Identifying Novel Therapeutic Strategies for Cachexia: Targeting AMPK and Inducible Nitric Oxide Synthase

Derek Thomas Hall

Department of Biochemistry

McGill University, Montreal

August 2019

A thesis submitted to McGill University in partial fulfillment

of the requirements of the degree of Doctor of Philosophy

For Pop, who taught me that if you choose to do something, do the best you can, and you will have no regrets.

Table of Contents

Abstract

Treatment of chronic disease is a growing burden in the healthcare system. Development of muscle wasting syndrome, known as cachexia, is one of the hallmarks of numerous chronic diseases, contributing to the loss of patient quality of life, mortality, and increased financial cost. However, despite being known of for centuries, our understanding of the molecular etiology of cachexia is relatively nascent. As such, there are no available effective treatments for cachexia, which is managed primarily through palliative care. Thus, there is a need to better understand the molecular mechanisms of cachexia and identify novel therapeutic targets. In this thesis, I have identified two novel targets for cachexia treatment: AMP-activated protein kinase (AMPK) and inducible nitric oxide synthase (iNOS). In Chapter 2, I showed that direct activation of AMPK can prevent metabolic dysfunction and muscle atrophy in cytokine, cancer, and septic-driven atrophy. Importantly, I also showed that indirect activation of AMPK through metabolic impairment is not effective at preventing atrophy, highlighting the importance of directly targeting AMPK for therapeutic potential. This work also demonstrates the critical role of altered mitochondrial homeostasis in the development of cachexia. In an effort to better understand the underlying cause of mitochondrial dysfunction, in Chapter 3 I demonstrated that iNOS, which is highly induced in response to inflammatory stimuli in muscle, significantly inhibits mitochondrial electron transport chain (ETC) activity. In particular, I identified Complex II and Complex IV of the ETC as potential sites of nitric oxide-mediated inhibition. I showed that inhibition of iNOS with a highly specific, clinically developed inhibitor can prevent metabolic dysfunction, atrophy, and loss of strength in a model of cancer cachexia. This work provides both insight into the mechanisms of disease progression in cachexia and identifies the repurposing of clinical iNOS inhibitors as a potential avenue of drug development. Collectively, the work from this thesis lays the groundwork for two novel strategies for cachexia treatment. In addition, it highlights the potential and importance of metabolic function in cachectic muscle. Further advancement of our understanding of metabolic regulation in cachexia will thus be critical for the development of future therapies.

Résumé

Le traitement des maladies chroniques est un fardeau croissant dans le système de santé. Le développement du syndrome de dépérissement musculaire, appelé cachexie, est l'un des signes distinctifs de nombreuses maladies chroniques, responsables de la perte de qualité de vie des patients, de la mortalité et d'une augmentation des coûts financiers. Cependant, bien que connu depuis des siècles, notre compréhension de l'étiologie moléculaire de la cachexie est relativement naissante. En tant que tel, il n'existe aucun traitement efficace disponible pour la cachexie, qui est principalement prise en charge par les soins palliatifs. Il est donc nécessaire de mieux comprendre les mécanismes moléculaires de la cachexie et d'identifier de nouvelles cibles thérapeutiques. Dans cette thèse, j'ai identifié deux nouvelles cibles pour le traitement de la cachexie: la protéine kinase activée par l'AMP (AMPK) et l'oxyde nitrique synthase inductible (iNOS). Au chapitre 2, je montre que l'activation directe de l'AMPK peut prévenir le dysfonctionnement métabolique et l'atrophie musculaire induits par les cytokines, le cancer et une atrophie d'origine septique. De manière importante, je montre également que l'activation indirecte de l'AMPK par le biais d'une déficience métabolique n'est pas efficace pour prévenir l'atrophie, soulignant l'importance de cibler directement l'AMPK pour son potentiel thérapeutique. Ce travail démontre également le rôle critique de l'homéostasie mitochondriale modifiée dans la progression de la cachexie. Dans un effort pour mieux comprendre la cause sous-jacente du dysfonctionnement mitochondrial, au chapitre 3, j'ai montré que l'iNOS, qui est fortement induit en réponse à des stimuli inflammatoires du muscle, inhibe de manière significative l'activité de la chaîne de transport d'électrons (ETC) mitochondriale. En particulier, j'ai identifié le complexe II et le complexe IV de l'ETC comme sites potentiels d'inhibition à médiation par l'oxyde nitrique. Je montre que l'inhibition d'iNOS avec un inhibiteur hautement spécifique, développé cliniquement, peut prévenir le dysfonctionnement métabolique, l'atrophie et la perte de force dans un modèle de cachexie cancéreuse. Ce travail fournit à la fois des informations sur les mécanismes de progression de la maladie dans la cachexie et identifie la réaffectation des inhibiteurs cliniques de l'iNOS comme une avenue potentielle du traitement de la cachexie. Ensemble, les travaux de cette thèse jettent les bases du développement de deux nouvelles stratégies pour le traitement de la cachexie. En outre, il souligne le potentiel et

l'importance de la fonction métabolique dans le muscle cachectique. Développer davantage notre compréhension de la régulation métabolique dans la cachexie sera donc essentiel pour le développement de futurs traitements.

Acknowledgements

I am of the firm opinion that pursuit of a Doctoral thesis cannot be undertaken alone. It is only with the support of my friends and family that I have been able to arrive at this point. I would like to thank Imed for taking me into his lab as an undergraduate student. You have directed both my development as a scientist and my growth as a person. I will always value what you have taught me, and I will aspire to achieve your unique blend of stubborn humility. In a similar vein, I would like to thank Sergio for guiding me through the nitty-gritty of it all. You are both more than mentors to me, and you will always be family.

To the lab members who were there at the beginning, your mentorship and companionship has been invaluable. Chris, you were an amazing TA and your passion brought me to this path. Jennifer, you helped me navigate the hurdles of graduate school and I would have been lost without you, literally. Brenda, we will always be bench-buddies, and I will miss our talks.

For those I have had the pleasure of mentoring, I thank you for your patience as I also learned how to be a better teacher. Amr, Souad, and Jason, you have become exceptional scientists. Watching your growth has been inspirational to my own, and I wish you the best of luck.

To Xian, Anne-Marie, Kholoud, and all the other members of the lab who I have had the pleasure of working with, you helped build a sense of community that was invaluable to me.

I would like to thank my Research Advisory Committee, Dr. Simon Wing, Dr. John Silvius, Dr. Russell Jones, and Dr. Gerardo Ferbeyre for their advice over the years. I would also like to thank the Biochemistry administrative staff, especially Christine Laberge and Vicky Kottis, for their continual support.

To “The Crew”, I would like to give my eternal gratitude for listening and nodding along to my ramblings on many a late night. David, Sayara, and PA, you helped keep me sane and taught me more than you know.

Finally, to my family, Mom, Ross, and Lise, I love you. Your unyielding support and encouragement have kept me going through the highs and the lows, especially in this final stretch.

Author Contributions

This is a manuscript-based thesis comprised of one published research article (Chapter 2), one research manuscript under preparation for submission (Chapter 3). Specific contributions of co-authors are outlined below.

Chapter 2 | Investigating the Potential of AMPK Activation for Cachexia Therapy

The contents of this chapter were originally published in

Hall DT, Griss T, Ma JF, Sanchez BJ, Sadek J, Tremblay AK, Mubaid S, Omer A, Ford RJ, Bedard N, Pause A, Wing SS, Di Marco S, Steinberg GR, Jones RG, Gallouzi IE (2018) "The AMPK agonist 5-Aminoimidazole-4-carboxamide ribonucleotide (AICAR), but not metformin, prevents inflammation-associated cachectic muscle wasting." (2018) *EMBO Mol. Med*. 10(7), pii: e8307

I was responsible for experimental design and conducted all experimental investigations, with assistance from other co-authors. I also performed the formal analysis and visualization of experimental findings. I prepared the original manuscript and participated in the review and preparation of the final submitted manuscript. TG assisted with the experimental design and performance of the extracellular flux experiments. JFM, BJS, JS, AKT, SM, and AO assisted with sample collection and processing for both *in vivo* and *in vitro* experiments. RJF and NB helped with the design of animal studies. AP contributed reagents and assisted with the interpretation of results. SSW contributed to the design of animal experiments and helped interpret the results. SDM assisted with experimental design and data analysis. RGJ contributed reagents, provided equipment, and helped interpret the extracellular flux experiments. IEG supervised experimental design, execution, and data interpretation. AP, SSW, SDM, and RGJ helped review and edit the manuscript. IEG reviewed, edited, and prepared the final manuscript for submission.

Chapter 3 | Identification of iNOS as a Driver of Metabolic Dysfunction in Cachexia

The contents of this chapter are adapted from

Hall DT, Sadek J, Colalillo B, Tremblay AK, Di Marco S, and Gallouzi IE. "Inducible Nitric Oxide Synthase Impairs Mitochondria Oxidative Phosphorylation in Cachexia" *Manuscript in preparation.*

I was responsible for experimental design and conducted all experimental investigations, with assistance from other co-authors. I also performed the formal analysis and visualization of experimental findings and prepared the original manuscript. JS assisted with sample collection and processing for western blot analyses for *in vitro* studies and assisted with the animal studies. CB assisted with western blot analysis for *in vitro* studies. SDM assisted with experimental design and data analysis. IEG supervised experimental design, execution, and data interpretation. Manuscript review and preparation is currently being conducted by myself, SDM, and IEG.

Chapter 4 | General Discussion

All novel experimental results reported in this section were conceptualized, performed, analyzed, and interpreted by myself, with supervision from Dr. Imed Gallouzi. AMPK muscle-specific knockout mice were generously provided by Dr. Gregory Steinberg.

Original Contributions to Knowledge

Chapter 2: Investigating the Potential of AMPK Activation for Cachexia Therapy

- Demonstrated that direct activators of AMPK, such as AICAR and A-769662, can protect against muscle atrophy in models of cachexia.
- Showed that activation of AMPK indirectly through mitochondrial inhibition, either during the normal progression of atrophy or by treatment with metformin, does not protect against muscle wasting and may promote atrophy.
- Identified differential effects on mitochondrial function and iNOS gene expression as potential explanations for the different outcomes of direct versus indirect AMPK activation.
- Collectively, this work demonstrates a dual role for AMPK activation in cachexia, where direct, early activation of AMPK can protect mitochondrial function and reduce atrophy, but activation of AMPK after mitochondrial inhibition may contribute to atrophy. Understanding this dual role is important for the development of therapeutic strategies that target AMPK for the treatment of cachexia.

Chapter 3: Identification of iNOS as a Driver of Metabolic Dysfunction in Cachexia

- Found that inhibition of mitochondrial oxidative phosphorylation was dependent on iNOS activity, implicating iNOS as a driver of metabolic dysfunction during cachexia.
- Performed a comprehensive bioenergetic profiling of cytokine-treated myotubes, revealing that the shift towards aerobic glycolysis induced by cytokines is not sufficient to maintain cellular energy homeostasis.
- Demonstrated that a clinically developed iNOS inhibitor recovers muscle ETC complex activity and reduces muscle weakness and atrophy in a pre-clinical model of cancer cachexia. This provides a proof-of-principle for the repurposing clinical iNOS inhibitors for the treatment of cachexia.
- Collectively, this work contributes to our understanding of how iNOS promotes muscle atrophy and dysfunction and validates it as a viable therapeutic target for the treatment of cachexia.

Chapter 1 | Clinical Impact and Molecular Mechanisms of Cachexia

"When the flesh on the body has disappeared, the carrying of the bones becomes a burden, it pulls you into the ground" – Herta Müller, *Atemschaukel*, 2009

1.1 Clinical Definitions, Prevalence, and Impact of Cachexia

1.1.1 What is Cachexia?

One of the hallmarks of end-stage chronic disease is a progressive, involuntary loss of body mass. The term cachexia was first coined by ancient Greek physicians, derived from *kakos*, meaning "bad", and *hexis*, meaning "condition," to describe the extreme levels of emaciation seen in very sick, chronically ill patients (Bennani-Baiti and Walsh, 2009). Importantly, cachectic wasting is distinct from malnutrition and cannot be reversed by caloric supplementation (Gullett et al., 2011). It arises in a variety of common chronic diseases, such as cancer, chronic obstructive pulmonary disorder, chronic heart and kidney failure, sepsis, and HIV infection (Vaughan et al., 2013; von Haehling et al., 2016). It is characterized primarily by the loss of skeletal muscle mass, which is often accompanied by loss of adipose tissue (Blum et al., 2014; Fearon et al., 2011). In addition, cachexia is associated with several other metabolic perturbations, such as anorexia, increased resting energy expenditure, and altered liver function (Baracos et al., 2018; Fearon et al., 2012; Porporato, 2016; Tisdale, 2009). Progression of cachexia leads to dramatic functional impairment in patients, who ultimately become bed-ridden before succumbing to their illness. Often, progression of cachexia, and not the overlying condition, is a direct or indirect cause of death. For example, loss of function in the respiratory muscles can make breathing difficult and increase susceptibility to pneumonia (Gullett et al., 2011). Indeed, the development of cachexia has historically been considered terminal; as Hippocrates famously described, "This illness is fatal" (Bennani-Baiti and Walsh, 2009).

1.1.2 Clinical Definitions of Cachexia

While cachexia has been known of for centuries, it has historically been underdiagnosed and under-researched due to the misconception that it is simply a symptom of the overlying

condition, rather than a separate syndrome with a unique etiology. In recent years, there have been several methodologies put forward to better standardize the diagnosis of cachexia and establish its clinical significance as a syndrome and predictor of poor outcome.

In 2008, a group of researchers and clinicians established a consensus definition of cachexia (Evans et al., 2008). They stated that cachexia was a "complex metabolic syndrome associated with underlying illness and characterized by loss of muscle with or without loss of fat mass" (Evans et al., 2008). Diagnosis criteria for cachexia was established as weight loss of at least 5% in the past 12 months or less with at least 3 of 5 additional markers of either decreased muscle strength, fatigue, anorexia, low fat-free mass index, or biochemical indications of chronic inflammation (Evans et al., 2008). Subsequently, several classification systems were proposed for the staging of cachexia patients (Argiles et al., 2017; Argiles et al., 2011; Blum et al., 2014; Fearon et al., 2011; Martin et al., 2015; Muscaritoli et al., 2010; Vigano et al., 2012; Vigano et al., 2017; Zhou et al., 2018).

From the consensus definition, Fearon *et al.* established four categories of disease progression: (1) non-cachectic, (2) pre-cachexia, (3) cachexia, and (4) refractory cachexia. Pre-cachexia was defined as body weight loss ≤ 5% with accompanying risk factors, such as cancer type, markers of inflammation, low food intake, or lack of response to treatment. Cachexia was defined as weight loss > 5% over the past 6 months or >2% if the patient's body mass index (BMI) was less than 20 kg/m^2. A patient was also considered cachectic if they were diagnosed with age-related muscle loss (sarcopenia) and >2% body weight loss. Refractory cachexia was identified as the stage in disease progression where the burden of intervention was likely to outweigh potential benefits. It was defined as weight loss in the preterminal stage of advance cancer or in cancer with rapid progression and no response to treatment, with a life expectancy of less than three months (Fearon et al., 2011). These definitions were subsequently refined to account for the impact of BMI on body weight loss criteria and assessed for their predictive power in patient outcome (Blum et al., 2014; Martin et al., 2015; Vigano et al., 2012). While patients classified as cachectic or refractory cachectic were found to have significantly worse prognosis and survival, there was no significant separation between pre-cachexia and non-cachectic patients (Blum et al., 2014; van der Meij et al., 2013; Vigano et al., 2012; Wesseltoft-Rao et al., 2015). Further

refinement of the classification system by Vigano *et al*. was able to establish a relevant and significant separation in measured outcomes between pre-cachectic patients and non-cachectic patients, though there was no separation between pre-cachectic and fully cachectic patients (Vigano et al., 2017).

In parallel to the four stages classification system, Argiles *et al.* developed a Cachexia Score (CASCO) diagnostic scale based on the initial consensus definition of Evans *et al.* (Argiles et al., 2011; Evans et al., 2008). The scoring accounts for body weight loss (40%), plasma markers of inflammation and metabolic disruption (20%), physical performance (15%), a nutritional assessment questionnaire (15%), and a quality of life questionnaire (10%) (Argiles et al., 2011). The CASCO scale was subsequently validated by comparing it to the Eastern Cooperative Oncology Group (ECOG) performance status and subjective scoring by specialized oncologists. Significant correlation was detected between CASCO and the other two scoring systems, indicating that CASCO is a valid clinical assessment tool (Argiles et al., 2017). The proposed advantage of the CASCO is that it provides a quantitative assessment of cachexia. However, more studies are required to see if it correlates with patient outcomes, such as survival. In addition, the CASCO requires a significant amount of specialized measurements and extensive questionnaires, potentially precluding its use in medical centers with limited resources. However, in the same validation study, Argiles *et al*. addressed this issue by developing a simplified scoring system, termed the miniCASCO (MCASCO), which was shown to correlate strongly with the full CASCO (Argiles et al., 2017).

Recently, Zhou *et al.* established and validated a new scoring methodology that effectively distinguished all four stages of cachexia development (Zhou et al., 2018). The cachexia staging score (CSS) system uses 5 variables consisting of assessments for weight loss, sarcopenia and muscle function (SARC-F), the ECOG performance status, appetite loss, and abnormal plasma markers, such as low albumin levels. The CSS system was able to stratify patients into the four stages of cachexia and, importantly, statistically separated them in metrics of both patient quality of life, functionality, and survival (Zhou et al., 2018). While promising, further studies are needed to see if the diagnostic value of the CSS is reproducible and valid across multiple clinical centers.

In conclusion, significant progress has been made towards the establishment of cachexia diagnostic criteria over the past decade. Future studies will focus on further refinement of the different staging methodologies and continued validation of their clinical relevancy.

1.1.3 Prevalence in Chronic Diseases

Estimations of the prevalence of cachexia can vary, partially due to the lack of a consistent definition for its diagnosis. In addition, the majority of studies have focused on the frequency of cachexia in cancer due to its higher overall prevalence and severity in cancer compared to other conditions (Arthur et al., 2014; von Haehling et al., 2016). Nevertheless, cachexia prevalence estimates for chronic obstructive pulmonary disease (COPD), sepsis, chronic heart failure (CHF), and HIV infection have been made, and it is clear that cachexia plays a relevant role in patient outcomes in these diseases (von Haehling et al., 2016; von Haehling and Anker, 2014). A study using data from the Nationwide Inpatient Sample database estimated that, in 2009, 161,898 cachexia related admissions were made in the US. The most common comorbidity was malignancy, followed by COPD, pneumonia, heart failure, renal failure, and HIV infection (Arthur et al., 2014). Interestingly, septicemia was the most common primary diagnosis when cachexia was secondarily diagnosed, highlighting the potential relevance of cachexia during sepsis (Arthur et al., 2014). Subsequent estimates using additional data from Europe and Japan suggested that cachexia rates in COPD were 15-25% and 20-40% in CHF and chronic kidney disease (CKD) (von Haehling et al., 2016). Cachexia rates in COPD have also been estimated to be as high as 40% depending on the definition used (Sanders et al., 2016). An estimate of cachexia in optimally treated, non-diabetic CHF patients found that the cachexia rate was only approximately 10%, suggesting that differences in comorbidities and treatment of the overlying condition can cause variations in measured cachexia rates (Christensen et al., 2013). Significant advancement in the treatment of HIV has reduced its disease burden in developed countries (Atta et al., 2019). However, there is evidence to suggest that successful treatment of HIV does not always abrogate the progression of cachexia, and the incidence of unintentional weight loss in HIV infected populations was estimated to be as high as 38% by Mangili *et al.* in 2006 (Mangili et al., 2006; Tang et al., 2005; Wanke et al., 2000). Furthermore, HIV/AIDS still represents a significant health burden in developing countries (Shao and Williamson, 2012). Thus, continued studies on the

epidemiology of cachexia in various chronic inflammatory diseases like COPD, CHF, HIV infection, and sepsis are warranted to better understand its frequency. However, it is clear that a significant portion of these patients suffer from cachexia.

In comparison to other chronic inflammatory conditions, incidence of cachexia in cancer is relatively high. The most common stated estimates of cancer cachexia range from approximately 30-50% of all cancer patients (Aoyagi et al., 2015; Argiles et al., 2014; Arthur et al., 2014; Baracos et al., 2018; Gannavarapu et al., 2018; Teunissen et al., 2007; Thoresen et al., 2013; Tisdale, 2009; Vigano et al., 2017; von Haehling et al., 2016; von Haehling and Anker, 2014; Zhou et al., 2018). However, the prevalence of cancer cachexia varies dramatically depending on definition used, potentially varying from 12-85% (Wallengren et al., 2013). In addition, the prevalence is known to vary depending on the cancer subtype. For example, breast and prostate cancers are estimated to have the lowest prevalence of cachexia (<25%) while pancreatic and gastroesophageal cancers are believed to have some of the highest rates of cachexia (>60%) (Baracos et al., 2018). The reasons behind these differences are unknown. It is possible that differences in inflammatory status contribute to the variability in cachexia incidence. It is also possible that localized disruption of organ function in the primary tumor site drives the differences in cachexia rates. For example, gastroesophageal cancers could interfere with nutritional status, and the pancreas plays a key role in regulating whole body metabolic homeostasis (Reim and Friess, 2016; Yabar and Winter, 2016). Furthermore, the prevalence of cachexia is believed to be significantly higher in patients with more advanced cancer stages (>80%) (Teunissen et al., 2007; von Haehling et al., 2016). Therefore, differences in the pathological progression of different cancers might underly the variations in cachexia rates. Regardless, cachexia is highly prevalent in cancer, and its strong correlation with disease progression highlights its connection to patient morbidity and mortality.

1.1.4 Clinical Impact of Cachexia

Development of cachexia has a severe negative impact on patients and their families, and it represents a significant burden to healthcare systems (Tan and Fearon, 2008). Patients with cachexia have significantly reduced survival rates compared to non-cachectic patients (Ozorio et al., 2017; Takayama et al., 2016; Utech et al., 2012; Vazeille et al., 2017; Vigano et al., 2017; Zhou et al., 2018). The one-year mortality rate of cachexia patients in COPD and CHF has been

estimated to be approximately 20% and 30%, respectively (von Haehling et al., 2016). In cancer, the one-year mortality rate can be as high as 80% in advanced cases (von Haehling et al., 2016). Indeed, cachexia has been estimated to be directly responsible for 20% and present in 50% of all cancer-related deaths (Warren, 1932) (von Haehling and Anker, 2010). The causative relationship between cachexia and increased mortality has not been fully developed (Kalantar-Zadeh et al., 2013). However, it has been demonstrated that cachexia reduces both the effectiveness of and tolerance to chemotherapy, reducing effective management of the primary condition and potentially contributing to increased mortality (Andreyev et al., 1998; Dewys et al., 1980; Prado et al., 2007). In addition, loss of respiratory muscle function has been associated with increased pneumonia rates in cachexia patients (Arthur et al., 2014; Windsor and Hill, 1988). Cachexia-induced loss of cardiac function may also lead to increased risk of heart failure and death (Barkhudaryan et al., 2017; Kalantar-Zadeh et al., 2013; Ponikowski et al., 1999). Finally, impaired immune system function may increase susceptibility to infection, as demonstrated by increased septicemia rates detected in cachexia patients (Arthur et al., 2014; Kalantar-Zadeh et al., 2013). It is likely that the direct cause of death varies from patient to patient. Ultimately, cachectic patients are frailer, less responsive to treatment, and more likely to develop complications, all of which significantly increases their mortality risk.

Compounding on the deadly nature of cachexia is its dramatic impact on patient quality of life. The progressive skeletal muscle wasting in patients leads to increased fatigue and reduced physical function and mobility (Dahele et al., 2007; Fearon et al., 2003; Fouladiun et al., 2007; Ozorio et al., 2017; Vigano et al., 2017; Zhou et al., 2018). Cachexia has also been associated with pain, poor sleep, nausea, altered taste and smell perception, and anorexia (Del Fabbro et al., 2011; Vigano et al., 2017; Yavuzsen et al., 2009; Zhou et al., 2018; Zhou et al., 2017). In addition, as described above, cachexia increases the risk of developing other complications or having a negative response to treatment (Andreyev et al., 1998; Arthur et al., 2014; Dewys et al., 1980; Prado et al., 2007; Windsor and Hill, 1988). As a result, cachexia patients consistently score worse in assessments of quality of life (Takayama et al., 2016; Vigano et al., 2017; Wheelwright et al., 2013; Zhou et al., 2018). Not to be overlooked is the impact of cachexia on the family and loved ones of afflicted patients. Cachectic patients require significantly more support. Furthermore,

the dramatic progression of cachexia negatively impacts not only the mental health of the patient, but also those close to them who bear witness to their progressive wasting (Hopkinson, 2014).

Besides its physiological and psychological impact, cachexia also represents a significant financial burden to both patients and healthcare networks. While there is a lack of studies on the cost of cachexia specifically (Tarricone et al., 2016), malnutrition status in cancer is well known to be associated with higher healthcare costs and hospitalization (Arends et al., 2017). In their analysis of the Nationwide Inpatient Sample database, Arthur *et al.* found that length of stay of hospitalization of cachexia patients was twice that of non-cachexia patients, with their hospitalization costs also being approximately double (Arthur et al., 2014). These results were corroborated by a small study of elderly Japanese patients with later stage non-small-cell lung cancer (NSCLC), where cachexia patients were found to have approximately double the number of unplanned hospital visits or hospitalizations, amounting to roughly 50% more in-patient medical costs (Naito et al., 2017). In a follow-up analysis focusing specifically on five cancers with the highest incidence of cachexia, Arthur *et al.* found that cachexia was still associated with more hospitalization and medical costs, but the effects were much smaller than previously reported (Arthur et al., 2016). Thus, there is some uncertainty as to the true cost of cachexia, and more studies are warranted to understand the financial impact of cachexia.

Despite the clear clinical impact of cachexia, at present there are no widely available, effective treatments. Patients diagnosed with cachexia are largely managed with palliative care (Baracos et al., 2018). To develop an effective therapy, a robust and comprehensive understanding of the etiology of cachexia is necessary.

1.2 Mechanisms of Cachexia

The causes of cachexia are complex and multimodal, involving crosstalk between numerous tissues throughout the body. While much remains to be understood about the underlying mechanisms, significant progress has been made in recent years. In general, it is believed cachexia arises due to the chronic inflammation induced by the overlying condition (e.g. cancer, COPD, etc.) (Aoyagi et al., 2015; Argiles et al., 2014; Baracos et al., 2018). Persistent elevation of

inflammatory signaling causes changes throughout the body, resulting in cachexia-associated phenotypes in numerous organs. In particular, the brain, liver, heart, adipose tissue, and skeletal muscle have been the primary sites of investigation (Argiles et al., 2015b; Baracos et al., 2018; Fearon et al., 2012). However, recent studies have also revealed changes in gut physiology (Bindels et al., 2016; Bindels et al., 2018; Potgens et al., 2018; Puppa et al., 2011). Ultimately, the combination of altered function in all these tissues, as well as crosstalk between them and with the immune system, induce an overall catabolic state, leading to muscle wasting.

1.2.1 Initiation of Cachexia: The Role of Humoral Factors

The initiation of cachexia is believed to be mediated by elevated levels of inflammatory humoral factors. Specifically, inflammatory hormones known as cytokines have been identified as key drivers of cachexia (Baracos et al., 2018). However, altered signaling from non-cytokine factors, such as insulin-like growth factor 1 (IGF-1) and glucocorticoids, also plays a role (Baracos et al., 2018). In addition, other factors, such as parathyroid hormonal signaling, exosome secretion, and zinc ion homeostasis have also recently been identified as potential initiators of cachexia (Chitti et al., 2018; Kir et al., 2016; Wang et al., 2018b).

1.2.1.1 Interleukins

Interleukins are a family of cytokines first discovered as secretory factors derived from leukocytes (Akdis et al., 2016). Interleukins can have pro-inflammatory (e.g. IL-6) or anti-inflammatory (e.g. IL-10) function (Akdis et al., 2016). In cachexia, IL-6 has been identified in numerous animal models and human patients as an important pro-cachectic factor (reviewed in (Narsale and Carson, 2014) and (Carson and Baltgalvis, 2010)). IL-6 is elevated in human cachexia patients and this increase negatively correlates with survival (Iwase et al., 2004; Songur et al., 2004). In addition, IL-6 is required for the induction of muscle wasting in several well-known mouse models of cancer cachexia (Baltgalvis et al., 2008; Bonetto et al., 2012; Puppa et al., 2014a; Strassmann et al., 1992a). In the C26 adenocarcinoma model of cancer cachexia, elevation of IL-6 secretion directly from tumor cells has been shown to correlate with induction of cachexia after implantation (Fujimoto-Ouchi et al., 1995). Furthermore, the secretion of IL-6 from tumor cells has been shown to be augmented by IL-1, implicating IL-1 as another pro-cachectic interleukin (Strassmann et al., 1992b; Strassmann et al., 1993). In addition to effects on IL-6 secretion, IL-1

has been linked to inflammation in the hypothalamus, trigging altered hormonal signaling and anorexia (reviewed in (McDonald et al., 2018)).

Other pro-inflammatory interleukins in the IL-6-like family may also play a role in cachexia. Leukemia inhibitor factor (LIF), IL-11, and oncostatin M (OSM) have all been shown to be upregulated in mouse models of cachexia and to induce atrophy in muscle cells and lipolysis in adipose tissue (Arora et al., 2018; Barton and Murphy, 2001; Iseki et al., 1995; Seto et al., 2015; Terawaki et al., 2014). Also, muscle-specific depletion of their common receptor, the gp130 receptor, protects against muscle wasting in the Lewis Lung Carcinoma (LLC) mouse model of cancer cachexia (Puppa et al., 2014a). There is some evidence to suggest that other interleukins may also be involved in the etiology of cachexia. For example, elevated levels of IL-8 has been associated with cachexia in pancreatic cancer patients (Hou et al., 2018) and IL-17 overexpression in mice has been reported to induce muscle wasting (Tang et al., 2010). Thus, while IL-6 and the IL-6-like family of cytokines have well established roles in cachexia, other pro-inflammatory interleukins may also be involved.

Suppression of anti-inflammatory interleukins may also contribute to the progression of cachexia. Indeed, IL-10 has been shown to supresses IL-6 expression in the C26 mouse model, and polymorphisms in IL-10 have been associated with risk of developing cachexia (Deans et al., 2009; Fujiki et al., 1997; Sun et al., 2010). Furthermore, IL-10 expression negatively correlates with muscle wasting in epithelial ovarian cancer patients (Aust et al., 2015). IL-4, another anti-inflammatory interleukin, has been shown to be downregulated in the liver of pancreatic cancer patients and to protect against cachexia during acute infection in mice (Brunet et al., 1997; Prokopchuk et al., 2017). Finally, levels of the anti-inflammatory IL-13 are lower in the tumor of cachectic cancer patients when compared to weight-stable cancer patients (de Matos-Neto et al., 2015). More work is needed to understand if decreased expression of anti-inflammatory interleukins is a wide-spread phenomenon during cachexia and if it plays a causative role. However, these studies do suggest that the balance of pro- and anti-inflammatory interleukins could contribute to the progression of cachexia.

1.2.1.2 Tumor Necrosis Factor-α and TWEAK

Tumor necrosis factor α (TNFα) is likely one of the most well-known inducers of cachexia (reviewed in (Patel and Patel, 2017)). Indeed, one of the first humoral factors to be identified that could induce cachexia was originally termed cachectin (Beutler et al., 1985b; Tracey et al., 1988), but it was subsequently discovered to be TNFα (Beutler et al., 1985a). Interestingly, despite numerous studies showing that TNFα can induce cachexia or that blocking TNFα signaling can prevent cachexia (Tisdale, 1997), serum TNFα levels are often found to not be elevated in cachexia patients when compared to weight stable patients (Hou et al., 2018; Kayacan et al., 2006; Socher et al., 1988; Tisdale, 1997). However, TNFα is elevated in disease-bearing patients when compared to healthy patients (Adami et al., 1994; Hou et al., 2018; Kayacan et al., 2006; Shaarawy and Abdel-Aziz, 1992). Thus, it seems that TNFα is likely necessary and permissive for the progression of cachexia, but not sufficient alone for its induction. In keeping with this, it has been shown that a solubilized receptor of TNFα can block atrophy in the LLC mouse model, despite no elevation in serum TNFα being detected (Llovera et al., 1998). Furthermore, TNFα has been shown to synergize with IFNγ and IL-1 to induce atrophy, in keeping with its function as a facilitator of cachexia (Acharyya et al., 2004; Di Marco et al., 2005; Flores et al., 1989; Ma et al., 2017).

Another member of the TNF family implicated in muscle wasting is the tumor necrosis factor-like weak inducer of apoptosis (TWEAK). TWEAK has been shown to impair muscle regeneration and induce wasting in a variety of atrophic conditions (reviewed in (Kumar et al., 2012)). In a model of chemically induced breast cancer, TWEAK is elevated in the serum, heart, and skeletal muscle (Padrao et al., 2017; Padrao et al., 2015). Also, an antibody targeting the TWEAK receptor Fn14 was found to prevent cachexia in the C26 mouse model (Johnston et al., 2015). However, the anti-cachectic effects of the antibody were found to be independent of TWEAK, as TWEAK knockout mice and mice treated with a monoclonal antibody targeting TWEAK were not resistant to cachexia (Johnston et al., 2015). Instead, a tumor-specific Fn14 function was found to be required, but the mechanism by which it induces cachexia is unknown (Johnston et al., 2015). Therefore, it is unclear if TWEAK itself is a trigger of cachectic muscle wasting, though it seems to be involved in other types of muscle atrophy. Nevertheless, targeting the Fn14 receptor

remains a promising therapeutic avenue, though the underlying mechanism of its pro-cachectic function remains to be determined.

1.2.1.3 Interferon-γ

IFNγ is another often cited inducer of cachexia. Administration of IFNγ in rats can induce cachexia-like symptoms, and anti-IFNγ antibodies can impair tumor growth and cachexia in murine cancer cachexia models (Langstein et al., 1991; Matthys et al., 1991a; Matthys et al., 1991b). Furthermore, inoculation of mice with Chinese Hamster Ovary (CHO) tumor cells expressing IFNγ can induce cachexia (Matthys et al., 1991a). However, cachexia was only detected when IFNγ and cancer cells were administered together, suggesting that IFNγ could not induce cachexia on its own (Matthys et al., 1991a). It was later found that IFNγ can act synergistically with other cytokines to induce the cachectic phenotype. Namely, IFNγ co-treatment with TNFα has been shown to induce atrophy in muscle cells in a synergistic manner (Guttridge et al., 2000). Thus, similar to TNFα, a basal level of elevated IFNγ seems to be permissive, but not in and of itself sufficient, for the induction of cachexia.

1.2.1.4 Transforming Growth Factor-β Super Family

The TGFβ superfamily is a group of cytokines that bind to a set of common receptors and impact numerous cellular functions, such as growth and differentiation (Massague, 2012). They are well known to play an important role in muscle physiology and development (Massague, 2012). Of particular note, myostatin, Activin A, and TGFβ1 have all been shown to have a role in the development of cachexia. Myostatin is best known for its role as a suppressor of hypertrophy, with myostatin depletion resulting in excessive muscular growth (Rodriguez et al., 2014). In addition, excessive production of myostatin can promote atrophy (Rodriguez et al., 2014; Zimmers et al., 2002). Inhibiting myostatin with a targeted antibody has been shown to prevent cancer cachexia in mice (Murphy et al., 2011). Furthermore, genetic depletion of myostatin from cardiac myocytes has been shown to protect against heart failure induced cachexia (Heineke et al., 2010). Inhibition of Activin A, another member of the TGFβ family, has also been shown to reduce cancer cachexia (Chen et al., 2017). Activin A has been found to be elevated in cachexia (Loumaye et al., 2015; Loumaye et al., 2017), and, like myostatin, its over expression triggers muscle atrophy (Chen et al., 2016). Finally, release of TGFβ from bone during osteolytic

metastatic cancers has been shown to drive oxidative stress and weakness in muscle (Waning et al., 2015). Administration of TGFβ has also been shown to induce cachexia in cancer-bearing mice (Zugmaier et al., 1991). Thus, collectively, TGFβ cytokines have been shown to be potent inducers of muscle atrophy.

Given that numerous members of the TGFβ family have been implicated in cachectic muscle atrophy, it is likely that they serve redundant functions in the induction of atrophic signaling. In keeping with this, inhibition of both Activin A and myostatin was found to be more effective than inhibiting either one alone (Chen et al., 2017). Several studies, then, have looked at the potential of targeting the TGFβ receptor, instead of the ligands, as a method of preventing TGFβ-mediated cachexia. In three separate studies, a solubilized activin receptor type II B (ActRIIB) was found to be very effective at preventing muscle atrophy and weakness in mouse models of cancer cachexia (Benny Klimek et al., 2010; Busquets et al., 2012; Zhou et al., 2010). Of interest from a therapeutic perspective, Zhou *et al.* demonstrated that delayed administration of the antibody did more than just prevent further loss, but actually reversed wasting after it had begun (Zhou et al., 2010). Also, Benny Klimek *et al*. showed that while the soluble ActRIIB receptor could prevent cachexia, myostatin knockout mice were in fact more susceptible to wasting, highlighting the potential redundancies of the TGFβ family ligands (Benny Klimek et al., 2010). Thus, it is clear that TGFβ signaling contributes to the induction of cachexia, and targeting receptor signaling may prove to a be an effective therapy for cachexia.

1.2.1.5 Insulin-like Growth Factor-1

Insulin-like growth factor-1 (IGF-1) is well known for its hypertrophic and anti-atrophic effects in muscle, mediated by AKT kinase signaling (Reviewed in (Schiaffino and Mammucari, 2011)). IGF-1 levels have been observed to decrease in rodent models of CHF, sepsis, and cancer (Brink et al., 1996; Costelli et al., 2006; Fan et al., 1994) and are also decreased in human cachexia patients in cancer and CHF (Attard-Montalto et al., 1998; Hambrecht et al., 2002). Also, administration of IGF-1 prevents muscle loss in several models of atrophy, such as muscular dystrophy, disuse, or glucocorticoid treatment (Kumar et al., 2011; Schakman et al., 2005; Shavlakadze et al., 2004; Ye et al., 2013). However, several studies have shown a lack of efficacy of IGF-1 injection in models of cachexia. Indeed, subcutaneous injection of IGF-1 in rats bearing

cachectic AH-130 hepatoma tumors did not protect against muscle loss (Costelli et al., 2006). In contrast, a separate study found that a significantly lower dose of IGF-1 subcutaneous injection could increase muscle mass in the same rat model (Schmidt et al., 2011). However, the recovery was not dose responsive, as higher doses of IGF-1 failed to recover muscle mass. This suggests that toxicity or reduced sensitivity might limit the effects of systemically administered IGF-1 (Schmidt et al., 2011). In a model of CHF cachexia, infusion of IGF-1 was unable to prevent atrophy induced by angiotensin II infusion, further demonstrating a lack of efficacy from systemically delivered IGF-1 (Brink et al., 2001). Several possible explanations have been suggested to explain why IGF-1 treatment does not reduce atrophy in cachexia models (Costelli et al., 2006; Schmidt et al., 2011). For one, the hypertrophic effects of IGF-1 have been suggested to be driven by its autocrine signaling, and local IGF-1 production may be more relevant than systemic production. In keeping with this, serum IGF-1 levels were found to be unchanged in CHF patients, but muscle expression of IGF-1 was decreased and correlated with reduced muscle fiber size (Hambrecht et al., 2002). Also, muscle-specific IGF-1 overexpression was found to block angiotensin II induced cachexia in mice (Song et al., 2005; Yoshida et al., 2010). However, similar muscle-specific overexpression experiments were ineffective in both a rat and mouse model of cancer cachexia, despite being able to prevent age-related muscle wasting (sarcopenia) (Penna et al., 2010). Thus, other confounding factors may limit the efficacy of IGF-1 administration. For example, the balance between IGF-1 and IGF binding proteins (IGFBPs) may limit the bioavailability of circulating IGF-1. In rheumatoid arthritis patients, circulating IGF-1 levels were unaffected, but IGFBP-1 was significantly upregulated, reducing the overall bioavailability of IGF-1 (Engvall et al., 2008). Also, several pro-cachectic cytokines, such as IL-1, IL-6, and TNF have been shown to limit IGF activity or impair IGF signaling, potentially limiting the efficacy of its administration in cachexia (Al-Shanti and Stewart, 2012; Anwar et al., 2002; Lazarus et al., 1993). Therefore, while it is likely that diminished IGF-1 levels contribute to cachexia, especially during CHF, establishment of causality, specifically in cancer cachexia, is complicated due to confounding factors that limit the efficacy of IGF-1 administration.

1.2.1.6 Glucocorticoids

Glucocorticoids are a class of steroidal hormones, such as cortisol, that are produced by the adrenal gland in response to stress (Zhou and Cidlowski, 2005). Glucocorticoids are known to induce a catabolic state in muscle through a variety of mechanisms, including suppression of mTOR signalling and increased proteasomal activity and autophagy (reviewed in (Schakman et al., 2013) and (Braun and Marks, 2015)). Indeed, treatment of muscle cells with glucocorticoids, like dexamethasone, is a commonly used model of muscle atrophy (Hasselgren et al., 2010). Glucocorticoids are known to be upregulated in cachexia (Cala et al., 2018; Drott et al., 1988; Flint et al., 2016; Suzuki et al., 2015). Furthermore, muscle-specific knockout of the glucocorticoid receptor (GR) prevents muscle loss in mouse models of sepsis and cancer cachexia (Braun et al., 2013). Thus, elevated glucocorticoid levels likely contribute to the progression of muscle wasting during cachexia.

1.2.1.7 Other Circulating Factors

Other mechanisms that may contribute to cachexia continue to be identified. For example, parathyroid hormone (PTH) signaling has recently been recognized as a potential driver of cachexia. In mouse models of kidney failure and cancer cachexia, elevated PTH in kidney failure and parathyroid hormone related protein (PTHrP) in cancer cachexia were shown to induce adipose tissue browning and muscle atrophy (Kir et al., 2016; Kir et al., 2014). Intriguingly, adipose tissue-specific knockout of the PTH receptor (PTHR) was able to prevent adipose tissue browning and also muscle atrophy, suggesting that crosstalk between fat and lean body tissue contributes to the progression of cachexia (Kir et al., 2016). Elevated PTHrP in human cancer patients was also associated with reduced muscle mass and increased resting energy expenditure (REE) (Hong et al., 2016; Kir et al., 2014). Another example is the growing interest in the potential role of exosomes in cachexia signaling. Numerous studies have begun to emerge showing that tumor-secreted exosomes can drive both muscle and adipose tissue wasting (Chitti et al., 2018; Hu et al., 2018; Marinho et al., 2017; Wu et al., 2018; Zhang et al., 2017). Finally, a recent study investigating the transcriptome of cachectic muscle in mouse models of metastatic cancer identified the zinc transporter ZIP14 as an inducer of atrophy, implicating altered zinc homeostasis as a potential driver of cachexia (Wang et al., 2018b). Therefore, despite

considerable progress over many years of research, new mechanisms of cachectic induction continue to be identified, highlighting the complexity and multifactorial nature of the syndrome.

1.2.2 Impact of Cachexia on Non-muscle Organs

While the primary clinical impact of cachexia is largely derived from loss of skeletal muscle mass and function, there is a growing appreciation for the role of non-muscle organs in the development of cachexia. Indeed, a growing body of evidence suggests that altered function in organs throughout the body contributes to an overall pro-inflammatory and catabolic state. In addition, it is now evident that significant “cross-talk” pathways between organs likely contributes to the etiology of cachexia, emphasizing the complex, multimodal nature of this syndrome (Fig. 1.1).

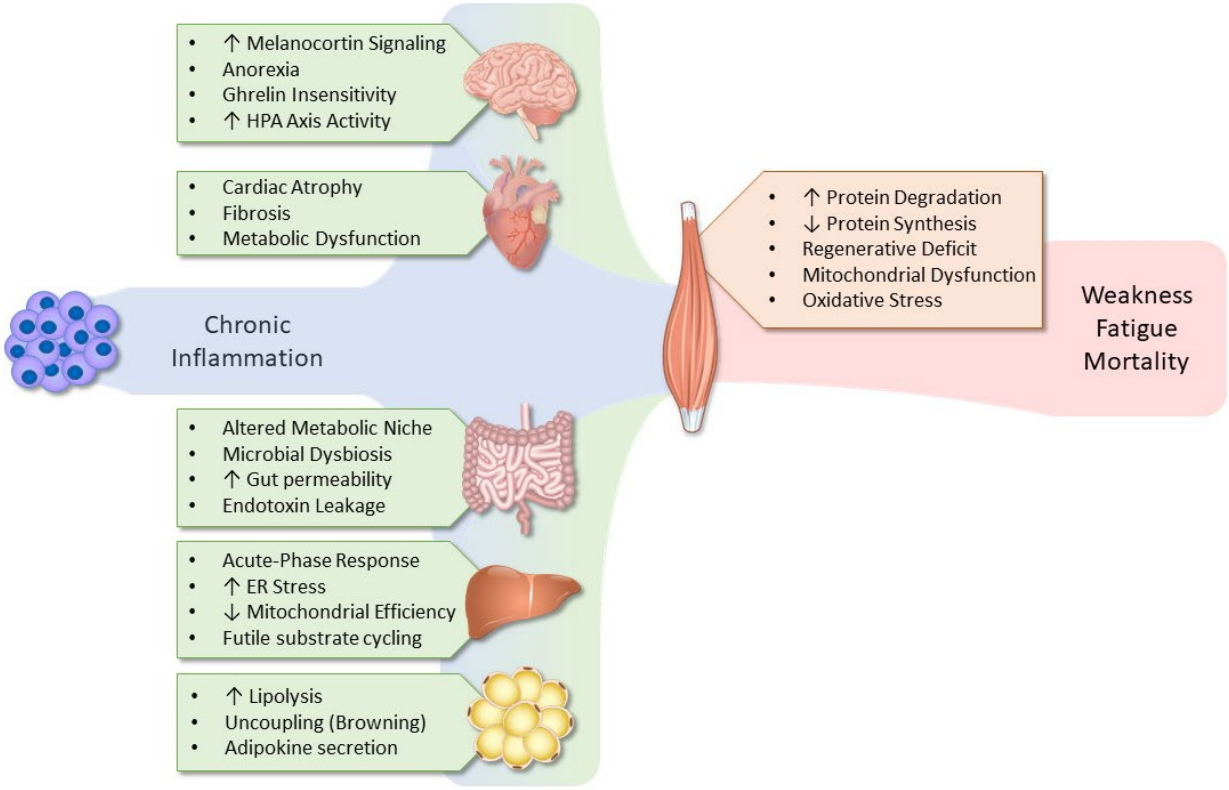

Figure 1.1: The role of non-muscle organs in the development of cachexia.

Pro-inflammatory diseases, such as cancer, induce a systemic level of chronic inflammation that alters the function of numerous tissues throughout the body to promote cachexia. Inflammation in the hypothalamus promotes anorexia and sickness behavior and stimulates the release of catabolic glucocorticoids from the adrenal glands through the HPA axis. In the heart, metabolic inefficiency, fibrosis, and atrophy lead to reduced cardiac function, which can contribute to exercise intolerance and fatigability and may result in sudden cardiac death. Inflammatory-induced alterations in the gut microenvironment lead to a bloom of pathogenic *Enterobacteriaceae* (microbial dysbiosis), which increases gut permeability and leakage of bacteria endotoxins into the systemic circulatory system. In the liver, the acute-phase protein response contributes to systemic inflammation, while altered metabolic function and increased flux of substrates through futile cycles promotes a negative energy balance. In adipose tissue, wasting from increased lipolysis and thermogenic uncoupling has been found to precede muscle loss and likely contributes to the whole-body negative energy balance. In addition, secretion of adipokines may contribute to chronic inflammation during cachexia. The combination of these systemic effects promotes a catabolic state and reinforces inflammatory signaling, which can subsequently act directly and indirectly on muscle tissue to promote atrophy, impair regeneration, and induce metabolic dysfunction and oxidative stress. Loss of skeletal muscle mass and function then leads to the weakness, fatigue, and mortality associated with the cachexia syndrome.

1.2.2.1 Central Nervous System

The chronic inflammation associated with cachexia promotes altered neuronal and hormonal signaling in the central nervous system (CNS) (reviewed in (Grossberg et al., 2010) and (van Norren et al., 2017)). Peripheral inflammation triggers inflammation in the brain, specifically in the brain stem and hypothalamus (Laflamme and Rivest, 1999). Inflammatory signaling in these regions subsequently induces altered neuronal signaling that contributes to sickness behavior, anorexia, and altered metabolic rates (Grossberg et al., 2010). For example, inflammation promotes melanocortin signaling in the hypothalamic feeding centers, which supresses appetite and increases energy expenditure (Grossberg et al., 2010). Inhibition of melanocortin signaling, through pharmacological or genetic approaches, has been shown to prevent anorexia and muscle wasting in various mouse models of cachexia (Cheung et al., 2005; Marks et al., 2001; van Norren et al., 2017; Wisse et al., 2001). Altered neuronal signaling may also affect hormonal signaling in the CNS. Two key regulators of appetite and energy balance are ghrelin, produced mainly by the stomach, and leptin, produced mainly by adipose tissue (Klok et al., 2007). Ghrelin is known to promote appetite, while leptin supresses appetite (Klok et al., 2007). Interestingly, cachexia patients have low leptin levels and normal or high ghrelin levels, in keeping with their starvation-like state (Engineer and Garcia, 2012; Porporato, 2016; Takahashi et al., 2009; Wolf et al., 2006). However, cachexia is consistently associated with anorexia and catabolism, indicating a breakdown of a normal hormonal response. Ghrelin and leptin act on the same melanocortin neural pathways that are affected by inflammation (Klok et al., 2007). Therefore, it is likely that the inflammatory signaling in cachexia overrides the hormonal stimuli (Engineer and Garcia, 2012; Porporato, 2016). Finally, CNS inflammation, specifically the activity of IL-1β, leads to the activation of the hypothalamic-pituitary-adrenal (HPA) axis and the release of glucocorticoids, which can induce muscle atrophy, as detailed above (van Norren et al., 2017). Ultimately, the collective affects of these altered neuronal and hormonal signaling pathways in the brain promote a negative energy balance through reduced energy intake and increased energy expenditure, promoting a catabolic state that contributes to wasting.

1.2.2.2 Liver

One of the hallmarks of chronic inflammation is the activation of the acute phase protein response in the liver. Inflammatory cytokines induce secretion of positive acute phase proteins, such as C-reactive protein (CRP), and repress secretion of negative acute phase proteins, such as albumin, from hepatocytes (Jain et al., 2011). Acute phase proteins, in turn, contribute to the innate immune response through a variety of functions (Jain et al., 2011). Although no causative role of increased CRP levels has been established in cachexia, elevated CRP/albumin ratios are strongly correlated with weight loss and decreased survival in cancer patients (Engvall et al., 2008; Ozorio et al., 2017; Shibutani et al., 2016; Vazeille et al., 2017; Wallengren et al., 2013). As such, CRP and/or albumin levels are used as a diagnostic criterion for cachexia, serving as an indicator of the overall inflammatory status (Argiles et al., 2011; Fearon et al., 2011; Vigano et al., 2017; Zhou et al., 2018). In addition to acute phase response, altered metabolic function in the liver, induced by inflammation, may play a more causative role in cachexia. Inflammation in the liver has been associated with ER stress, decreased mitochondrial energy generation efficiency, and steatosis (lipid accumulation), which may all contribute to a negative energy balance (Berriel Diaz et al., 2008; Dumas et al., 2011; Jones et al., 2013; Julienne et al., 2014; Narsale et al., 2015; Peyta et al., 2015; Porporato, 2016). However, more work is needed to understand the molecular mechanisms of liver metabolic dysfunction and how it influences progression of cachexia.

The liver may also contribute to cachexia through its role in the recycling of amino acids, lipids, and lactate through gluconeogenic futile cycles (Argiles et al., 1997). For example, the Cori cycle, in which lactate produced from anaerobic glycolysis is converted back to glucose by hepatocytes, is a net negative energy pathway that has been shown to be elevated in cancer patients (Fig. 1.2)(Vaughan et al., 2013). In addition, alanine, glutamine, and glycerol derived from the breakdown of triacylglycerides can all be utilized in hepatic gluconeogenesis (Zhang et al., 2018a). Increased activity of these recycling pathways can contribute to the resting energy expenditure (REE) and overall negative energy balance during cachexia (Argiles et al., 1997). The negative energy balance may be further exacerbated by uncoupling and thermogenesis in adipose tissue and, potentially, skeletal muscle (discussed below; Fig. 1.2). In the case of cancer cachexia,

release of amino acids and lipids can be taken up by cancer cells, supporting tumor growth (Fig. 1.2) (Beloribi-Djefaflia et al., 2016; Lukey et al., 2017). Furthermore, gluconeogenic substrate recycling, particularly lactate produced from glycolytic tumors, helps support glucose-dependent anaerobic metabolism in cancer cells (Fig. 1.2). Indeed, the extent of anaerobic metabolism has been shown to influence the energetic demand of tumors, with more anaerobic cancer cells requiring significantly more energy (Friesen et al., 2015). In addition, anaerobic metabolism in cancer promotes the onset of cachexia and increase hepatic gluconeogenesis independently of secreted factors, indicating that the energetic demand of the tumor plays a role in the development of cachexia (Wang et al., 2018a). Therefore, in cancer cachexia, substrate recycling in the liver plays a critical role in both the onset of cachexia and tumor growth. Whether liver substrate cycling is also part of the development of cachexia in non-cancer contexts remains to be determined.

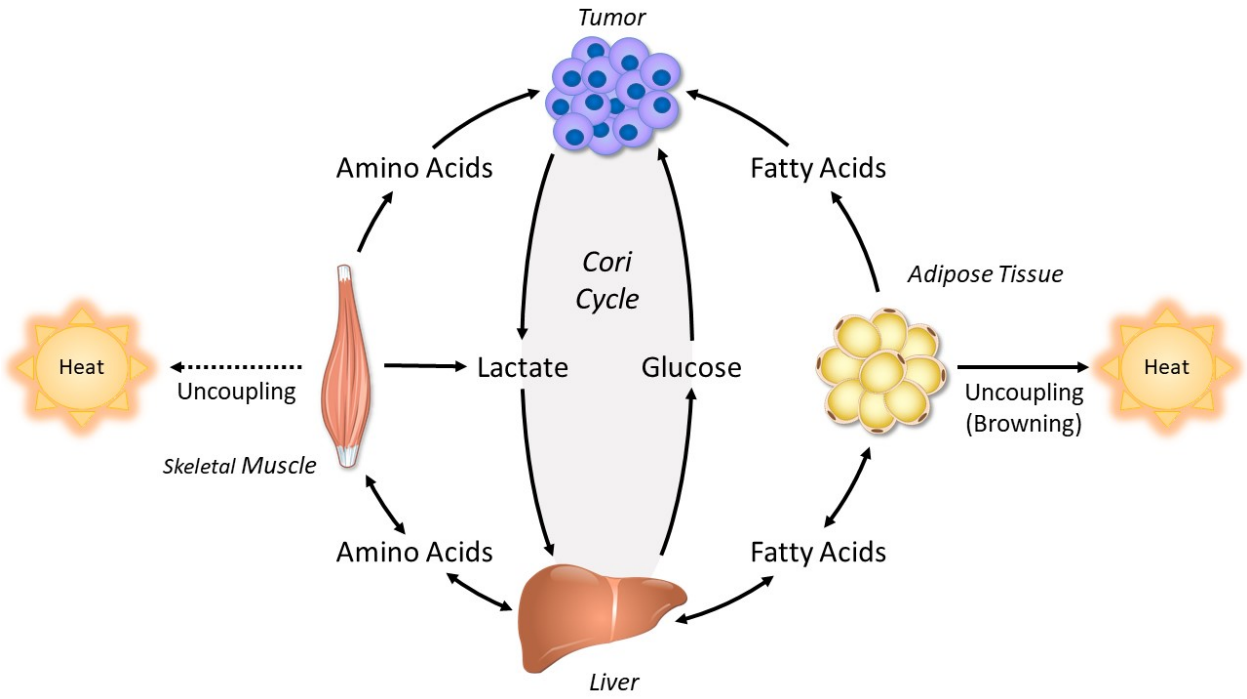

Figure 1.2: Energetic and Substrate Distribution during Cancer Cachexia.

In cancer cachexia, interplay between the growing tumor and metabolic tissues throughout the body leads to a negative energy and substrate balance in the host metabolism. Increased substrate cycling through futile cycles, such as the conversion of lactate to glucose in the Cori cycle (net loss of four ATP), contributes to energetic inefficiency. Mitochondrial uncoupling (browning) in white adipose tissue leads to the loss of energy through heat dissipation. Uncoupling may also be present in skeletal muscle, though experimental evidence for this is conflicting (dashed arrow). Release of amino acids, such as glutamate and alanine, and free fatty acids from muscle and adipose tissue, respectively, during wasting are cycled through the circulatory system. These macromolecular substrates can be consumed by the liver for gluconeogenesis or utilized by tumor cells to support their proliferation and growth. As a result, the expansion of cancer cells acts as a nutrient sink, drawing substrates from the peripheral tissue. The combination of these effects is an overall catabolic state in the host, where the body's resources are utilized inefficiently and diverted to support an anabolic state in the tumor.

1.2.2.3 Heart

Altered cardiac function is a predominant feature of many of the conditions associated with cachexia, namely chronic heart failure and COPD (de Miguel Diez et al., 2013; von Haehling et al., 2007). However, cardiac dysfunction has also been identified in cancer and septic cachexia (Callahan and Supinski, 2009; Murphy, 2016). Cardiac atrophy, fibrosis, myocardium structural impairment, and altered metabolic function have all been identified in various models of cachexia (Reviewed in (Belloum et al., 2017)). Loss of cardiac structural integrity leads to loss of function and a reduction in aortic pressure and ejection fraction, similar to what is seen in classical heart failure (Tian et al., 2010; Zimmers et al., 2017). In addition, altered mitochondrial morphology and accumulation of triacylglycerides (a marker of reduced beta-oxidation) in cachectic cardiac tissue indicate impaired mitochondrial function (Belloum et al., 2017; Muhlfeld et al., 2011; Tian et al., 2010). Mitochondrial beta-oxidation of fatty acids is the primary source of energy generation in healthy cardiomyocytes, which have a high energy need due to the demanding nature of maintaining the heartbeat rhythm, and so impaired mitochondrial energy generation may also contribute to reduced cardiac function during cachexia (Lionetti et al., 2011). Cardiac dysfunction can subsequently contribute to the reduced exercise tolerance and quality of life observed in cachectic patients. Furthermore, sudden cardiac death due to arrhythmia may be one of the primary mechanisms of cachexia-induced mortality (Kalantar-Zadeh et al., 2013). Thus, understanding the role of cardiac wasting and dysfunction in the development of cachexia, as well as the underlying mechanisms of induction, is a critical area of future research.

1.2.2.4 Adipose Tissue

After muscle wasting, adipose tissue wasting is likely the second most recognizable phenotype of cachexia. White adipose tissue (WAT) is a primary site of energy storage, containing the majority of the body's lipid stores (Dalal, 2019). Inflammatory cytokines (especially TNFα and IL-6), as well as PTH signaling and β-adrenergic signaling, have been shown to promote lipolysis and thermogenic uncoupling ("browning") in WAT (Dalal, 2019). Lipolysis during cachexia is mediated by the activity of hormone-sensitive lipase (HSL) and adipose triglyceride lipase (ATGL) (Agustsson et al., 2007; Das et al., 2011). Free-fatty acids (FFA) released from lipolysis are at least partially secreted, as demonstrated by the fact that cachectic adipocytes secrete FFA at a

significantly higher rate (Tsoli et al., 2014). In addition, cachexia is consistently associated with increased circulatory levels of FFAs (Agustsson et al., 2012; Dahlman et al., 2010; Han et al., 2018; Tsoli et al., 2014). Increased circulating FFAs may then contribute to increased lipid accumulation in cachectic liver and heart, and are taken up by cancer cells during cancer cachexia (Fig. 1.2) (Berriel Diaz et al., 2008; Muhlfeld et al., 2011; Mulligan et al., 1992). Released fatty acids may also be utilized intracellularly during "browning". Cachectic WAT has been shown to have increased expression of genes associated with brown adipose tissue (BAT) (Kir et al., 2014; Petruzzelli et al., 2014; Rohm et al., 2016). In BAT and browning WAT ("beige"), expression of uncoupling protein 1 (UCP1) in the mitochondria uncouples fatty acid oxidation from ATP generation, resulting in the release of heat (Dalal, 2019). This thermogenic process plays a critical role in temperature regulation, but in cachexia may contribute to a negative energy balance (Fig. 1.2) (Dalal, 2019). The combination of increased lipolysis, fatty acid secretion, and thermogenic uncoupling ultimately leads to the loss of adipose tissue in cachexia.

Intriguingly, while fat and muscle loss can be triggered independently by inflammatory cytokines, there appears to be significant crosstalk between fat tissue and skeletal muscle during cachexia (Baracos et al., 2018). In numerous mouse models, adipose tissue wasting has been shown to precede the loss of skeletal muscle (Kir et al., 2016; Kir et al., 2014; Petruzzelli et al., 2014; Rohm et al., 2016). Furthermore, several studies have shown that interventions that specifically prevent adipose tissue wasting can indirectly prevent muscle wasting, suggesting that the mechanisms of adipose tissue loss contribute to muscular atrophy in cachexia (Das et al., 2011; Kir et al., 2016; Rohm et al., 2016). However, skeletal muscle atrophy can occur in cachexia in the absence of fat loss, indicating that these mechanisms may be heterogenous in the cachexia patient population (Baracos et al., 2019; Choi et al., 2015). The mechanism of crosstalk is, at present, unclear. Increased energy expenditure due to increased lipolysis and browning may contribute to a holistic negative energy balance that leads to muscle wasting. In addition, endocrine signaling between fat tissue and muscle due to the release of adipokines and myokines may be involved (Argiles et al., 2018). Given the clear evidence of crosstalk between fat tissue and skeletal muscle, fat wasting should not be considered just a secondary effect of cachexia, but a critical component of its progression.

1.2.2.5 Gut

In recent years, investigations on the role of gut microbiota in chronic disease have become an area of growing interest. While only a handful of studies have been performed investigating the role of gut function in cachexia, the evidence suggests that altered gut homeostasis contributes significantly to its pathogenesis. In the $APC^{Min/+}$ and C26 mouse models of cancer cachexia, gut permeability has been found to increase in an IL-6-dependent manner (Bindels et al., 2018; Puppa et al., 2011). Subsequently, elevated levels of endotoxins and LPS binding protein (LBP) were detected in the plasma of cachectic mice and in human cachectic patients, indicating that gut permeability can contribute to systemic inflammation during cachexia (Bindels et al., 2018; Puppa et al., 2011). Increased gut permeability was accompanied by altered microbiota composition (microbial dysbiosis). Cachexia in mouse models has been associated with a decrease in *Lactobacillus* spp., *Ruminococcaceae*, and *Lachnospiraceae and an increase in Enterobacteriaceae* (Bindels et al., 2016; Bindels et al., 2018; Potgens et al., 2018). Interestingly, probiotic administration of *Lactobacilli* or prebiotic treatment of nondigestible carbohydrates reverse gut dysfunction and cachexia symptoms in murine cancer models (Bindels et al., 2012; Bindels et al., 2016; Bindels et al., 2015). In contrast, administration of the *Enterobacteriaceae* strain *Klebsiella oxytoca* promoted gut dysfunction and muscle atrophy, highlighting the importance of microbiota composition in cachexia (Potgens et al., 2018). The causative mechanisms of altered gut flora have yet to be conclusively demonstrated. However, it has been proposed that changes in epithelial cell metabolism and a depletion of regulator T cells alters the gut microenvironment, promoting the expansion of pro-cachectic *Enterobacteriaceae*, which are known to promote gut permeability (Palmela et al., 2018). Further work is needed to validate the underlying causes of microbial dysbiosis in cachexia and to determine if similar mechanisms of gut dysfunction occur in other types of cachexia, such as during COPD and CHF.

1.2.3 Inflammatory Signal Transduction Pathways in Skeletal Muscle During Cachexia

Lean body mass loss is the primary feature of cachexia, and the mechanisms that underly cachectic muscle wasting are complex and multimodal. As detailed above, the impact of chronic inflammation on whole body homeostasis creates a highly catabolic environment that promotes muscle atrophy. In addition to these systemic effects, muscle tissue responds directly to

inflammatory signaling, leading to a variety of biochemical changes that promote atrophy. Inflammatory pro-cachectic cytokines can act in concert, sometimes synergistically, to induce atrophy and dysfunction in skeletal muscle. As such, several convergent pathways have been identified as critical components in the induction of inflammatory signaling in skeletal muscle during cachexia.

1.2.3.1 NF-κB

The nuclear factor κ-light-chain-enhancer of activated B cells (NF-κB) family of transcription factors are master regulators of the induction of inflammatory gene expression in response to numerous inflammatory cytokines, such as TNFα, IL-1, and IL-6 (Liu et al., 2017). The family is composed of five members, p50/p105 (NF-κB1), p52/p100 (NF-κB2), p65 (RELA), c-REL and RELB (Li and Verma, 2002). NF-κB can be activated by both a canonical and an alternative pathway (Li et al., 2008). In the canonical pathway, convergent signaling from numerous inflammatory stimuli lead to the activation of inhibitor of κB kinase-β (IKKβ), which in turn phosphorylates the inhibitor of κB-α (IκBα) (Li et al., 2008). IκBα binding to NF-κB sequesters it in the cytoplasm and prevents transcriptional activation. Upon phosphorylation, IκBα is degraded by the 26S-proteasome, releasing NF-κB and allowing nuclear translocation (Li et al., 2008). In the alternative pathway, phosphorylation of the p100 precursor protein by IKKα leads to ubiquitin-mediated processing to form the p52 subunit, which heterodimerizes with RelB and translocates to the nucleus (Li et al., 2008). In muscle, both mechanisms of activation have been found to induce atrophy (Li et al., 2008).

NF-κB is a critical component of cachexia signaling in skeletal muscle. Muscle-specific expression of a phospho-mutant IκBα super-repressor, which constitutively inhibits NF-κB activation, has been shown to prevent atrophy and inhibit inflammatory signaling in both mouse and cellular models of cachexia (Cai et al., 2004; Di Marco et al., 2005; Guttridge et al., 2000; He et al., 2013; Ma et al., 2017). The role of NF-κB in atrophy is often ascribed to the elevated expression of the muscle-specific E3-ligase muscle RING-finger protein-1 (MuRF1), which plays a critical role in protein degradation during muscle atrophy (Cai et al., 2004). However, reduced regenerative potential and expression of pro-myogenic genes have also been associated with NF-κB activity during cachexia (Di Marco et al., 2005; Guttridge et al., 2000; He et al., 2013).

Furthermore, NF-κB has been shown to induce the expression of inducible nitric oxide synthase (iNOS) in cachectic muscle, which produces high levels of reactive nitrogen species and induces oxidative stress (Di Marco et al., 2012; Di Marco et al., 2005; Ma et al., 2017). Finally, a specific inhibitor of NF-κB was found to partially reverse altered metabolism in the muscle of C26-bearing mice, suggesting that NF-κB also contributes to metabolic dysfunction during cachexia (Der-Torossian et al., 2013). Thus, while the induction of proteasomal protein degradation is a well-established mechanism of NF-κB-mediated atrophy, inhibition of regenerative potential, induction of oxidative stress, and impairment of metabolic function can also be attributed to NF-κB activity.

1.2.3.2 STAT3

Signal Transducers and Activators of Transcription-3 (STAT3) is a member of the STAT family of transcription factors that mediate signal induction in a variety of cells in response to cytokines and growth factors (Mali, 2015). In unstimulated conditions, STAT3 localization is predominantly cytoplasmic, but it is known to shuttle continuously between the nucleus and the cytoplasm (Reich, 2013). Phosphorylation of STAT3 in the SH2 domain leads to homo- and heterodimerization of STAT3 and its accumulation in the nucleus, where it promotes the expression of inflammatory response genes (Delgoffe and Vignali, 2013; Huynh et al., 2019). Phosphorylation of STAT3 is mediated primarily by Janus-kinases (JAK), but it can also be activated by Src family kinases and MAPK/ERK signaling (Mali, 2015). In addition, heterodimerization with NF-κB has been shown to lead to the accumulation of STAT3 in the nucleus in a phosphorylation-independent manner (Kim and Yoon, 2016; Ma et al., 2017). Cachexia-associated STAT3 activity has largely been linked to IL-6 signaling (Bonetto et al., 2012; Bonetto et al., 2011). However, STAT3 responds to numerous cytokines and inflammatory signals and has been shown to be activated by TNFα and IFNγ in an IL-6-independent, NF-κB-dependent manner during cachexia, highlighting its importance as an integrator of cytokine signaling (Ma et al., 2017).

The mechanism by which STAT3 induces muscle atrophy in cachexia is an area of active research. The causative role of STAT3 in cachexia was first demonstrated by Bonetto *et al.*, who showed that chemical or genetic inhibition of STAT3 could prevent cachexia in a variety of

models, and that muscle-specific, constitutively active STAT3 overexpression could spontaneously induce muscle atrophy (Bonetto et al., 2012). Subsequently, several causative mechanisms have been proposed for STAT3-mediated muscle wasting. STAT3 has been shown to promote protein degradation by inducing the transcription of the muscle-specific E3-ligases atrogin-1/MAFbx and MuRF1, as well as caspase-3 (a promotor of proteasomal activity) (Silva et al., 2015). In addition, STAT3 has been shown to promote myostatin expression through upregulation of the C/EBPδ transcription factor (Silva et al., 2015; Zhang et al., 2013). Collaboration between STAT3 and NF-κB has also been shown to be required for the expression of iNOS, an inducer of nitrosative stress (Ma et al., 2017). Interestingly, STAT3 has been shown to localize to the mitochondria and regulate oxidative phosphorylation, as well as promote expression of glycolytic genes in the nucleus (Huynh et al., 2019). However, the role of mitochondrial-STAT3 and STAT3 metabolic regulation in cachexia has yet to be explored.

1.2.3.3 FOXO

Members of the Forkhead box protein (FOXO) family of transcription factors, specifically FOXO1 and FOXO3, play a critical role in the activation of protein degradation pathways in cachexia. Indeed, FOXOs induce the expression of proteins involved in ubiquitin-mediated proteasomal degradation (e.g. MuRF1 and atrogin-1/MAFbx), as well as autophagy (e.g. LC3, Bnip3, PINK) (Reviewed in (Sandri, 2016)). FOXO activity can be regulated by several extracellular and intracellular signaling pathways. The activity of FOXO in the nucleus is inhibited by phosphorylation by AKT (Manning and Cantley, 2007). AKT activity, in turn, is stimulated by anabolic signaling from IGF-1/PI3K and a positive feedback loop involving mTOR activity (Schiaffino and Mammucari, 2011). In contrast, the AKT pathway is inhibited by inflammatory cytokine signaling, such as TNFα and TGFβ (myostatin), leading to FOXO activation (Schiaffino and Mammucari, 2011). In addition, FOXO can be activated directly by intracellular stress signaling from oxidative stress and energetic stress via AMP-sensitive kinase (AMPK) (Schiaffino and Mammucari, 2011). Interestingly, FOXO proteins have been shown to reduce the expression of mitochondrial genes and impact other metabolic pathways, such as glycolysis in other cell types (Ferber et al., 2012; Gross et al., 2008; Ma et al., 2018). As such, FOXO signaling may play a role in integrating atrophic and metabolic signaling during cachexia.

1.2.3.4 Smads

The Smad family of transcription factors are key mediators of TGF-β signal transduction (Moustakas et al., 2001). Receptor activated Smads (R-Smad; 1,2,3,5, and 8) are activated downstream of activin receptor-like kinases (ALKs), and subsequently form oligomeric complexes with co-Smad4 (Moustakas et al., 2001). In contrast, inhibitory Smads (I-Smad; 6 and 7) compete with R-Smads for binding to activated receptors and target them for degradation (Moustakas et al., 2001). The importance of Smad signaling in cachexia is highlighted by the fact that inhibiting R-Smad2/3 can induce hypertrophy and block atrophy (Chen et al., 2017; Sartori et al., 2009). In addition, viral gene therapy inducing overexpression of I-Smad7 in muscle has been shown to block muscle atrophy in a mouse model of cachexia, independently of its effects on tumor growth and systemic inflammation (Winbanks et al., 2016). R-Smad2/3 activation is believed to promote atrophy by supressing AKT activity, leading to reduced mTORC1 signaling and protein synthesis (Goodman et al., 2013; Sartori et al., 2009; Trendelenburg et al., 2009). R-Smad3 also binds to the Atrogin-1, but not the MuRF-1 promoter, indicating that Smad may also promote protein degradation (Goodman et al., 2013; Sartori et al., 2009). However, it is not presently clear if Smad signaling promotes Atrogin-1 expression directly or through AKT/FOXO signaling (Goodman et al., 2013). Also, Atrogin-1 expression is not consistently upregulated by Smad2/3 signaling, making the importance of protein degradation in Smad-mediated atrophy uncertain (Trendelenburg et al., 2009). Interestingly, Smad3 has been shown to decrease peroxisome proliferator-activated receptor-gamma coactivator 1-α (Pgc1-α; a critical regulator of oxidative metabolism) promoter activity and expression and impair metabolic responses to exercise (Bohm et al., 2016; Goodman et al., 2013; Tiano et al., 2015). Thus, in combination with it's known effects on Akt/mTORC signaling and protein synthesis, impairment of metabolic function may also play a role in Smad-induced atrophy, though more studies are needed to establish if this is the case.

1.2.4 Mechanisms of Muscle Atrophy

Classically, the balance of protein turnover and protein synthesis in skeletal muscle has been considered the main driving mechanism of atrophy in cachexia. Direct cytokine signaling in

muscle promotes proteasomal protein degradation, as well as autophagy (Sandri, 2016). In addition, protein synthesis is often supressed in cachexia, leading to an overall negative protein balance (Tisdale, 2009). Recent evidence suggests that cachectic muscle may also have a reduced regenerative potential due to diminished muscle differentiation (myogenesis) capacity in adult muscle stem cells (satellite cells) (He et al., 2013). Ultimately, the negative protein balance from increased degradation and decreased synthesis and the reduced regenerative potential leads to the loss of skeletal muscle mass at the molecular and physiological levels.

1.2.4.1 Increased Protein Degradation

The ubiquitin-proteasome pathway (UPP) allows for the targeted turnover of select proteins within the cell (Lecker et al., 2006). Specificity is mediated by poly-ubiquitination of target proteins through the coordinated actions of E1, E2, and E3 enzymes (Lecker et al., 2006). E1 serves to activate ubiquitin, which is subsequently transferred to an E2 carrier protein (Lecker et al., 2006). E3 ligases, which contain ubiquitin transfer and substrate recognition domains, then coordinate the transfer of ubiquitin onto lysine residues of target proteins (Lecker et al., 2006). Subsequent reactions transfer additional ubiquitin units to lysine residues within ubiquitin, creating a poly-ubiquitin chain that is recognized by the 26S proteasome complex (Lecker et al., 2006). The 26S proteasome then degrades the protein into small peptides that are further degraded by the activity of cytosolic peptidases (Lecker et al., 2006). In cachexia, increased activity of the UPP has long been associated with the progression of muscle atrophy (Tisdale, 1999). Specifically, upregulation of the muscle-specific E3 ligases MuRF1 and atrogin-1/MAFbx, as well as the more recently identified TRAF6 and MUSA1, are believed to drive the degradation of myofibrillar and myogenic proteins required for the maintenance of skeletal muscle (Sandri, 2016). In addition, non-degradatory ubiquitin signaling may also be involved in crosstalk between the UPP and autophagy, as well as metabolic function (Sandri, 2016).

Macroautophagy is a conserved mechanism by which cells degrade and recycle intracellular components (Parzych and Klionsky, 2014). Two other forms of autophagy, microautophagy and chaperone-mediated autophagy, allow for more targeted degradation, but their role in cachexia is unknown (Parzych and Klionsky, 2014; Sandri, 2016). In macroautophagy, cellular components are engulfed by a lipid bilayer membrane, forming an autophagosome (Parzych and Klionsky,

2014). Merger of autophagosomes with lysosomes, which contain hydrolytic enzymes in a low pH environment, results in the degradation and subsequent release of the contents of the autophagosome (Parzych and Klionsky, 2014). Increased macroautophagy has been detected in several murine cachexia models and in the muscle of human cachexia patients (Chacon-Cabrera et al., 2014; Johns et al., 2014; Penna et al., 2013; Pigna et al., 2016; Puig-Vilanova et al., 2015; Stephens et al., 2015; Tardif et al., 2013). However, it is unclear if upregulated macroautophagy plays a detrimental or protective role in cachexia. In fact, macroautophagy in muscle is critical for the turnover of damaged cellular components, particularly mitochondria (mitophagy), and loss of autophagic function can promote atrophy (Carnio et al., 2014; Drake and Yan, 2017). In keeping with this, treatments that promote macroautophagy and exercise, which is known to upregulate autophagy, have all been shown to reduce atrophy during cachexia (Grumati et al., 2011; Pigna et al., 2016; Puppa et al., 2012). The evidence suggests, then, that autophagic turnover may be a protective mechanism during cachexia, but more work is needed to conclusively establish this.

1.2.4.2 Supressed Protein Synthesis

Protein synthesis is a highly regulated process that dynamically responds to numerous extra- and intracellular signaling pathways. Most notably for cachexia, the rate of protein synthesis can be modulated by nutrient availability, hormonal and inflammatory signaling, exercise, and oxidative stress (Atherton and Smith, 2012; Heberle et al., 2015; Mercier et al., 2002; Velloso, 2008). Regulation of protein synthesis is incredibly complex, occurring at multiple stages of initiation, elongation, and ribosomal release (Hershey et al., 2012). In addition, synthesis of specific mRNA can be modulated by a variety of regulatory factors, such as RNA-binding proteins and miRNA (Ma et al., 2012; van de Worp et al., 2018; von Roretz et al., 2011). While a decrease in general protein translation has been detected in several cachectic models and cohorts of human cachexia patients, the mechanisms underlying inhibition of translation during cachexia are still only partially understood (Brown et al., 2018; Eley and Tisdale, 2007; Emery et al., 1984b; Rennie et al., 1983; White et al., 2011b).

The most widely studied anabolic pathway in cachexia is the AKT/mTOR/GSK3β pathway. In response to growth factors, such as IGF-1, AKT activation leads to the phosphorylation and activation of mTOR and inhibition of glycogen synthase kinase 3β (GSK3β) (Schiaffino and

Mammucari, 2011). GSK3β phosphorylates eukaryotic initiation factor 2B (eIF2B), inhibiting recruitment of the initiation methionine tRNA to the translation initiation complex (Kimball, 1999; Schiaffino and Mammucari, 2011). mTOR is a critical regulator of protein translation, with numerous downstream targets, notably ribosomal protein S6 kinase (S6K) and 4E binding proteins (4EBPs) (Heberle et al., 2015). Decreased phosphorylation of AKT, GSK3β, mTOR, and mTOR downstream targets have all been demonstrated in cachexia (Quan-Jun et al., 2017; Schmitt et al., 2007; White et al., 2011b). The mechanisms of reduced AKT/mTOR signaling are still being explored. As discussed above, SMAD activity and reduced IGF-1 may contribute to suppression of AKT activity (Goodman et al., 2013; Sartori et al., 2009; Schiaffino and Mammucari, 2011; Trendelenburg et al., 2009). In addition, the energy-sensitive kinase AMPK has been identified as a negative regulator of mTOR signaling during cachexia (White et al., 2013). However, despite numerous studies showing supressed AKT/mTOR signaling, several studies have found that mTOR signaling was unaffected or even increased during cachexia (MacDonald et al., 2015; Penna et al., 2010). In one recent study, the general protein synthesis rate was found to be decreased during the progression of cachexia, despite minimal changes in AKT, S6K, and 4EBP phosphorylation (Brown et al., 2018). This suggests that other mechanisms of protein translation inhibition may be activated during cachexia. Furthermore, anabolic stimuli, such as feeding or exercise, can have significant and temporal impacts on protein synthesis signaling, which may complicate interpretation of results. While cachexia is associated with a reduced sensitivity to these stimuli (anabolic resistance), an anabolic response is still present in the early stages of cachexia (Antoun and Raynard, 2018). Thus, more work is needed to clarify these discrepancies and to decipher the role of anabolic signaling and anabolic resistance in cachectic muscle atrophy.

1.2.4.3 Regeneration Deficit

In addition to intracellular protein turnover rates, muscle mass is also influenced by the growth and differentiation of adult muscle stem cells (Blaauw and Reggiani, 2014). In adult muscle tissue, resident stem cells known as satellite cells are spaced along the length of mature myofibers (Le Grand and Rudnicki, 2007). In response to stimuli, such as injury, exercise, or growth factors, these stem cells expand to form a pool of committed mononuclear cells known as myoblasts

(Blaauw and Reggiani, 2014; Le Grand and Rudnicki, 2007). Myoblasts further expand, and eventually fuse with each other or into existing myofibers, regenerating damaged muscle or inducing hypertrophy (Blaauw and Reggiani, 2014; Le Grand and Rudnicki, 2007). Reduced regenerative capacity in aging and genetic myopathies has been linked with progressive atrophy (Boyden et al., 2012; Joanisse et al., 2017; Kudryashova et al., 2012; Lagalice et al., 2018; Schaaf et al., 2018). For example, in Duchenne's muscular dystrophy, impaired satellite cell function has been identified as a contributing factor to muscle wasting (Chang et al., 2016). Only a handful of studies have investigated regenerative defects in cachexia but results from these studies strongly suggest that cachectic muscle has a significant regenerative deficit.

Myogenesis is controlled by the coordinated regulation of several pro-myogenic transcription factors. In brief, expression of Paired box 7 (Pax7) is necessary for the establishment and maintenance of the satellite stem cell pool (Olguin and Pisconti, 2012). Upon commitment to differentiation, satellite cells begin expressing the early stage transcription factors myogenic factor 5 (Myf5) and MyoD and eventually downregulate Pax7 (Olguin and Pisconti, 2012). In the later stages of differentiation, Myf5 and MyoD expression is reduced as myogenin, a late stage transcription factor, is expressed (Olguin and Pisconti, 2012). Several studies have reported a decrease in the expression of both MyoD and myogenin in mature muscle cells and muscle tissue in models of cachexia (Acharyya et al., 2004; Brown et al., 2018; Costelli et al., 2005; Di Marco et al., 2012; Di Marco et al., 2005; He et al., 2013). This down regulation has been shown to be dependent on NF-kB and the activity of iNOS, although the causative mechanisms of decreased expression are not fully understood (Acharyya et al., 2004; Di Marco et al., 2005). In a comprehensive assessment of myogenic potential in cachexia, He *et al.* showed that cachectic muscle is associated with a severe regenerative deficit in response to injury (He et al., 2013). The loss of regenerative potential was discovered to be the result of precocious activation of both satellite and non-satellite stem cells due to increased Pax7 expression (He et al., 2013). Downregulation of Pax7 is required for commitment to differentiation, and so persistence of Pax7 impairs the expression of MyoD and myogenin and the progression of myogenesis (He et al., 2013). Importantly, reduction of Pax7 expression or ectopic overexpression of Pax7 were found to prevent or promote atrophy, respectively, demonstrating that the regenerative defect impacts

muscle mass in cachexia (He et al., 2013). Pax7 overexpression, reduced myogenic potential, and impaired regeneration were subsequently confirmed in another study of murine cancer cachexia (Marchildon et al., 2015).

Collectively, the evidence shows that in cachexia, regenerative potential is reduced due to dysregulation of the myogenic regulatory program. However, the mechanisms driving this dysfunction require further investigation. In these studies, increased Pax7 expression depended on the NF-κB and CCAAT/enhancer-binding protein β (C/EBPβ) transcription factors (He et al., 2013; Marchildon et al., 2015). C/EBPβ regulates Pax7 transcription directly, but this has not been demonstrated for NF-κB, so it is not known if NF-κB acts on Pax7 directly or indirectly (Marchildon et al., 2012). Furthermore, the mRNA of Pax7 was recently found to be decreased in cachectic muscle, despite the increase in Pax7 protein previously reported (Brown et al., 2018). This suggests that Pax7 regulation in cachexia may be more complex than just transcriptional upregulation. More work is needed to understand the molecular mechanisms of myogenic dysregulation in cachexia. In addition, the potential of regenerative therapy for the treatment of cachexia needs to be explored.

1.2.5 Metabolic Dysfunction in Cachexia

Muscle atrophy and a negative protein balance in skeletal muscle has been the primary focus of a significant portion of cachexia research. However, growing evidence indicates that, like in many of the other organs affected by chronic inflammation, there is significant metabolic dysfunction in skeletal muscle during cachexia (Argiles et al., 2015a). Due to the energy-demanding nature of contraction, skeletal muscle is particularly sensitive to aberrations in metabolic function. This is highlighted by the fact that mitochondrial defects often result in myopathy (Pfeffer and Chinnery, 2013; Smeitink et al., 2001). In cachexia, metabolic abnormalities have been observed to precede atrophy, suggesting that skeletal muscle mass loss may be a secondary symptom following loss of metabolic function (Brown et al., 2017; Fukawa et al., 2016; Op den Kamp et al., 2012). Therefore, understanding the nature of metabolic dysfunction, as well as the underlying molecular mechanisms, is critical to the development of effective therapies against cachexia.

1.2.5.1 Altered Metabolic Profiles in Cachexia

Metabolomic profiling is a powerful technique that allows for the simultaneous assessment of numerous metabolites and metabolic pathways. Several studies have performed metabolomic-based analysis on cachectic muscle, identifying common metabolic perturbations associated with cachexia (Cui et al., 2019a; Cui et al., 2019b; Der-Torossian et al., 2013; Lautaoja et al., 2019; Pin et al., 2019a; Tseng et al., 2015). One pathway that is commonly identified as altered during cachexia is glycolysis. In glycolysis, glucose is broken down into pyruvate, which can be converted to acetyl-CoA by pyruvate dehydrogenase (PDH) in the matrix of the mitochondria or converted to lactate by lactate dehydrogenase (LDH) in the cytoplasm (Fig. 3) (Saunier et al., 2016; Valvona et al., 2016). Acetyl-CoA can subsequently enter the tricarboxylic acid (TCA) cycle, where reducing equivalents (NADH, $FADH_2$) can be generated to drive the activity of the electron transport chain (ETC) and the production of ATP through oxidative phosphorylation (OXPHOS) (Bowtell et al., 2007). When fermented to lactate (anaerobic), glucose breakdown generates a net two ATP (Mookerjee et al., 2017). In contrast, complete oxidation of glucose through OXPHOS (aerobic) leads to a net production of approximately 31-32 ATP (Mookerjee et al., 2017). While less efficient than aerobic metabolism, anaerobic glycolysis is believed to generate ATP at a faster rate, supplying energy rapidly during muscle contraction (Baker et al., 2010). Several studies of cachectic muscle have identified signs of elevated glycolysis, namely depletion of intracellular glucose and glycogen content (Cui et al., 2019a; Cui et al., 2019b; Der-Torossian et al., 2013; Lautaoja et al., 2019; Tseng et al., 2015). Levels of other glycolytic intermediates vary between studies. For example, intramuscular lactate has been shown to remain unchanged (Der-Torossian et al., 2013; Pin et al., 2019a) or decrease (Cui et al., 2019a; Cui et al., 2019b). However, without metabolite tracing, it is difficult to assess the true rate of lactate production, as it is also affected by the secretion and clearance rates. Indeed, several studies have shown increased serum lactate levels, but this may also be associated with increased glycolytic activity in the tumor (Cui et al., 2019a; Cui et al., 2019b; Lautaoja et al., 2019).

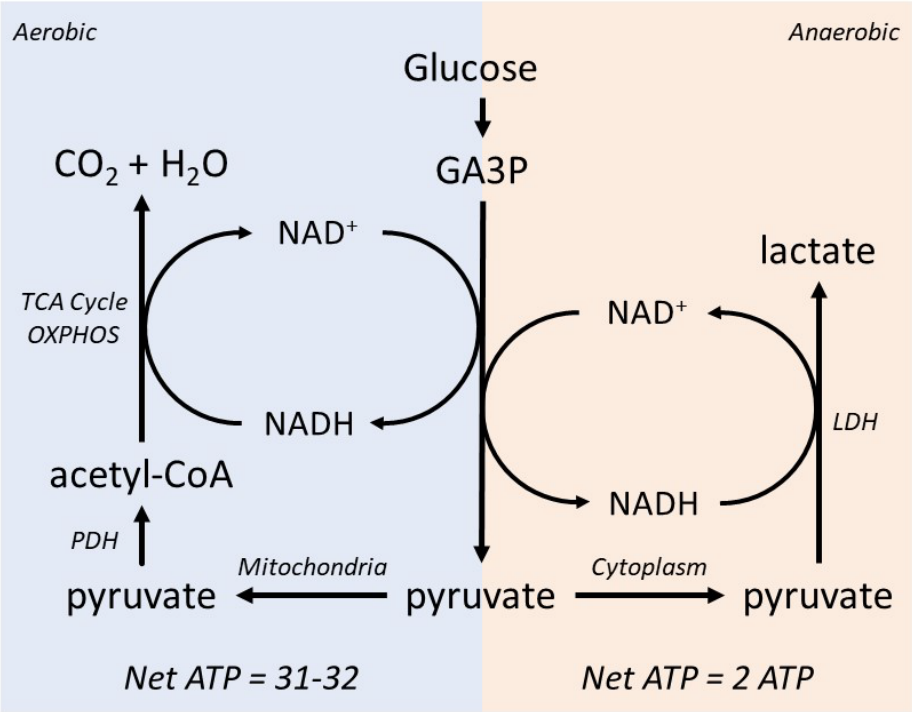

Figure 1.3: Glucose catabolism in skeletal muscle.

Breakdown of glucose for energy can be performed either aerobically or anaerobically. In glycolysis, glucose is broken down into pyruvate through a series of enzymatic reactions. Transport of pyruvate to the mitochondrial matrix and conversion to acetyl-CoA by pyruvate dehydrogenase (PDH) feeds into the Tricarboxylic Acid (TCA) cycle and aerobic oxidative phosphorylation (OXPHOS). Alternatively, pyruvate can be converted to lactate anaerobically by lactate dehydrogenase (LDH) in the cytoplasm. Fermentation to lactate regenerates the NAD^+ needed for glycolysis. If pyruvate is utilized aerobically, the NADH produced from glycolysis can be shuttled to the mitochondria and used in OXPHOS. Aerobic metabolism produces approximately net 31-32 ATP per glucose, whereas anaerobic metabolism produces net 2 ATP per glucose.

Another major pathway found to be affected in cachexia is the TCA cycle. As mentioned above, pyruvate from glycolysis can feed into the TCA cycle after conversion to acetyl-CoA (Saunier et al., 2016). Acetyl-CoA can also be generated from the breakdown of fatty acids (Houten et al., 2016). Citrate synthase, the first enzyme in the TCA cycle, converts acetyl-CoA and oxaloacetate to citrate (Bowtell et al., 2007). Subsequent reactions lead to the regeneration of oxaloacetate and the generation of the reducing equivalents required for OXPHOS (Bowtell et al., 2007). In cachexia, TCA cycle intermediates have been found to be reduced (Cui et al., 2019a; Der-Torossian et al., 2013; Pin et al., 2019a). This reduction is likely mediated, at least in part, by reduced flux of pyruvate from glycolysis into the TCA cycle due to decreased PDH activity (Pin et al., 2019a). PDH is negatively regulated by pyruvate dehydrogenase kinase 4 (PDK4), which inactivates PDH through phosphorylation of the E1α subunit (Gray et al., 2014). PDK4 expression is upregulated in muscle in cancer and sepsis models of cachexia (Asp et al., 2011; Constantinou et al., 2011; Kliewer et al., 2015; Pin et al., 2019b; Tzika et al., 2013). Furthermore, inhibition of PDK4 in myotubes treated with cancer-conditioned media has been shown to reduce atrophy, whereas overexpression of PDK4 spontaneously induces atrophy, demonstrating the causative role of altered pyruvate utilization in muscle wasting (Pin et al., 2019b). The mechanisms of increased PDK4 expression have not been demonstrated in cachexia. However, PDK4 is known to be transcriptionally regulated by several factors associated with cachexia, such as FOXO, the glucocorticoid receptor, and C/EBPβ (Jeong et al., 2012).

When TCA cycle intermediates are depleted from reduced carbohydrate flux or high energetic demand, free amino acids can be consumed in anaplerotic reactions to replenish them (Owen et al., 2002; Shimomura et al., 2004). Given the high rate of protein degradation and suppression of protein synthesis in cachexia, there is potentially an elevated pool of free amino acids to utilize. However, during muscle breakdown amino acids are also funneled through transamination reactions to form glutamine and alanine, which are subsequently secreted into the circulatory system (Owen et al., 2002). Several anaplerotic amino acids, such as glutamine, glutamate, and branch-chain amino acids (BCAAs), are altered in cachectic muscle, though there is inconsistency in the directionality, with some studies showing increases (Cui et al., 2019a; Cui et al., 2019b; Tseng et al., 2015) and others showing decreases in amino acid levels (Der-Torossian et al., 2013;

Pin et al., 2019a). It is difficult to ascertain from steady-state levels if these alterations are resulting from increased protein breakdown, increased anaplerotic demand, or amino acid secretion. Interestingly, ^{13}C tracing of glutamine in muscle of cancer-bearing mice found that muscle glutamine was utilized for the formation of TCA cycle intermediates and secreted (Luo et al., 2014). This suggests that amino acids from protein breakdown can still be utilized in anaplerotic reactions to replenish diminished TCA cycle intermediates despite also being secreted.

Discrepancies between studies of metabolomics in cachexia have likely arisen due to a variety of variables, such as different sample preparation and processing procedures, different model systems, and different methods of analysis. In addition, as discussed, it is difficult to assess metabolic flux, which is often the more relevant variable, from steady state metabolite levels. However, collectively, these studies point towards several recurrent metabolic signatures of cachexia. Namely, increased glycolytic flux, reduced entry of pyruvate into the TCA cycle, and altered amino acid metabolism favoring anaplerosis and secretion. The next steps, then, will be to validate these metabolic profiles in human cachexia patients and to use results from these and future studies to identify key points of regulation that can be targeted therapeutically. Future studies should also use, where feasible, metabolite tracing to better assess metabolic flux.

1.2.5.2 Mitochondrial Dysfunction

The metabolic aberrations identified in the metabolic profiles of cachectic muscle are consistent with impaired mitochondrial function. Mitochondrial dysfunction can reduce aerobic energy production, leading to energetic stress and compensatory upregulation of glycolysis (Gaude et al., 2018; Smith et al., 2018). In addition, as described above, the TCA cycle in the mitochondrial matrix is a central hub of amino acid metabolism (Owen et al., 2002; Shimomura et al., 2004). Numerous studies have found that muscle mitochondria in cachexia display signs of altered dynamics and morphology and reduced oxidative phosphorylation with or without inner-membrane uncoupling.

Mitochondrial content is controlled by mitochondrial biogenesis and degradation through mitophagy (Palikaras et al., 2015). In addition, mitochondria are subject to dynamic cycles of fission and fusion that allow for recycling of mitochondrial material and repair or disposal of

damaged mitochondria (Youle and van der Bliek, 2012). All forms of mitochondrial turnover and dynamics are affected in cachectic muscle (reviewed in (VanderVeen et al., 2017)). For example, PGC-1α, a master regulator of mitochondrial biogenesis, is downregulated in models of cancer cachexia (Sandri et al., 2006; White et al., 2011a; White et al., 2012). Also, the increase in autophagy associated with cachexia likely promotes mitophagy (VanderVeen et al., 2017). Mitophagy is mediated by both the Bnip3 and PINK1-PARKIN regulatory pathways (Brown et al., 2017). Bnip3, but not PINK1-PARKIN, has consistently been found to be elevated in mouse and human cachectic muscle, suggesting that increased mitophagy in cachexia is mediated through Bnip3 signaling (Aversa et al., 2016; Brown et al., 2017; Op den Kamp et al., 2013; Stephens et al., 2010). In addition, cachexia is associated with reduced expression of mitochondrial fusion genes (Mfn1/2) and increased expression of fission genes (Fis1), indicating an overall dynamics imbalance towards fission (Brown et al., 2018; White et al., 2011a; White et al., 2012). Increased fission and formation of smaller mitochondria is associated with mitochondrial damage and is believed to promote clearance through mitophagy (Twig et al., 2008). Also, swelling and disrupted cristae structures have been observed in cachectic muscle mitochondria, another sign of mitochondrial damage (Fontes-Oliveira et al., 2013; Shum et al., 2012). Together, these observations indicate that cachectic muscle is characterized by increased mitochondrial damage, resulting in elevated mitochondrial turnover through increased fission and mitophagy and decreased biogenesis. However, the nature and underlying causes of mitochondrial damage are still being investigated.

Aerobic energy generation through OXPHOS is one of the primary functions of mitochondria and is critical for the maintenance of muscle energy homeostasis (Smeitink et al., 2001). OXPHOS is carried out by the ETC, which is composed of 4 complexes that utilize reducing equivalents from the TCA cycle to generate an electro-chemical proton gradient across the inner mitochondrial membrane, and ATP synthase (Complex V), which uses the proton gradient to drive ATP synthesis (Fig. 1.4) (Smeitink et al., 2001). ETC activity has been shown to be reduced in cachexia in a handful of experimental studies. In particular, the activity of complex IV has been shown to be decreased, but Complex I and II have also been shown to have reduced activity (Fermoselle et al., 2013; Fontes-Oliveira et al., 2013; Julienne et al., 2012; Padrao et al., 2013; Pin

et al., 2019a; VanderVeen et al., 2019; VanderVeen et al., 2018). OXPHOS can also be modulated by the activity of uncoupling proteins (UCPs), which allow protons to flow across the inner mitochondrial membrane and uncouple the ETC from ATP synthase (Rousset et al., 2004). Increased expression of UCP2, UCP3, or both has been detected in mouse models and human patients (Busquets et al., 2005; Busquets et al., 2001; Collins et al., 2002; Sanchis et al., 1998; Tseng et al., 2015). In addition, Tzika *et al.* found that the rate of ATP synthesis was decreased approximately two-fold more than flux through the TCA cycle in cachectic mice, an indicator of uncoupling between TCA cycle activity and ATP production (Tzika et al., 2013) However, when Julienne *et al.* directly measured respiration rates in isolated mitochondria from tumor-inoculated rats, they found no uncoupling of respiration, despite increased UCP2 expression (Julienne et al., 2012). UCPs have been shown to have antioxidant functions, reducing mitochondrial reactive oxygen species (ROS) production without affecting respiration rates (MacLellan et al., 2005). Therefore, upregulation of UCPs in muscle does not necessarily mean that mitochondrial respiration is uncoupled. Instead, it is possible that the upregulation of UCPs is an antioxidant response. Indeed, in addition to reducing energy production, impaired ETC activity can lead to ROS production, inducing oxidative stress (Murphy, 2009). More studies measuring the coupling state of respiration directly are needed to determine if UCP upregulation in cachexia leads to physiological uncoupling. In addition, the role of UCPs in the antioxidant response may have therapeutic significance.

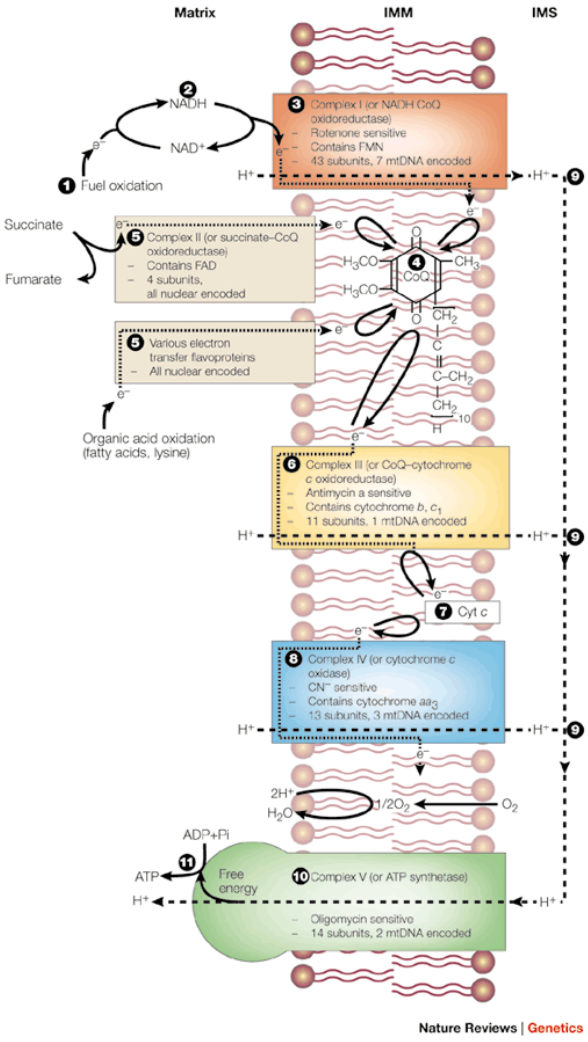

Figure 1.4: OXPHOS system in mammalian mitochondria.

Electrons (e−) from carbon oxidations (step 1 and dotted lines) are transferred via NADH (step 2) into OXPHOS complex I (step 3), which is embedded in the lipid bilayer of the inner mitochondrial membrane (IMM), then transported to coenzyme Q (CoQ) (step 4). Some electrons from organic-acid oxidations are transferred, via other flavin-containing enzyme complexes (step 5), directly to CoQ. CoQ delivers electrons via complex III (step 6) and cytochrome c (Cyt c) (step 7) to the final electron acceptor complex IV (step 8). Here, oxygen is reduced to water. The electrons lose free energy at each transfer step, and in complexes I, III and IV, the energy is harnessed and coupled to the movement of H+ (step 9 and dashed lines) from the mitochondrial matrix to the intermembrane space (IMS). The proton gradient thus generated is used for the production of ATP by complex V (step 10). Except for complex II, all complexes contain some proteins encoded by the mitochondrial genome and others encoded by the nuclear genome. The number of subunits for each complex is indicated. (CN, cyanide; FMN, flavin mononucleotide; mt, mitochondrial.) *Reprinted from Smeitink, J., van den Heuvel, L., and Di Mauro, S. "The genetics and pathology of oxidative phosphorylation" Nature Reviews Genetics* ***2****, 342-352 (© 2001) with permission from Springer Nature.*

1.2.6 Energetic Stress and AMPK

1.2.6.1 Energetic Stress in Cachectic Muscle

Impaired OXPHOS in mitochondria reduces energy generation, leading to energetic stress in cachectic muscle. In keeping with impaired ETC activity, the rate of ATP synthesis in cachectic muscle has been shown to decrease, coinciding with decreased ATP and increased AMP levels (Constantinou et al., 2011; Fontes-Oliveira et al., 2013 Pin, 2019 #5065; Julienne et al., 2012; Tzika et al., 2013). In addition, reduced phospho-creatine and glycogen, two important forms of energy storage in muscle, have also been detected in models of cachexia (Constantinou et al., 2011; Tseng et al., 2015). Reduced energy in muscle can promote fatigue and reduce strength, two common features of cachexia (Wan et al., 2017). In addition, low energy levels may promote protein degradation and supress protein synthesis in skeletal muscle, leading to atrophy (Carbone et al., 2012). Therefore, induction of energetic stress may be a critical component of the progression of muscle dysfunction and atrophy in cachexia.

1.2.6.2 AMPK and Energy Homeostasis

Energetic stress leads to the activation of AMPK, a master regulator of energy homeostasis. AMPK is a heterotrimeric serine/threonine kinase that regulates a wide breadth of metabolic-related pathways (Hardie et al., 2012). It is composed of a catalytic kinase α-subunit, a regulatory β-subunit that contains a glycogen binding domain, and a regulator γ-subunit that is responsible for sensing AMP and ATP levels in the cell (Hardie et al., 2012). There are two isoforms of the α- and β-subunits and three isoforms of the γ-subunit, all of which are expressed in skeletal muscle (Tobias et al., 2018). AMPK activation is mediated by both allosteric interactions and covalent modification. One of the most critical modifications of AMPK is phosphorylation of Thr172 in the alpha subunit, which is required for the release of an auto-inhibitory domain from the catalytic pocket (Stein et al., 2000; Xiao et al., 2011). Thr172 phosphorylation is mediated by upstream kinases, such as liver kinase B1 (LKB1), Ca^{2+}/calmodulin-dependent protein kinase kinase-β (CaMKKβ), and transforming growth factor-β (TGF-β)-activated kinase 1 (TAK1) (Carling et al., 2008; Neumann, 2018). The phosphorylation status of AMPK is also regulated by allosteric interactions with the β- and γ-subunits. Binding of adenosine nucleotides to Bateman domains composed of CBS motifs in the γ-subunit allosterically regulates AMPK and alters its susceptibility

to phosphorylation and dephosphorylation by protein phosphatases (Hardie et al., 2012; Salminen et al., 2016). AMP/ADP binding induces activity and promotes phosphorylation while inhibiting dephosphorylation, while ATP binding has the opposite effects (Hardie et al., 2012; Salminen et al., 2016). In addition, glycogen binding to the β-subunit can inhibit enzymatic activity and phosphorylation (McBride et al., 2009). These regulatory events allow AMPK to act as a sensor of cellular energy levels. When the AMP/ATP ratio increases or glycogen levels are depleted, AMPK is activated and promotes energy generating pathways while inhibiting energy consuming pathways.

Many aspects of metabolism are regulated by AMPK (Fig. 1.5). For example, mTOR signaling, autophagy and proteasomal protein degradation, fatty acid β-oxidation, glycolysis, and mitochondrial biogenesis are all regulated by AMPK activity. AMPK inhibits mTOR through inhibitory phosphorylation of Raptor and TSC2 (Shaw, 2009). AMPK inhibition of mTOR can indirectly activate autophagy, and AMPK also directly phosphorylates autophagy proteins, such as ULK1, Beclin1, ATG9, and VPS34 (Herzig and Shaw, 2018). AMPK also promotes mitochondrial fission, facilitating mitophagy (Toyama et al., 2016). In addition, AMPK phosphorylates and activates FOXO, promoting autophagic and proteasomal gene expression (Bonaldo and Sandri, 2013). Another target of AMPK is fatty acid metabolism. Acetyl-CoA carboxylase (ACC), which catalyzes the conversion of acetyl-CoA to malonyl-CoA in the first step of lipid synthesis, is a well-known target of AMPK (Herzig and Shaw, 2018). Malonyl-CoA is also an allosteric inhibitor of the mitochondrial fatty acid transporter CPT1, the rate limiting step of beta-oxidation (Herzig and Shaw, 2018). Thus, inhibition of ACC both blocks lipid synthesis and promotes beta-oxidation. A series of AMPK targets are also believed to directly or indirectly promote glucose uptake and glycolytic flux (Herzig and Shaw, 2018). Finally, AMPK is known to promote mitochondrial biogenesis by activating and increasing the expression of biogenic regulators, such as PGC-1α (Jager et al., 2007; Marin et al., 2017; Zong et al., 2002). Collectively, these changes serve to reduce energy consumption and promote energy production in cells.

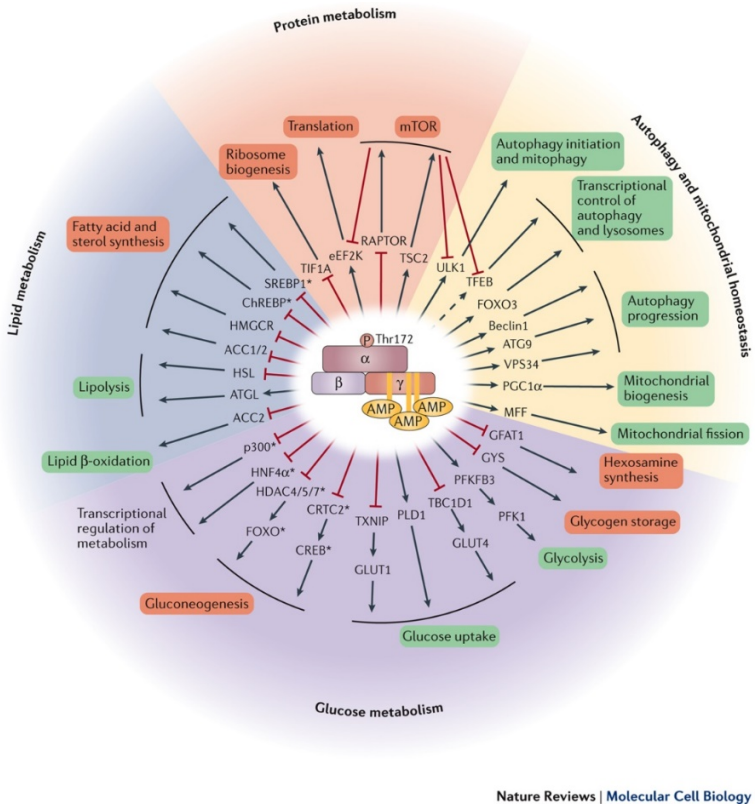

Figure 1.5: AMPK regulates a variety of metabolic processes.
Once activated, the AMP-activated protein kinase (AMPK) complex phosphorylates key targets to rewire metabolism. The direct targets of AMPK are shown in the first concentric circle. The arrow indicates whether the phosphorylation is activating or inhibitory for the function of the target protein. The general process in which each target is involved is indicated in the next circle, and the box colour indicates whether that general process is activated (green) or inhibited (red). For certain targets, an intermediate mediator of the effect is indicated between the two circles. The pathways modulated by AMPK are grouped into four general categories — protein metabolism, lipid metabolism, glucose metabolism, and autophagy and mitochondrial homeostasis — denoting the wide range of processes that are controlled by AMPK. mTOR is modulated by AMPK while also modulating several direct or indirect targets of AMPK. This is illustrated by arrows from mTOR to its targets and serves to emphasize the complex relationship between these two signalling pathways. Transcriptional regulators are denoted by an asterisk. It is important to note that only a subset of AMPK substrates is included in the figure. ChREBP, carbohydrate-responsive element-binding protein; CREB, cAMP response element-binding protein; FOXO, forkhead box protein O; HDAC, histone deacetylase; HMGCR, HMG-CoA reductase; HNF4α, hepatocyte nuclear factor 4α; MFF, mitochondrial fission factor; PGC1α, peroxisome proliferator-activated receptor-γ co-activator 1α; PLD1, phospholipase D1; SREBP1, sterol regulatory element-binding protein 1; TFEB, transcription factor EB. *Reprinted from Herzig, S., Shaw, R. J. "AMPK: guardian of metabolism and mitochondrial homeostasis" Nature Reviews Mol. Cell Biol.* ***19****, 121-135 (© 2018) with permission from Springer Nature.*

Another aspect of AMPK activation relevant to cachexia is the regulation of cellular inflammatory responses. In general, AMPK acts as an anti-inflammatory factor, though this is still an area of active research (Fig. 1.6; reviewed in (Salt and Palmer, 2012)). AMPK inhibits NF-κB indirectly, potentially through inhibition of IKKβ (Bess et al., 2011), or reduced acetylation of p65 through inhibition of the acetyl transferase p300 (Zhang et al., 2011) and activation of the deacetylase SIRT1 (Chen et al., 2002). Another potential mechanism of NF-κB inhibition is upregulation of PGC-1α, which is known to have a reciprocal relationship with NF-κB; NF-κB can promote loss of PGC-1α (Alvarez-Guardia et al., 2010), but PGC-1α also inhibits NF-κB activity (Eisele et al., 2013). AMPK has also been shown to inhibit IL-6 stimulated STAT3 phosphorylation and DNA binding (Kim et al., 2012; Nerstedt et al., 2010). The mechanisms of the inhibition of STAT3 phosphorylation are unknown, but DNA binding appears to be inhibited by interactions with orphan nuclear receptor small heterodimer partner (SHP), whose expression is increased by AMPK activation (Kim et al., 2012). Several other potentially anti-inflammatory functions of AMPK have also been identified, such as increased expression of anti-inflammatory cytokines, suppression of MAPK/ERK signaling, and suppression of ROS and reactive nitrogen species (RNS) production (Salt and Palmer, 2012). However, the role of these anti-inflammatory functions in cachexia have not been explored.

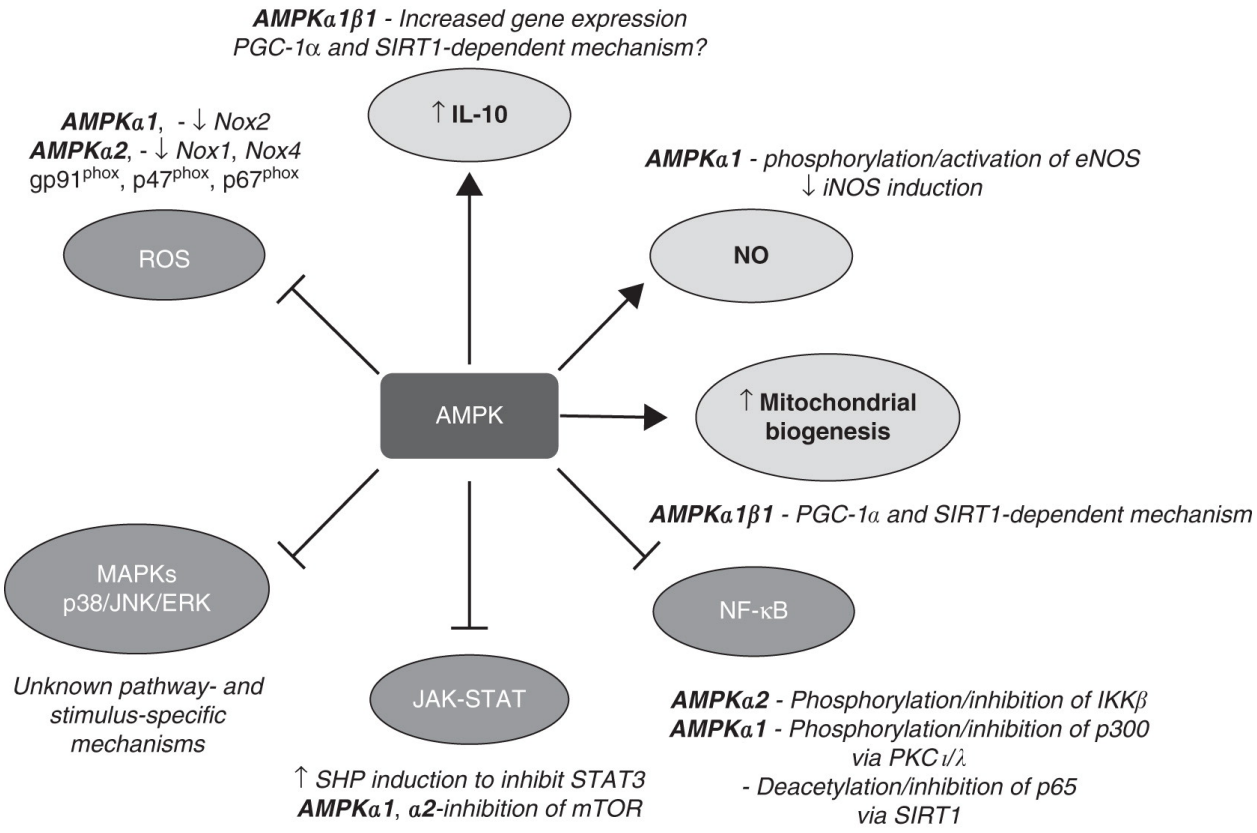

Figure 1.6: Specific AMPK isoforms inhibit pro-inflammatory processes via multiple mechanisms.

Summary of the proposed molecular mechanisms by which AMPK can suppress inflammation, where the known identities of the AMPKα and β subunit(s) thought to be responsible for a given phenomenon are indicated. *Reprinted from Salt, I.P. and Palmer, T.M. "Exploiting the anti-inflammatory effects of AMP-activated protein kinase activation" Expert Opin. Investig. Drugs* ***8****, 1155-67 (© 2012) with permission from Taylor & Francis.*

1.2.6.3 Duality of AMPK in Muscle Wasting: Does AMPK Promote or Protect From cachexia?

The pro-catabolic functions of AMPK suggest that it could promote atrophy in skeletal muscle during cachexia in response to energetic stress. Indeed, AMPK activation may promote atrophy and can impair hypertrophy (Thomson, 2018). Increased AMPK activation has been demonstrated in several mouse models of cancer cachexia (Cui et al., 2019b; Halle et al., 2019; Hardee et al., 2018; Puppa et al., 2014a; Puppa et al., 2014b; White et al., 2011b; White et al., 2013). Activation of AMPK during cachexia has been associated with the suppression of mTOR signaling (White et al., 2013). Treatment with Compound C, an inhibitor of AMPK, reduced suppression of mTOR in IL-6 treated and LLC conditioned media treated myotubes, indicating that AMPK is at least partially responsible for the inhibition of protein synthesis by cytokine signaling (Gao and Carson, 2016; White et al., 2013). However, while it is clear that AMPK is activated during the progression of cachexia, it remains to be shown if AMPK inhibition can prevent muscle atrophy and protect muscle function in cachexia.

AMPK activation may also have beneficial effects during cachexia due to its anti-inflammatory and mitochondrial protective functions. Indeed, muscle-specific knockout of AMPK has been shown to promote myopathy in aging due to accumulation of dysfunctional mitochondria (Bujak et al., 2015). Also, AMPK activation in mice treated with Angiotensin II has been shown to reduce muscle atrophy (Tabony et al., 2011). Furthermore, AMPK activation has been shown to be protective in a variety of neuromuscular disorders, such as Duchenne muscular dystrophy (DMD), spinal muscular atrophy, and myotonic dystrophy (reviewed in (Dial et al., 2018)). In cachexia, loss of AMPK expression in adipose tissue may drive metabolic dysfunction and adipose tissue wasting (Rohm et al., 2016). However, the protective potential of AMPK in cachectic skeletal muscle wasting has never been explored. In Chapter 2 of this thesis, we addressed this question and assessed whether and how AMPK activation could be used to prevent cachexia.

1.2.6.4 Pharmacological Activation of AMPK

Many drugs have been developed to activate AMPK (reviewed in (Kim et al., 2016)). In general, AMPK activators can be classified as direct or indirect (Fig. 1.7). Direct AMPK activators bind to AMPK and induce its activation through allosteric mechanisms. The two main allosteric sites on AMPK are the adenosine binding Bateman domains and a regulatory site between the β- and α-

subunits called the allosteric drug and metabolite (ADaM) site (Kemp, 2004; Langendorf and Kemp, 2015). Binding of drugs to the Bateman domains likely activates AMPK by mimicking the effects of AMP binding (Bung et al., 2018; Kim et al., 2016). The mechanisms of activation through the ADaM site are less understood. However, phosphorylation of Ser108 seems to be required for drug binding (Dite et al., 2017). Also, the ADaM site can induce AMPK activation allosterically, with or without phosphorylation of Thr172 (Calabrese et al., 2014). Furthermore, it has been shown that simultaneous binding of different compounds to the ADaM site and Bateman domains can induce synergistic activation of AMPK (Ducommun et al., 2014; Langendorf et al., 2016; Scott et al., 2014). Recently, another mechanism of direct AMPK activation was identified in which the kinase inhibitor SU6656 was shown to paradoxically activate AMPK through a unique mechanism involving binding to the catalytic site and promotion of Thr172 phosphorylation (Ross et al., 2017). Indirect activation of AMPK is caused by the elevation of endogenous AMP, usually through the inhibition of mitochondrial function (Kim et al., 2016).

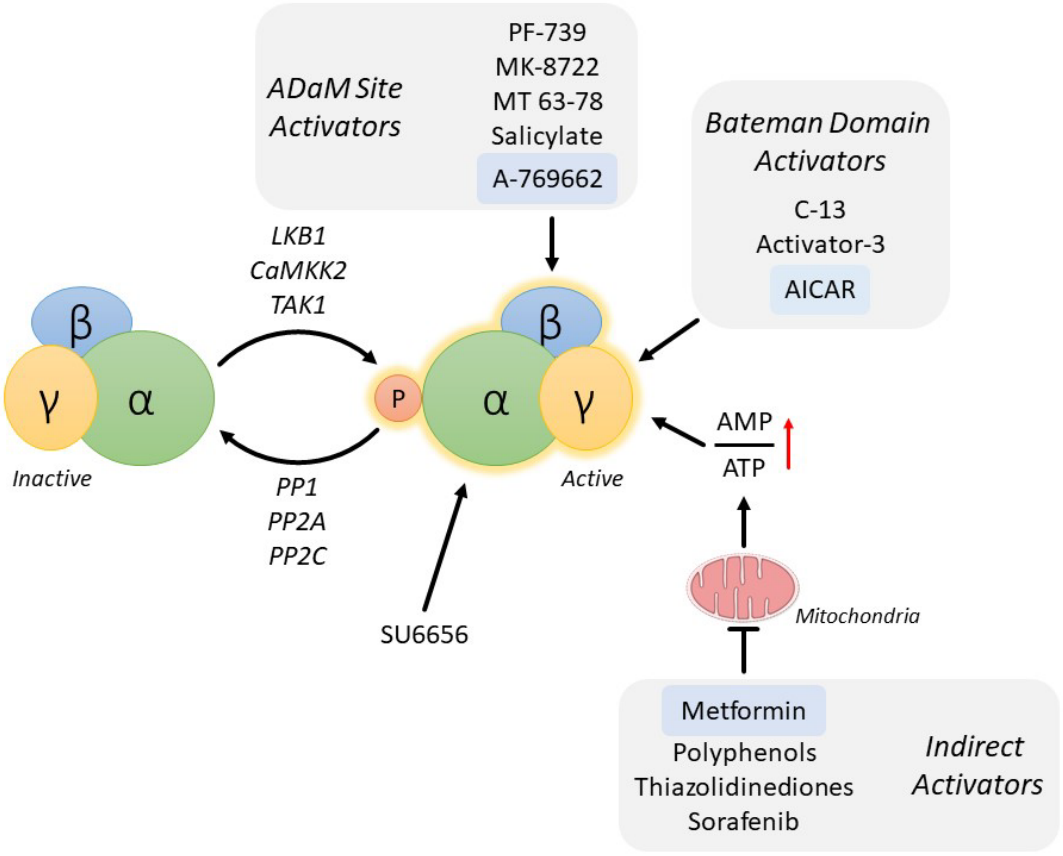

Figure 1.7: Activators of AMPK and their proposed mechanisms of action.

AMPK activation is mediated through allosteric interactions and the phosphorylation of Thr172 in the activation loop of the α-subunit. Phosphorylation is controlled by three known kinases (LKB1, CaMMK2, and TAK1) and three known phosphatases (PP1, PP2A, and PP2C). Drug or AMP binding to the regulatory β- and γ-subunits induces activation both allosterically and by promoting and inhibiting the phosphorylation and dephosphorylation, respectively, of Thr172. Mechanisms of direct AMPK activation include binding to the Bateman domains in the γ-subunit and to the ADaM site in the β-subunit. SU6656 has also been shown to induce activation through a unique binding mechanism in the catalytic pocket of the α-subunit. Indirect activators of AMPK increase cellular AMP levels, usually through the inhibition of mitochondrial ATP synthesis. Activators used for studies performed in Chapter 2 are highlighted in blue.

1.2.7 Oxidative and Nitrosative Stress in Cachexia

Impairment of mitochondria can lead to the production of ROS. Excessive ROS production causes oxidative stress through the chemical modification of proteins, lipids, and nucleic acids (Birben et al., 2012). Furthermore, reaction of ROS with nitric oxide (NO) can lead to the formation of reactive nitrogen species (RNS), further contributing to oxidative stress (Pacher et al., 2007). Increased oxidative stress has been identified as an underlying cause of many pathologies associated with inflammation (Khansari et al., 2009; Liguori et al., 2018). In muscle, oxidative stress has been shown to promote mitochondrial dysfunction and impair contraction due to modification of contractile proteins (Beckendorf and Linke, 2015; Bonnard et al., 2008). Oxidative stress also affects calcium homeostasis in muscle (Espinosa et al., 2016). In addition, extended oxidative stress exposure promotes autophagy and proteasomal protein degradation and can supress protein synthesis (reviewed in (Powers et al., 2016)). Collectively, these effects can promote atrophy and reduce muscle function. As such, oxidative stress may be an important component of cachectic muscle wasting and dysfunction.

1.2.7.1 Evidence of Oxidative Stress in Cachectic Muscle

Increased oxidative stress from either increased production of ROS/RNS or reduced antioxidant potential leads to the modification of intracellular components. In particular, carbonylation or nitration of proteins can be used as markers of oxidative stress (Radi, 2013b; Suzuki et al., 2010). In addition, ROS levels can be measured directly with oxidative-sensitive dyes (Dikalov and Harrison, 2014). Several studies have looked at markers of oxidative stress in models of cachexia and in human patients. In cancer-bearing rodents, increases in muscle protein carbonylation and nitration have been observed (Barreiro et al., 2005; Buck and Chojkier, 1996; Chacon-Cabrera et al., 2014; Salazar-Degracia et al., 2017). In addition, elevated ROS levels have been demonstrated in muscle lysates from cachectic mice (Pin et al., 2019a; Sullivan-Gunn et al., 2011). Signs of oxidative stress in murine cachexia have also been detected through measuring the redox state of several sensitive metabolites, such as glutathione, which were shown to be more oxidized in cachectic muscle (Der-Torossian et al., 2013). Interestingly, in one recent study, it was demonstrated that while oxidative protein modifications were elevated in the gastrocnemius, they were not elevated in the diaphragm, suggesting that oxidative stress may be muscle-type

specific (Salazar-Degracia et al., 2017). Diaphragm muscle is known to be less sensitive to oxidative damage induced by sepsis, potentially due to a more efficient antioxidant response (Talarmin et al., 2017). In human patients, oxidative stress has been detected in the muscle of cancer, AIDS, and COPD patients, indicating that oxidative stress occurs in cachexia across several different disease (Puig-Vilanova et al., 2015; Ramamoorthy et al., 2009). Short-term antioxidant treatment has been shown to improve performance status in cancer patients, highlighting the importance of oxidative stress in the progression of muscle dysfunction in cachexia (Assi and Rebillard, 2016). However, antioxidant treatment can promote cancer growth in the later stages of cancer development, complicating their use in cancer cachexia specifically (Assi et al., 2016; Assi and Rebillard, 2016). Therefore, understanding the molecular mechanisms of oxidative stress induction and the downstream impact of oxidative stress in muscle is critical for the development of more targeted therapies.

1.2.7.2 Potential Sources of ROS

One of the primary sources of intracellular ROS is the mitochondria. Electron leakage from the mitochondrial ETC can react with molecular oxygen to form superoxide (O_2^-) (Murphy, 2009). Superoxide can then react with other biomolecules or with nitric oxide to form peroxynitrite ($ONOO^-$) (Szabo et al., 2007). Alternatively, superoxide can be converted to hydrogen peroxide by superoxide dismutase (Buettner, 2011). In addition to mitochondria, superoxide can also be produced by cellular oxidases (Phaniendra et al., 2015). The potential sources of ROS in cachexia have been recently reviewed (Abrigo et al., 2018; Assi and Rebillard, 2016). Mitochondrial ROS (mtROS), cytoplasmic xanthine oxidase, and membrane-bound NADPH oxidases (NOX) have all been implicated in the onset of oxidative stress in cachexia (Fig. 1.8) (Abrigo et al., 2018). mtROS is of particular interest given the importance of mitochondrial dysfunction in the progression of cachexia, but the mechanism of mtROS formation in cachexia is unclear. The ETC, particularly Complex I and III, is considered to be the primary site of mtROS formation (Murphy, 2009). It has been demonstrated that increased fatty acid β-oxidation can induce elevated ROS levels and promote atrophy (Fukawa et al., 2016). However, as discussed above, cachectic muscle often presents with reduced ETC activity. The mechanisms of reduced ETC activity are unknown, but ROS induces mitochondrial dysfunction and inhibits the ETC (Abrigo et al., 2018). Paradoxically,

inhibition of the ETC complexes can then lead to the production of more mtROS, creating a positive feedback loop (Brookes et al., 2004). As discussed above, UCP expression may be an antioxidant response, reducing mtROS production from the dysfunctional ETC (MacLellan et al., 2005). More research is needed, however, to clarify the mechanisms of elevated mtROS in cachectic muscle.

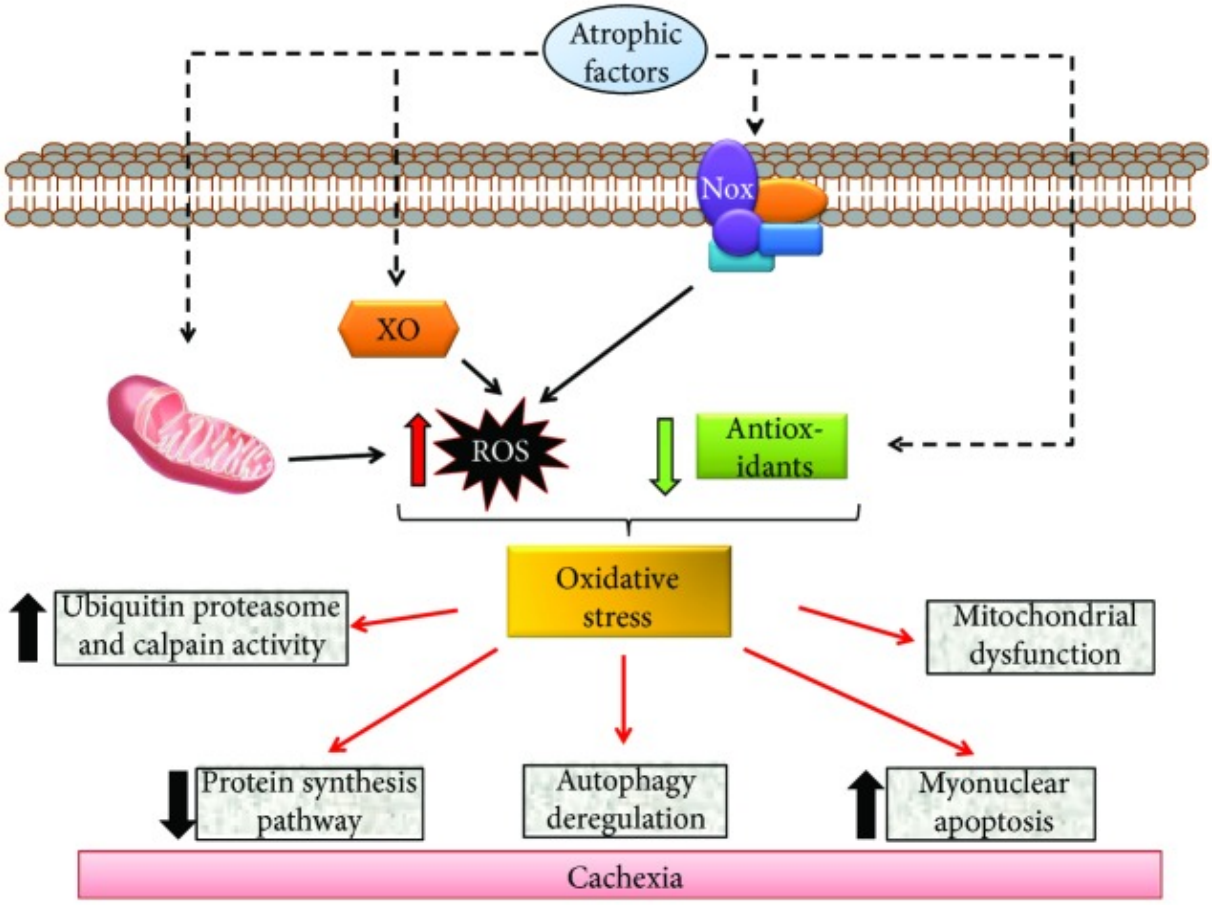

Figure 1.8: Molecular mechanisms involved in cachexia are modulated by oxidative stress.

Atrophic factors can generate oxidative stress in skeletal muscle by the activation of different sources of reactive oxygen species, such as the mitochondria, xanthine oxidase (XO), and NADPH oxidase complex with Nox subunit, in addition to the decrease in antioxidant species. Oxidative stress is able to produce mitochondrial dysfunction, increase ubiquitin proteasome system activity, increase myonuclear apoptosis, decrease the protein synthesis pathway, and deregulate autophagy, all of which are involved in cachexia-skeletal muscle atrophy. *Reprinted from Abrigo, J., et al. "Role of Oxidative Stress as a Key Regulator of Muscle Wasting during Cachexia" Oxid. Med. Cell Longev.* ***2018*** *2063179, 17 (© 2018) under the Creative Commons Attribution License.*

1.2.7.3 Inducible Nitric Oxide Synthase and Nitrosative Stress

Indications of nitrosative stress have also been detected in the muscle of murine cachexia models and in human cachexia patients (Barreiro et al., 2005; Salazar-Degracia et al., 2017). Nitrosative stress is mediated by the formation of peroxynitrite from the reaction of superoxide with nitric oxide (Szabo et al., 2007). Nitric oxide is produced by nitric oxide synthases (NOS). There are three mammalian NOS isoforms; endothelial (eNOS), neuronal (nNOS), and inducible (iNOS) (Strijdom et al., 2009). All three isoforms can be expressed by skeletal muscle (Kapur et al., 1997). eNOS and nNOS are basally expressed, have relatively low enzymatic activity, and are involved in physiological nitric oxide signaling (Kapur et al., 1997; Stamler and Meissner, 2001; Strijdom et al., 2009). In contrast, iNOS is rapidly induced under certain stress conditions and leads to the production of higher levels of NO (Strijdom et al., 2009). These higher NO levels are an important part of the cytotoxic immune response but have also been associated with numerous pathological conditions (Radi, 2013a). For example, iNOS-induced nitrosative stress has been associated with calcium leakage in the *mdx* mouse model of Duchenne muscular dystrophy (Bellinger et al., 2009). iNOS expression is elevated in the skeletal muscle cachectic of patients (Adams et al., 2003; Agusti et al., 2004; Ramamoorthy et al., 2009). Also, our research group and others have previously shown that iNOS is involved in cytokine-driven muscle wasting in experimental models (Buck and Chojkier, 1996; Di Marco et al., 2012; Di Marco et al., 2005; Ma et al., 2017). Chemical inhibition of iNOS prevents wasting in nude mice injected with CHO-TNFα overexpressing cells and in myotubes treated with TNFα and IFNγ (Buck and Chojkier, 1996; Di Marco et al., 2005). In addition, we have demonstrated that iNOS knockout mice are resistant to wasting induced by intramuscular injection of IFNγ and TNFα (Ma et al., 2017). However, the potential of iNOS inhibition in pre-clinical models of cachexia has never been explored.

Expression of iNOS is mediated by both transcriptional and post-transcriptional regulation (reviewed in (Pautz et al., 2010)). In response to inflammatory stimuli, iNOS transcription is activated by inflammatory transcription factors, such as NF-κB (Pautz et al., 2010). In cachexia, we have recently demonstrated that cytokine-induced iNOS expression in muscle is mediated by collaboration between STAT3 and NF-κB (Ma et al., 2017). Once transcribed, the iNOS mRNA is destabilized by AU-rich elements in the 3'-untranslated region (UTR). This allows for the rapid

turnover and clearance of the iNOS mRNA transcript (Pautz et al., 2010). Degradation is mediated by KSRP, which binds to the AU-rich elements and recruits the exosome complex (Linker et al., 2005). In response to inflammatory signals, KSRP binding is antagonized by zinc-finger protein tristetraprolin (TTP) (Linker et al., 2005). Release of KSRP also promotes the binding of Human antigen R (HuR) to the AU-rich elements, stabilizing iNOS expression (Linker et al., 2005; Rodriguez-Pascual et al., 2000). We have previously demonstrated that HuR-mediated stabilization is required for iNOS expression in muscle cells during inflammation (Di Marco et al., 2005). Other posttranscriptional regulatory mechanisms, including regulation by small non-coding RNAs, also modulate iNOS expression (Pautz et al., 2010). Thus, iNOS expression is a tightly controlled mechanism that allows for the rapid induction and eventual clearance of iNOS in response to inflammatory signaling.

The mechanisms of iNOS-mediated muscle wasting are poorly understood. iNOS has been shown to negatively regulate the activity and expression of Jun-D and MyoD, respectively (Buck and Chojkier, 1996; Di Marco et al., 2005). These transcription factors are critical for the expression of muscle-specification genes, such as myosin heavy chain or creatine-kinase (Buck and Chojkier, 1996; Di Marco et al., 2005). The effects on Jun-D are likely mediated by direct oxidative modification (Buck and Chojkier, 1996). We have shown that the destabilization of MyoD mRNA is mediated by the formation of peroxynitrite, indicating that the cachectic effects of iNOS are likely due to nitrosative stress arising from peroxynitrite production (Di Marco et al., 2005). However, we do not know how peroxynitrite induces the destabilization of MyoD. iNOS expression in muscle cells has also been shown to supress mTOR signaling, though the mechanism of inhibition is also unknown (Fig. 1.9) (Frost et al., 2009). Thus, while there is some evidence to suggest iNOS-mediated nitrosative stress contributes to the cachectic phenotype, there is a lack of mechanistic understanding of the role of iNOS in cachexia. In Chapter 3, we demonstrate that iNOS is a mediator of cytokine-induced mitochondrial dysfunction, providing new insight into how iNOS-NO signaling contributes to cachexia.

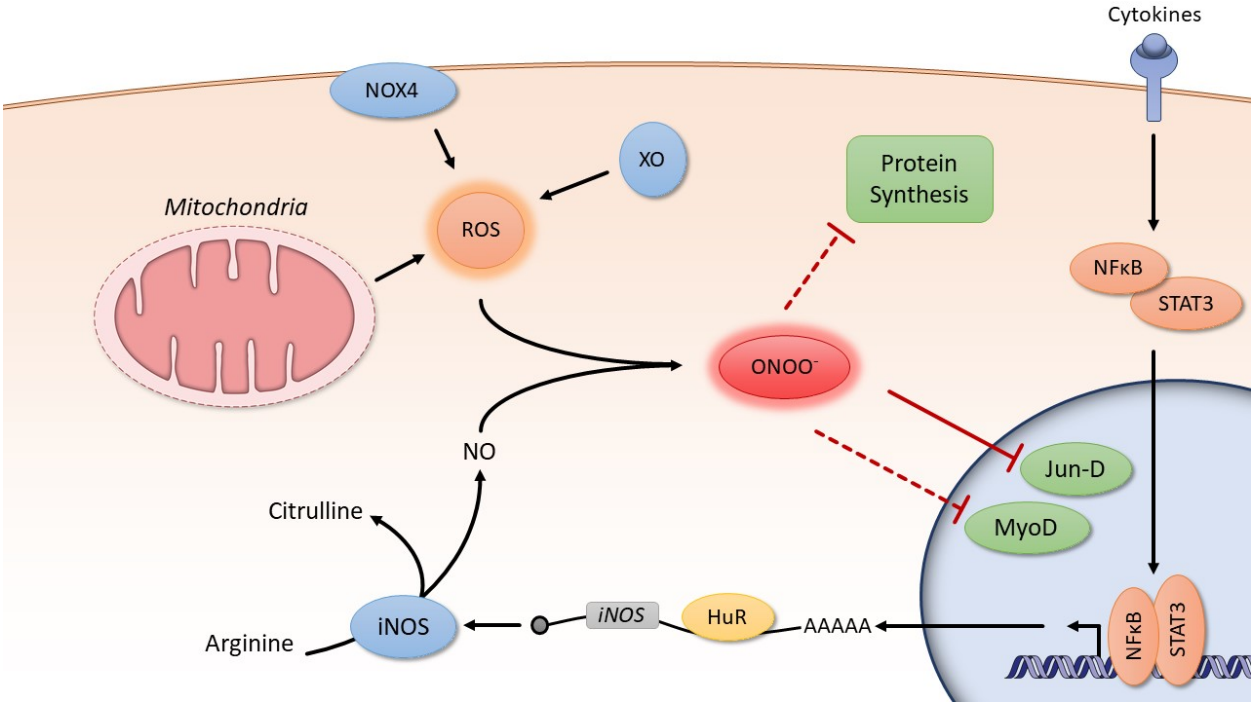

Figure 1.9: Potential mechanisms of iNOS induced muscle atrophy.

Inflammatory cytokines, such as TNFα, activate the transcription factors NF-κB and STAT3. NF-κB and STAT3 then induce the transcription of the iNOS transcript, which is subsequently bound by HuR at an ARE in the 3'-UTR and stabilized. This results in a dramatic increase in iNOS mRNA and protein levels. iNOS converts arginine into citrulline, releasing nitric oxide (NO). NO then reacts with ROS (i.e. superoxide) to form peroxynitrite ($ONOO^-$). Several NO/$ONOO^-$-dependent pathways may be responsible for the induction of muscle wasting. First, oxidative modification of Jun-D impairs its DNA binding, inhibiting expression of several key skeletal muscle-specific proteins. Second, MyoD expression is compromised due to the destabilization of its mRNA transcript through an unknown mechanism, further reducing transcription of muscle-specific proteins. Finally, NO-production may inhibit protein synthesis by inhibiting mTOR signaling, though the mechanism by which this occurs is unknown. *Modified from Hall, D.T., Ma, J.F., Di Marco, S., Gallouzi, I.E. "Inducible nitric oxide synthase (iNOS) in muscle wasting syndrome, sarcopenia, and cachexia" Aging (Albany NY)* ***3*** *8,702-715 (© 2011) under the Creative Commons Attribution License.*

1.3 Thesis Rationale and Objectives

Cachexia is a devastating syndrome that affects an estimated 9 million patients in industrialized countries (von Haehling and Anker, 2010). While significant progress has been made in the diagnosis and management of cachexia, there are still no effective interventions available (Baracos et al., 2018). Development of future therapies is predicated on an in-depth understanding of its underlying mechanisms. A growing body of research has shown that although muscle atrophy represents the ultimate outcome of cachexia, significant metabolic aberrations and functional deficits are apparent preceding atrophy. AMPK is a master regulator of metabolic homeostasis that regulates many of the systems known to be affected by cachexia. AMPK can reduce inflammation and promote mitochondrial health. However, AMPK also activates protein degradation and inhibits protein synthesis. While some studies have shown that AMPK activation can be beneficial in muscle atrophy, AMPK activation has been implicated in the impairment of anabolic signaling in cachexia. Therefore, it is unclear how AMPK should be targeted for cachexia. Nevertheless, we hypothesized that the protective metabolic and anti-inflammatory effects of AMPK activation would predominate and protect against cachectic muscle wasting. Thus, the objective of my research in Chapter 2 was to determine if drug-induced AMPK activation could prevent atrophy and metabolic dysfunction in established models of cachexia. During these studies, we demonstrated that inflammatory cytokines robustly inhibit oxidative phosphorylation in myotubes, and I subsequently became curious to understand the underlying cause of this inhibition. In Chapter 3, I identified iNOS as an inducer of cytokine-driven mitochondrial impairment. I then investigated the mechanisms of this impairment and the effects of iNOS inhibition on metabolic dysfunction and muscle atrophy.

Chapter 2 | Investigating the Potential of AMPK Activation for Cachexia Therapy

2.1 Preface

An increasingly apparent paradigm in research on AMPK is its ability to serve opposing functions depending on the context of its activation. For example, in cancer, AMPK can inhibit growth by suppressing anabolism, but it can also promote growth by protecting cancer cells from metabolic stress (Jeon and Hay, 2015). Given the protective role of AMPK in metabolic function, and the importance of metabolism during cachexia, as well as its potentially anti-inflammatory function, it is possible that AMPK activation could be protective for cachexia (Herzig and Shaw, 2018; Salt and Palmer, 2012). However, its role in suppressing mTOR and protein synthesis after the onset of energetic stress in cachectic muscle may contribute to atrophy (White et al., 2013). Therefore, in this chapter, we set out to determine if activation of AMPK would be beneficial or detrimental for the treatment of cachexia.

These findings and discussions were originally published in EMBO Molecular Medicine in the following manuscript:

Hall DT, Griss T, Ma JF, Sanchez BJ, Sadek J, Tremblay AMK, Mubaid S, Omer A, Ford RJ, Bedard N, Pause A, Wing SS, Di Marco S, Steinberg GR, Jones RG, and Gallouzi IE. “The AMPK agonist 5-aminoimidazole-4-carboxamide ribonucleotide (AICAR), but not metformin, prevents inflammation-associated cachectic muscle wasting.” *EMBO Mol Med*. 2018 Jul;10(7). pii: e8307.

2.2 Abstract

Activation of AMPK has been associated with pro-atrophic signaling in muscle. However, AMPK also has anti-inflammatory effects, suggesting that in cachexia, a syndrome of inflammatory-driven muscle wasting, AMPK activation could be beneficial. Here we show that the AMPK agonist AICAR suppresses IFNγ/TNFα-induced atrophy, while the mitochondrial inhibitor metformin does not. IFNγ/TNFα impair mitochondrial oxidative respiration in myotubes and promote a metabolic shift to aerobic glycolysis, similarly to metformin. In contrast, AICAR partially restored metabolic function. The effects of AICAR were prevented by the AMPK inhibitor Compound C and were reproduced with A-769662, a specific AMPK activator. AICAR and A-769662 co-treatment was found to be synergistic, suggesting that the anti-cachectic effects of these drugs are mediated through AMPK activation. AICAR spared muscle mass in mouse models of cancer and LPS induced atrophy. Together, our findings suggest a dual function for AMPK during inflammation-driven atrophy, wherein it can play a protective role when activated exogenously early in disease progression but may contribute to anabolic suppression and atrophy when activated later through mitochondrial dysfunction and subsequent metabolic stress.

2.3 Introduction

Cachexia is a wasting syndrome that often occurs as a comorbidity with chronic pro-inflammatory diseases, such as cancer, HIV infection, and sepsis (Blum et al., 2014; Fearon et al., 2011). Cachexia is primarily characterized by a progressive and extensive loss of skeletal muscle mass and strength, but can also present with loss of fat mass, anorexia, and cardiac atrophy and remodeling (Fearon et al., 2012; Groarke et al., 2013). The prevalence of cachexia in patients varies depending on the type of disease. For example, it is estimated that approximately half of all cancer patients experience cachexia (von Haehling and Anker, 2010, 2014). It is well-established that onset of cachexia negatively impacts disease outcome, reducing the effectiveness of primary disease treatment and increasing patient morbidity and mortality (Andreyev et al., 1998; Prado et al., 2007; Utech et al., 2012; Vaughan et al., 2013; Vigano et al., 2017).

While there are numerous symptoms of the cachectic state, one of the more debilitating aspects of this condition is the dramatic loss of skeletal muscle tissue (Fearon et al., 2011). Although the mechanisms behind cachectic muscle wasting are complex, it is believed that one of the primary triggers of muscle atrophy is the chronic elevation of pro-inflammatory cytokines (e.g. IL-1, IL-6, TNFα, IFNγ) (Argiles et al., 2009; Fearon et al., 2012; Morley et al., 2006; Tisdale, 2009). In keeping with this, induction of muscle atrophy can be recapitulated in culture and *in vivo* by exposure to different cytokine combinations (e.g. IFNγ and TNFα (Acharyya et al., 2004; Di Marco et al., 2012; Di Marco et al., 2005; Guttridge et al., 2000) or IL-6 (Bonetto et al., 2012; White et al., 2012)). Extended cytokine exposure results in the continued activation of inflammatory signaling within muscle cells, leading to the expression of pro-cachectic genes (Bonaldo and Sandri, 2013; Bonetto et al., 2011; Fearon et al., 2012; Guttridge et al., 2000; Hall et al., 2011). For example, we and others have demonstrated that inducible nitric oxide synthase (iNOS) is dramatically upregulated during cytokine-driven muscle wasting and that the production of reactive nitrogen compounds, such as nitric oxide (NO), by this enzyme contributes to the pathogenesis of cachexia (Buck and Chojkier, 1996; Di Marco et al., 2012; Di Marco et al., 2005; Hall et al., 2011; Ramamoorthy et al., 2009). Recent evidence suggests that cytokine exposure also alters the metabolism of muscle. Indeed, it has been shown in several models of

cachexia and inflammation-driven wasting that muscle undergoes a Warburg-like increase in aerobic glycolysis and mitochondrial abnormalities (Barreiro et al., 2005; Der-Torossian et al., 2013; Fontes-Oliveira et al., 2013; Julienne et al., 2012; McLean et al., 2014; White et al., 2012).

The metabolic regulating enzyme, AMP-activated protein kinase (AMPK), has been associated with cytokine- and cancer-driven muscle wasting (White et al., 2011b; White et al., 2013). AMPK is a heterotrimeric complex (composed of a catalytic α-subunit, linker β-subunit, and regulatory γ-subunit) that responds to cellular energy levels (Hardie et al., 2012). Activation of AMPK has been shown to suppress anabolic signaling through mTOR and has been found to increase the expression of muscle-specific E3-ligases (Krawiec et al., 2007; Nakashima and Yakabe, 2007; Shaw, 2009). However, AMPK has also been shown to have potent anti-inflammatory effects in a variety of cell types (Galic et al., 2011; Mounier et al., 2013; O'Neill and Hardie, 2013; Salminen et al., 2011). The anti-inflammatory function suggests that AMPK activation could be beneficial for muscle atrophy induced by chronic inflammation. Consistent with this concept, genetic deletion of skeletal muscle AMPK leads to the acceleration of aging-induced sarcopenia (Bujak et al., 2015). Further, an AMPK stabilizing peptide was recently shown to be effective at preventing adipose tissue wasting in cancer cachexia (Rohm et al., 2016). Therefore, there is an apparent contradiction for the role of AMPK during cachectic muscle wasting: While its association with atrophic signaling suggests AMPK can contribute to muscle wasting during cachexia, the anti-inflammatory functions of AMPK suggest that it could also prevent cytokine-driven atrophy.

Here, we tested the hypothesis that compounds that activate AMPK could prevent cytokine-driven muscle wasting. To do so, we assessed the impact of two well-known AMPK activators – AICAR and metformin – on atrophy in cultured myotubes treated with the pro-inflammatory cytokines IFNγ and TNFα (Towler and Hardie, 2007; Viollet et al., 2012). These compounds activate AMPK through distinct mechanisms. AICAR is phosphorylated by cellular kinases to form ZMP, which acts as an AMP mimetic, binding directly to and activating AMPK (Towler and Hardie, 2007). In contrast, the biguanide metformin inhibits Complex I of the electron transport chain, leading to an indirect activation of AMPK by increasing cytoplasmic AMP levels (Viollet et al., 2012). Surprisingly, we found that while AICAR, metformin, and IFNγ/TNFα treatment activated AMPK, only AICAR prevented IFNγ/TNFα-induced atrophy. In addition, AICAR, but not metformin,

was found to partially restore normal metabolic function and inhibit the pro-cachectic iNOS/NO pathway. The effects of AICAR were blocked by co-treatment with the AMPK inhibitor Compound C and recapitulated with the more specific AMPK activator A-769662 (Cool et al., 2006; Goransson et al., 2007). In addition, A-769662 and AICAR were found to synergistically prevent wasting, suggesting that the effects of these compounds are through AMPK. Finally, AICAR was able to restore muscle mass in multiple murine models of cachectic muscle wasting.

2.4 Results

2.4.1 Activation of AMPK by AICAR but not metformin prevents muscle wasting

To assess whether AMPK activation could prevent cytokine-induced muscle atrophy we performed studies in C2C12 myotubes treated with IFNγ and TNFα. These pro-cachectic cytokines are a well-established model to induce a muscle wasting-like phenotype *in vitro* that begins with signaling events occurring within the first 24h, followed by atrophy detectable by 48h and culminating in loss of integrity by 72h (Di Marco et al., 2012; Di Marco et al., 2005). To activate AMPK, we used two AMPK activators, AICAR and metformin. As expected, both AICAR and metformin showed increased AMPK phosphorylation at Thr172 (pAMPK), a post-translational modification that is required for AMPK activity, 24h after treatment (Hardie et al., 2012) (Fig. 2.1A). AICAR and metformin treatment also led to the increased phosphorylation of acetyl-CoA carboxylase (ACC) at Ser79 (pACC) (Fig. 2.1A). ACC is a well-established downstream target of AMPK and is often used to demonstrate increased AMPK activity within cells (Munday, 2002). Interestingly, IFNγ/TNFα treatment alone also increased pAMPK and pACC levels at 24h, corroborating previous reports that AMPK phosphorylation increases during the progression of cachexia-induced muscle wasting (Fig. 2.1A) (Penna et al., 2010; White et al., 2011b; White et al., 2013). To further understand the dynamics of AMPK activation in this model, we tested the phosphorylation status of AMPK and ACC over a time course of the first 24h of cytokine treatment. We observed that while cytokine treatment alone resulted in detectable phosphorylation of ACC at 6-12h, respectively, co-treatment with AICAR resulted in detectable levels by 30min (Fig. 2.2). Metformin treatment, in turn, induced detectable ACC phosphorylation by 1h (Fig. 2.2). Thus, while AMPK does seem to be activated by cytokine treatment eventually, treatment with the AMPK agonists increased AMPK activity at a time when it was not normally induced by cytokine treatment.

Having established the AMPK activation status across the different treatment regimes, we next sought to determine what would be the effect of AMPK agonists on the progression of muscle wasting. Surprisingly, we found that AICAR treatment, but not metformin, was able to prevent the loss of integrity in myotubes exposed to IFNγ/TNFα over a 72h period (Fig. 2.1B). To determine whether the AICAR treatment also protected myotubes from the initial atrophying

that precedes myotube collapse, we measured myotube widths 48h after cytokine treatment. Again, only AICAR treatment prevented the cytokine-induced atrophy of muscle myotubes (Fig. 2.1C). In contrast, metformin had no effect on cytokine-induced atrophy and showed a trend toward smaller widths when used alone (Fig. 2.1C). Finally, we assessed the mRNA expression levels of the pro-myogenic transcription factors MyoD and myogenin, which are down-regulated within the first 24h of IFNγ/TNFα treatment (Figs. 2.1D, 2.1E). We observed that, AICAR treatment, but not metformin, significantly increased the mRNA levels of MyoD in cytokine-treated myotubes compared to cytokine treatment alone, though they were not restored to non-treated control levels (Fig. 2.1D). However, AICAR treatment did restore Myogenin mRNA to basal levels during cytokine treatment (Fig. 2.1E). Taken together, these results clearly demonstrate that, despite both compounds activating AMPK, only co-treatment with AICAR prevents the progression of cytokine-induced myotube wasting.

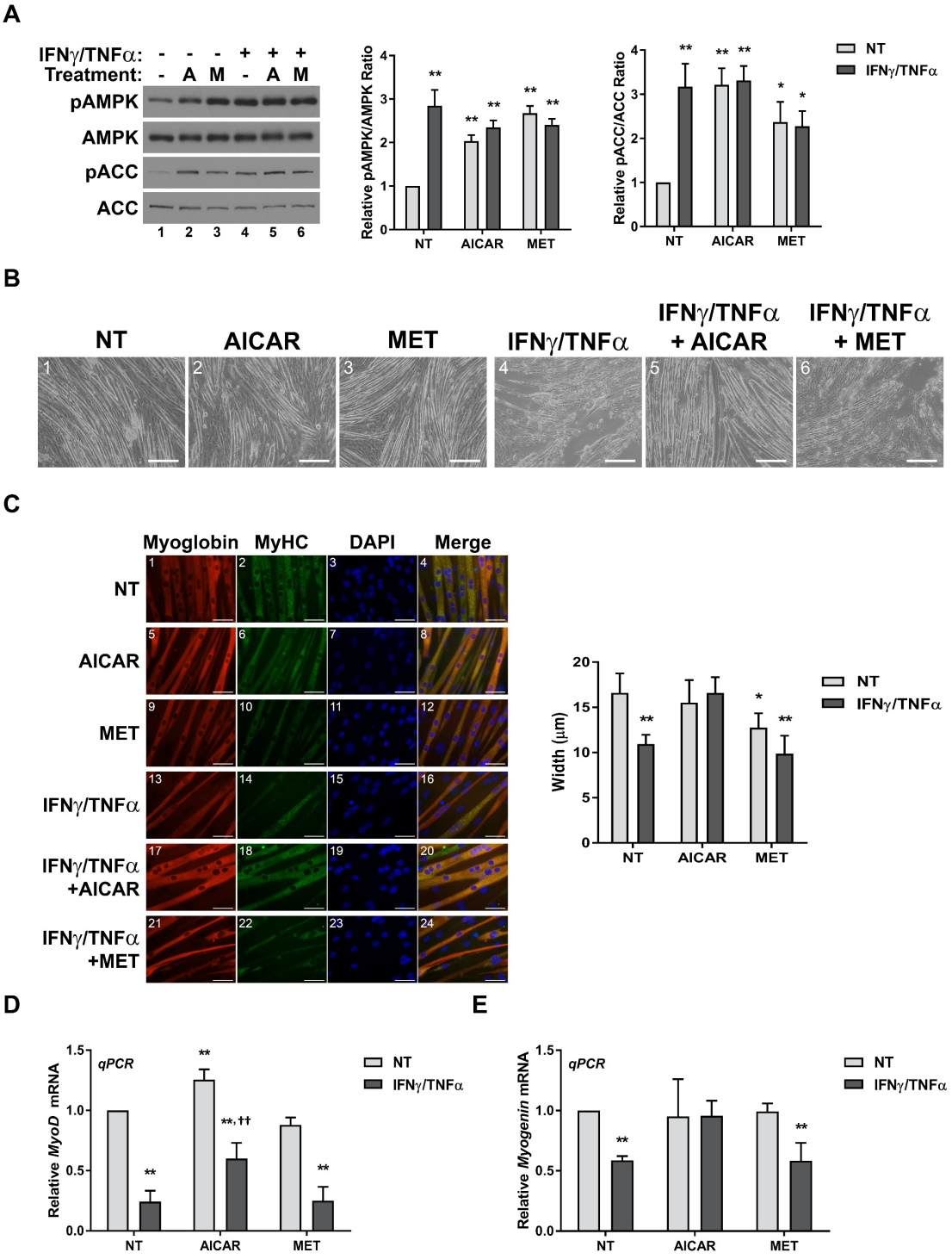

Figure 2.1 AICAR but not metformin prevents IFNγ/TNFα-induced myotube atrophy.

(A) Western blotting for phospho-Thr172-AMPK (pAMPK), total AMPK, phospho-Ser79-ACC (pACC), and total ACC 24h after treatment. Quantification represents the pAMPK/AMPK and pACC/ACC ratios relative to the non-treated (NT) control.

(B) Phase contrast images of fibers 72 h after treatment. Scale bars represent 0.25 mm.

(C) Immunofluorescence staining for myoglobin and myosin heavy chain (MyHC) 48 h after treatment. Scale bars represent 50 µm. Quantification represents the average myotube width.

(D, E) RT–qPCR analysis of the mRNA levels of MyoD (D) and myogenin (E) 24 h after treatment relative to the NT control.

Data information: All quantifications are of three independent experiments (n = 3) and error bars represent standard error of the mean (SEM). Significance between means was first determined using ANOVA. Significance P-values were calculated using Fisher's LSD. *P < 0.05; **P < 0.01 from NT controls; †† P < 0.01 from IFNγ/TNFα-treated controls.

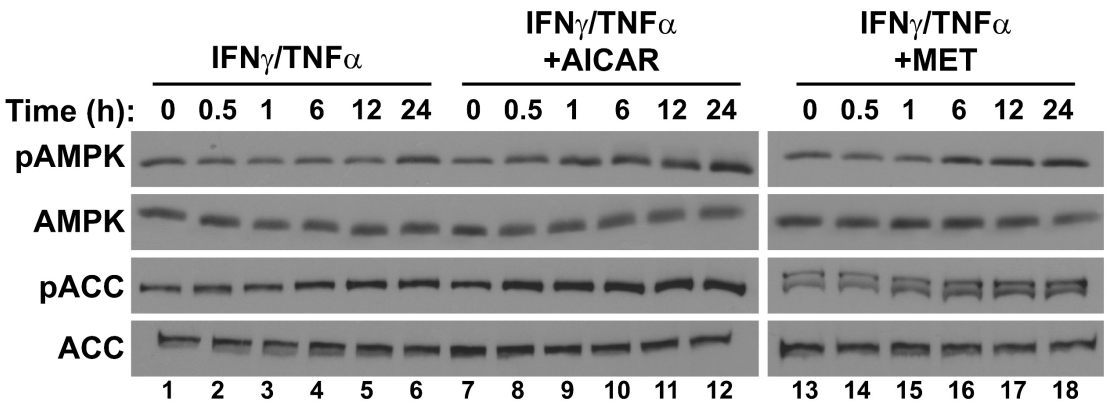

Figure 2.2: Time course of AMPK activation during cytokine and AICAR or metformin co-treatment.

Western blotting for phospho-Thr172 AMPKα (pAMPK), total AMPKα (AMPK), phospho-Ser79-ACC (pACC), and total ACC during the first 24 h of treatment.

2.4.2 AICAR-mediated activation of AMPK restores normal muscle metabolism

In recent years, it has been demonstrated that muscle undergoing cachectic wasting exhibit altered metabolic profiles compared to healthy fibers (Der-Torossian et al., 2013; Fontes-Oliveira et al., 2013; Julienne et al., 2012). Further, given that AMPK is intimately involved in metabolism, we predicted that cytokine treatment would significantly alter metabolic activity in myotube cells, and that the treatment with the AMPK agonists may affect these changes (Hardie et al., 2012). It has been shown that tumor-bearing mice with cachexia exhibit a metabolic signature in muscle characterized by a Warburg-like increase in glycolysis (Der-Torossian et al., 2013). To assess whether this was also the case in our model, we measured the rate of glucose consumption and lactate production, which are indicative of the rate of glycolytic flux. We observed a significant increase in lactate production and glucose consumption in myotubes treated with IFNγ/TNFα, indicative of elevated glycolysis induced by this treatment (Fig. 2.3A and B). Metformin, a known inhibitor of mitochondrial respiration that induces a compensatory increase in glycolysis, also increased lactate production and glucose consumption, as expected, with no additional increase when co-treated with inflammatory cytokines (Fig. 2.3A and B) (Viollet et al., 2012). AICAR, on the other hand, did not affect glycolysis on its own and reduced the increase in glycolysis caused by cytokine treatment (Fig. 2.3A and B). Therefore, in keeping with their ability to protect or not against IFNγ/TNFα-induced wasting, AICAR but not metformin was able to prevent the increased glycolytic rate induced by these cytokines.

Changes in glycolytic activity are often, though not always, associated with changes in oxidative respiration in the mitochondria. Cytokine exposure has been associated with impaired mitochondrial function and reduced oxidative capacity. In addition, several reports have found evidence of mitochondrial dysfunction in pre-clinical models of cachexia (Constantinou et al., 2011; Julienne et al., 2012; Tzika et al., 2013). Therefore, we assessed mitochondrial respiration in C2C12 myotubes using the Seahorse XF extracellular flux system. We found that cytokine treatment significantly reduced both the basal and maximal oxygen consumption rates (OCR; Fig. 2.3C). This was associated with a dramatic increase in the extracellular acidification rate (ECAR), in keeping with our findings that cytokine treatment increases glycolytic flux (Fig. 2.3D). Together, the shifts in OCR and ECAR show a dramatic shift in C2C12 myotubes treated with IFNγ/TNFα

from an aerobic to glycolytic metabolism (Fig. 2.3E). As expected, metformin, a known mitochondrial inhibitor, induced a similar inhibition of OCR and elevation of ECAR, though not to the same magnitude as cytokine-treatment (Fig. 2.3C-E). Metformin co-treatment with IFNγ/TNFα had no additional effects (Fig. 2.3C-E). In contrast, AICAR co-treatment partially restored both basal and maximal respiration and reduced the ECAR (Fig. 2.3C-E). To assess mitochondrial coupling, we compared the respiration rates before and after injection of the ATP-synthase inhibitor oligomycin (Brand and Nicholls, 2011). We found that the decreases in basal respiration during cytokine and metformin treatment were the result of reductions in both coupled and uncoupled respiration (Fig. 2.3F). However, while metformin did not affect the coupling efficiency, IFNγ/TNFα significantly reduced it (Fig. 2.3F). Interestingly, although AICAR co-treatment did not restore basal respiration to its non-treated levels, it did fully recover the coupling efficiency (Fig. 2.3F). Therefore, in cytokine-treated cells co-treated with AICAR, but not metformin, there is a recovery of ATP synthesis dependent mitochondrial respiration. In contrast, metformin alone impairs mitochondrial respiration and has no recovery effect during cytokine co-treatment. Collectively, the metabolomics analysis shows that cytokines induce a shift toward glycolysis associated with severely impaired mitochondrial oxidative respiration that is blunted by co-treatment with AICAR. In contrast, metformin treatment alone impairs mitochondrial respiration and has no additive effect during co-treatment with cytokines. This suggests that the inability of metformin to recover atrophy during cytokine treatment, unlike AICAR, could be due to a lack of recovery of mitochondrial function.

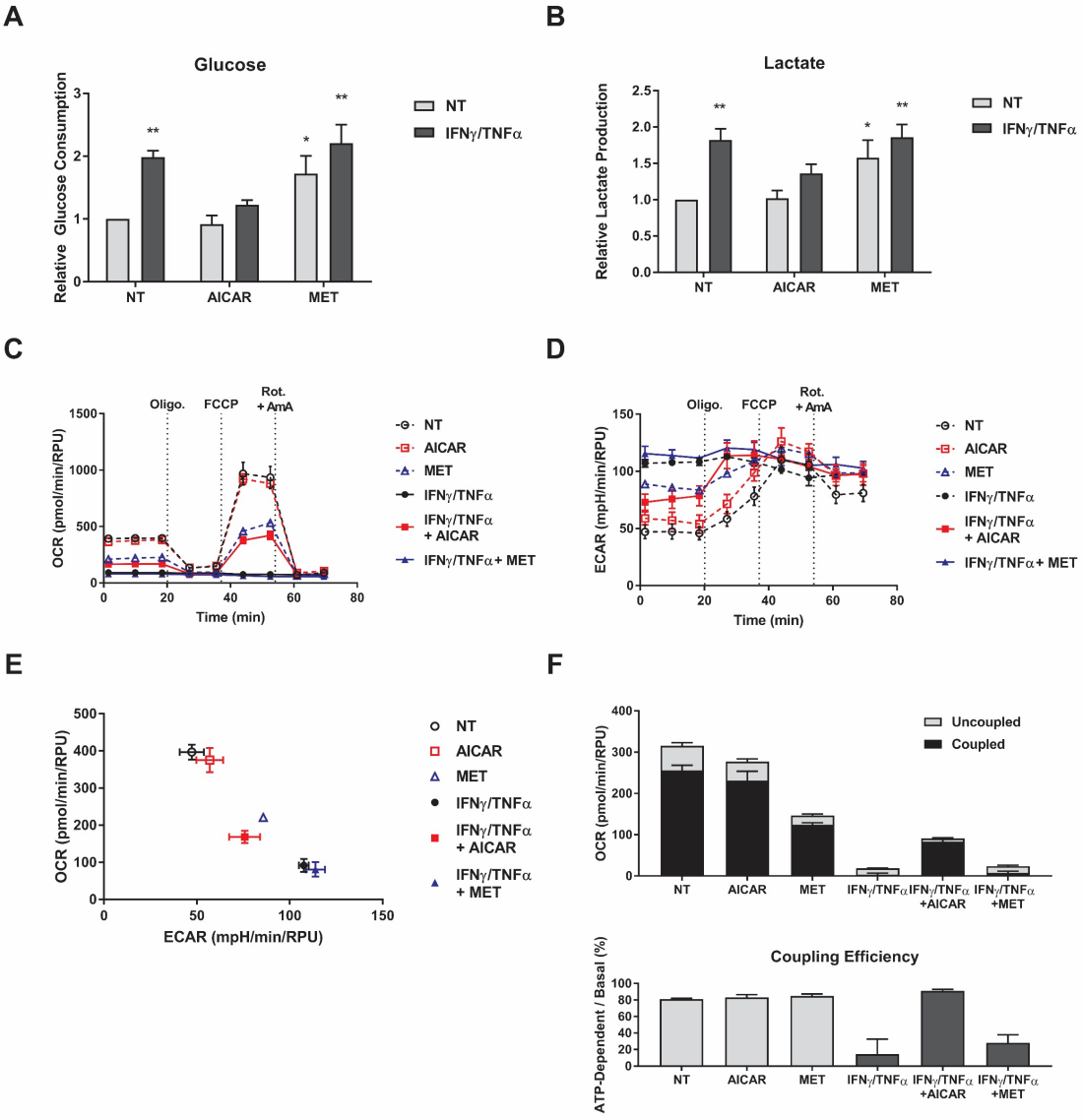

Figure 2.3: AICAR corrects cellular metabolic changes in cytokine-treated myotubes.

(A, B) Rates of glucose consumption (A) and lactate production (B) measured in the media 24 h after treatment relative to the non-treated (NT) control from three independent experiments (n = 3). Error bars represent the SEM.

(C–F) Seahorse XF extracellular flux analysis performed on cells 24 h after treatment. Sequential injections of oligomycin (Oligo.), FCCP, and a combination of rotenone and antimycin A (Rot. + AmA) were performed to assess mitochondrial fitness. Flux was normalized to relative protein units (RPU) measured after the run with an SRB assay. Data are representative of three independent experiment (n = 3). Error bars represent the standard deviation of biological replicates (SD). (C) Oxygen consumption rates (OCR). (D) Extracellular acidification rates (ECAR).

(E) Coordinate plot of OCR and ECAR showing the cellular metabolic profile. (F) Measurements of uncoupled (oligomycin-resistant) and coupled (oligomycin-sensitive) respiration. Coupling efficiency was calculated as the percentage of basal respiration associated with coupled respiration.

Data information: Significance between means was first determined using ANOVA. Significance P-values were calculated using Fisher's LSD. *P < 0.05; **P < 0.01 from NT controls.

One potential consequence of altered metabolism is reduced anabolism. Indeed, the inhibition of anabolic signaling is considered to be a key mechanism underlying atrophy in a variety of overlying pro-inflammatory conditions (Rennie et al., 1983; Smith and Tisdale, 1993). Furthermore, AMPK activation has been implicated in suppressing anabolic signaling in cancer cachexia by inhibiting mTOR (White et al., 2013). To assess how AICAR and metformin treatments affect anabolic signaling in cytokine-treated myotubes, we determined the phosphorylation status of the ribosomal protein S6 kinase (S6K) at Thr389 and its target ribosomal protein S6 (S6) at Ser235/236, a downstream target of signaling mTOR (Hornberger et al., 2007; Roux et al., 2007). As expected, cytokine treatment resulted in hypo-phosphorylation of S6K and S6 48 hours after treatment, which is indicative of reduced translation initiation (Fig. 2.4A) (Roux et al., 2007). AICAR treatment, but not metformin, was able to prevent this decrease (Fig. 2.4A). It is important to note that, while previous reports have demonstrated that exogenous activation of AMPK leads to mTOR suppression, the dosage and timing of AICAR and metformin used here had no significant effect on phosphorylation of S6K or S6 on its own (Fig. 2.4A) (Williamson et al., 2006; Xu et al., 2012).

We next sought to directly determine whether these effects on anabolic signaling correlated with changes in general protein biosynthesis. To do so, we performed radio-labeling experiments in which myotubes treated with IFNγ/TNFα in combination with AICAR or metformin were incubated with L-[^{35}S]-methionine and L-[^{35}S]-cysteine. Cells treated with IFNγ/TNFα showed a significant decrease in the incorporation of radioactivity, indicating that cytokine-treatment suppresses *de novo* protein synthesis (Fig. 2.4B). AICAR treatment, but not metformin, prevented this suppression (Fig. 2.4B). Hence, correlating with a restoration in normal metabolic function, only AICAR appears to be able to restore anabolic signaling in wasting myotubes.

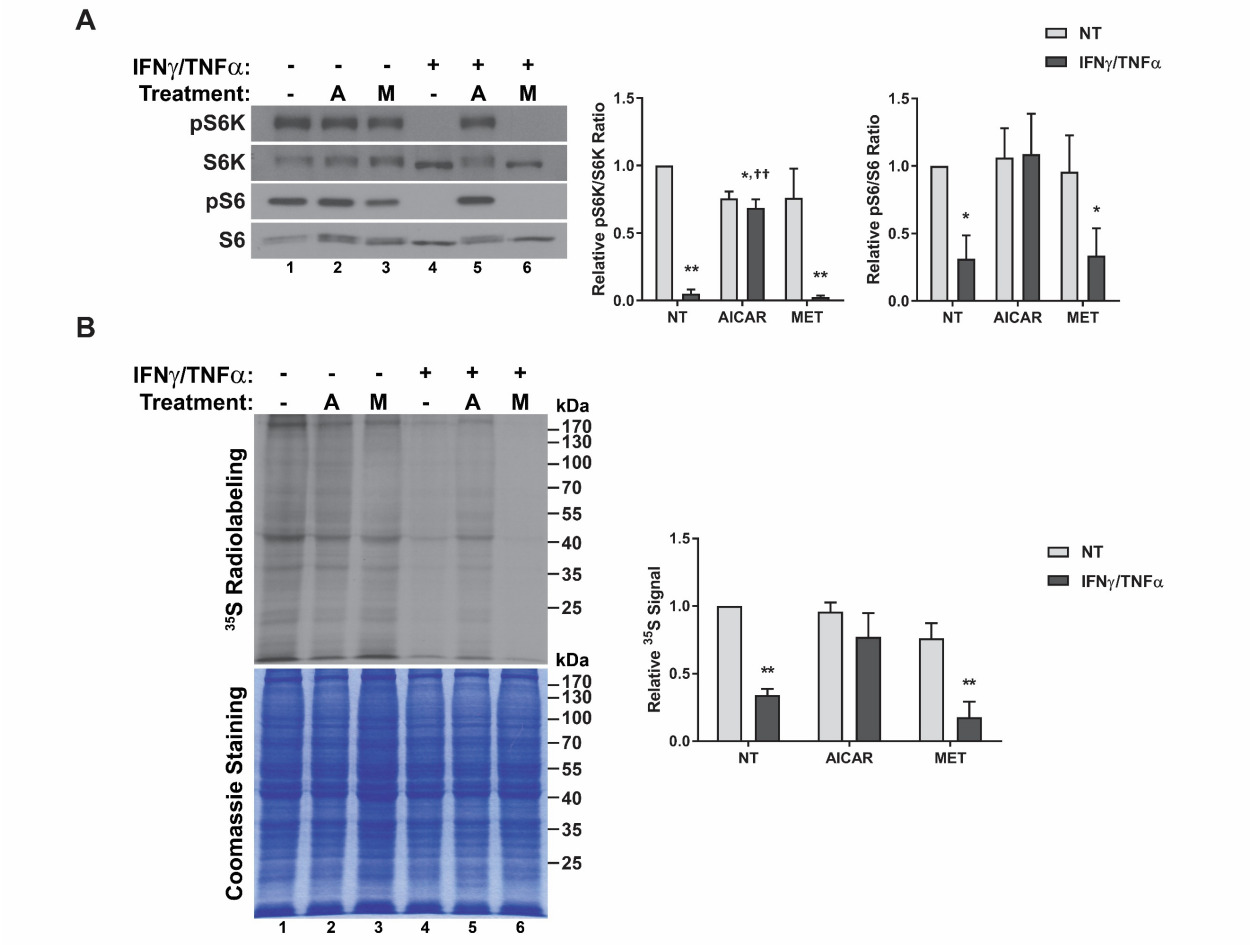

Figure 2.4: AICAR restores anabolic signaling and de novo protein synthesis in cytokine-treated myotubes.

(A) Western blotting of phospho-Thr389-p70S6K (pS6K), total p70S6K (S6K), phospho-Ser235/236-S6 (pS6), and total S6. Quantification represents the pS6K/S6K (n = 3) and pS6/S6 (n = 4) ratios relative to the non-treated (NT) control.

(B) Radiographic analysis of de novo protein synthesis using 35S-labeling. Quantification represents whole lane radiation signal density standardized to Coomassie staining and relative to NT control levels (n = 3).

Data information: Error bars represent the SEM. Significance between means was first determined using ANOVA. Significance P-values were calculated using Fisher's LSD. *P < 0.05; **P < 0.01 from NT controls; †† P < 0.01 from IFNγ/TNFα-treated controls.

2.4.3 AICAR treatment prevents the activation of the iNOS/NO pathway

In order to determine why these two different compounds, despite both activating AMPK, appear to have such varied effects, we began to look at how treatment with the different AMPK agonists affects the induction of inflammatory pathways during this process. We and others have previously reported that in response to inflammatory signaling, muscle significantly upregulates the expression of the iNOS enzyme, leading to NO release. Furthermore, treatments that inhibit the iNOS/NO pathway are able to prevent cytokine-induced atrophy, suggesting that this pathway is a key downstream mediator of wasting (Buck and Chojkier, 1996; Di Marco et al., 2012; Di Marco et al., 2005; Ma et al., 2017; Ramamoorthy et al., 2009). Thus, we assessed the effect of treatment on the expression of iNOS and if this effect correlated with the ability of AICAR to prevent wasting. Indeed, AICAR, but not metformin, dramatically reduced iNOS protein and mRNA levels by 24h (Fig. 2.5A, 4B), with a corresponding decrease in the levels of NO in the culture media (Fig. 2.5C). Interestingly, at higher doses, metformin does not affect iNOS expression and, in fact, induced myotube atrophy similarly to when myotubes are treated with inflammatory cytokines. (Fig. 2.6). Therefore, these results suggest that one of the reasons for the differential effects of AICAR and metformin is their ability or inability to modulate iNOS expression, respectively.

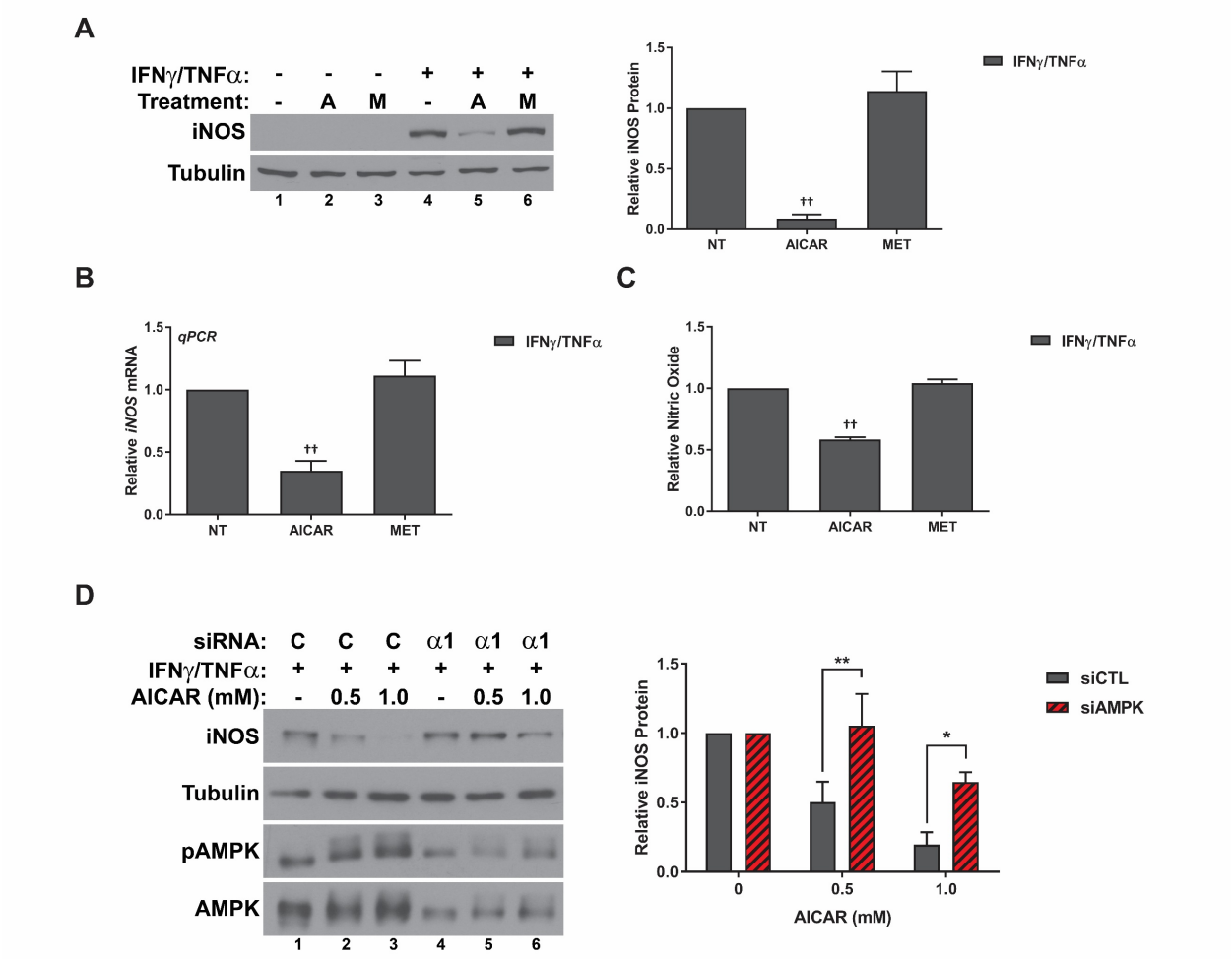

Figure 2.5: The differential effects of AMPK agonists correlates with the expression of inducible nitric oxide synthase (iNOS).

(A) Western blotting for iNOS and tubulin protein levels 24 h after treatment. Quantification represents the levels of iNOS protein normalized to tubulin and relative to the IFNγ/TNFα control.

(B) RT–qPCR analysis of iNOS mRNA levels relative to the IFNγ/TNFα control 24 h after treatment.

(C) Nitric oxide (NO) levels in the culture media of cells relative to the IFNγ/TNFα control 24 h after treatment.

(D) C2C12 myoblast cells were transfected with control (siCTL) or AMPKα1 (siAMPKα-1) targeting siRNA. Cells were subsequently treated with IFNγ/TNFα and the indicated doses of AICAR for 24 h. Western blotting for iNOS, tubulin, phospho-Thr172 AMPKα (pAMPK), and AMPK protein levels. Quantification represents the levels of iNOS protein normalized to tubulin and relative to the siCTL, IFNγ/TNFα control.

Data information: All quantifications are of three independent experiments (n = 3), and error bars represent the SEM. Significance between means was first determined using ANOVA. Significance P-values were calculated using Fisher's LSD. *P < 0.05; **P < 0.01 from equivalent siCTL samples; †† P < 0.01 from IFNγ/TNFα-treated controls.

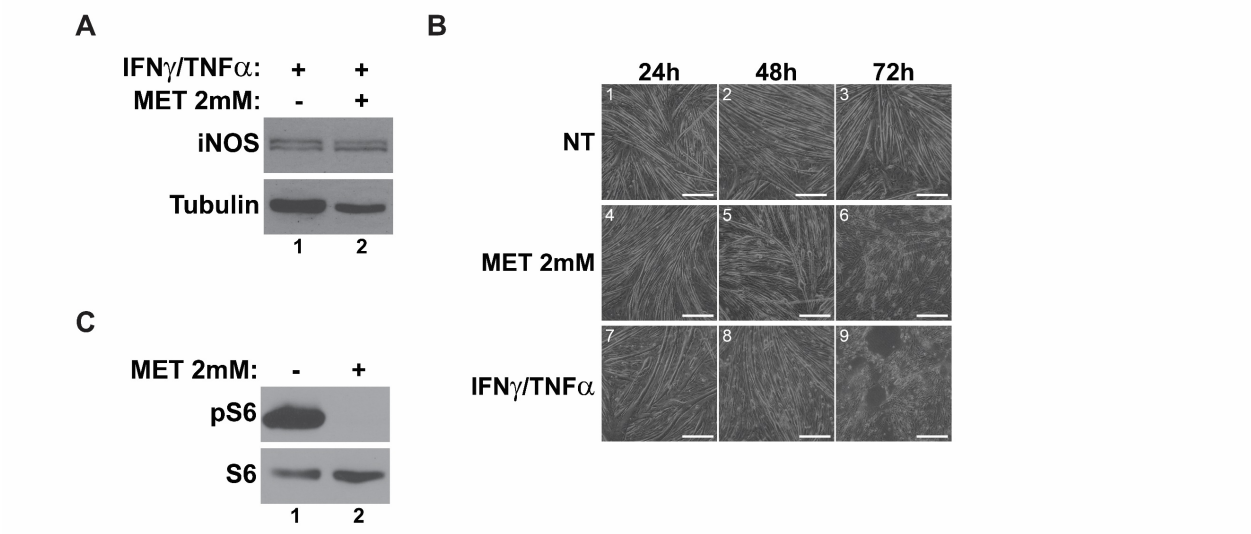

Figure 2.6: Higher doses of metformin induce atrophy and do not inhibit iNOS.

(A) Western blotting for iNOS and tubulin protein levels in cells treated with IFNγ/TNFα with or without metformin (2 mM) for 24 h.

(B) Phase contrast images at 24 h, 48 h, and 72 h post-treatment with either metformin or IFNγ/TNFα. Scale bars represent 0.25 mm.

(C) Western blotting of phospho-Ser235/236-S6 (pS6) and total S6 48 h after treatment with metformin.

2.4.4 AICAR mechanism of action is likely dependent on AMPK

As described above, AICAR was found to activate AMPK much faster than cytokines (Fig. 2.2). Therefore, the beneficial effects of AMPK activation likely depend on the timing of activation. However, it is still unclear whether these effects of AICAR are in fact dependent on AMPK activity. To address this, we conducted knockdown experiments using siRNA targeting AMPK. Fully differentiated muscle cells express a large pool of AMPK. In addition, several isoforms of each subunit are present in muscle, making the AMPK system in muscle especially resistant to experimental attempts at knockdown (Steinberg and Kemp, 2009). Therefore, we conducted our studies in muscle pre-cursor cells (myoblasts), which express a lower level of AMPK and only one isoform of the catalytic subunit (AMPKα1). Importantly, while myoblasts cannot be assessed for atrophy, they maintain a similar response to inflammatory stimulus as seen in fully differentiated cells (Di Marco et al., 2005). Indeed, like myotubes, myoblasts will induce expression of iNOS and phosphorylation of AMPK 24h after treatment with IFNγ/TNFα (Fig. 2.5D). Therefore, we assessed whether the inhibition of iNOS by AICAR treatment could be impaired by AMPK knockdown in myoblasts. In myoblasts, knockdown of AMPKα1 prevented the ability of AICAR to inhibit iNOS, indicating that the effects on iNOS expression were AMPK-dependent (Fig. 2.5D). In keeping with this, overexpression of human AMPKα1 increased sensitivity of myoblasts to AICAR treatment (Fig. 2.7).

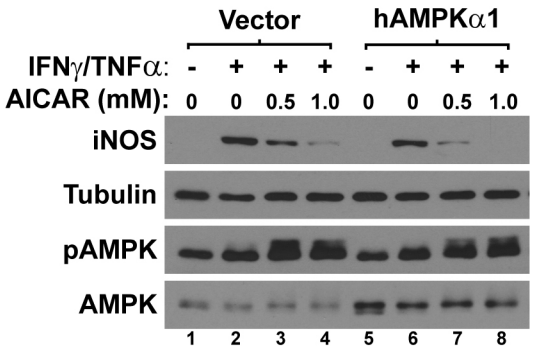

Figure 2.7: Overexpression of AMPKα increases C2C12 sensitivity to AICAR.

C2C12 myoblast cells were transfected with constructs expressing human AMPKα1 (hAMPKα1) or an empty vector negative control (Vector). Cells were then treated with IFNγ/TNFα and the indicated doses of AICAR. Western blot analysis performed for protein levels of iNOS, tubulin, and phosphor-Thr172-AMPK (pAMPK), and total AMPK.

To further assess the AMPK-dependency of the AICAR-mediated effects in differentiated myotubes, we conducted studies using the well-known AMPK inhibitor Compound C (Zhou et al., 2001). We first confirmed that Compound C treatment inhibited AICAR induced AMPK activation by measuring AMPK and ACC phosphorylation (Fig. 2.8A). We then assessed the effect of AMPK inhibition on the anti-atrophic properties of AICAR. We found that co-treatment with Compound C negated the AICAR-mediated restoration of myotube widths in cytokine-treated myotubes (Fig. 2.8B). This effect correlated with a 50% reduction in the recovery of normal glycolytic metabolism, as determined by glucose consumption and lactate production (Fig. 2.8C and D). In keeping with this, co-treatment with Compound C completely impaired the ability of AICAR to restore anabolic signaling in cytokine-treated myotubes (Fig. 2.8E). Finally, Compound C treatment was found to significantly reduce the inhibition of iNOS protein expression due to AICAR treatment (Fig. 2.8F). Taken together, these results show that inhibition of AMPK signaling can blunt the effects of AICAR treatment on cytokine-induced myotube wasting.

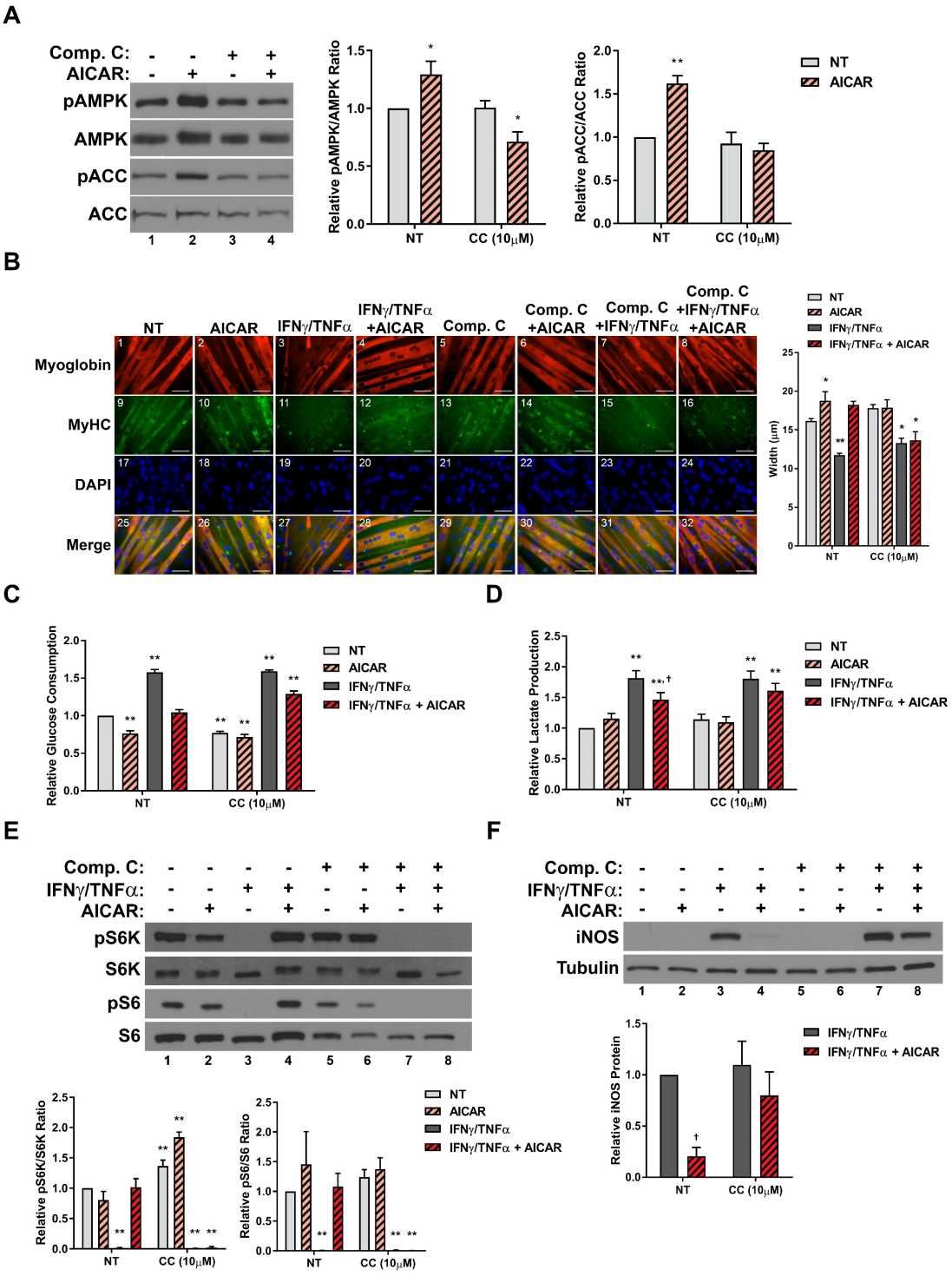

Figure 2.8: Compound C inhibits the effects of AICAR on cytokine-induced atrophy.

(A) Western blotting for phospho-Thr172 AMPKα (pAMPK), total AMPKα (AMPK), phospho-Ser79-ACC (pACC), and total ACC 24 h after treatment. Quantification of the pAMPK/AMPK and pACC/ACC ratios relative to the non-treated (NT) control from four and three independent experiments, respectively (n = 4, 3).

(B) Immunofluorescence staining for myoglobin and myosin heavy chain (MyHC) 48h after treatment. Scale bars represent 50 µm. Quantification represents the average myotube width.
(C, D) Rates of glucose consumption (C) and lactate production (D) measured in the media 24 h after treatment relative to the NT control.
(E) Western blotting of phospho-Thr389-p70S6K (pS6K), total p70S6K (S6K), phospho-Ser235/236-S6 (pS6), and total S6. Quantification represents the pS6K/S6K and pS6/S6 ratios relative to the NT control.
(F) Western blotting for iNOS and tubulin protein levels 24 h after treatment. Quantification represents the levels of iNOS protein normalized to tubulin and relative to the IFNγ/TNFα control.
Data information: All quantifications are of three independent experiments (n = 3), unless otherwise stated, and error bars represent the SEM. Significance between means was first determined using ANOVA. Significance P-values were calculated using Fisher's LSD. *P < 0.05; **P < 0.01 from non-treated (NT) controls; † P < 0.05 from IFNγ/TNFα-treated controls.

If these AICAR-mediated effects are AMPK-dependent, other direct AMPK activators should be able to reproduce the effects of AICAR. To test this hypothesis, we conducted similar studies to those described above with another, more specific AMPK agonist, A-769662. A-769662 is a direct activator of AMPK that binds to the beta1 subunit to allosterically activate the kinase (Cool et al., 2006; Goransson et al., 2007; Sanders et al., 2007; Scott et al., 2008). Importantly, this mechanism, while still direct, is distinct from that of AICAR, as shown by the fact that co-treatment with both agonists has a synergistic effect (Ducommun et al., 2014). When we co-treated C2C12 myotubes with IFNγ/TNFα and A-769662, we found that A-769662 prevented myotube atrophy similarly to AICAR (Fig. 2.9A). In addition, A-769662 replicated the effect of AICAR on aerobic glycolysis (Fig. 2.9B and C), S6K/S6 phosphorylation (Fig. 2.9D) and the activation of the iNOS/NO pathway (Fig. 2.9E-G). Therefore, A-769662 treatment replicated the effects of AICAR on cytokine-induced atrophy.

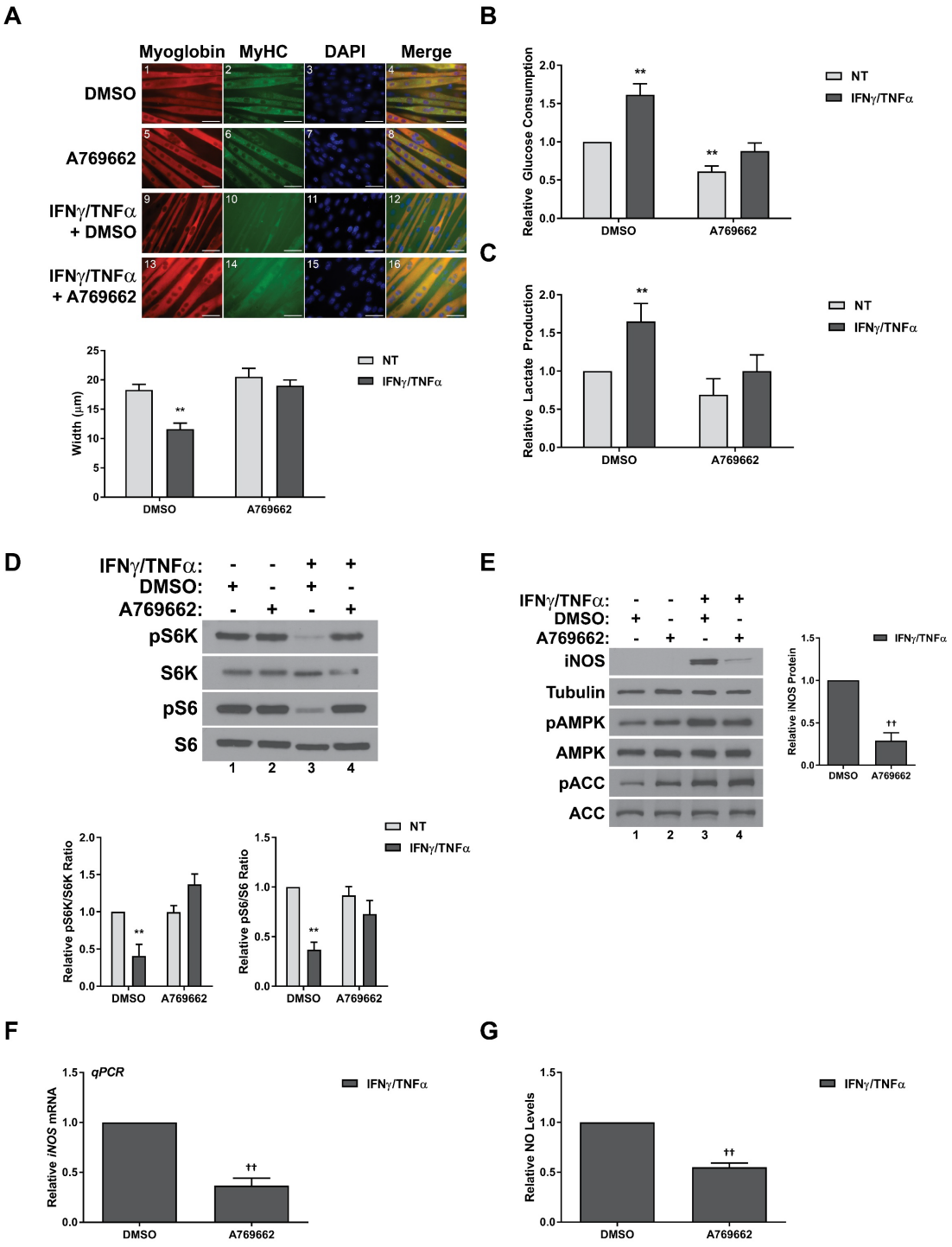

Figure 2.9: A-769662 prevents iNOS expression and is anti-cachectic

(A) Immunofluorescence staining for myoglobin and myosin heavy chain (MyHC) 48 h after treatment. Scale bars represent 50 μm. Quantification represents the average myotube width.

(B,C) Rates of glucose consumption (B) and lactate production (C) measured in the media 24 h after treatment relative to the DMSO-treated control.

(D) Western blotting of phospho-Thr389-p70S6K (pS6K), total p70S6K (S6K), phospho-Ser235/236-S6 (pS6), and total S6. Quantification represents the pS6K/S6K and pS6/S6 ratios relative to the DMSO-treated control.

(E) Western blotting of iNOS, tubulin, phospho-Thr172 AMPKα (pAMPK), total AMPKα (AMPK), phospho-Ser79-ACC (pACC), and total ACC. Quantification represents the levels of iNOS protein normalized to tubulin and relative to the IFNγ/TNFα control.

(F) RT–qPCR analysis of iNOS mRNA levels relative to the IFNγ/TNFα control 24 h after treatment.

(G) Nitric oxide (NO) levels in the culture media of cells relative to the IFNγ/TNFα control 24 h after treatment.

Data information: All quantifications are of three independent experiments (n = 3), and error bars represent the SEM. For panels (A–D), significance between means was first determined using ANOVA. Significance P-values were calculated using Fisher's LSD. For panels (E–G), P-values were calculated using the Student's t-test. *P < 0.05; **P < 0.01 from DMSO controls; †† P < 0.01 from IFNγ/TNFα-treated controls.

As mentioned above, AICAR and A-769662 have been shown to act synergistically on AMPK by activating the kinase from distinct allosteric sites (Ducommun et al., 2014). Therefore, if the effects of these compounds are indeed through AMPK and not through different off-target pathways, they should be able to synergistically prevent the effects of cytokines on myotube wasting. To test this, we titrated co-treatments of sub-optimal doses of both AICAR and A-769662 and assessed their effect on cytokine-treated myotubes. Importantly, while treatment of these lower doses of the two compounds did not significantly affect myotube atrophy in response to IFNγ/TNFα alone, combined treatments significantly recovered myotube size (Fig. 2.10A). Furthermore, co-treatment was able to synergistically inhibit the expression of iNOS (Fig. 2.10B) and restore anabolic signaling (Fig. 2.10C). Thus, AICAR and A-769662 can synergistically prevent cytokine-induced atrophy and signaling events, likely through AMPK. Taken together, the results of Compound C and A-769662 treatment and co-treatment strongly suggest that the effects of AICAR on inflammatory atrophy are mediated through direct AMPK activation.

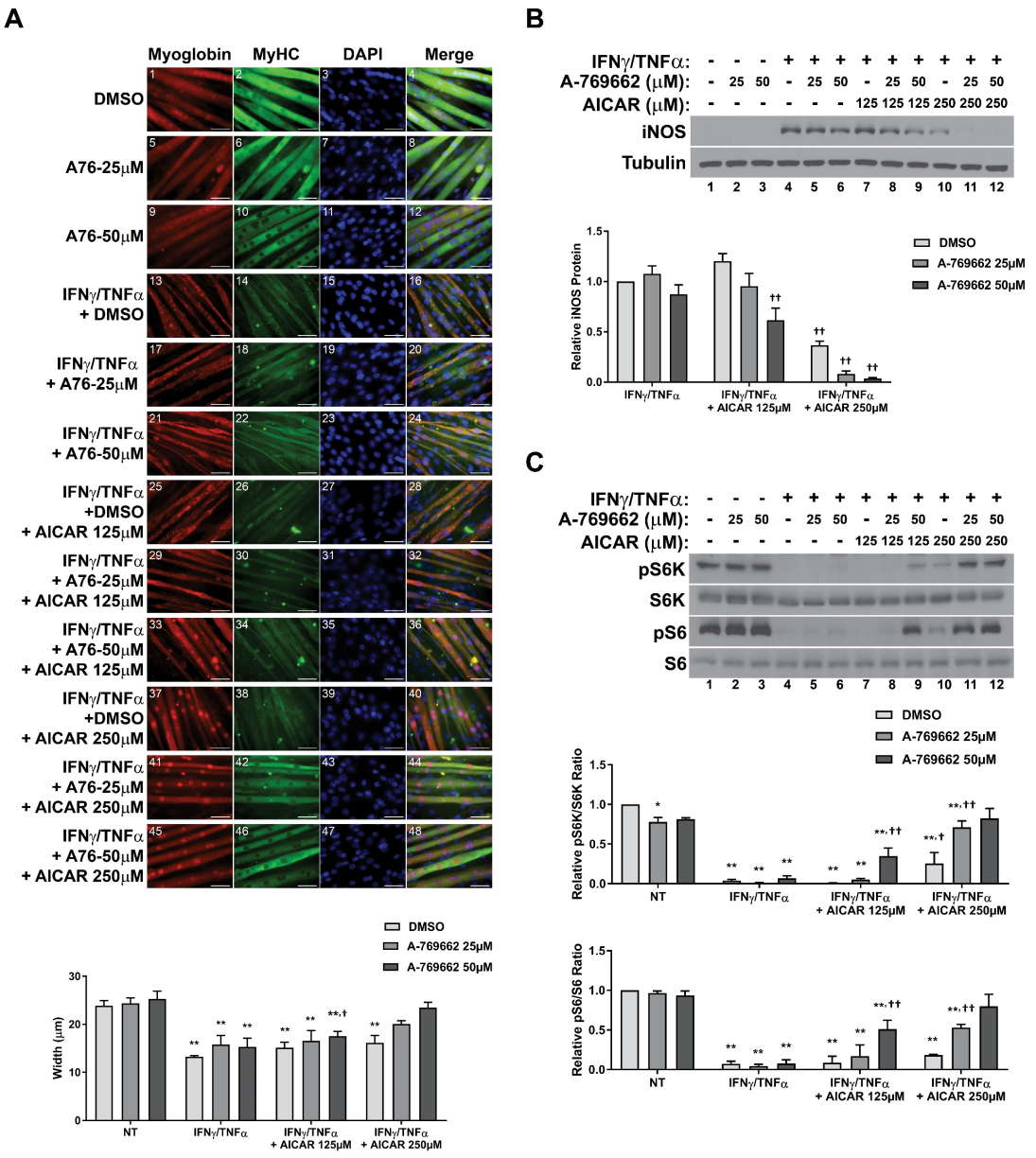

Figure 2.10: AICAR and A-769662 synergistically prevent cytokine-induced myotube atrophy.

(A) Immunofluorescence staining for myoglobin and myosin heavy chain (MyHC) 48 h after treatment. Scale bars represent 50 μm. Quantification represents the average myotube width.

(B) Western blotting for iNOS and tubulin protein levels 24 h after treatment. Quantification represents the levels of iNOS protein normalized to tubulin and relative to the IFNγ/TNFα control.

(C) Western blotting of phospho-Thr389-p70S6K (pS6K), total p70S6K (S6K), phospho-Ser235/236-S6 (pS6), and total S6. Quantification represents the pS6K/S6K and pS6/S6 ratios relative to the NT control.

Data information: All quantifications are of three independent experiments (n = 3), and error bars represent the SEM. Significance between means was first determined using ANOVA. Significance P-values were calculated using Fisher's LSD. *P < 0.05; **P < 0.01 from non-treated (NT) controls; † P < 0.05; †† P < 0.01 from IFNγ/TNFα-treated controls.

2.4.5 AICAR, but not metformin, prevents muscle atrophy in the C26 murine model of cancer cachexia

In order to assess whether the inhibition of cytokine-driven muscle wasting by AMPK is relevant in disease models of cachexia, we first performed *in vivo* studies in the BALB/C mouse strain. It has previously been shown that the subcutaneous injection of C26-adenocarcinoma cells into the flank of these mice leads to the development of cancer cachexia-like symptoms due to the production of pro-inflammatory cytokine, such as IL-6 (Tanaka et al., 1990). Both AICAR and metformin have been associated with anti-tumorigenic effects, and so the possibility exists that AICAR or metformin treatment could affect the growth of the C26 cells and, in doing so, prevent the onset and progression of cancer cachexia independent of muscle-specific effects (Faubert et al., 2013; Jose et al., 2011; Kourelis and Siegel, 2012). Indeed, daily intraperitoneal injections of AICAR or metformin at early stages of tumor development (day 9, when the C26 tumors were just palpable) triggered a robust reduction in tumor burden and subsequent muscle atrophy (Fig. 2.11). Therefore, we decided to begin treatment with these two agonists only after tumors had become well established (day 12) to assess the effects of these drugs on muscle loss independently from their effect on tumor growth. We observed that AICAR treatment, but not metformin, significantly reduced the extent of body weight loss in C26 bearing animals (Table 2.1). This recovery was associated with an improvement in overall musculature (Fig. 2.12A) and an approximately 50% reduction in the extent of muscle mass loss, assessed in both the gastrocnemius and tibialis anterior muscles (Table 2.1). However, there was no effect on adipose tissue wasting, assessed in the inguinal fat pad (Table 2.1). In this treatment regime, neither AICAR nor metformin significantly affected end-point tumor burden (Table 2.1). Serum levels of IL-6 were elevated in all cancer-bearing mice, though there was a trend towards decreased levels in AICAR (non-significant) and metformin (significant) treated mice (Table 2.1). There was no significant effect of AICAR or metformin treatment alone in non-tumor bearing mice on body weight change or gastrocnemius weight (Fig. 2.13A and B). Activation of AMPK in muscle was confirmed by detection of ACC phosphorylation, which was increased in mice treated with AICAR, metformin, or in cancer-bearing mice, as expected (Fig. 2.12B). To confirm that AICAR treatment successfully reduced the extent of cancer-induced muscle atrophy, myofiber cross-sectional area (CSA) was determined in gastrocnemius muscle samples. C26 tumor-bearing animals had

reduced CSA, which showed recovery with AICAR, but not metformin, following the same trend seen in the overall muscle weight (Figs. 8C). In addition, the expression of the muscle-specific E3-ligase Atrogin-1/MAFbx was found to be decreased in the muscle of AICAR, but not metformin, treated mice and there was a non-significant trend toward decreased expression of MuRF1 (Fig. 2.12D-E). Treatment with AICAR or metformin alone had no significant effect on the basal expression of Atrogin-1/MAFbx or MuRF1 (Fig. 2.13C and D). Thus, AICAR, but not metformin, was found to reduce the extent of muscle wasting in the C26 model independent of tumor growth.

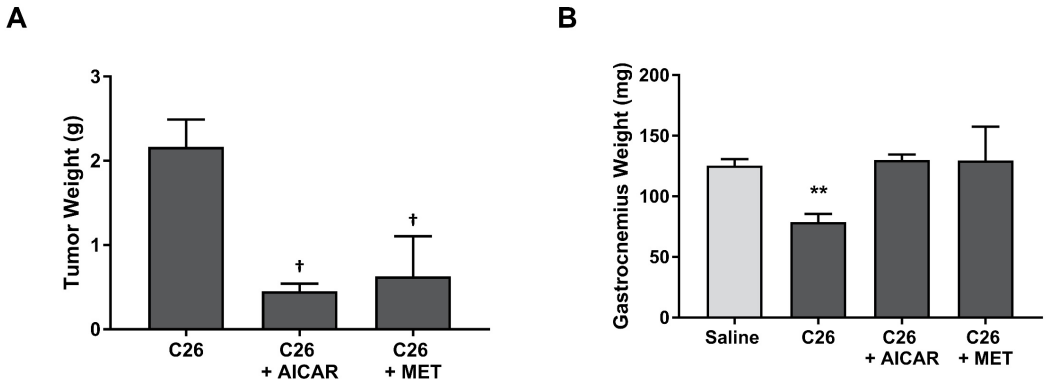

Figure 2.11: Early treatment with AMPK agonists impairs tumor development in the C26 model.

Starting 9 days post-C26 cell subcutaneous injection, mice were intraperitoneally injected daily with either AICAR (500 mg/kg/day), metformin (250 mg/kg/day), or an equivalent volume of saline.

(A) Final tumor masses.

(B) Gastrocnemius muscle weights.

Data information: Results are derived from three mice per cohort (n = 3), and error bars represent the SEM. Significance between means was first determined using ANOVA. Significance P-values were calculated using Fisher's LSD. **P < 0.01 from saline controls; † P < 0.05 from C26 controls.

Table 2.1: AICAR, but not metformin, mitigates muscle atrophy in the C26 murine model of cancer cachexia.

	Saline	C26	C26 + AICAR	C26 + Metformin
Body Weight Change (%)	5.0 ± 0.4	-19.0 ± 1.7 **	-9.6 ± 2.5 ** ††	-16.3 ± 1.5 **
Tibialis Anterior (mg)	37.6 ± 2.2	26 ± 1.5 **	31.3 ± 1.4 * †	25.4 ± 0.7 **
Gastrocnemius (mg)	122.6 ± 2.1	87.3 ± 3.9 **	101.8 ± 2.7 * †	83.8 ± 4.6 **
Fat Pad (mg)	137 ± 6.9	10.9 ± 6.4 **	15 ± 6.6 **	11.8 ± 3.1 **
Tumor (g)	NA	1.024 ± 0.060	1.038 ± 0.104	1.007 ± 0.065
n	9	10	6	8
IL-6 (pg/mL) (n = 4)	30.8 ± 1.7	253.9 ± 46.1 **	201.9 ± 55.2 *	127.7 ± 34.9

Values represent the mean ± standard error of the mean. * $p < 0.05$, ** $p < 0.01$ compared to Saline cohort. † $p < 0.05$, †† $p < 0.01$ compared to C26 cohort.

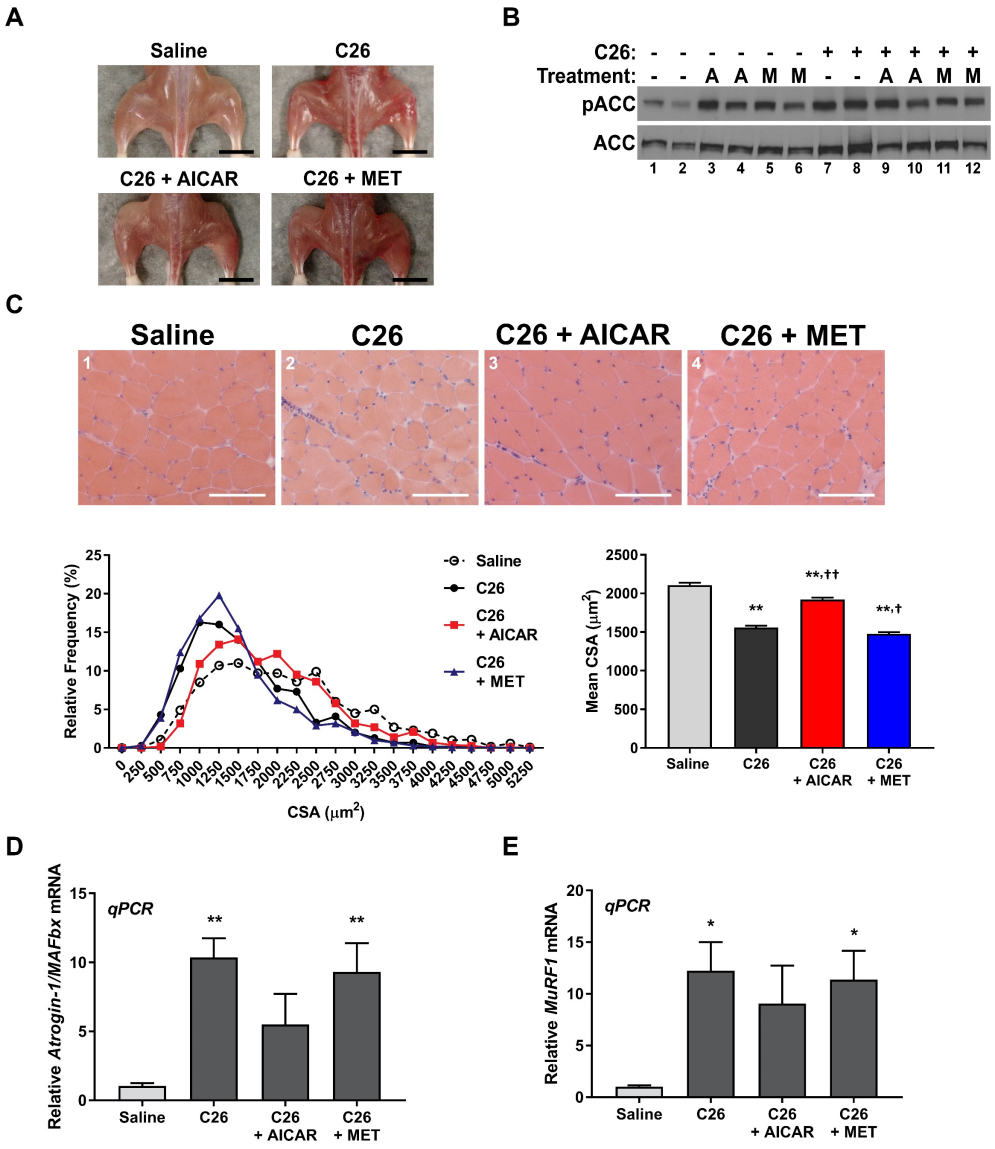

Figure 2.12: AICAR partially recovers muscle mass in the C26-mouse model of cancer cachexia

(A) Representative images of overall hind limb musculature. Scale bar represents 1 cm.

(B) Western blotting for phospho-Ser79-ACC (pACC) and total ACC.

(C) Cross-sectional analysis of the gastrocnemius muscle calculated from 250 fibers per mouse from four mice per cohort (n = 4). Cross-sections were stained by H&E. Scale bars represent 100 μm.

(D, E) RT–qPCR analysis of Atrogin-1/MAFbx (D) and MuRF1 (E) mRNA expression from the tibialis anterior of three mice per cohort (n = 3).

Data information: Error bars represent the SEM. Significance between means was first determined using ANOVA. Significance P-values were calculated using Fisher's LSD. *P < 0.05; **P < 0.01 from saline controls; † P < 0.05; †† P < 0.01 from C26 controls. Source data are available online for this figure.

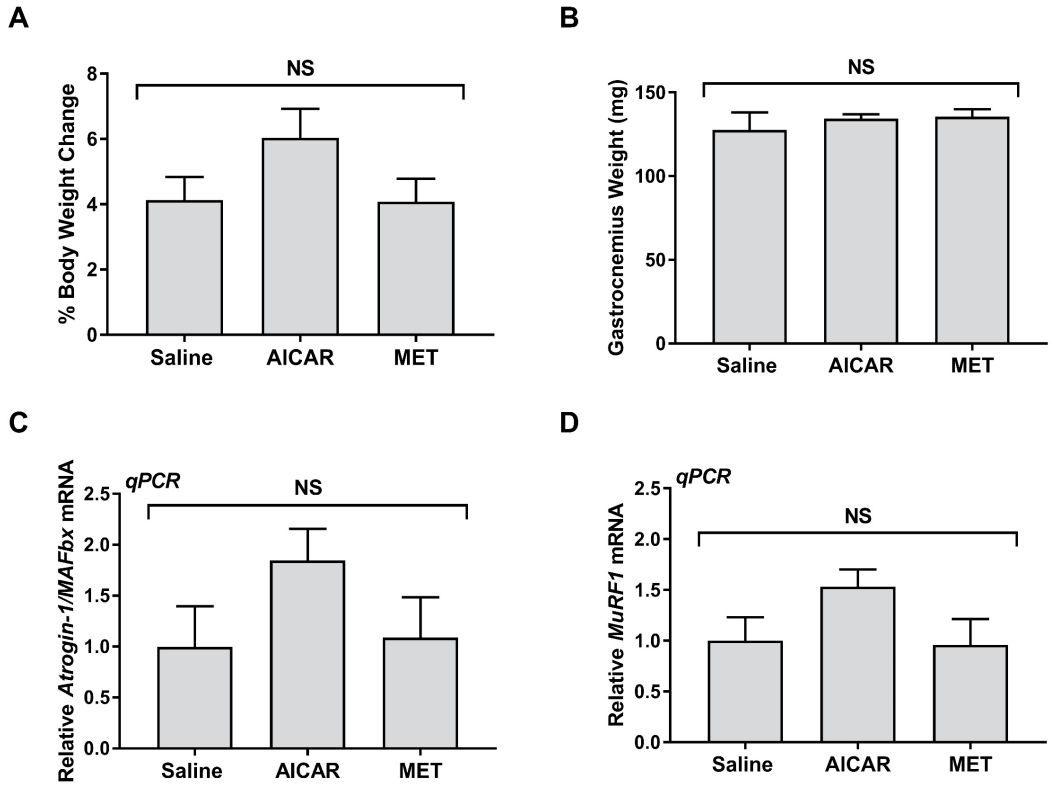

Figure 2.13: Consecutive daily AICAR or metformin treatment does not affect body weight or muscle mass.

BALB/C mice were intraperitoneally injected daily with AICAR (500mg kg^{-1} day^{-1}), metformin (250mg kg^{-1} day^{-1}), or an equivalent volume of saline for 7-9 days.

(A) Percent body weight change.

(B) Gastrocnemius muscle weights.

(C-D) RT-qPCR analysis of Atrogin-1/MAFbx (C) and MuRF1 (D) mRNA expression from the tibialis anterior.

Data information: Results are derived from four mice per cohort (n = 4) and error bars represent the SEM. Significance between means was determined using ANOVA. NS, not significant.

Given that the AICAR treatment was necessarily delayed to avoid affecting tumor growth, we hypothesized that AICAR treatment might be affecting the later stages of disease progression more strongly than the early stages. Indeed, we observed that the correlation between tumor growth and muscle weight loss in the gastrocnemius was lost in the AICAR treated C26 cohort (Fig. 2.14A). Therefore, we assessed the extent of muscle loss in mice at day 14 and day 21 post-C26 inoculation. At day 14, mice have only received 2 days of AICAR treatment, in comparison with day 21, where they have received 9 days of treatment. Interestingly, we found that approximately half of the wasting observed at day 21 had already occurred by day 14, and that this loss was not affected after only 2 days of AICAR treatment (Fig. 2.14B). However, AICAR treatment significantly and dramatically reduced the further loss of muscle mass between day 14 and day 21 (Fig. 2.14B). Furthermore, assessment of Atrogin-1/MAFbx and MuRF1 expression at day 14 showed that AICAR treatment had significantly reduced the expression of Atrogin-1/MAFbx, but not MuRF1, in keeping with our previous observations (Fig. 2.14C). Therefore, it appears that there is significant portion of muscle loss that occurs prior to AICAR administration, but that AICAR effectively prevents the further progression of muscle wasting once it has been administered to C26 tumor-bearing mice. It is likely, then, that earlier treatment with AICAR could be more beneficial, but due to the limitation of having to treat later to prevent the effects of AICAR on tumor growth, this was not possible in our model. Of note, this limitation would not be present in the clinical context, as both the anti-tumorigenic and anti-cachectic properties of AMPK activation early on in disease progression would be beneficial for the treatment of cancer cachexia. Nevertheless, results from this model show that AICAR administration can effectively prevent muscle wasting in the C26 cancer cachexia model, independent of effects on tumor progression.

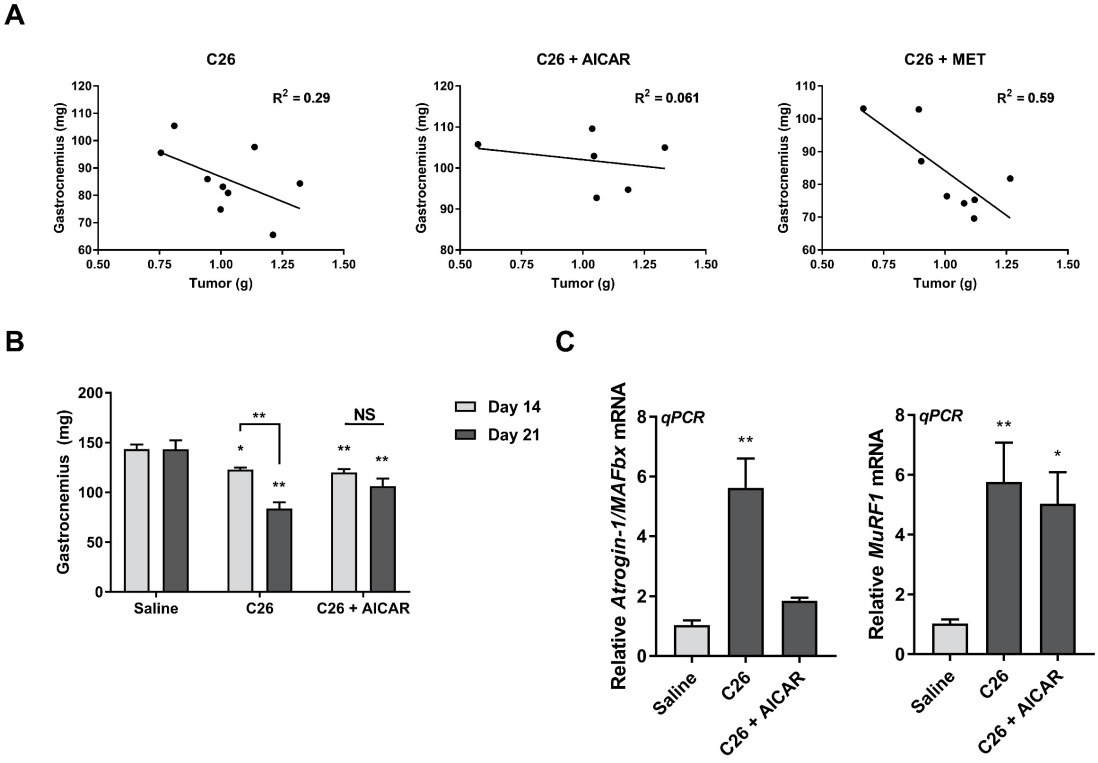

Figure 2.14: Delayed AICAR treatment prevents the further progression of cancer-related muscle atrophy.

(A) Correlation analysis between final tumor mass and gastrocnemius muscle mass in the C26 inoculated cohorts from Table 2.1.

(B, C) BALB/C mice were intraperitoneally injected daily with either AICAR (500 mg/kg/day), metformin (250 mg/kg/day), or an equivalent volume of saline starting 12 days after C26 inoculation. Tissues were collected from mice either two days later (Day 14) or nine days later (Day 21). (B) Gastrocnemius muscle weights. (C) RT–qPCR analysis of Atrogin-1/MAFbx and MuRF1 mRNA expression from the tibialis anterior at Day 14.

Data information: Results are derived from four mice per cohort for Day 14 (n = 4) and three mice per cohort for Day 21 (n = 3), and error bars represent the SEM. Significance between means was first determined using ANOVA. Significance P-values were calculated using Fisher's LSD. *P < 0.05; **P < 0.01 from saline controls or indicated comparisons.

2.4.6 AICAR, but not metformin, prevents muscle atrophy induced by IFNγ/TNFα injection

It is possible that the sparing of muscle mass in AICAR treatment is due to systemic effects, that impact muscle wasting indirectly (Galic et al., 2011; Mounier et al., 2013; O'Neill and Hardie, 2013). Indeed, both AICAR and metformin treatment showed decreased circulating IL-6, which is believed to be a driver of the cachectic phenotype in the C26 model (Aulino et al., 2010). However, given that metformin treatment reduced IL-6 levels more significantly than AICAR treatment but had no effect on muscle mass, it is likely that the levels of IL-6 seen in AICAR and metformin treatment are sufficient to induce cachexia. To further confirm that the effects of AICAR are specific to the interaction between inflammation and muscle, and not due to indirect effects on the tumor or circulating cytokine levels, we conducted wasting evaluations in mice that were intramuscularly injected with the inflammatory cytokines IFNγ/TNFα. We have previously shown that this tumor-free model can induce muscle wasting (Di Marco et al., 2012; Di Marco et al., 2005; Ma et al., 2017). Importantly, because the cytokines are administered directly to the muscle tissue, it is not possible for AICAR treatment to affect the initial inflammatory stimulus in this system. In this model, AICAR treatment had no effect on total body weight changes, but prevented muscle mass loss (Fig. 2.15). Therefore, it is likely that AICAR treatment can prevent muscle wasting, at least in part, by affecting the response to inflammation at the site of muscle tissue.

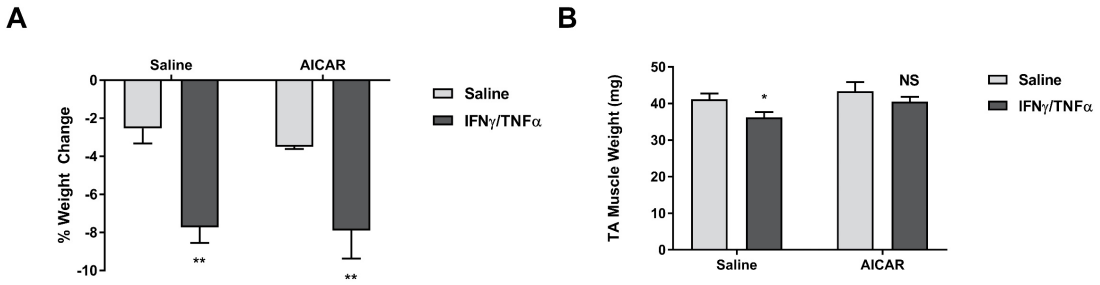

Figure 2.15: AICAR treatment prevents muscle wasting induced by intramuscular cytokine injection.

C57Bl/6 mice were intramuscularly injected with either IFNγ (7,500 U) and TNFα (3 µg) or an equivalent volume of saline in the right posterior thigh muscles daily for 5 days. Mice were also intraperitoneally injected with either AICAR (350 mg/kg/day) or an equivalent volume of saline. On the fifth day, mice were euthanized and tissue samples were collected.

(A, B) Body weight (A) and tibialis anterior muscle weight (B) analysis of saline (n = 8), IFNγ/TNFα (n = 8), AICAR (n = 3), and IFNγ/TNFα + AICAR (n = 7) cohorts.

Data information: Error bars represent the SEM. Significance between means was first determined using ANOVA. Significance P-values were calculated using Fisher's LSD. *P < 0.05; **P < 0.01 from saline controls. NS, not significant.

2.4.7 AICAR, but not metformin, prevents muscle atrophy in a murine model of septic cachexia

To further assess the efficacy of AICAR in models of inflammation-associated muscle wasting, we next assessed a model of septic cachexia. Intraperitoneal injection of LPS has been shown to induce a septic-like state in mice. While the immune response to LPS in mice does not completely reflect that seen in humans, it does induce the expression of TNFα and IL-6 in mice, and has previously been shown to induce muscle loss and the expression of the atrophic muscle E3 ligases, similar to human sepsis-associated cachexia, within 24h (Braun et al., 2013; Callahan and Supinski, 2009; Copeland et al., 2005; Doyle et al., 2011; Jin and Li, 2007). Therefore, we co-injected mice with LPS and either AICAR or metformin and assessed the effect on muscle wasting. It has previously been reported that LPS injected mice have significantly reduced food consumption rates (Braun et al., 2013). Therefore, we pair-fed our controls (PF) and our LPS and AICAR or metformin co-treated cohorts to the LPS cohort consumption rate in order to account for any variation that might have arisen from differences in food consumption. We observed that LPS mice have a significant reduction in body weight following LPS injection (Table 2.2). However, this body weight loss was largely accounted for by the decrease in food consumption, as observed by the fact that the PF cohort showed similar body weight loss (Table 2.2). Unlike in the C26 model, this acute model of inflammation did not significantly affect the weight of adipose tissue (Table 2.2). However, there was a significant loss of muscle mass in both the gastrocnemius and tibialis anterior in LPS treated mice when compared to PF controls, which was completely prevented by AICAR, but not metformin, treatment (Table 2.2). The effects on muscle atrophy were further confirmed by cross-sectional area analysis of the gastrocnemius muscle. As for the muscle weights, we observed that LPS injected mice had significantly reduced average muscle fiber CSA, which was completely abrogated by AICAR treatment and unaffected by metformin treatment (Fig. 2.16A). Furthermore, AICAR treatment, but not metformin, was able to prevent the increased expression of both Atrogin-1/MAFbx and MuRF1 in the skeletal muscle of LPS injected mice (Fig. 2.16B and C). Treatment with AICAR or metformin alone did not significantly affect body weight change, muscle mass, or E3 ligase expression, though there was a non-statistically significant trend toward decreased MuRF1 expression in the metformin control cohort (Fig. 2.17). However, in the LPS and metformin co-treated cohort, this reduction was not

observed (Fig. 2.16C). Thus, as in our other models, only AICAR prevented muscle wasting in a model of septic cachexia.

Table 2.2: AICAR, but not metformin, mitigates muscle atrophy in the LPS model of septic cachexia.

	Vehicle	PF	LPS	LPS + AICAR	LPS + Metformin
Body Weight Change (%)	2.1 ± 0.2 *	-9.5 ± 1.3	-10.4 ± 0.7	-6.5 ± 1 *	-11.4 ± 0.4
Tibialis Anterior (mg)	44.1 ± 3.4	43.2 ± 0.8	38.3 ± 1.5 **	42.2 ± 0.9	39.2 ± 1.2 *
Gastrocnemius (mg)	156.5 ± 4.8	145.7 ± 3.2	136.3 ± 3.6 *	144.8 ± 2.9	136.5 ± 2.2 *
Fat Pad (mg)	99.7 ± 10.6	97.6 ± 10.3	106.1 ± 16.8	95.5 ± 8.1	107.7 ± 12.1
n	4	11	11	11	11

Values represent the mean ± standard error of the mean. * $p < 0.05$, ** $p < 0.01$ compared to the pair-fed (PF) cohort.

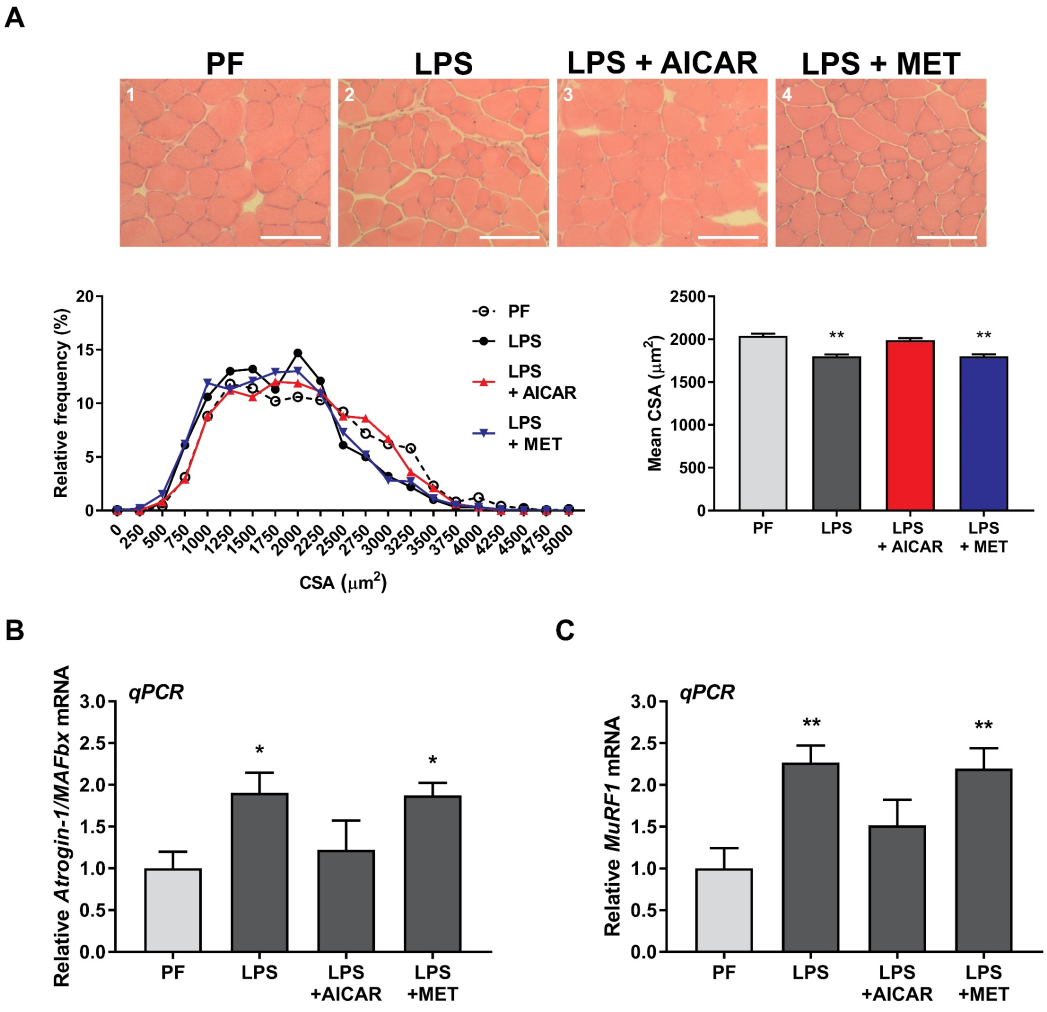

Figure 2.16: AICAR completely prevents muscle wasting in response to LPS injection.

(A) Cross-sectional analysis of the gastrocnemius muscle calculated from 250 fibers per mouse from four mice per cohort (n = 4). Cross-sections were stained by H&E. Scale bars represent 100 μm.

(B, C) RT–qPCR analysis of Atrogin-1/MAFbx (B) and MuRF1 (C) mRNA expression from the tibialis anterior of four mice per cohort (n = 4).

Data information: Error bars represent the SEM. Significance between means was first determined using ANOVA. Significance P-values were calculated using Fisher's LSD. *P < 0.05; **P < 0.01 from PF controls.

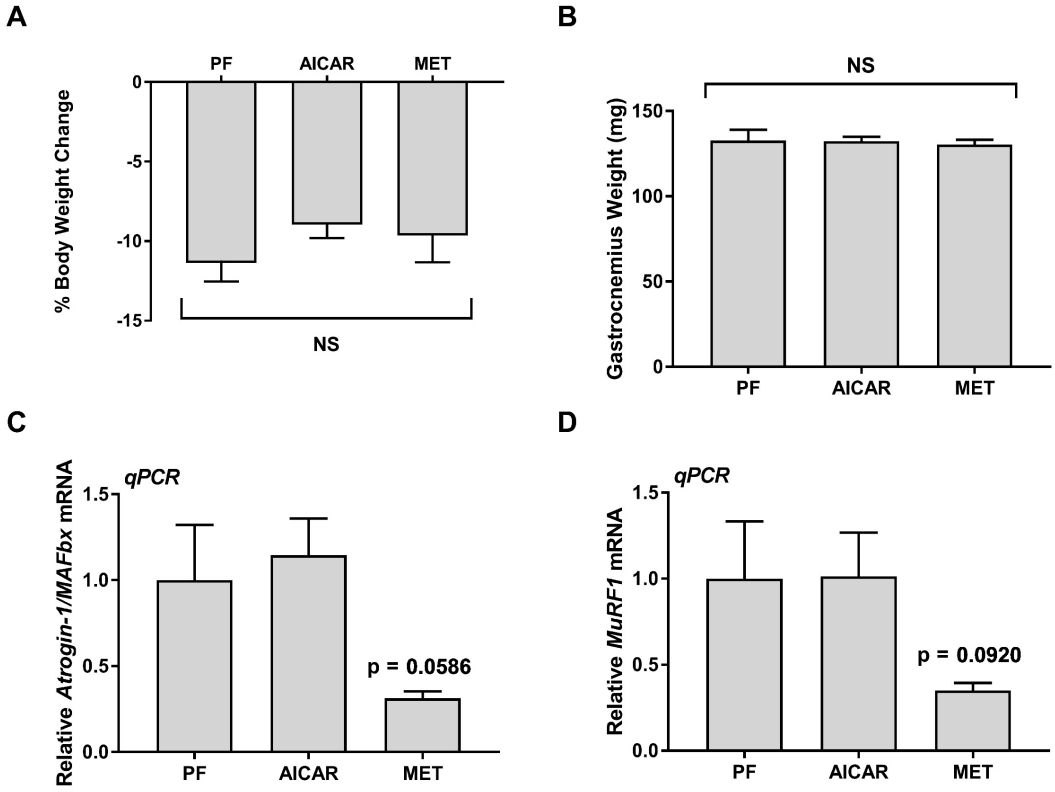

Figure 2.17: Single doses of AICAR or metformin alone do not affect body weight or muscle mass.

C57Bl/6 mice were intraperitoneally injected with either AICAR (500mg kg-1), metformin (250mg kg-1), or an equivalent volume of saline. All cohorts were pair-fed (PF) to the food consumption rate of LPS injected mice. Tissue samples were collected 18h later.

(A) Percent body weight change.

(B) Gastrocnemius muscle weights.

(C-D) RT-qPCR analysis of Atrogin-1/MAFbx (C) and MuRF1 (D) mRNA expression from the tibialis anterior.

Data information: Results are derived from four mice per cohort (n = 4) and error bars represent the SEM. Significance between means was first determined using ANOVA. Significance p-values were calculated using Fisher's LSD. NS, not significant.

Taken together, the results from these animal studies show that AICAR can mitigate or prevent muscle atrophy in a variety of inflammatory disease contexts, including both chronic (cancer) and acute (sepsis, cytokine injection) conditions. This suggests that AMPK agonists that do not affect mitochondrial function could be used as novel therapies, in conjunction with other treatments, to prevent the loss of muscle mass in patients with chronic or acute inflammatory conditions.

2.5 Discussion

While AMPK has been associated with the progression of cachexia, its anti-inflammatory properties suggest that AMPK activation could be anti-cachectic, since inflammation is the primary driver of cachectic muscle wasting (Tisdale, 2009). To understand whether AMPK activation could prevent inflammation driven atrophy, we tested the effects of drug-induced AMPK activation in models of inflammatory muscle wasting. Interestingly, we found that the AMP-mimic AICAR, but not the mitochondrial inhibitor metformin, prevented inflammation-associated atrophy in both *in vitro* and *in vivo* models, despite both being commonly used as AMPK activators (Figs. 2.1, 2.12, 2.14, 2.16) (Grahame Hardie, 2016). Prevention of atrophy correlated with restoration of oxidative metabolism and anabolic signaling, as well as impairment of one of the known effectors of muscle wasting, the iNOS/NO pathway (Figs. 2.3-2.5). Inhibition of AMPK activation with Compound C was found to block the protective effects of AICAR (Fig. 2.8). In addition, a more specific AMPK activator, A-769662, which activates AMPK through the beta subunit, was found to replicate the effects of AICAR (Fig. 2.9). AICAR and A-769662 were also found to be able to act synergistically to prevent atrophy in myotubes (Fig. 2.10). These results suggest that the beneficial effects of AICAR in cytokine-driven atrophy are likely to be AMPK-dependent. However, we also found that AMPK was activated by cytokines alone and metformin treatment. In these conditions, AMPK activation was instead associated with mitochondrial dysfunction, as well as impairment of mTOR and anabolism, in keeping with previous reports (White et al., 2011b; White et al., 2013) (Fig. 2.4, Fig. 2.6). Together, these observations indicate that the role of AMPK in inflammatory driven muscle atrophy is complex and likely context dependent.

The different outcomes of AMPK activation observed in our study are likely linked to the nature and timing of the activation. Our results indicate that cytokine-associated muscle wasting is accompanied by an elevation in the glycolytic rate and severely impaired mitochondrial oxidative respiration (Fig. 2.3). Importantly, metformin treatment alone had many of the same effects as inflammatory cytokine treatment. This is not surprising, as metformin has been shown to directly inhibit complex I in the electron transport chain (Andrzejewski et al., 2014; Bridges et al., 2014). Indeed, the activation of AMPK by metformin is believed to be an indirect consequence of the

metabolic stress induced by inhibition of oxidative phosphorylation and the resulting increase in cytoplasmic AMP levels (Grahame Hardie, 2016). Likely, this is also the mechanism behind the activation of AMPK during cytokine treatment alone. Importantly, we observed that both low and high doses of metformin induced wasting similar to cytokine treatment in C2C12 myotubes (Fig. 2.1C, 2.6). We also observed a reduction in both muscle mass (non-significant, Table 2.1) and CSA (significant, Fig. 2.12C) in the C26 and metformin co-treated cohort when compared to the C26 treated cohort. Therefore, it would appear that the mitochondrial toxicity of metformin supersedes any potential beneficial effects of the activation of AMPK in the context of inflammation associated atrophy, and it is possible that metformin treatment during inflammatory disease may even be detrimental to muscle mass, to an extent. From this, we conclude that AMPK activation during or after the induction of mitochondrial dysfunction, as is the case in cytokine and metformin treatment, but not AICAR, does not prevent muscle atrophy and likely contributes to the suppression of anabolic signaling through mTOR, as has previously been suggested (White et al., 2013). This activation, then, is likely to represent a later stage of inflammatory atrophic signaling. Consistent with this, we observed that AMPK is activated in the later stages of inflammatory signaling in muscle, both *in vitro* and *in vivo* (Fig. 2.1A, 2.2, 2.12B). This observation is corroborated by a previous study in the $Apc^{Min/+}$ colon cancer model that showed that AMPK activation occurs in the later stages of cachectic progression (White et al., 2011b). In contrast, ZMP, the active form of AICAR, and A-769662 both activate AMPK directly by binding to the gamma and beta subunits, respectively, and are not dependent on the energetic and metabolic status of the cell (Grahame Hardie, 2016). As a result, we observed that AICAR treatment was able to induce AMPK activation much earlier than cytokine treatment (Fig. 2.2). This early activation of AMPK by AICAR and/or A-769662, before the induction of metabolic stress, was associated with both a protection of metabolic function (Fig. 2.3) and the prevention of both myotube and muscle wasting (Fig. 2.1, 2.9, 2.10, 2.12, 2.16). Therefore, we propose that the activation of AMPK before the induction of metabolic stress, as is the case with AICAR and A-769662, can protect muscle from inflammation-induced atrophy, but that, induction of AMPK activity by metabolic stress, as is the case with metformin and cytokines, instead contributes to the suppression of anabolism.

One apparent contradiction that arises from this duality of AMPK function in inflammatory muscle wasting is the apparent ability for AMPK activation to be associated with both the suppression and recovery of anabolic signaling through mTOR and protein synthesis. Indeed, we observed that activation of AMPK during cytokine and metformin treatment was associated with a hypo-phosphorylation of both S6 kinase and S6 and a decreased rate of protein synthesis (Fig. 2.4, 2.6). As described above, this suppression has been linked to AMPK activity (White et al., 2011b; White et al., 2013). However, treatment with AICAR and/or A-769662 recovered S6K and S6 phosphorylation and protein translation, despite the fact that AMPK activity is known to inhibit mTOR (Inoki et al., 2012). Importantly, the doses of AICAR and A-769662 used in our studies were not associated with significant or persistent suppression of anabolic signaling when used alone (Fig. 2.4 and Fig. 2.9). Thus, we do not believe that AICAR or A-769662 induced AMPK activation directly affects mTOR signaling in our model, but rather indirectly restores it by inhibiting the upstream inflammatory events that eventually lead to anabolic repression. This suggests, again, that the context of AMPK activation during cachexia is likely to be critical, and that a therapeutic window exists for the use of AMPK agonists in cachexia. It is likely that activating AMPK would only be effective at the onset or early stages of cachexia development, before the induction of metabolic stress or anabolic signaling suppression. In contrast, in later stages of cachexia, AMPK inhibition might prove to be more therapeutically beneficial.

In addition to effects on metabolism and anabolic signaling, we found that the ability of the different AMPK activators to prevent, or not, the progression of muscle wasting correlated with inhibition of the expression of the pro-cachectic gene iNOS. We and others have previously shown that this enzyme plays a very important role as a downstream effector of inflammation driven wasting (Buck and Chojkier, 1996; Di Marco et al., 2012; Di Marco et al., 2005; Hall et al., 2011; Ma et al., 2017; Ramamoorthy et al., 2009). Also, we have previously shown that drugs that inhibit this enzyme can prevent cachexia, further highlighting the therapeutic relevancy of inhibiting iNOS expression (Di Marco et al., 2012; Di Marco et al., 2005; Ma et al., 2017). Therefore, it is likely that inhibition of iNOS is a key mechanism by which AMPK activation can prevent inflammation-driven muscle wasting.

A possible alternative explanation for the observations in this study is that the effects of AICAR

arise from an off-target pathway and are AMPK independent. Indeed AICAR treatment is known to activate AMPK-independent pathways (Quan et al., 2015; Rao et al., 2016). However, we found that the effects of AICAR treatment on atrophy, metabolism, mTOR signaling, and iNOS expression were all prevented by treatment with the AMPK inhibitor Compound C (Fig. 2.8). Importantly, Compound C has been described to inhibit inflammatory signaling independent of AMPK inhibition (Kim et al., 2011; Rao et al., 2016). If this effect was dominant in our model, Compound C treatment would be expected to enhance AICAR-mediated inhibition of the inflammatory phenotype. However, we observed the opposite effect, and found that Compound C impaired the anti-inflammatory effects of AICAR. Given this, it is likely that the observed effects of Compound C are dependent on the inhibition of AMPK activity. To further confirm that the effects of AICAR were AMPK dependent, we also tested A-769662, a more specific AMPK activating compound (Cool et al., 2006; Goransson et al., 2007; Sanders et al., 2007; Scott et al., 2008). We found that A-769662 had the same effects as AICAR in our models (Fig. 2.9). Importantly, A-769962 and the AICAR derivative ZMP have distinct chemical structures and bind to different subunits of AMPK heterotrimers (Grahame Hardie, 2016). In fact, A-769662 and AICAR have been shown to be able to activate AMPK synergistically (Ducommun et al., 2014). Consistent with this, our data show that co-treatments of sub-optimal doses of both AICAR and A-769662 were able to reverse the effects of cytokine treatment on myotubes (Fig. 2.10). Thus, given their chemical dissimilarity and the fact that co-treatment of the two compounds synergistically inhibits cytokine-induced myotube atrophy, it seems unlikely that the effects observed in our study can be explained by the convergence of separate off-target effects of these compounds. Therefore, there is strong evidence to suggest that the effects of AICAR and A-769662 treatment on inflammation-induced muscle wasting are through their ability to activate AMPK.

We found that AICAR administration was effective at preventing muscle atrophy in a variety of mouse models of cachexia. In the C26 model of cancer cachexia (Table 2.1, Fig. 2.12) and the LPS model of septic cachexia (Table 2.2, Fig. 2.16), as well as a model of cytokine-induced atrophy (Fig. 2.15), we found that AICAR, but not metformin prevented muscle loss. However, we did not see any effects on adipose tissue wasting, another important characteristic of cachectic wasting,

despite a previous study that found that an AMPK stabilizing peptide was effective at preventing adipose tissue wasting in cachexia (Table 2.1) (Rohm et al., 2016). This discrepancy is most likely due to the fact that AMPK protein levels are significantly depleted in cachectic adipose tissue, but not in skeletal muscle (Fig. 2.12) (Rohm et al., 2016). Therefore, administration of an AMPK agonist alone would be insufficient to recover adipose mass, as there would be no molecular target in said tissue. This suggests that the dual administration of an AMPK stabilizer and an AMPK agonist may effectively recover both lean muscle and adipose tissue mass during cachectic wasting.

Cachexia is a multifactorial disease, requiring a multimodal therapeutic approach. Our study strongly suggests that AMPK activators could represent a novel therapeutic development space for the treatment of a variety of cachectic conditions. Indeed, the therapeutic potential of AMPK activation is further unscored by the fact that AMPK activation can protect muscle in *mdx* mice and in Angiotensin II driven muscle atrophy (Pauly et al., 2012; Tabony et al., 2011). However, our findings, as discussed above, also indicate that there is likely a therapeutic window early on in the cachectic molecular pathophysiology during which AMPK activation is effective. In contrast, in the later stages of disease, AMPK inhibition might prove to be more beneficial, as has previously been suggested (White et al., 2013). It is clear that the role of AMPK in muscle related disease is complex, and more studies are needed to further understand how and when AMPK can be beneficial or detrimental, and when it is activation or inhibition could be used therapeutically. Greater understanding in this area could then lead to the development of novel therapeutics that could be used in concert with other treatments to combat the deadly cachexia syndrome.

2.6 Materials and Methods

Reagents and antibodies

IFNγ and TNFα were purchased from R&D Systems. AICAR and metformin were obtained from Toronto Research Chemicals (TRC) and Sigma-Aldrich, respectively. A-769662 and Compound C were obtained from TOCRIS Bioscience. Antibodies against pThr172-AMPKα (#2535), AMPKα (#2603), pSer79-ACC (#3661), ACC (#3662), pThr389-pS6K (#9205), S6K (#2708), pSer235/236-S6 (#2211), and S6 (#2317) were obtained from Cell Signaling Technology. Anti-iNOS antibody (#610431) was obtained from BD Transduction Laboratories. The anti-tubulin antibody (DSHB Hybridoma Product 6G7; deposited by Halfter, W.M.) and the anti-myosin heavy-chain antibody (DSHB Hybridoma Product MF20; deposited by Fischman, D.A.) were obtained from the Developmental Studies Hybridoma Bank, created by the NICHD of the NIH and maintained at The University of Iowa, Department of Biology, Iowa City, IA 52242. Anti-myoglobin antibody (ab77232) was obtained from Abcam.

Cell culture and treatment

C2C12 myoblast cells (ATCC, Manassas, VA, USA) were grown and maintained in Dulbecco's modified Eagle's medium (DMEM; Invitrogen) containing 20% fetal bovine serum (Sigma) and 1% penicillin/streptomycin (P/S) antibiotics (Invitrogen). Cells were routinely monitored for mycoplasma infection by DAPI staining. To differentiate, C2C12 cells were allowed to reach 90–100% confluence on plastic coated with a 0.1% gelatin solution and were then switched to DMEM containing 2% horse serum (Invitrogen) and 1% P/S. On the third or fourth day following induction of differentiation, myotubes were treated or not with IFNγ (100 U/ml) and TNFα (20 ng/ml; (Di Marco et al., 2012; Di Marco et al., 2005; Ma et al., 2017)). At the same time, cells were treated or not with either AICAR (0.5 mM), metformin (MET; 0.5 mM), or A-769662 (100 µM; (Goransson et al., 2007; Zhou et al., 2001)).

Animal models

All animal experiments were carried out with approval from the McGill University Faculty of Medicine Animal Care Committee and are in accordance with the guidelines set by the Canadian Council of Animal Care. Animals were randomly assigned to each treatment group by cage at the time of the experiment.

Cancer cachexia model

Male BALB/C mice, age 4–6 weeks weighing on average 23 g, were obtained from the Jackson Laboratory. Mice were injected subcutaneously in the right flank with either C26 colon cancer cells at 1.0–1.5 × 106 cells per animal or an equal volume of saline solution. Tumor growth was monitored by measuring tumor surface area every other day with calipers. On day 9 or day 12 post-injection, animals were injected intraperitoneally with either AICAR (500 mg/kg/day), metformin (250 mg/kg/day), or an equal volume of saline. Mice were injected every day thereafter at approximately the same time for the next 7 days. This dose of AICAR and metformin equate to a human equivalent dose of approximately 40 mg/kg/day and 20 mg/kg/day when accounting for surface area and are comparable to the doses reported in clinical trials using these compounds for cancer treatment (Bost et al., 2016; Nair and Jacob, 2016). On day 19–21 post-C26 cell injection, animals were euthanized by CO2 asphyxiation followed by cervical dislocation. Immediately following death, mice were exsanguinated and serum was frozen at −80°C. The muscle tissue and fat pad of each animal were then dissected and weighed immediately. After, muscles to be used for histological analysis were frozen in liquid nitrogen cooled isopentane (Sigma) and stored at −80°C. All other tissues were snap-frozen directly in liquid nitrogen.

LPS septic cachexia model

The LPS model of septic shock was performed on male C57Bl/6 mice age 8–12 weeks, weighing on average 26 g, obtained from Jackson Laboratory. LPS was prepared fresh the day of the experiment in a solution of 0.5% bovine serum albumin (BSA) in phosphate-buffered saline (PBS). LPS solution was then diluted with either additional saline for control cohorts or a PBS solution of either AICAR or metformin. The final dose of LPS administered was 1 mg/kg, which as previously been reported to induce muscle atrophy and muscle-specific E3 ligase expression (Braun et al., 2013; Doyle et al., 2011; Jin and Li, 2007). The final dose of AICAR was 500 mg/kg, and the final dose metformin was 250 mg/kg. Mice were injected intraperitoneally with the appropriate combination of compounds at the beginning of the dark cycle, between 18:30 and 19:30. All mice were separated into individual cages (1 mouse per cage) to allow for pair-feeding and food consumption monitoring. For pair-fed cohorts, mice were given the average food consumed by a pilot cohort of LPS-injected mice. Mice were euthanized the following day, approximately 18h after initial injection, as described above.

Intramuscular cytokine injection mouse model of atrophy

For intramuscular cytokine injection experiments, male C57Bl/6 mice age 4–6 weeks, weighing approximately 23 g were obtained from the Jackson Laboratory. Every day for 5 days, mice were intraperitoneally injected with either AICAR (350 mg/kg) or an equivalent volume of saline. One hour after, mice were intramuscularly injected with a cocktail of IFNγ/TNFα (7,500 U/mouse; 3 μg/mouse) or an equivalent volume of saline in the upper hind limb muscles. On the final day of injection, 3–4 h after the final injection of cytokines, mice were euthanized and tissues were weighed and collected as described in the C26 model of cancer cachexia.

Histological analysis of muscle cross-sectional area

Isopentane-frozen muscles were prepared for sectioning in a cryostat at −20°C to −30°C. Sections of 8–10 μm were obtained and stained using the hematoxylin and eosin (H&E) staining method. Stained samples were subsequently imaged by light microscopy. Muscle cross-sectional area was determined using ImageJ software to manually trace the circumference of individual fibers (Schneider et al., 2012).

Immunoblotting

Protein from C2C12 cells were extracted using a mammalian lysis buffer (50 mM HEPES pH 7.0, 150 mM NaCl, 10% glycerol, 1% Triton X-100, 10 mM sodium pyrophosphate, 100 mM NaF, 1 mM EGTA, 1.5 mM MgCl2). Immunoblotting analyses were performed using soluble fraction of whole protein lysates run on 7.5–12% acrylamide gels. Proteins were blotted on to nitrocellulose membranes, blocked with either 10% skim milk or 5% BSA in TRIS-buffered saline, 0.1% Tween (TBS-T) for 30–60 min, and probed with antibodies against iNOS (1:5,000 – 1:3,000), and pAMPK (1:5,000 – 1:1,000), AMPK (1:5000 – 1:1,000), pACC (1:5000–1:1,000), ACC (1:1,000), pS6K (1:2,000), S6K (1:5,000), pS6 (1:5,000), S6 (1:1,000), and α-tubulin (1:5,000). After washing with TBS-T, blots were subsequently probed with the appropriate horseradish peroxidase-conjugated secondary antibodies (1:5,000) and exposed to ECL reagent (Western Lightning Plus, Perkin Elmer). Signal was determined by exposure to photosensitive films. Quantifications of Western blot band signal density were performed using ImageJ software (Schneider et al., 2012).

Immunofluorescence and myotube diameter measurements

For immunofluorescence experiments, cells were first fixed in 3% paraformaldehyde for 30 min. Cells were then permeabilized in a solution containing 0.1% Triton X-100 and 1% goat serum in

phosphate-buffered saline. After washing with 1% goat serum phosphate-buffered saline, cells were incubated with antibodies against myosin heavy chain (MF-20; 1:1,000) and myoglobin (1:500) to visualize myotubes for 1 h at room temperature. Following further washing, cells were then incubated with appropriately labeled Alexa Fluor® (Invitrogen) secondary antibodies (1:500) for one hour at room temperature. Nuclei were visualized by DAPI staining (Miron et al., 2004). Cells were visualized using a Zeiss Observer.Z1 microscope with a 40× oil objective, and images were obtained using an AxioCam MRm digital camera. Myotube diameters were measured at 3 points along each cell using AxioVision Rel. 4.8 or Carl Zeiss Zen2 (blue) software.

Metabolic assays

Cellular glucose consumption and lactate production rates were determined by measuring media concentrations of glucose and lactate with a Flux Bioanalyzer (NOVA Biomedical) as previously described (Vincent et al., 2015). Extracellular flux rates were measured using the Seahorse Bioscience XFe24 Analyzer (Seahorse Bioscience—Agilent Technologies). On the day of seeding, the wells of an XF24 culture plate were coated with 1% gelatin for 30 min at room temperature. Excess gelatin was removed and C2C12 myoblasts were seeded at 2 × 104 cells/well in 20% FBS, 1% penicillin, streptomycin supplemented DMEM. The next day, cells were switched to 2% HS, 1% penicillin/streptomycin supplemented DMEM to initiate differentiation. On day 3 or day 4 of differentiation, cells were treated with IFNγ (100 U/ml)/TNFα (20 ng/ml) and/or AICAR or metformin (0.5 mM) in 2% HS, 1% pen./strep. media for 24 h. Approximately 1 h before beginning the assay, cells were switched to Seahorse Assay Media (Agilent 102353-100) supplemented with 25 mM glucose (Sigma—G7528) and 2 mM glutamine (ThermoFisher—25030149), adjusted to pH 7.4 at 37°C. Cells were subsequently incubated in a non-CO2 incubator for 1 h. The XF assay consisted of an initial 3 cycles of mix (3 min), pause (2 min), measure (3 min) to establish basal respiration. Oligomycin (final contraction 1 µM), FCCP (final concentration 1.5 µM), and rotenone and antimycin A (final concentrations 1 µM) were injected sequentially, with two measurement cycles (see above) following each injection. After the Seahorse assay was complete, cellular protein content was measured using an SRB assay as described in (Vichai and Kirtikara, 2006). In brief, cells were fixed in with trichloroacetic acid (TCA) at a final concentration of 3.3% (wt/vol) for 1 h at 4°C. After fixation, cells were washed with running distilled water and dried at room

temperature. Fixed cells were stained with a 1% acetic acid solution containing 0.057% SRB (wt/vol) for 30 min. at room temperature, followed by four washes with 1% acetic acid. Staining was solubilized by the addition of 10 mM Tris, pH 10.5, and absorbance at 510 nm was read using a Synergy Mx MultiMode Plate Reader. Absorbance at 510 nm was then relativized to the average absorbance for non-treated cells to determine the relative protein units (RPU). Extracellular flux rates were then normalized to the RPU for each well.

De novo protein synthesis

Analysis of de novo protein synthesis rates was performed as previously described (Di Marco et al., 2012). In brief, C2C12 myotubes were treated with IFNγ/TNFα and AMPK agonists, as described above. At the indicated time points, cells were incubated with EasyTag™ Express Protein Labelling Mix (PerkinElmer) at approximately 27.5 µCi/ml radioactivity for 30 min at 37°C. After, cells were lysed directly in SDS dye, resolved on a polyacrylamide gel, and stained with Coomassie Blue. Radioactivity was visualized by exposing dried gels to photosensitive film.

RT–qPCR

Total RNA was extracted from differentiated C2C12 cells treated as described above using TRIzol® (Invitrogen) according to the manufacturer's instructions. RNA quantity and quality were determined by spectrophotometric analysis using a Thermofisher NanoDrop™ reader (ND-1000) and by agarose gel electrophoresis. A reverse transcription reaction was performed using M-MLV Reverse Transcriptase (New England Biolabs). A negative control lacking the reverse transcriptase was also performed. Generated cDNA was then analyzed by qPCR using a Corbett RG-6000, and levels were normalized to GAPDH and subsequently relativized to the non-treated control for all experimental replicates. Primer sequences are given in Table 2.3.

Table 2.3: qPCR Primer Sequences

Gene	Protein	Gene ID	Forward Primer (5'-3')	Reverse Primer (5'-3')
Nos2	iNOS	18126	GTGCGCATGGCTCGGGATGT	GGCTGTCAGAGCCTCGTGGC
Gapdh	GAPDH	14433	AAGGTCATCCCAGAGCTGAA	AGGAGACAACCTGGTCCTCA
Myod1	MyoD	17927	CGACACCGCCTACTACAGTG	TTCTGTGTCGCTTAGGGATG
Myog	Myogenin	17928	CTACAGGCCTTGCTCAGCTC	AGATTGTGGGCGTCTGTAGG
Fbxo3	Atrogin-1 /MAFbx	67731	GACCGGCTACTGTGGAAGAG	CCAGGAGAGAATGTGGCAGT
Trim63	MuRF1	433766	GAGCAAGGCTTTGAGAACATGGACT	GCGTCCAGAGCGTGTCTCACT

AMPK siRNA knockdown and overexpression

C2C12 myoblast cells were transfected using jetPEI (Polyplus Transfection) according to the manufacturer's instructions. For myoblast knockdown experiments, cells were transfected at ~50% confluence with 50 nM of siRNA targeting the AMPKα1 subunit (Origene: #SR417172) or a universal scrambled negative control siRNA (Origene: #SR30004). 24 h after transfection, cells were treated with cytokines, as described above. 24 h after treatment, cells were collected and protein extracts were collected. For myoblast AMPK overexpression experiments, myoblasts were transfected as above with either a pcDNA3 vector expressing the cDNA sequence of the human AMPKα1 subunit or an empty vector control.

Statistics and data processing

For non-animal studies, n values indicate the number of times the experiment was independently replicated. For animal studies, n values indicate the number of animals per cohort. For animal studies, sample sizes were based on previous studies and expertise, with a minimum of three mice for any given statistical analysis. For in vitro studies, experimental replicates were excluded if the negative (non-treated) and positive (cytokine-treated) samples did not show an appropriate inflammatory response. For in vivo studies, mice were excluded if they developed complications unrelated to the cachexia phenotype or if they developed humane-intervention end-point complications early in the course of the study (e.g., ulceration of the tumor mass). Samples for measuring myotube widths and muscle fiber cross-sectional areas were blinded before

acquisition of images and during quantification. Graphs represent the mean, with error bars showing either the standard error of the mean for biological replicates or the standard deviation for technical replicates. Significance between means was first determined using ANOVA with Brown-Forsythe and D'Agostino & Person tests for variance similarity and normal distribution, respectively. Significance P-values were computed using Fisher's uncorrected LSD or the Student's t-test in GraphPad Prism version 6 and 7 for Windows, GraphPad Software, La Jolla California USA, http://www.graphpad. All P-values for main figures and tables and extended view figures can be found in Appendix Tables S2–S14 (online).

Data Availability

All relevant data pertaining to the studies conducted within this manuscript are available from the authors upon request.

2.7 Author Contributions

DTH contributed to conceptualization, conducted the investigation and validation of experimental findings, wrote the original draft, and performed the formal analysis and visualization of experimental findings. TG assisted with investigations, validations, and formal analysis of the metabolic studies, including the GC-MS and oxidative respiration studies. JFM, BJS, JS, AMKT, SM, and AO contributed to the investigations and validations of the cachectic models as well as to help with experiments to address reviewers' comments. RJF assisted in the conceptualization of animal and discussed results. NB helped with the design and execution of animal study. AP contributed with reagent, the interpretation of the results, and reviewed and edited the manuscript. SSW helped interpret the results, contributed to the design of animal studies, and reviewed and helped edit the manuscript. SDM assisted with conceptualization, data analysis, and helped edit and review the manuscript. GRS helped in the conceptualization of animal studies, discussed and helped in the analysis of the results, and reviewed and helped edit the manuscript. RGJ provided materials, equipment, and supervision for conducting the metabolic studies and discussed and helped the analysis of the results and reviewed and helped edit the manuscript. I-EG conceptualized, established, and directed the execution of research goals, interpreted the data, reviewed, and edited the manuscript.

2.8 Conflict of Interest

The authors declare that they have no conflict of interest.

2.9 Acknowledgements

We are grateful to Erzsebet Nagy Kovacs for assistance with the animal studies. We thank Dr. John Silvius and Dr. Gerardo Ferbeyre for their ideas, suggestions, and guidance. This work is funded by a Canadian Cancer Society Research Institute (CCSRI) Innovation Grant (702565), a CIHR operating grant (MOP-142399, PJT-156397), and a Qatar National Research Fund (QNRF) (NPRP8-457-3-101) to I.E.G, as well as a CIHR operating grant (MOP-93799) to R.G.J., Canadian Cancer Society Research Institute – Innovation grant (#703394) to S.S.W. G.R.S. is a Canada Research Chair in Metabolism and Obesity and the J. Bruce Duncan Chair in Metabolic Diseases and acknowledges funding from CIHR-125980-1 and the Canadian Cancer Society Research and Innovation Fund. D.T.H. was funded by a scholarship received from the Canadian Institute of Health Research (CIHR) funded Chemical Biology Program at McGill University.

Chapter 3 | Identification of iNOS as a Driver of Metabolic Dysfunction in Cachexia

3.1 Preface

Our study on AMPK in cachexia found that protection of metabolic function correlated with prevention of atrophy. We observed a dramatic inhibition of oxidative respiration during cytokine treatment, consistent with several other reports showing impaired mitochondrial function and loss of ETC complex activity in cachectic muscle (Der-Torossian et al., 2013; Fermoselle et al., 2013; Julienne et al., 2012; McLean et al., 2014; Padrao et al., 2013; Pin et al., 2019a; Puppa et al., 2012). Direct activation of AMPK partially restored mitochondrial respiration and prevented atrophy, whereas indirect activation through mitochondrial inhibition was associated with atrophy. These findings suggest that mitochondrial dysfunction, specifically the impairment of OXPHOS, may represent a critical component of cachexia. However, the molecular mechanisms underlying this impairment are unknown. Therefore, we wished to investigate how cytokines induce mitochondrial dysfunction. In our previous study, we also identified differential effects on iNOS expression between direct and indirect AMPK activation. While we and others have previously observed that iNOS can mediate cytokine-induced atrophy, the downstream effects of iNOS expression are only partially understood (Hall et al., 2011). Interestingly, NO has been demonstrated in other systems to inhibit the ETC (Brown, 2001; Brown and Borutaite, 2004). As such, we hypothesized that iNOS activity might be the cause of mitochondrial dysfunction during cytokine treatment. In this chapter, we investigated this possibility and assessed the efficacy of iNOS inhibition in a pre-clinical model of cancer cachexia.

These findings and discussions are part of a manuscript currently in preparation for submission.

Hall DT, Sadek J, Colalillo B, Tremblay AK, Di Marco S, and Gallouzi IE. “Inducible Nitric Oxide Synthase Impairs Mitochondria Oxidative Phosphorylation in Cachexia” *Manuscript in preparation.*

3.2 Abstract

Cachexia syndrome develops in patients with chronic inflammatory diseases, such as cancer, and is characterized by progressive muscle wasting. In addition, cachectic muscle has functional and metabolic defects that occur before the onset of atrophy. This has been linked to impaired mitochondrial function. However, the mechanisms driving mitochondrial dysfunction are unknown. In this study, we identified inducible nitric oxide synthase (iNOS) as an inhibitor of oxidative phosphorylation (OXPHOS) in cytokine-treated myotubes. We showed that inhibition of iNOS restores OXPHOS in myotubes treated with the cachectic cytokines IFNγ and TNFα. Also, we identified impairment of Complex II and Complex IV of the electron transport chain (ETC) as a potential cause of reduced mitochondrial respiration. We show that inhibition of OXPHOS in cytokine-treated cells reduces their bioenergetic capacity, leading to the onset of energetic stress, activation of AMPK, suppression of mTOR, and, ultimately, atrophy. Importantly, these effects were reversed by iNOS inhibition. We also demonstrate that the clinically developed iNOS inhibitor GW274150 can prevent loss of strength, impaired ETC complex activities, and atrophy in the C26 model of cancer cachexia. Together our data demonstrate a critical role for iNOS activity in the onset of muscle wasting and provide a proof-of-principle for the repurposing of iNOS inhibitors, such as GW274150, as novel therapeutics for the treatment of cachexia.

3.3 Introduction

Cachexia is a debilitating wasting syndrome that arises in numerous conditions, such as cancer, chronic obstructive pulmonary disorder (COPD), chronic heart failure (CHF), HIV infection, and sepsis (Farkas et al., 2013). It is characterized by a dramatic, involuntary loss of both lean muscle and adipose tissue mass (Blum et al., 2014; Fearon et al., 2011). Development of cachexia is associated with a significant increase in morbidity and mortality in patients due to loss of skeletal muscle function (Gannavarapu et al., 2018; Naito et al., 2017; Takayama et al., 2016; Vigano et al., 2017; Zhou et al., 2018). However, despite its significant impact on patient quality of life and chance for survival, there are currently no effective therapies for the treatment of cachexia. It is well accepted that cachexia is triggered by chronic inflammation and the upregulation of pro-cachectic inflammatory cytokines (Baracos et al., 2018; Fearon et al., 2012). However, efficacy from monotherapies targeting various pro-inflammatory cytokines has been difficult to develop due to the multifactorial nature of the condition (Jatoi et al., 2007; Jatoi et al., 2010; Wiedenmann et al., 2008). This highlights the need to identify downstream inducers of cachexia within effected tissues that integrate signals from multiple cytokines and which might be more effective targets for therapy.

Inflammatory cytokines are believed to induce muscle atrophy by triggering a catabolic state in muscle. Indeed, many cytokines induce the expression of the muscle-specific E3-ligases MuRF1 and Atrogin-1/MAFbx, which are well-established markers of atrophy during cachexia (Baracos et al., 2018; Fearon et al., 2012). Reduced anabolic signaling and protein synthesis have also been demonstrated in murine models of cachexia and human patients (Brown et al., 2018; Emery et al., 1984a; Hall et al., 2018; Puppa et al., 2014a; Smith and Tisdale, 1993; White et al., 2011b; White et al., 2013). Interestingly, recent observations have suggested that, in addition to alterations in protein homeostasis, cachectic muscle has significant functional impairment due to effects on metabolic function, primarily in mitochondria (Argiles et al., 2015a; Fearon et al., 2012; Hall et al., 2018; Porporato, 2016). Numerous studies have shown that cachectic muscle displays impaired oxidative phosphorylation (OXPHOS) that is associated with reduced electron transport chain (ETC) complex expression or activity (Brown et al., 2017; Der-Torossian et al., 2013; Fermoselle et al., 2013; Hall et al., 2018; Julienne et al., 2012; McLean et al., 2014; Padrao

et al., 2013; Pin et al., 2019a; Puppa et al., 2012; VanderVeen et al., 2018). In particular, reduced cytochrome c oxidase (Complex IV), succinate dehydrogenase (Complex II), and NADH dehydrogenase (Complex I) activity has been observed in cachectic muscle (Fermoselle et al., 2013; Julienne et al., 2012; Pin et al., 2019a; VanderVeen et al., 2018; White et al., 2012). In addition, other mitochondrial defects, such as increased uncoupling, altered fission and/or fusion, and abnormal morphology have been described (Antunes et al., 2014; Fontes-Oliveira et al., 2013; Shum et al., 2012; Tzika et al., 2013; White et al., 2012). This loss of mitochondrial function is correlated with a reduction in the rate of ATP production, suggesting that the energy balance of muscle is negatively impacted (Antunes et al., 2014; Constantinou et al., 2011; Pin et al., 2019a; Tzika et al., 2013). Many studies investigating metabolic impairment in cachectic muscle have demonstrated that these changes are induced by proinflammatory cytokines, such as TNFα and IL-6 (Der-Torossian et al., 2013; Fermoselle et al., 2013; White et al., 2012). Furthermore, mitochondrial dysfunction has been linked to NF-kB activity, suggesting that transcription of pro-inflammatory genes may be driving the affects on metabolic function (Der-Torossian et al., 2013; Fermoselle et al., 2013). However, the gene targets that drive inflammatory-mediated mitochondrial dysfunction in cachexia have yet to be identified.

Increased expression of inducible nitric oxide synthase (iNOS; *NOS2*) has previously been demonstrated to be a transcriptional target for pro-cachectic signaling (Buck and Chojkier, 1996; Di Marco et al., 2012; Di Marco et al., 2005; Hall et al., 2018; Hall et al., 2011; Ma et al., 2017; Ramamoorthy et al., 2009). iNOS is one of three isoform of nitric oxide synthase, along with endothelial (eNOS) and neuronal (nNOS), that produce nitric oxide (NO) from the breakdown of L-arginine to L-citrulline (Strijdom et al., 2009). While eNOS and nNOS are associated with physiological NO production and cellular signaling, iNOS expression and activity is strongly induced by inflammation and is associated with excessive NO production (Strijdom et al., 2009). The high levels of NO lead to the formation of peroxynitrite (ONOO-), a highly reactive species that induces nitrosative and oxidative stress (Szabo et al., 2007; Wiseman and Thurmond, 2012). Nitrosylation of proteins has been shown to be elevated in cachexia (Barreiro et al., 2005). Furthermore, we and others have demonstrated that chemical inhibition of iNOS or iNOS knockout can prevent TNFα or IFNγ/TNFα driven muscle wasting (Buck and Chojkier, 1996; Di

Marco et al., 2012; Di Marco et al., 2005; Hall et al., 2018; Ma et al., 2017). Importantly, in a recent study we have reported that iNOS knockout mice are resistant to wasting induced by intramuscular injection of IFNγ/TNFα (Ma et al., 2017), despite still expressing the E3 ligase MuRF1 (Di Marco et al., 2005). This suggests that iNOS drives atrophy independently from protein degradation. However, the mechanisms by which iNOS induction contributes to cachexia are still unknown.

In other systems NO and peroxynitrite have been shown to inhibit mitochondrial ETC activity (Brown, 2001; Brown and Borutaite, 2004). However, it is unknown if this inhibition plays a role in cachexia. Thus, we investigated if iNOS could be a driver of metabolic dysfunction in cachexia. Here, we show that cytokine treatment in C2C12 myotubes severely inhibits mitochondrial respiration, leading to a shift to glycolysis. Impairment of mitochondrial respiration correlated with the expression and activity of iNOS. Also, inhibition of iNOS with the clinically relevant iNOS inhibitor GW274150 or the investigational inhibitor aminoguanidine reversed the inhibition of mitochondrial respiration. Impaired mitochondrial activity was associated with a significant reduction in bioenergetic capacity and reduced ATP levels, leading to activation of AMP activated protein kinase (AMPK) and inhibition of mammalian target of rapamycin (mTOR). Importantly, these effects were reversed by inhibiting iNOS. Furthermore, mice treated with GW274150 are resistant to cancer cachexia-associated metabolic dysfunction and muscle wasting. These results demonstrate that iNOS is a key inducer of mitochondrial dysfunction in murine models of cachexia. They also show that inhibition of iNOS activity could represent a novel target to reduce cachectic muscle atrophy and restore metabolic function.

3.4 Results

3.4.1 Cytokine impairment of oxidative phosphorylation correlates with NO production

Several studies have shown that cachectic muscle has impaired mitochondrial function (Argiles et al., 2015a; Fearon et al., 2012; Porporato, 2016). In keeping with this, we have previously shown that C2C12 myotubes treated with the pro-cachectic cytokines IFNγ and TNFα have significantly reduced oxidative respiration, resulting in a shift to aerobic glycolysis (Hall et al., 2018). However, the mechanisms by which oxidative respiration is supressed are unknown. To determine how cytokine treatment impairs oxidative metabolism, we first assessed the timing of inhibition over the first 24h of treatment using a Seahorse Extracellular Flux analyzer. As we had previously seen, IFNγ/TNFα dramatically reduced the mitochondrial oxygen consumption rate (OCR_{mito}) after 24h (Fig. 3.1A) (Hall et al., 2018). However, inhibition of OCR_{mito} was not observed to occur until after 12 hours of treatment (Fig. 3.1A). This timing of inhibition was in keeping with a transcriptional signal transduction, as induction of gene expression can take several hours, whereas post-translational modification cascades, such as phosphorylation, typically occur rapidly (Deribe et al., 2010). We and others have previously shown that inducible nitric oxide synthase (iNOS) is a key mediator of cytokine driven atrophy that is transcriptionally induced following inflammatory stimulation (Buck and Chojkier, 1996; Di Marco et al., 2012; Di Marco et al., 2005; Hall et al., 2018; Ma et al., 2017; Ramamoorthy et al., 2009). In addition, NO has previously been associated with inhibition of ETC activity (Brown, 2001; Brown and Borutaite, 2004). Therefore, we speculated that iNOS could be driving the metabolic dysfunction in our model. We found that the timing of OCR inhibition coincided with a substantial increase in the levels of media nitrite, a stable product formed from the oxidation of NO, and iNOS protein expression, which were not detected until after 12h of treatment (Fig. 3.1B,C) . This correlation suggests that iNOS derived NO could indeed be the inducer of inhibition of mitochondrial respiration during cytokine treatment.

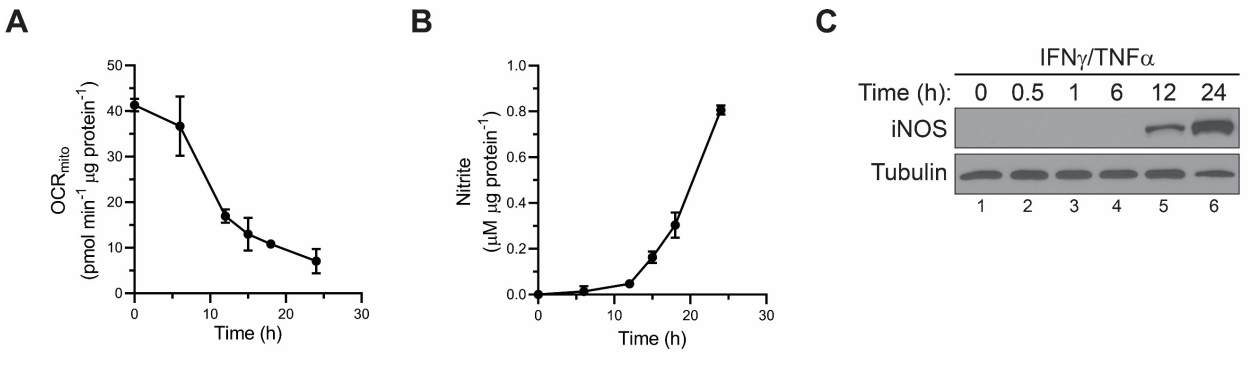

Figure 3.1: iNOS expression correlates with inhibition of oxidative respiration.

C2C12 myotubes were treated with IFNγ (100U/mL) and TNFα (20ng/mL) and assessed over 24h.

(A) Mitochondrial oxygen consumption rate (OCR_{mito}) was measured with a Seahorse XF analyzer.

(B) Media nitrite levels determined with GRIESS reagent.

(C) Western analysis of iNOS and Tubulin protein expression.

Data information: Results are a representative example of two independent experiments (n = 2). Error bars represent the standard deviation of technical triplicates.

3.4.2 Inhibition of iNOS activity restores oxidative metabolism

To test if iNOS mediates cytokine-driven impairment of mitochondrial respiration, we inhibited iNOS activity with the clinically developed iNOS inhibitor GW274150 (GW) and with the irreversible iNOS inhibitor aminoguanidine (AMG). GW is a highly specific inhibitor for iNOS over eNOS and nNOS and has been shown to have minimal toxicity (Vitecek et al., 2012). AMG is also a specific inhibitor of iNOS, but it is not under clinical development (Thornalley, 2003). Inhibition of iNOS with GW or with AMG reversed the effects of IFNγ/TNFα on OCR and the extracellular acidification rate (ECAR) (Fig. 3.2, Fig. 3.3). Using the methodology outlined by Mookerjee *et al*., we determined the theoretical basal and maximal rates of oxidative and glycolytic ATP production (J-ATP) from the OCR and ECAR and assessed the bioenergetic profile of the cells (Mookerjee et al., 2017, 2018). Determination of the initial J-ATP rates, when the cells are primarily consuming exogenous glucose, allows for the assessment of the cells basal energetic state ($J\text{-}ATP_{total}$), as well as preferences for either glycolytic ATP production ($J\text{-}ATP_{glycolytic}$) or mitochondrial oxidative phosphorylation ATP production ($J\text{-}ATP_{oxidative}$). By assessing the production rates following FCCP and monensin treatment, the theoretical maximal $J\text{-}ATP_{oxidative}$ and $J\text{-}ATP_{glycolytic}$ rates, respectively, can be determined. When plotted on perpendicular axes, the area defined by these maximal rates represent the bioenergetic profile, with the intersection of these two rates defining the maximal bioenergetic capacity of the cell (Mookerjee et al., 2017, 2018). Our analysis revealed that while control C2C12 cells have a highly oxidative metabolism, IFNγ/TNFα caused a dramatic shift in both basal and maximal metabolic activity towards glycolysis (Fig. 3.4A-B, Fig. 3.5A-B,). This shift was prevented by treatment with GW in a dose dependent manner and by treatment with AMG (Fig. 3.4A-B, Fig. 3.5A-B). These changes were reflected in the glycolytic index, a measure of how much of the total basal ATP production comes from glycolytic activity. In IFNγ/TNFα treated cells, the glycolytic index was 60%-95%, a dramatic increase from the approximately 10% index observed in control untreated cells (Fig. 3.4C, Fig. 3.5C). Treatment with GW or AMG had no significant effects on the glycolytic index in untreated cells but reduced the glycolytic index in cytokine treated cells (Fig. 3.4C, Fig. 3.5C). Importantly, control cells had a large capacity for oxidative respiration, which was dramatically reduced by cytokine treatment (Fig. 3.4A, Fig. 3.5A). While cytokines did increase the glycolytic capacity, it

was not sufficient to compensate for the loss of oxidative capacity. As a result, the total bioenergetic capacity in cytokine treated cells was significantly reduced (Fig. 3.4D, Fig. 3.5D). In addition, the basal rate of J-ATP production decreased in cytokine treated cells by 25-30% when compared to their control counterparts (Fig. 3.4B, Fig. 3.5B). However, treatment with GW, in addition to reverting the metabolism profile back to a more oxidative state, was able to partially recover the bioenergetic capacity and restore the basal ATP production rate (Fig. 3.4B,D). Treatment with AMG was also able to restore basal ATP production, but did not have as robust an affect on bioenergetic capacity (Fig. 3.5B,D). Nevertheless, the overall trend indicates that inhibition of iNOS prevents the shift towards glycolytic metabolism and loss of bioenergetic capacity induced by cytokines. Importantly, the extent of recovery of oxidative metabolism in GW treated and AMG treated cells correlated with the reduction of media nitrite levels (Fig. 3.4E, 3.5E). Indeed, when comparing the individual technical replicates of all IFNγ/TNFα, IFNγ/TNFα + GW 10μM, and IFNγ/TNFα + GW 100μM samples across all experimental replicates, there was a strong negative correlation between the media nitrite levels and the J-$ATP_{oxidative}$ rate (Fig. 3.4F). Therefore, our results indicate that nitric oxide production is the primary driver of cytokine-mediated oxidative respiration inhibition in our model.

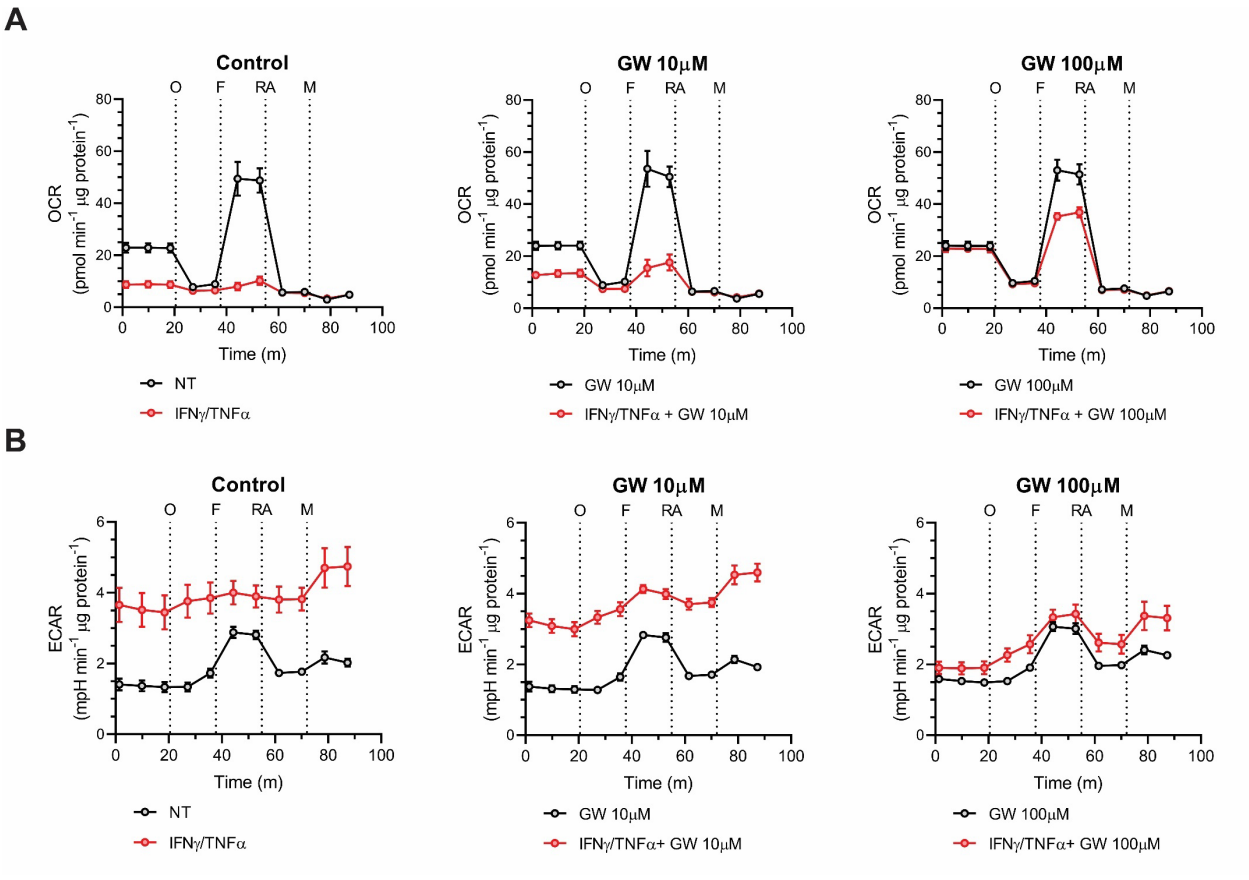

Figure 3.2: GW274150 reverses IFNγ/TNFα-induced suppression of OCR and elevation of ECAR.

C2C12 myotubes were treated with or without IFNγ (100U/mL) and TNFα (20ng/mL) and the indicated doses of GW274150 (GW). Extracellular flux was measured after 24h with a Seahorse XF Analyzer. Sequential injections of oligomycin (O, 1μM), FCCP (F, 1.5μM), Rotenone + Antimycin A (RA, 1μM), and monensin (M, 20μM) were performed to assess the bioenergetic profile.

(A) Oxygen consumption rate (OCR).

(B) Extracellular acidification rate (ECAR).

Data Information: Results are a representative example of three independent experiments (n = 3). Error bars represent the standard deviation of technical triplicates.

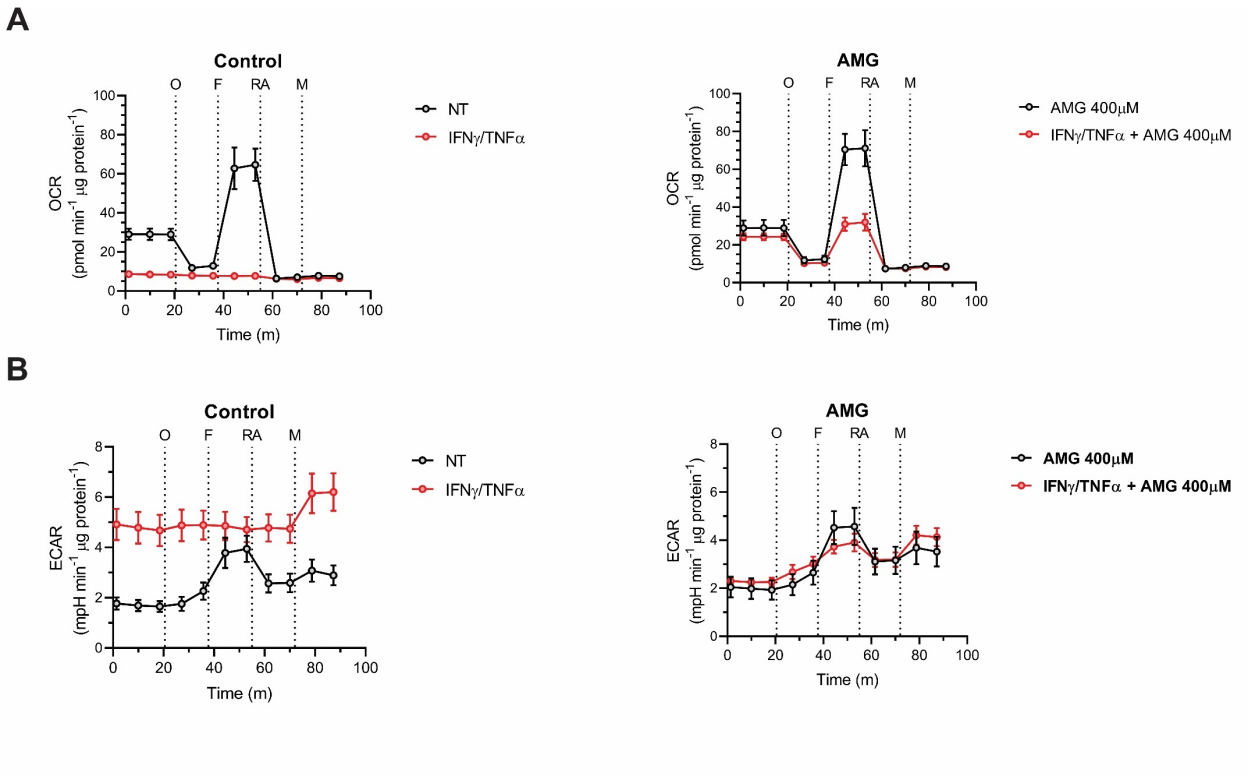

Figure 3.3: Aminoguanidine reverses IFNγ/TNFα-induced suppression of OCR and elevation of ECAR.

C2C12 myotubes were treated with or without IFNγ (100U/mL) and TNFα (20ng/mL) and aminoguanidine (AMG; 400µM). Extracellular flux was measured after 24h with a Seahorse XF analyzer. Sequential injections of oligomycin (O, 1µM), FCCP (F, 1.5µM), Rotenone + Antimycin A (RA, 1µM), and monensin (M, 20µM) were performed to assess the bioenergetic profile.

(A) Oxygen consumption rate (OCR).

(B) Extracellular acidification rate (ECAR).

Data Information: Results are a representative example of three independent experiments (n = 3). Error bars represent the standard deviation of technical triplicates.

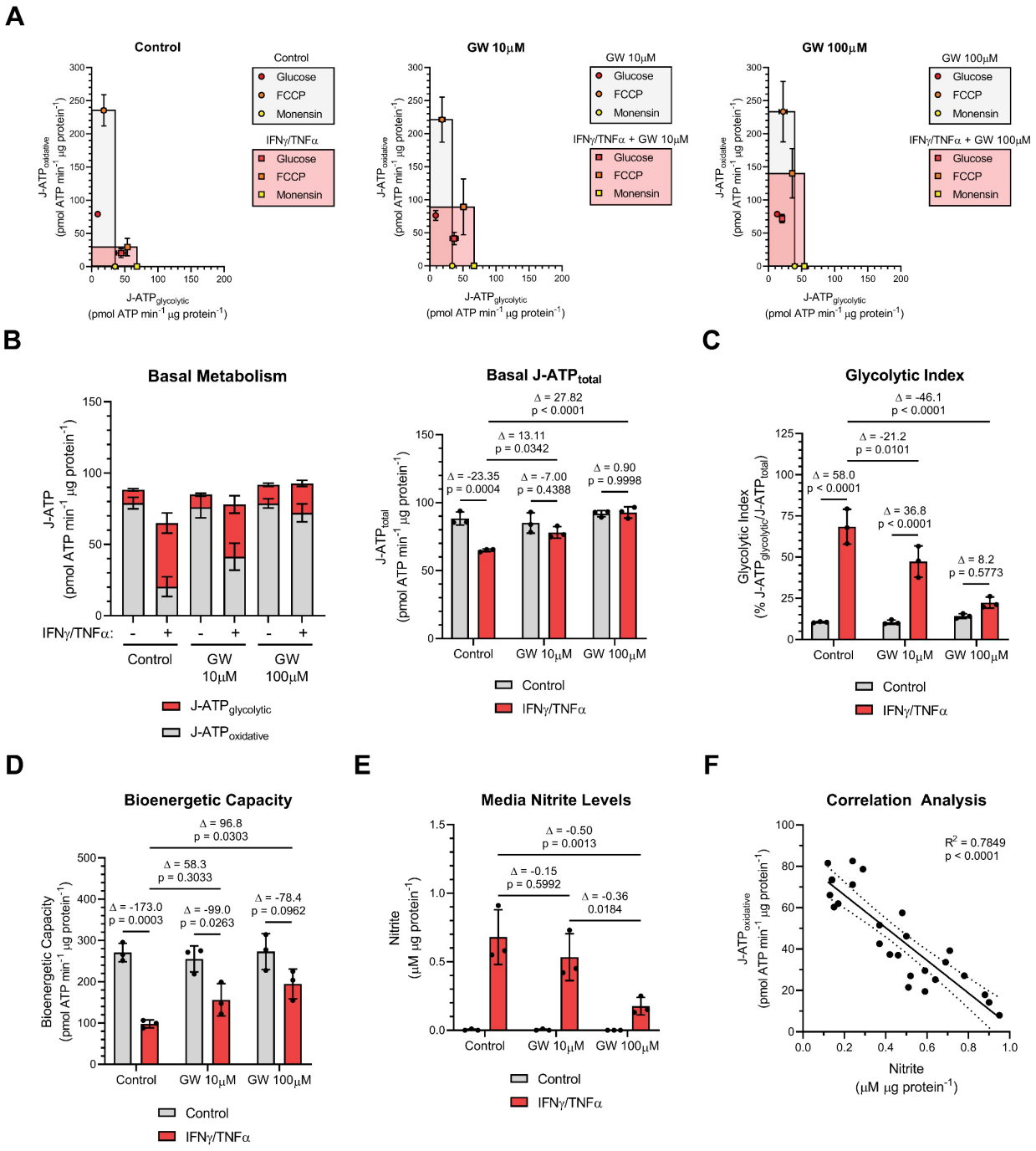

Figure 3.4: GW274150 prevents a cytokine-induced shift to aerobic glycolysis in C2C12.

C2C12 myotubes were treated with or without IFNγ (100U/mL) and TNFα (20ng/mL) and the indicated doses of GW274150 (GW). ATP production rates (J-ATP) from oxidative phosphorylation (oxidative) and glycolysis (glycolytic) were determined from measurements of extracellular flux 24h after treatment.

(A) Bioenergetic profiles. Highlighted squares are defined by the theoretical maximal $J\text{-}ATP_{oxidative}$ and $J\text{-}ATP_{glycolytic}$ rates.

(B) (*left)* Basal J-ATP$_{glycolytic}$ and J-ATP$_{oxidative}$ rates. (*right*) Total basal J-ATP rate.

(C) Glycolytic index (% J-ATP$_{glycolytic}$ / J-ATP$_{Total}$) of basal metabolism.

(D) Total bioenergetic capacity (sum of maximal J-ATP$_{glycolytic}$ and J-ATP$_{oxidative}$ rates).

(E) Media nitrite levels measured with standardized GRIESS reagent.

(F) Correlation analysis of replicate media nitrite levels to basal J-ATP$_{oxidative}$.

Data information: Individual data points represent the average of technical replicates from three independent experiments (n = 3). Error bars represent the standard deviation (SD) of the mean. For statistical comparisons, Δ indicates the fold change of mean values and p-values were calculated with an ANOVA followed by a Tukey's post-hoc test for multiple comparisons. Correlation was determined using linear regression and the p-value of the slope was determined with an F-test.

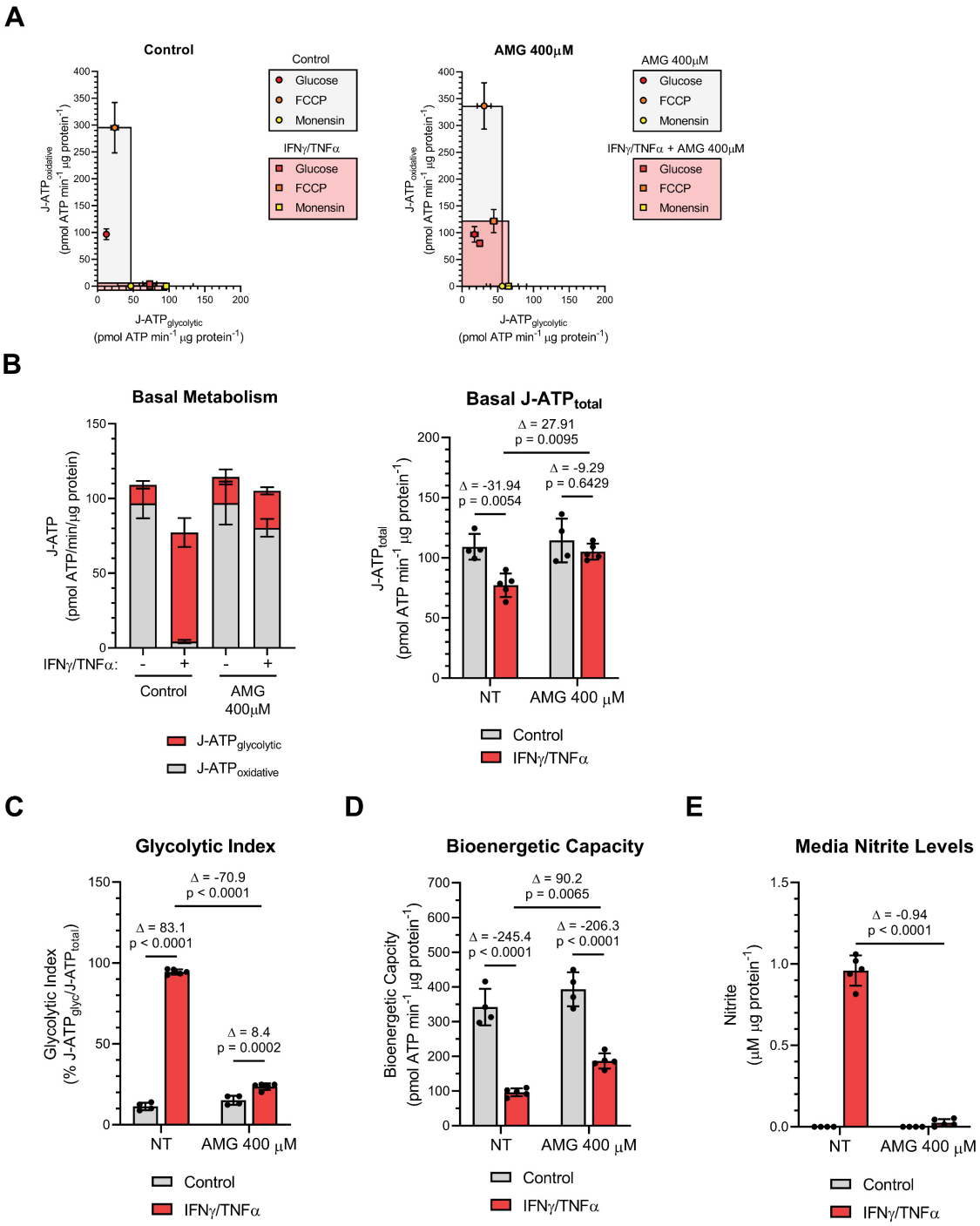

Figure 3.5: Aminoguanidine prevents a cytokine-induced shift to aerobic glycolysis in C2C12.

C2C12 myotubes were treated with or without IFNγ (100U/mL) and TNFα (20ng/mL) and aminoguanidine (AMG; 400μM). ATP production rates (J-ATP) from oxidative phosphorylation (oxidative) and glycolysis (glycolytic) were determined from measurements of extracellular flux 24h after treatment.

(A) Bioenergetic profiles. Highlighted squares are defined by the theoretical maximal J-$ATP_{oxidative}$ and J-$ATP_{glycolytic}$ rates.

(B) (*left)* Basal J-$ATP_{glycolytic}$ and J-$ATP_{oxidative}$ rates. (*right*) Total basal J-ATP rate.

(C) Glycolytic index (% J-$ATP_{glycolytic}$ / J-ATP_{Total}) of basal metabolism.

(D) Total bioenergetic capacity (sum of maximal J-$ATP_{glycolytic}$ and J-$ATP_{oxidative}$ rates).

(E) Media nitrite levels measured with standardized GRIESS reagent.

Data Information: Results are a representative example of three independent experimental replicates (n = 3). Individual data points are technical replicates from a representative experiment. Error bars represent the standard deviation (SD) of the mean. For statistical comparisons, Δ indicates the fold change of mean values and p-values were calculated with an ANOVA followed by a Tukey's post-hoc test for multiple comparisons.

To determine how nitric oxide affects oxidative respiration, we assessed the integrity of the ETC complexes. To do so, we performed a Western blot analysis probing for subunits of each complex. We found that cytokine treatment significantly reduced the levels of MTCO1 and SDHB, subunits of cytochrome c oxidase (COX; Complex IV) and succinate dehydrogenase (SDH; Complex II) by approximately 90% and 50% respectively (Fig. 3.6, Fig. 3.7). Expression of these subunits was re-established by treatment with GW or AMG (Fig. 3.6, Fig. 3.7). This indicates that the integrity of COX and SDH in the ETC is compromised during cytokine treatment in a NO-dependent manner. Interestingly, GW 10μM did not significantly affect ETC complex subunit expression (Fig. 3.6), despite partially restoring oxidative phosphorylation (Fig. 3.4). This suggests that the activity of the complexes is likely inhibited even in the absence of effects on complex subunit expression. Importantly, the expression levels of VDAC, an outer mitochondrial membrane pore protein, as well as the other complex subunits, were relatively stable, indicating that mitochondrial content was unaffected (Colombini et al., 1996). In keeping with this, mitochondrial content and expression of PGC-1α, a promoter of mitochondrial biogenesis, were not affected by cytokine treatment (Fig. 3.8). Therefore, the loss of oxidative phosphorylation appears to arise, at least in part, from the specific loss of integrity of Complex IV and Complex II in the ETC, rather than depletion of total mitochondrial content.

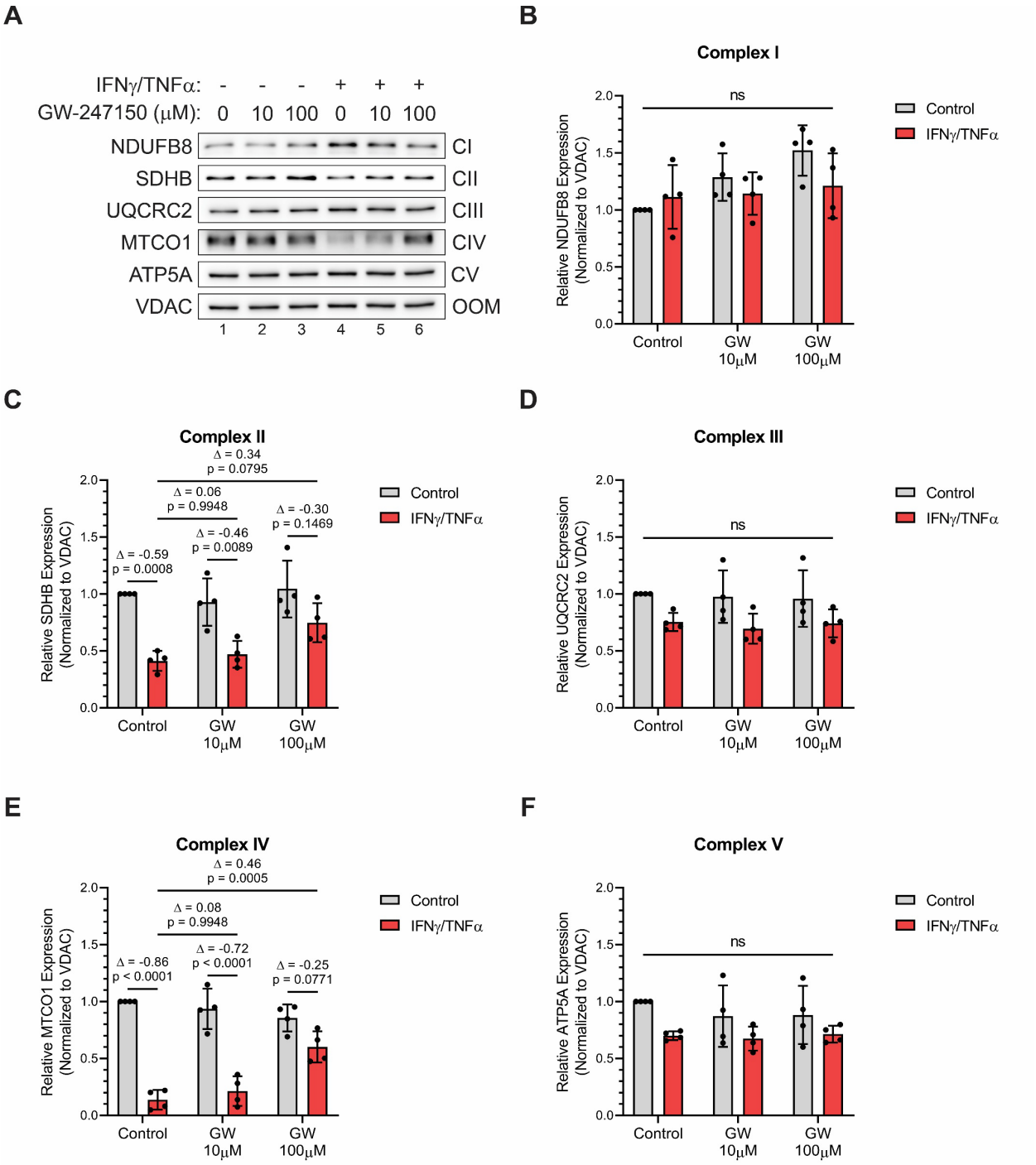

Figure 3.6: Cytokine-mediated loss of Complex II and IV integrity are reversed with GW274150.

C2C12 myotubes were treated with or without IFNγ (100U/mL) and TNFα (20ng/mL) and the indicated doses of GW274150 (GW). Protein content was extracted 24h after treatment.

(A) Western blot analysis for ETC protein complex subunits.

(B-F) Quantification of protein expression of complex subunits normalized to VDAC (Outer Mitochondrial Membrane; OMM) and relative to untreated control. (B) NDUFB8 (Complex I; CI)

(C) SDHB (Complex II; CII) (D) UQCRC2 (Complex III; CIII) (E) MTCO1 (Complex IV; CIV) (F) ATP5A (Complex V; CV).

Data information: Individual data points are from four independent experimental replicates (n = 4). Error bars represent the standard deviation (SD) of the mean. For statistical comparisons, Δ indicates the difference of mean values and p-values were calculated with an ANOVA followed by a Tukey's post-hoc test for multiple comparisons. Data sets where no statistically significance ($p > 0.05$) comparisons were observed are indicated as non-significant (ns).

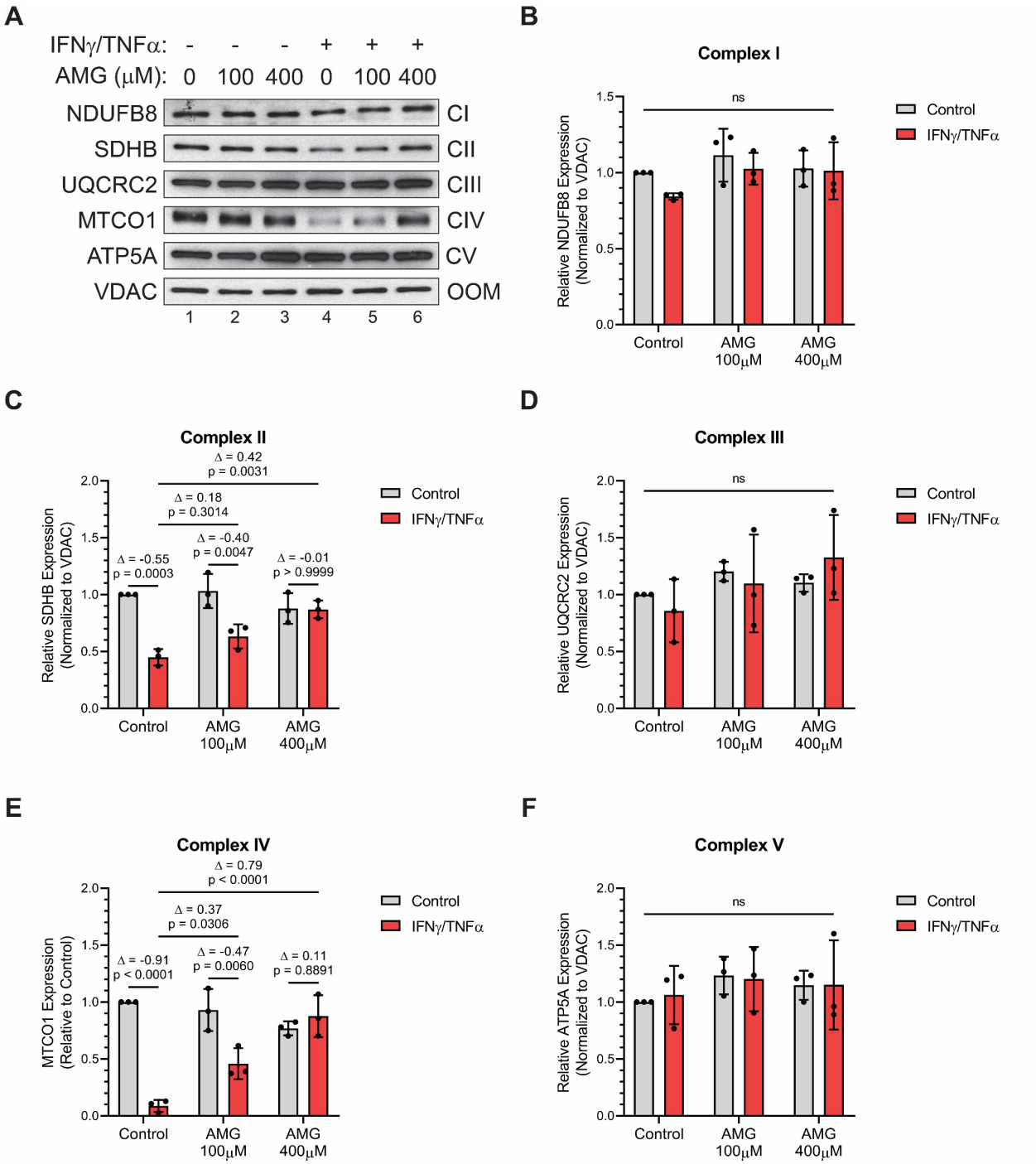

Figure 3.7: Cytokine-mediated loss of Complex II and IV integrity are reversed with aminoguanidine.

C2C12 myotubes were treated with or without IFNγ (100U/mL) and TNFα (20ng/mL) and the indicated doses of aminoguanidine (AMG). Protein content was extracted 24h after treatment.

(A) Western blot analysis for ETC protein complex subunits.

(B-F) Quantification of protein expression of complex subunits normalized to VDAC (Outer Mitochondrial Membrane; OMM) and relative to untreated control. (B) NDUFB8 (Complex I; CI) (C) SDHB (Complex II; CII) (D) UQCRC2 (Complex III; CIII) (E) MTCO1 (Complex IV; CIV) (F) ATP5A (Complex V; CV).

Data information: Individual data points are from three independent experimental replicates (n = 3). Error bars represent the standard deviation (SD) of the mean. For statistical comparisons, Δ indicates the difference of mean values and p-values were calculated with an ANOVA followed by a Tukey's post-hoc test for multiple comparisons. Data sets where no statistically significance ($p > 0.05$) comparisons were observed are indicated as non-significant (ns).

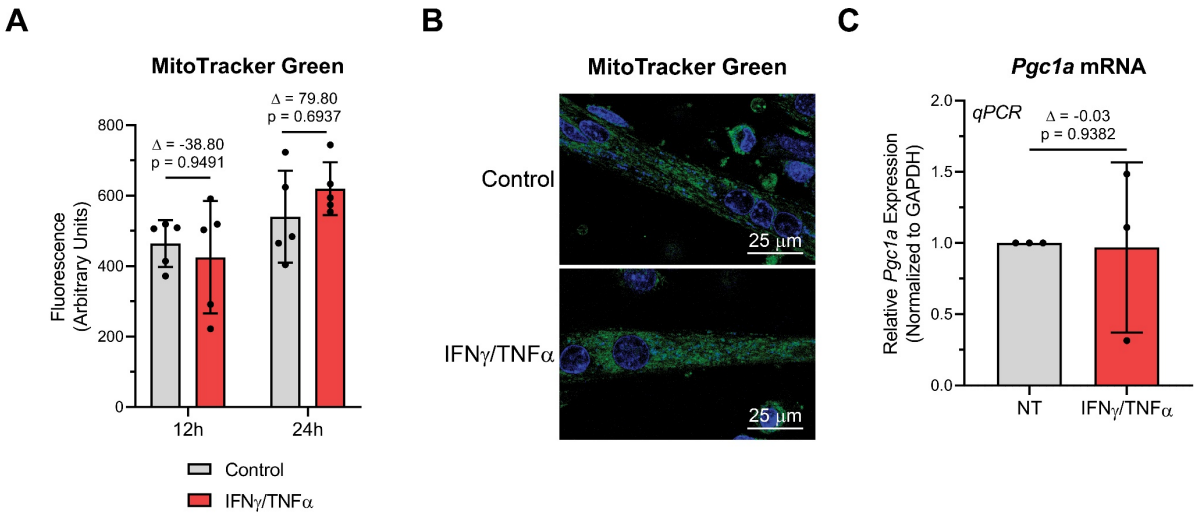

Figure 3.8: Mitochondrial content is unaffected by IFNγ/TNFα.

C2C12 myotubes were treated with or without IFNγ (100U/mL) and TNFα (20ng/mL) for 12h or 24h.

(A) Mitochondria content was assessed by MitoTracker™ Green FM staining (100nM).

(B) Confocal fluorescence microscopy images of MitoTracker™ Green FM (Green) and Hoechst 33342 (Blue) in cells treated for 24h.

(C) RT-qPCR analysis of *Pgc1a* mRNA expression in cells treated for 24h.

Data information: (A) Individual data points represent technical replicates. (B) Representative image of two independent experiments (n = 2). (C) Individual data points represent values from three independent experiments (n = 3). Error bars represent the standard deviation (SD) of the mean. For statistical comparisons, Δ indicates the fold change of mean values and p-values were calculated with either an ANOVA followed by a Tukey's post-hoc test for multiple comparisons (A) or a paired student's t-test (B).

3.4.3 Aerobic glycolysis during cytokine treatment is associated with energetic stress

The reduced ATP production rate observed in cytokine treated cells, as well as their overall lower bioenergetic capacity, suggests that the altered metabolic state in cytokine-treated myotubes might result in reduced ATP levels and energetic stress. In keeping with this, the cellular ATP levels were reduced by approximately 35% in cytokine treated cells, which was prevented by GW and AMG treatment (Fig. 3.9A-B). Depletion of ATP and subsequent accumulation of AMP can lead to the activation of AMP activated protein kinase (AMPK), an important regulator of energy homeostasis (Hardie et al., 2012). AMPK activation is dependent on phosphorylation at Thr172 (pAMPK) (Stein et al., 2000). In addition, AMPK activation is often highly correlated with phosphorylation of its downstream target ACC at Ser79 (Munday, 2002). Therefore, we assessed if the altered energetics correlated with AMPK activity by assessing AMPK and ACC phosphorylation. As we have previously shown, cytokine treatment induced AMPK phosphorylation, as well as phosphorylation of its downstream target ACC (Fig. 3.9C-D) (Hall et al., 2018). Induction of AMPK activity was reversed when cells were co-treated with GW, in keeping with the observed restoration of cellular ATP content (Fig. 3.9). Therefore, iNOS inhibition was able to prevent reduction of ATP content and the subsequent induction of energetic stress signaling in cytokine-treated myotubes.

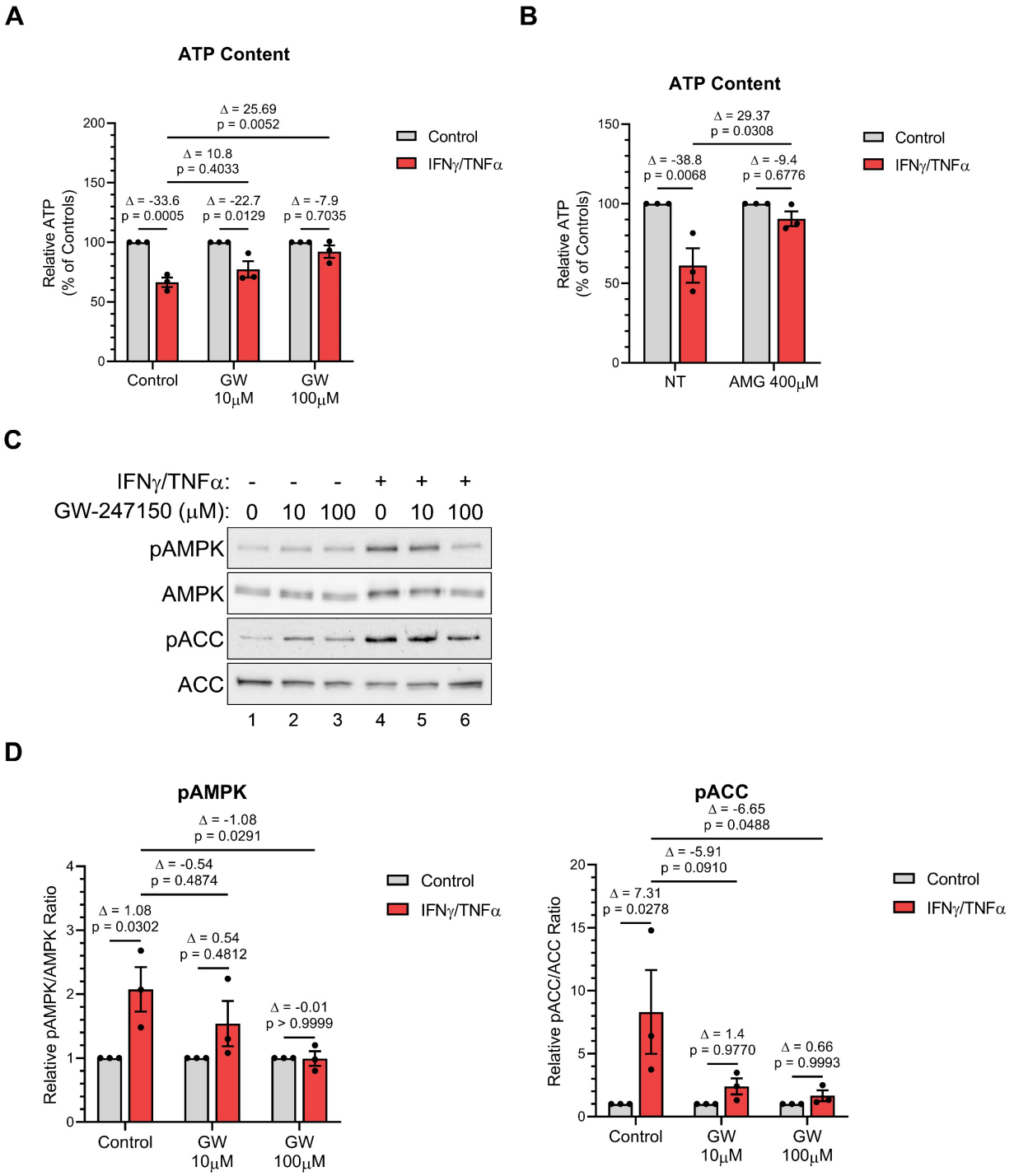

Figure 3.9: iNOS inhibition recovers cellular ATP levels and reduces AMPK activation.

C2C12 myotubes were treated with or without IFNγ (100U/mL) and TNFα (20ng/mL) and the indicated doses of GW274150 (GW) or aminoguanidine (AMG) for 24h.

(A-B) Cellular ATP content in (A) GW treated and (B) AMG treated cells. Quantified as a percentage of the corresponding control treatment ATP levels.

(C) Western blot analysis for pThr172-AMPK (pAMPK), total AMPK (AMPK), pSer79-ACC (pACC), and total ACC (ACC).

(D) Quantification of the (*left*) pAMPK to AMPK ratio and the (*right*) pACC to ACC ratio. Ratios are expressed relative to the corresponding control treatment ratios.

Data information: Individual data points are from three to four independent experimental replicates (n = 3-4). Error bars represent the standard deviation (SD) of the mean. For statistical comparisons, Δ indicates the difference of mean values and p-values were calculated with an ANOVA followed by a Tukey's post-hoc test for multiple comparisons.

3.4.4 Inhibition of iNOS recovers anabolic signaling through mTOR and prevents atrophy

One consequence of energetic stress is the inhibition of protein synthesis. mTOR is a central regulator of protein translation that is sensitive to both growth factors and cellular energy levels (Heberle et al., 2015). AMPK activation in cachexia has previously been linked to mTOR suppression and reduced protein synthesis and we have previously demonstrated that mTOR is heavily supressed in IFNγ/TNFα treatment (Hall et al., 2018; White et al., 2013). Therefore, we tested if suppression of mTOR could be reversed by iNOS inhibition by assessing phosphorylation of the mTOR targets ribosomal protein S6 kinase (S6K) and its target, ribosomal protein S6 (S6). We found that GW restored S6K and S6 phosphorylation in a dose dependent manner (Fig. 3.10). To assess if this had an impact on atrophy induced by cytokines, we assessed myotube widths by immunofluorescence staining for myosin heavy chain and myoglobin in cells treated with or without cytokines and GW and found that GW was able to prevent atrophy (Fig. 3.11). Thus, the restoration of metabolic function and prevention of energetic stress was also correlated with a restoration of protein synthesis signaling and prevention of atrophy.

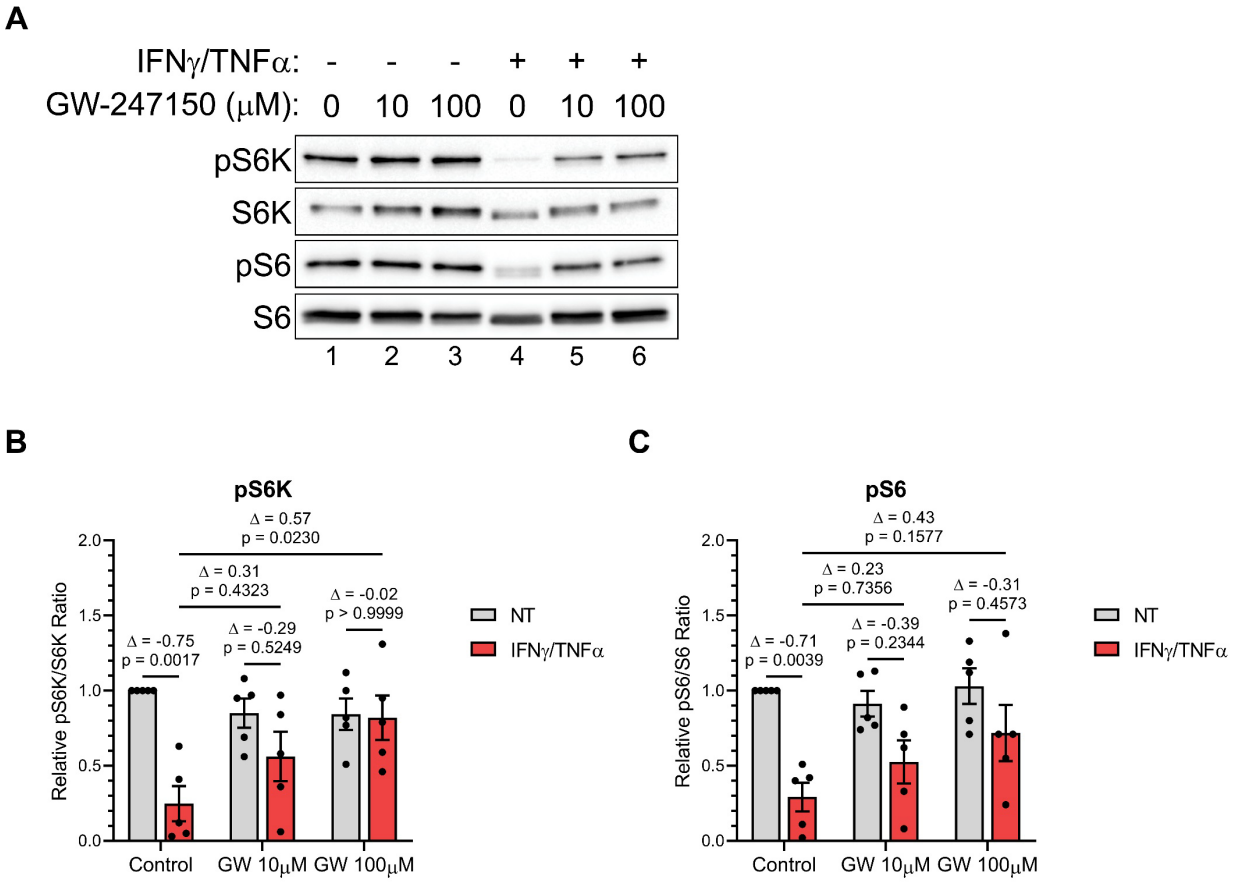

Figure 3.10: iNOS inhibition restores mTOR signaling in cytokine-treated myotubes.

C2C12 myotubes were treated with or without IFNγ (100U/mL) and TNFα (20ng/mL) and the indicated doses of GW274150 (GW). Protein content was extracted 48h after treatment.

(A) Western blot analysis for pThr389-S6K (pS6K), total S6K (S6K), pSer235/236-S6 (pS6), and total S6 (S6).

(B) Quantification of the pS6K to S6K ratio. Ratios are expressed relative to the untreated control.

(C) Quantification of the pS6 to S6 ratio. Ratios are expressed relative to the untreated control.

Data information: Individual data points are from five independent experimental replicates (n = 5). Error bars represent the standard deviation (SD) of the mean. For statistical comparisons, Δ indicates the difference of mean values and p-values were calculated with an ANOVA followed by a Tukey's post-hoc test for multiple comparisons.

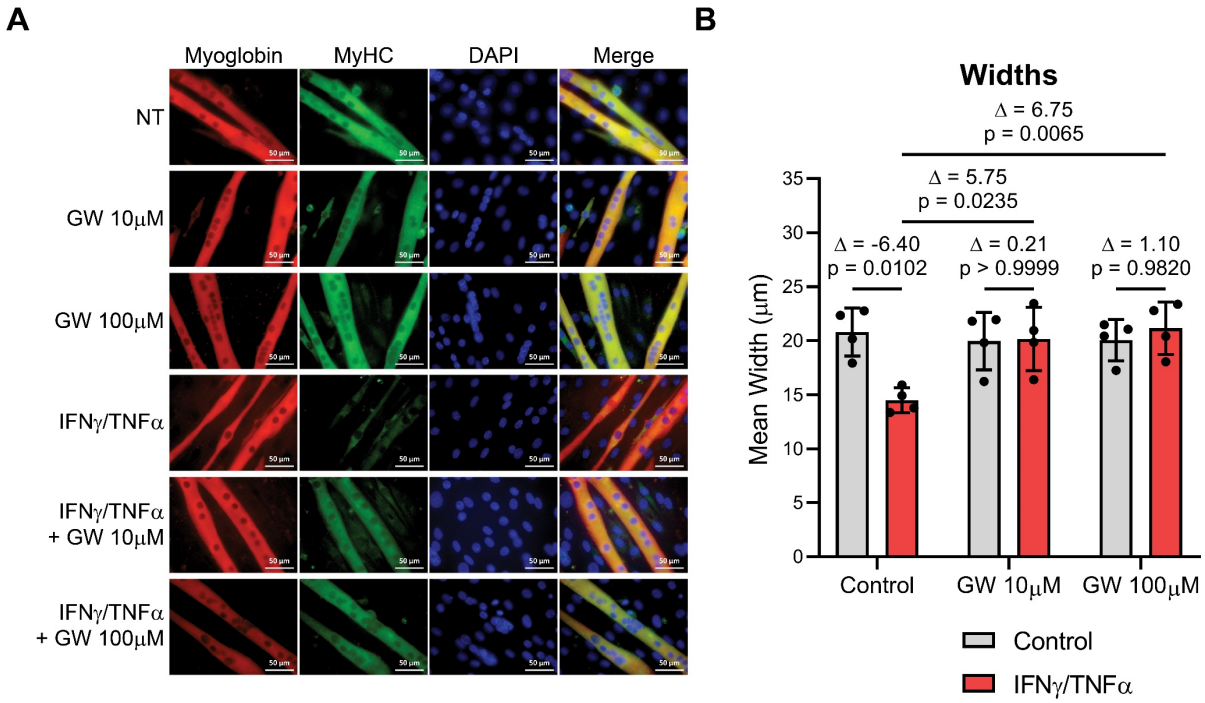

Figure 3.11: GW274150 treatment prevents cytokine-induced atrophy.

C2C12 myotubes were treated with or without IFNγ (100U/mL) and TNFα (20ng/mL) and the indicated doses of GW274150 (GW). Cells were fixed after 48h of treatment.

(A) Representative immunofluorescence imaging for myoglobin and myosin heavy chain (MyHC). Nuclei were visualized with DAPI staining.

(B) Quantification of mean fiber widths. Individual fiber widths were measured at three points along the fiber and averaged.

Data information: Individual data points are from four independent experimental replicates (n = 4). Error bars represent the standard deviation (SD) of the mean. For statistical comparisons, Δ indicates the difference of mean values and p-values were calculated with an ANOVA followed by a Tukey's post-hoc test for multiple comparisons.

3.4.5 GW274150 prevents muscle loss and metabolic dysfunction in a murine model of cancer cachexia.

We next wished to assess if iNOS inhibition could recover muscle function in a pre-clinical mouse model of cachexia. To do so, we tested the efficacy of GW treatment in the C26 adenocarcinoma model. Male BALB/C mice were injected with C26 colon cancer cells, which induce a cachectic phenotype over the course of 14-19 days (Bonetto et al., 2016). First, we confirmed that iNOS was induced in the muscle of C26-bearing mice (Fig. 3.12), as we have previously seen in our culture model (Di Marco et al., 2012). Importantly, iNOS inhibition has been shown to impair tumor growth (Garrido et al., 2017; Granados-Principal et al., 2015; Kostourou et al., 2011). Therefore, we delayed treatment for 5 days to allow tumors to establish before treating with GW. GW was administered at a dose of 5mg kg^{-1}, which has previously been shown to reduce collagen-induced arthritis symptoms in mice to an extent similar to that observed in iNOS knockout mice (Cuzzocrea et al., 2002). Delay of GW treatment did not affect tumor growth rates (Fig. 3.13). As such, final tumor burdens in C26 and C26 + GW cohorts were equivalent (Fig. 3.14A). In addition, swelling of the spleen, a marker of general inflammation, was equivalent in both cohorts (Fig. 3.14B). Therefore, tumor growth and general inflammation appeared to be unaffected by GW treatment.

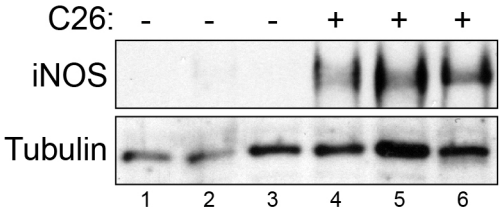

Figure 3.12: iNOS expression is elevated in muscle in the C26 model.

Male BALB/C mice were injected subcutaneously with C26 cells ($1.25x10^6$ cells) or an equivalent volume of saline. After 19 days, protein content was extracted from the gastrocnemius and assessed by Western blot analysis for iNOS and Tubulin expression.

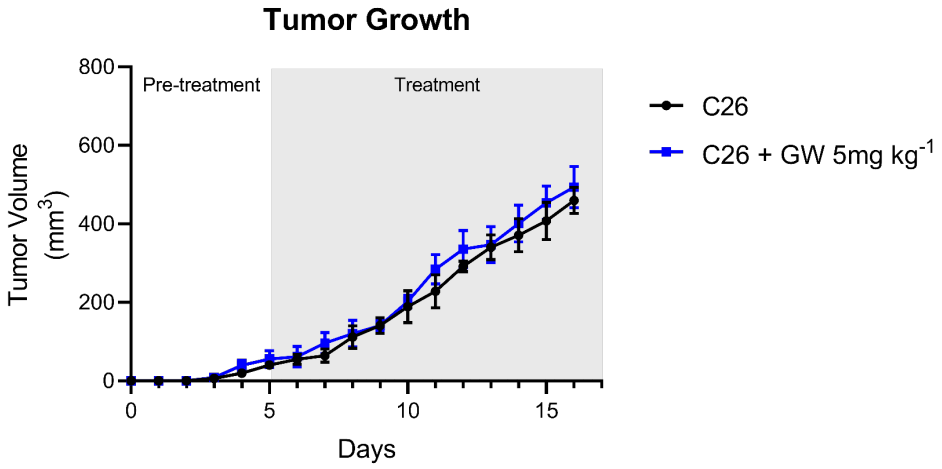

Figure 3.13: Tumor growth regression during GW274150 treatment.

Male BALB/C mice were injected subcutaneously with C26 cells ($1.25x10^6$ cells). After 5 days and everyday thereafter, mice were injected with either saline or GW 5mg kg^{-1}.

Data information: Data points represent the mean volumes of three mice in each cohort (n = 3). Error bars represent the standard deviation (SD) of the mean.

We next assessed the progression of cachexia in mice with normal tumor progression. In both C26 and C26 + GW treated cohorts, significant body weight loss was observed, though there was a trend towards increased weight in the C26 + GW (Fig. 3.14C). GW treatment did not affect adipose tissue wasting, which likely contributes significantly to the overall body weight change (Fig. 3.14D). However, in skeletal muscle tissue, GW treatment significantly improved mass. Indeed, in both the tibialis anterior and gastrocnemius, muscle wasting was reduced by approximately 50% (Fig. 3.14E-F). Thus, while overall body weight loss was unaffected, lean body weight was preserved by GW treatment.

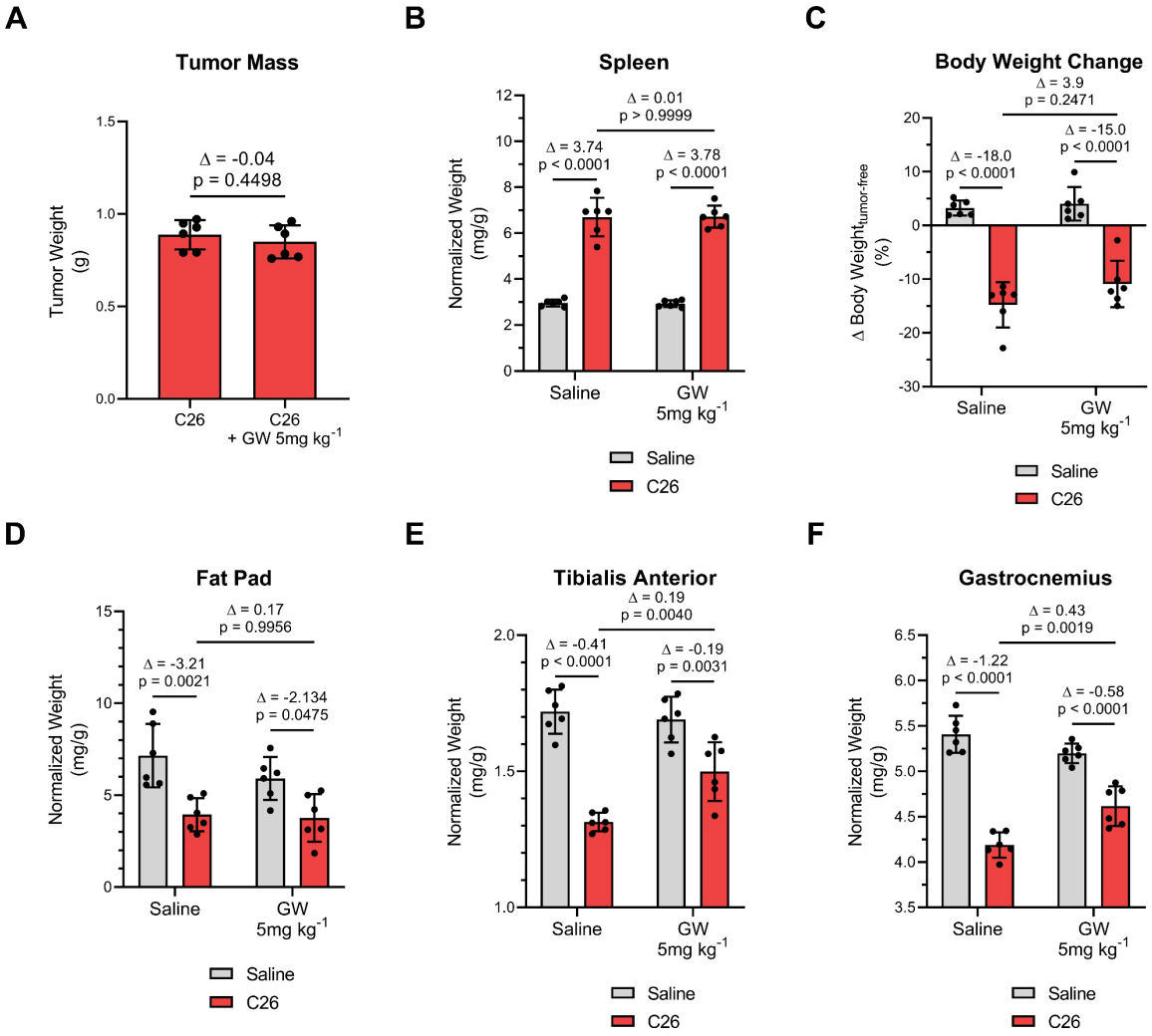

Figure 3.14: GW274150 treatment reduces muscle wasting in the C26 model.

Male BALB/C mice were injected subcutaneously with C26 cells ($1.25x10^6$ cells) or an equivalent volume of saline. After 5 days and everyday thereafter, mice were injected with either saline or GW 5mg kg^{-1}. After 16 days, mice were euthanized and body weight tissue mass was assessed.

(A) Tumor weight.

(B) Spleen weight normalized to initial body weight.

(C) Percent body weight change from day 0.

(D) Inguinal fat pad weight normalized to initial body weight.

(E) Tibialis anterior weight normalized to initial body weight.

(F) Gastrocnemius weight normalized to initial body weight.

Data information: Individual data points represent values from individual mice, with a total of six mice per cohort (n = 6). Error bars represent the standard deviation (SD) of the mean. For statistical comparisons, Δ indicates the difference of mean values and p-values were calculated with an ANOVA followed by a Tukey's post-hoc test for multiple comparisons.

In addition to wasting, cachexia is often associated with a functional deficit in muscle strength, possibly due to metabolic impairment (Murphy et al., 2012). Therefore, we measured grip strength changes in our model. As expected, C26 mice showed a substantial loss of grip strength (-17.6%) over the course of the experiment (Fig. 3.15A). However, there was no substantial loss of grip strength in GW treated mice, despite observable muscle mass wasting (Fig. 3.15A, 3.14E-F). This would suggest that, while GW treatment only partially prevented atrophy, muscle function was more significantly affected. To determine if GW treatment restored mitochondrial function, as we had seen in our culture model, we assessed Complex II and Complex IV activity in the lysates extracted from extensor digitorum longus (EDL) muscle. In keeping with previous reports of impaired Complex II and Complex IV activity in models of cachexia (Fermoselle et al., 2013; Julienne et al., 2012; Padrao et al., 2013; Pin et al., 2019a; VanderVeen et al., 2019; VanderVeen et al., 2018), we observed trends towards decreased activity in both complexes, though there was insufficient power in our experiment to detect statistical significance (achieved power: 0.79 (Complex II), 0.33 (Complex IV); Fig. 3.15B-C). Treatment with GW significantly increased Complex II activity in C26-bearing mice and showed a trend towards increased Complex IV activity, reflecting the recovery in metabolic function we had seen in our culture model (Fig. 3.15B-C). We also assessed ETC complex stability by assessing the protein levels of labile subunits of each complex, as we had done in our culture model. Interestingly, unlike in our culture model, we observed no changes in complex stability in the muscle of C26 mice (Fig. 3.16). This suggests that metabolic dysfunction in mice is less severe than what we observed in culture. Nevertheless, our results indicate that the C26 pre-clinical model is characterized by a loss of ETC function and muscle strength, which is restored by inhibition of iNOS. This confirms, in an *in vivo* model, that iNOS can drive metabolic dysfunction in cachexia.

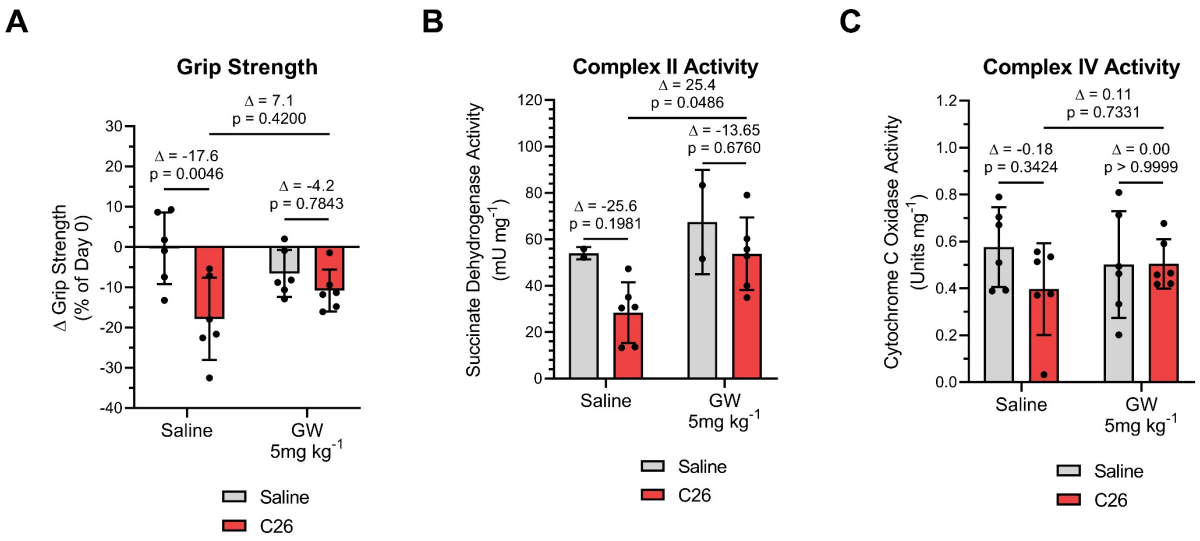

Figure 3.15: GW274150 treatment restores strength and metabolic function in the C26 model.

Male BALB/C mice were injected subcutaneously with C26 cells ($1.25x10^6$ cells) or an equivalent volume of saline. After 5 days and everyday thereafter, mice were injected with either saline or GW 5mg kg^{-1}.

(A) Change in grip strength from before tumor cell injection (day 0) and before endpoint collection (day 16).

(B) Complex II activity, normalized to protein content, measured in EDL muscle lysates collected after endpoint (day 16).

(C) Complex IV activity, normalized to protein content, measured in EDL muscle lysates collected after endpoint (day 16).

Data information: Individual data points represent values from individual mice, with a total of two or six mice per cohort (n = 2, n = 6). Error bars represent the standard deviation (SD) of the mean. For statistical comparisons, Δ indicates the difference of mean values and p-values were calculated with an ANOVA followed by a Tukey's post-hoc test for multiple comparisons.

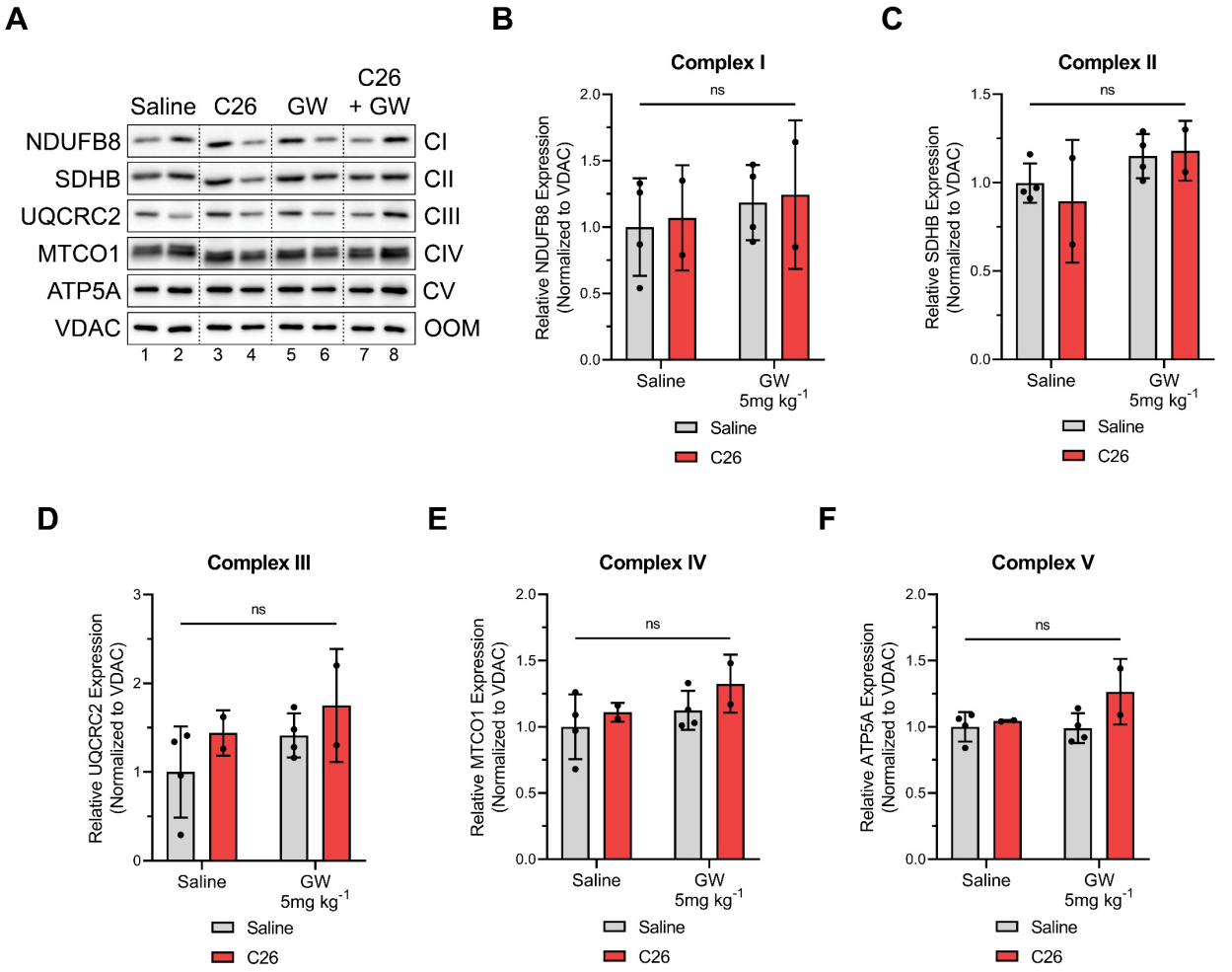

Figure 3.16: ETC complex integrity is not compromised in the C26 mouse model.

Male BALB/C mice were injected subcutaneously with C26 cells ($1.25x10^6$ cells) or an equivalent volume of saline. After 5 days and everyday thereafter, mice were injected with either saline or GW 5mg kg^{-1}. After 16 days, mice were euthanized and protein content was extracted from the quadriceps muscle.

(A) Western blot analysis for ETC protein complex subunits. Dashed lines indicate cropped segments. All images for each protein were obtained on the same exposure.

(B-F) Quantification of complex subunits normalized to VDAC (Outer Mitochondrial Membrane; OMM) and relative to untreated control. (B) NDUFB8 (Complex I; CI) (C) SDHB (Complex II; CII) (D) UQCRC2 (Complex III; CIII) (E) MTCO1 (Complex IV; CIV) (F) ATP5A (Complex V; CV).

Data information: Individual data points represent values from individual mice, with a total of two mice in C26-bearing cohorts or four mice in Saline control cohorts (n =2, n = 4). Error bars represent the standard deviation (SD) of the mean. Statistical comparisons were performed using an ANOVA, which found no statistically significant ($p > 0.05$) differences.

3.5 Discussion

The importance of metabolic function in cachectic muscle has become more apparent in recent years. In particular, mitochondrial dysfunction has been linked to impaired muscle function and atrophy during cachexia (Argiles et al., 2015a; VanderVeen et al., 2017). While numerous studies have demonstrated reduced activity of ETC complexes, the molecular origins of this dysfunction are unknown (Fermoselle et al., 2013; Julienne et al., 2012; Padrao et al., 2013; Pin et al., 2019a; VanderVeen et al., 2019; VanderVeen et al., 2018). Here, we identify iNOS as a potential inducer of inflammatory-dependent mitochondrial dysfunction. We show that reduced OXPHOS in IFNγ/TNFα-treated myotubes correlates with and is dependent on iNOS activity (Fig. 3.1-5). Loss of oxidative respiration is associated with a shift towards glycolysis, which has also been observed in murine models of cachexia (Cui et al., 2019a; Der-Torossian et al., 2013). Our bioenergetic analysis indicates that this shift towards glycolysis is not sufficient to maintain the basal ATP production rate or bioenergetic capacity (Fig. 3.4-5). Diminished ATP production was confirmed by a depletion of cellular ATP levels and activation of AMPK (Fig. 3.9). Reduced energy generation in muscle can limit contractile function and anabolic metabolism, which are hallmarks of the cachectic condition (Baker et al., 2010; Conley, 2016; Smiles et al., 2016). In keeping with this, we observed a suppression of mTOR signaling and onset of atrophy that were reversed by inhibition of iNOS (Fig. 3.10-11). Collectively, our study identifies iNOS as an inhibitor of mitochondrial function in cachectic muscle, which promotes energetic stress and the onset of muscle atrophy.

In this study, we report that reduced oxidative phosphorylation in cytokine-treated myotubes was associated with the loss of expression of SDHB and MTCO1, subunits of Complex II and IV respectively, indicating these complexes may be the primary targets of iNOS-derived NO (Fig. 3.6-7). This is in keeping with other reports showing that Complex II and Complex IV expression or activity are reduced in models of cachexia (Brown et al., 2017; Der-Torossian et al., 2013; Fermoselle et al., 2013; Julienne et al., 2012; McLean et al., 2014; Padrao et al., 2013; Pin et al., 2019a; Puppa et al., 2012; VanderVeen et al., 2019; VanderVeen et al., 2018). NO is known to be a reversible inhibitor of Complex IV, competing with oxygen binding (Taylor and Moncada, 2010). In addition, our group has previously identified the formation of the highly reactive peroxynitrite, formed from the reaction of superoxide with NO, as a driver of NO-mediated atrophy (Di Marco

et al., 2005). As the ETC is a direct source of ROS production, which is elevated in cachexia, it is possible that there is a higher local concentration of peroxynitrite near the ETC in mitochondria (Murphy, 2009). In addition, peroxynitrite-mediated nitration of Complex II and Complex IV has been demonstrated to impair their activity (Cassina and Radi, 1996; Chen et al., 2008; Radi et al., 1994; Sharpe and Cooper, 1998). Therefore, while our data does not reveal how NO inhibits Complex II and IV activity, it is possible that direct nitration of these complexes is involved. However, this will need to be confirmed experimentally, as NO may also have indirect effects on mitochondrial function. Importantly, we did not detect a loss of subunit expression in the muscle of C26 mice, despite seeing a trend towards decreased activity of both Complex II and Complex IV, which was reversed by treatment with GW274150 (Fig. 3.15, 3.16). Our study was not sufficiently powered to achieve statistical significance for these observed effects. However, the extent of reduced complex activity observed in our C26 mice is consistent with previous studies of Complex II activity in the C26 model (Pin et al., 2019a) and Complex IV in other cancer cachexia models (Fermoselle et al., 2013; Julienne et al., 2012; Padrao et al., 2013; VanderVeen et al., 2018). Therefore, the loss of complex activity, despite lack of reduced subunit expression, is likely a bona fide phenotype. This discrepancy may be due to differences in the severity of inhibition between our culture and animal models. Indeed, complex activity was only observed to decrease by approximately 20-25% in cachectic mice, whereas ETC activity in cytokine-treated myotubes was almost completely lost (Fig. 3.15B-C, Fig. 3.4, Fig. 3.5). We have found that iNOS expression and activity are extremely high in our culture model compared to *in vivo* (unpublished observation). Therefore, the extent of nitrosative stress is likely more severe than one might expect *in vivo*, manifesting a more extreme loss of ETC activity and loss of ETC protein expression. Nevertheless, the molecular targets of NO signaling, namely Complex II and Complex IV, appear to be consistent between our culture and animal models.

iNOS inhibition recovered basal metabolic function in our study. However, there was only limited recovery of maximal oxidative capacity, even when the activity of iNOS was almost completely inhibited, as determined by media nitrite levels (Fig. 3.4, 3.5). This suggests that other, iNOS-independent mechanisms may affect metabolic function. Total oxidative capacity is dependent both on the function of the ETC and the ability of the cell to utilize substrates for the

generation of reducing equivalents through the Tricarboxylic Acid (TCA) Cycle (Baker et al., 2010). While iNOS inhibition clearly restores ETC activity, altered substrate utilization has also been demonstrated in cachexia. Indeed, cachexia is associated with reduced pyruvate dehydrogenase (PDH) activity, which catalyzes the formation of acetyl-CoA from pyruvate (Pin et al., 2019a). This switch may be due to increased activity of pyruvate dehydrogenase kinase 4 (PDK4), which inhibits PDH and limits the flow of carbohydrate-derived pyruvate into the TCA cycle (Pin et al., 2019a; Pin et al., 2019b). Carbohydrate oxidation is a key source of energy generation during exercises, and so the reduced capacity to utilize carbohydrates for oxidative phosphorylation may limit muscle function during exercise (Melzer, 2011). While the restoration of ETC activity in our culture model was sufficient to recover basal ATP production, these cells are not under the same energetic demand of *in vivo* muscle during contraction. Therefore, combination therapies, such as co-treatment with iNOS and PDK4 inhibitors, that restore both ETC activity and normal substrate utilization, may be required to achieve full functional recovery in patients.

We and other have previously implicated iNOS as a potential target for therapeutic intervention (Hall et al., 2011). In mouse models of elevated cytokine treatment, either through CHO cells overexpressing TNFα or direct intramuscular injection of IFNγ/TNFα, chemical inhibition or genetic knockout of iNOS has been shown to prevent atrophy (Buck and Chojkier, 1996; Ma et al., 2017). However, the mechanism of iNOS-induced atrophy is not well understood. Previous evidence suggests that iNOS can negatively regulate myogenic gene expression by affecting MyoD expression and Jun-D activity (Buck and Chojkier, 1996; Di Marco et al., 2005). Here, we show that iNOS expression likely contributes to atrophy, at least in part, by impairing mitochondrial oxidative phosphorylation and inducing energetic stress. Furthermore, we show that iNOS inhibition can restore metabolic function and reduce muscle atrophy in the pre-clinical C26 model of cancer cachexia (Fig. 3.14-15). This demonstrates, for the first time, that iNOS inhibition has therapeutic potential in a disease-driven model of cachexia. Importantly, increased iNOS expression has been shown in the skeletal muscle of cancer, AIDS, chronic heart failure, and COPD cachexia patients, suggesting that iNOS may be involved in the onset of cachexia under a variety of overlying conditions (Adams et al., 2003; Agusti et al., 2004; Ramamoorthy et al., 2009). The inhibitor used in our studies, GW274150, has been developed clinically for other

inflammatory conditions, such as asthma, arthritis, and migraines (Vitecek et al., 2012). While efficacy in these diseases has been limited, the drug has been largely well tolerated, with good pharmacokinetics and minimal adverse events (Vitecek et al., 2012). As such, drug repurposing of GW274150, or other clinical iNOS inhibitors, may be warranted for the treatment of cachexia. Use of iNOS inhibitors may be particularly effective in cancer cachexia, given the potential pro-tumorigenic function of iNOS. Indeed, several studies have shown that iNOS inhibition can reduce tumor growth and metastasis (Garrido et al., 2017; Granados-Principal et al., 2015; Kostourou et al., 2011). More studies are warranted to firmly established the therapeutic potential of iNOS inhibitors in cachexia, especially in cancer cachexia, where inhibition may play a dual role in the treatment of both cancer and muscle wasting.

3.6 Materials and Methods

Reagents and Antibodies

IFNγ (485-MI) and TNFα (410-MT) were purchased from R&D systems. GW274150 (HY-12119) was purchased from MedChemExpress. Aminoguanidine (396494), DAPI (10236276001), oligomycin (75351), Rotenone (R8875), Antimycin A (A8674), and monensin (M5273) were purchased from Sigma-Aldrich. Hoechst 33342 (62249) and MitoTracker™ Green FM (M7514) were purchased from ThermoFisher Scientific. ECL Western Blotting Detection Reagent (RPN2106) was purchased from GE Healthcare Life Sciences.

The iNOS antibody (610431) was purchased from BD Transduction Laboratories. The tubulin antibody (DSHB Hybridoma Product 6G7; deposited by Halfter, W.M.) was obtained from the Developmental Studies Hybridoma Bank (DSHB), created by the NICHD of the NIF and maintained at The University of Iowa, Department of Biology, Iowa City, IA 52242. Total OXPHOS Rodent Antibody Cocktail (ab110413) containing five antibodies, one against a subunit of each ETC complex, was purchased from Abcam. VDAC (48665), pThr172-AMPKα (2535), total AMPKα (2603), pSer79-ACC (3661), total ACC (3662), pThr389-S6K (9205), total S6K (2708), pSer235/236-S6 (2211), and S6 (2317) antibodies were purchased from Cell Signaling Technology. The myoglobin antibody (ab77232) was purchased from Abcam. The myosin heavy chain antibody (DSHB Hybridoma Product MF20; deposited by Fischman, D.A.) was obtained from the DSHB. Horseradish Peroxidase (HRP) conjugated goat secondary antibodies against mouse (315-035-003) and rabbit (111-035-003) primary antibodies were obtained from Jackson ImmunoResearch Laboratories. Alexa Fluor™ 488 conjugated goat anti-mouse secondary (A11029) and Alex Fluor™ 594 conjugated goat anti-rabbit secondary (A11072) antibodies were purchased from ThermoFisher Scientific.

Cell Culture

C2C12 myoblast cells (ATCC, Manassas, VA, USA) were cultured as previously described (Hall et al., 2018). Cells were grown on 0.1% gelatin coated culture dishes (purchased from Corning) in DMEM (ThermoFisher 11995-065) supplemented with 20% fetal bovine serum (Sigma-Aldrich F1051) and 1% penicillin/streptomycin (Sigma-Aldrich P0781). Cells were differentiated upon reaching 90-100% confluence by switching to DMEM containing 2% horse serum (Invitrogen

16050122) and 1% penicillin/streptomycin. After three to four days, when cells had formed visible myotubes, cells were treated as described. Cells were monitored for mycoplasma infection by DAPI staining.

Media Nitrite Levels

Media nitrite levels were measured using GRIESS reagent as previously described (Di Marco et al., 2005). GRIESS reagent 1 (1% sulphanilamide, 5% phosphoric acid) and GRIESS reagent 2 (0.1% N-(1-napthyl)-ethylenediamine dihydrochloride) were mixed in a 1:1 ratio to make GRIESS assay reagent. A standard curve was generated using a serial dilution of sodium nitrite solution. Standards and unknown media samples were mixed in a 1:1 ratio with GRIESS assay reagent and left at room temperature for 5 minutes. Absorbance was subsequently measured at a wavelength of 543 nm and the nitrite concentration of unknown samples was determined by comparison to the standard curve.

Immunoblotting

Protein content was extracted from cells using a detergent lysis buffer (50mM HEPES pH 7.0, 150mM NaCl, 10% glycerol, 1% Triton® X-100, 10mM sodium pyrophosphate, 100mM NaF, 1mM EGTA, 1.5mM $MgCl_2$). Protein content from muscle was extracted by homogenizing muscle in ice cold muscle protein extraction buffer (PBS supplemented with 1% NP-40, 0.5% sodium deoxycholate, 50mM NaF, 5mM $Na_4P_2O_7$, and 0.1% SDS). The soluble protein fraction was clarified by centrifugation at 12,000g for 5 minutes at 4°C. and diluted with laemmli loading dye. Western blot analysis was performed with the Bio-Rad system. Proteins were resolved on acrylamide gels and transferred to nitrocellulose membranes using the Trans-Blot® Turbo™ system according to the manufacturer's instructions. Successful transfer was confirmed by reversible Ponceau S staining. Membranes were blocked in 10% skim milk and washed three times in TRIS-buffered saline containing 0.1% Tween (TBS-T). Membranes were incubated in primary antibodies diluted in either 0.5% skim milk or 0.5% BSA containing TBS-T overnight. Total OXPHOS Rodent antibody cocktail was diluted 1:1000. VDAC was diluted 1:5000. All other antibodies were diluted as previously reported (Hall et al., 2018). Primary antibodies were removed by washing three times in TBS-T. Membranes were then incubated in the appropriate HRP conjugated secondary antibodies diluted 1:5000-1:10,000 in 0.5% skim milk, TBS-T for 1h at

room temperature. Membranes were washed three times in TBS-T and exposed using ECL reagent. Chemiluminescent signal was detected using either photosensitive film or a Bio-Rad ChemiDoc™ imaging system. Densitometry quantification was performed using either ImageJ software (Schneider et al., 2012) or Bio-Rad Image Lab™ software.

Extracellular Flux and Bioenergetics Analysis

OCR and ECAR were determined using an Agilent Seahorse XFe24 Analyzer. Cells were grown and differentiated in XFe24 culture plates (1007777-004) as previously described (Hall et al., 2018). One hour before assessment, cells were carefully switched to XF Base Medium (103575-100) supplemented with 10mM D-glucose (Sigma G7528) and cultured in a CO_2-free incubator at 37°C, as described by the manufacturer. A XFe24 sensor cartridge (102340-100), calibrated overnight in a CO_2-free 37°C incubator according to the manufacturer's instructions, was loaded with Oligomycin (final concentration 1µM), FCCP (final concentration 1.5µM), Rotenone (final concentration 1µM) and Antimycin A (final concentration 1µM), and monensin (final concentration 20µM). After calibration, basal extracellular flux was measured in three cycles. Drugs were subsequently injected in the indicated order, with two measurement cycles between each injection. Measurement cycles consisted of a 3 minute mix, a 2 minute wait, and a 3 minute measurement. Media buffering capacity was determined at the time of the experiment using a sequential injection of HCl in two wells and ranged from 0.061 to 0.065mpH pmol $H^{+\,-1}$. Following completion of the run, individual well protein content was determined as previously described (Mookerjee et al., 2017). Cells were carefully washed three times in room temperature albumin-free Krebs-Ringer phosphate HEPES (KRPH) medium (2mM HEPES, 136mM NaCl, 2mM NaH_2PO_4, 3.7mM KCl, 1mM $MgCl_2$, 1.5mM $CaCl_2$, pH 7.4). Cells were lysed by adding 25µL of RIPA lysis buffer (150mM NaCl, 50 mM Tris, 1mM EGTA, 1mM EDTA, 1% Triton® X-100, 0.5% sodium deoxycholate, 0.1% SDS, pH 7.4) to each well. Plates were incubated on ice for 30 minutes and then agitated on a plate shaker for 5 min. Plates were placed back on ice and well protein content was determined using a BCA assay (ThermoFisher 23225) according to the manufacturer's instructions. Extracellular flux rates were normalized to protein content. Bioenergetic profiling was determined as detailed by Mookerjee *et al*. (Mookerjee et al., 2017, 2018).

RT-qPCR

RT-qPCR was performed as previously described (Hall et al., 2018). In brief, total RNA was extracted using TRIzol® (ThermoFisher 15596018) according to the manufacturer's instructions. RNA quality and quantity were determined using a ThermoFisher NanoDrop™ reader (ND-1000) and agarose gel electrophoresis. Following reverse transcription, cDNA was analyzed by qPCR in a Corbett RG-6000 with SsoFast™ Evagreen® Supermix (BioRad 1725200) using primers for *Pgc1α* (F: 5'-CAG GAA CAG CAG AGA CA-3', R: 5'-GTT AGG CCT GCA GTT CCA GA-3') and *Gapdh* (F: 5'-AAG GTC ATC CCA GAG CTG AA-3' R: 5'-AGG AGA CAA CCT GGT CCT CA-3').

MitoTracker Staining

C2C12 cells were grown and differentiated in 0.1% gelatin-coated black wall, clear bottom 96 well plates (Corning C3603) and ibidi® µ-Slides (80826) as described above. After 24h of treatment with or without cytokines, cells were washed twice with warm PBS and incubated at 37°C in base DMEM media (ThermoFisher A14430-01) supplemented with 25mM D-glucose, 2mM glutamine, 100nM of MitoTracker™ Green FM, and 10µM Hoechst 33342 for 30 minutes. After, cells were washed twice with warm PBS and refreshed with warm, supplemented DMEM without MitoTracker™ Green FM. For quantification of fluorescence signal, fluorescence in the 96 well plate was measured using a BioTek™ Synergy™ Mx Monochromator-Based MultiMode Reader. Signal was acquired using the bottom-read, auto-gain settings and 490/9 excitation and 516/9 emission filters. For imaging, cells in the ibidi® µ-Slides were live imaged in a 37°C, 5% CO_2 chamber using a Zeiss LSM710 Confocal Microscope.

ATP Content

Cellular ATP content was determined using the Invitrogen ATP Determination Kit (A22066) as described by the manufacturer. To prepare cell lysates, media was removed from a few wells at a time by manual pipetting to avoid drying. Wells were quickly washed once with room temperature PBS and then cells were lysed in ATP Assay Lysis Buffer (25mM Tris-HCl, 2mM DTT, 2mM EDTA, 10% glycerol, 1% Triton® X-100). After lysis buffer was added to all wells, the plate was agitated on a plate shaker for 5 minutes at room temperature. Plate was then placed on ice and ATP content was determined.

Immunofluorescence

Immunofluorescence was performed as previously described (Hall et al., 2018). In brief, cells were fixed in 3% paraformaldehyde for 30 minutes, permeabilized and blocked in 0.1% Triton® X-100, 1% goat serum (ThermoFisher 16210-064), incubated in primary antibodies against myosin heavy chain (MF-20; 1:1,000) and myoglobin (1:500) for one hour and, after washing, Alexa Fluor® secondary antibodies (1:500) for one hour, stained with DAPI, and mounted on coverslips with VECTASHIELD® Antifade Mounting Medium (Vector Laboratories H-1000). Samples were then blinded to the experimenter and cells were imaged with a Zeiss Observer Z1 microscope and AxioCam MRm digital camera. Myotube diameters were measured at three points along each cell using the Carl Zeiss Zen2 (blue) software.

Animal Models

Animal experiments were carried out with approval from the McGill University Faculty of Medicine Animal Care Committee and are in accordance with the guidelines set by the Canadian Council of Animal Care. Male BALB/C age 6-8 weeks were obtained from Jackson Laboratory. Mice were randomly assigned by cage to each treatment group. C26 cancer cells (kindly provided by Dr. Denis Guttridge) were thawed approximately 5 days before the planned injection day. Cells were cultured in DMEM supplemented with 10% fetal bovine serum and 1% penicillin/streptomycin. Cells were kept below 70% confluency and passed a minimal number of times before injection (typically 1-2 times). C26 were prepared in chilled, sterile PBS at a concentration of 1.25×10^7 cells mL^{-1}. Cells were briefly warmed before injection and 100µL was injected subcutaneously into the right flank (1.25×10^6 cells per mouse). For saline controls, an equivalent volume of saline was injected. Tumor growth was monitored by manual measurement with calipers. GW274150 was prepared ahead of time to a final concentration of 0.5mg mL^{-1} in PBS under sterile conditions and stores in single-use aliquots at -20°C. Five days after C26 injection and every day thereafter, mice were intraperitoneally injected with 10mL kg^{-1} of either GW274150 (final dose: 5mg kg^{-1}) or PBS. On day 16 post-C26 injection, mice were anesthetised with isoflurane gas and exsanguinated by cardiac puncture. Following cervical dislocation, tissues were rapidly dissected, weighed, and snap frozen in liquid nitrogen. One mouse in the C26 + GW cohort was excluded due to complete regression of the tumor during treatment. Two mice in the C26 cohort and one mouse in the C26+GW cohort were not included in the analysis due to no

detectable body weight change (non-cachectic) at the time of collection, despite normal tumor growth. Two mice in the C26 + GW cohort were excluded from the analysis due to development of complications determined to be independent from cachexia progression.

ETC Complex Activity Assays

The EDL muscle was rapidly removed from mice following euthanasia. Tendons were removed and muscle tissue was homogenized on ice in SDH Assay Buffer obtained from the Sigma-Aldrich Succinate Dehydrogenase Assay Kit (MAK197). Insoluble material was removed by centrifugation at 12,000g for 5 minutes at 4°C. Succinate dehydrogenase (Complex II) and cytochrome c oxidase (Complex IV) activities were then determined using the Sigma-Aldrich Succinate Dehydrogenase Assay Kit and the Cytochrome c Oxidase Assay Kit (CYTOCOX1) according to the manufacturer's instructions. Protein content was determined using the BCA assay kit and enzyme activity was normalized to protein concentration.

3.7 Acknowledgements

We are thankful to Shawn McGuirk for his help in understanding the intricacies of bioenergetic profiling. This work was funded by a CIHR operating grant (MOP-142399) and a CIHR project grant (PJT-159618) to Dr. Imed-Eddine Gallouzi. Derek Thomas Hall was funded by and a recipient of the James O. & Maria Meadows Studentship, the Maysie MacSporran Award, and the Charlotte and Leo Karassik Foundation Oncology PhD Fellowship.

Chapter 4 | General Discussion

4.1 Overview

The goal of this thesis was to further our understanding of the molecular mechanisms of cachexia and to identify novel potential targets for therapeutic development. To this end, we have uncovered a role for AMPK activation and iNOS in the regulation of metabolic function in muscle during cachexia. In Chapter 2, we show that although AMPK is activated during the normal progression of cachexia, direct AMPK activation, potentially before the onset of mitochondrial dysfunction, can protect mitochondria and prevent atrophy. In contrast, activation of AMPK following mitochondrial inhibition may contribute to muscle wasting. In Chapter 3, we demonstrate that inhibition of mitochondrial OXPHOS is mediated, at least in part, by the activity of iNOS. We also identify Complex II and Complex IV as targets of nitric oxide signaling. In both chapters, we observed that loss of mitochondrial energy generation was accompanied by an increase in glycolytic fermentation. However, in Chapter 3, we show that this switch to glycolysis is insufficient to maintain normal energy homeostasis, which is likely the underlying cause of AMPK activation during normal cachectic progression. Our data also show that loss of energy homeostasis leads to robust suppression of mTOR signaling and protein synthesis, culminating in atrophy. To assess the therapeutic potential of these findings, we tested the ability of the AMPK activator AICAR and the iNOS inhibitor GW274150 to prevent muscle atrophy in pre-clinical murine models of cachexia. We found that both direct AMPK activation and iNOS inhibition can prevent muscle atrophy in a cancer cachexia model. In addition, we show that AMPK activation can prevent muscle wasting in a model of septic cachexia. Together, this work demonstrates that restoring or protecting metabolic function, specifically in the mitochondria, can protect against cachectic muscle wasting. In addition, we also provide proof-of-principle in support of the use of AICAR-like drugs and the clinically tested compound GW274150 as novel tools to combat cancer-induced muscle wasting.

Although these studies advance our understanding of the mechanisms of cachexia, several unanswered questions remain. Of particular interest is dissecting the mechanisms underlying the paradoxically beneficial effects of AMPK activation, despite the fact that AMPK is also involved in promoting cachectic atrophy (White et al., 2013). Our work shows that direct AMPK activation

protects mitochondrial function and inhibits iNOS expression. However, it is unclear why metabolic dysfunction and iNOS expression are refractory to the AMPK activation that occurs during inflammation. In order to understand this, it will be necessary to discover how direct AMPK activation protects metabolic dysfunction and inhibits iNOS. Given that our results show that iNOS inhibits mitochondrial OXPHOS, it is possible that inhibition of iNOS might underly the recovery of metabolic dysfunction, but other mechanisms may also be involved. Ultimately, while our work provides proof-of-principle, future studies are needed to validate the therapeutic potential of AMPK activation and iNOS inhibition. As well, our studies focused mainly on mechanisms within mature muscle cells, but clinical cachexia involves complex interactions with numerous organs throughout the body. In addition, both AMPK and iNOS have been shown to affect muscle regeneration and satellite stem cell function (Fu et al., 2015; Rigamonti et al., 2013). Therefore, investigations on how AMPK activation or iNOS inhibition will affect other mechanisms of cachexia are needed.

4.2 How should AMPK be targeted for treatment of cachexia?

While our work suggests that AMPK activation can be beneficial for cachexia, others have shown that AMPK inhibition can also be beneficial (White et al., 2013). Interestingly, this paradoxical role for AMPK is not an uncommon paradigm, as AMPK activation has also been shown to be both pro- and anti-tumorigenic depending on the context (Faubert et al., 2015). Our current explanation for the dual role of AMPK in cachexia is that direct, early activation of AMPK protects metabolic function and impairs inflammatory signaling, but activation of AMPK following energetic stress promotes anabolic and catabolic pathways, contributing to atrophy. Both our study and the study by White *et al.* used the AMPK inhibitor Compound C to establish causative dependency on AMPK activation (White et al., 2013). However, Compound C is known to have numerous non-specific targets (Dasgupta and Seibel, 2018). Although we also used a second, more specific AMPK activator A-769662 to validate our results with AICAR and showed that these two compounds can synergize, the possibility remains that non-specific drug off-target effects might contribute to our findings (Cool et al., 2006; Ducommun et al., 2014). Thus, validation of the two roles of AMPK in promoting or preventing cachexia using genetic based models of AMPK depletion or activation may be necessary to firmly establish causality. To this end, we have begun

developing and assessing models of AMPK knockout and dominant-active overexpression. A preliminary pilot study of the LLC cancer cachexia model in muscle-specific AMPK knockout mice (AMPK-MKO) has shown a trend towards reduced muscle atrophy in knockout mice, with no apparent affects on tumor growth or spleen inflammation (Fig. 4.1) (O'Neill et al., 2011). We have also established a transfection-based protocol to overexpress a dominant active mutant of the AMPK α-subunit in C2C12 myotubes (Fig. 4.2) (Crute et al., 1998). We plan to use this system to assess the impact of genetic AMPK activation on cytokine-induced metabolic dysfunction and atrophy. Results from these studies will help to confirm the dual-role of AMPK in cachectic muscle atrophy.

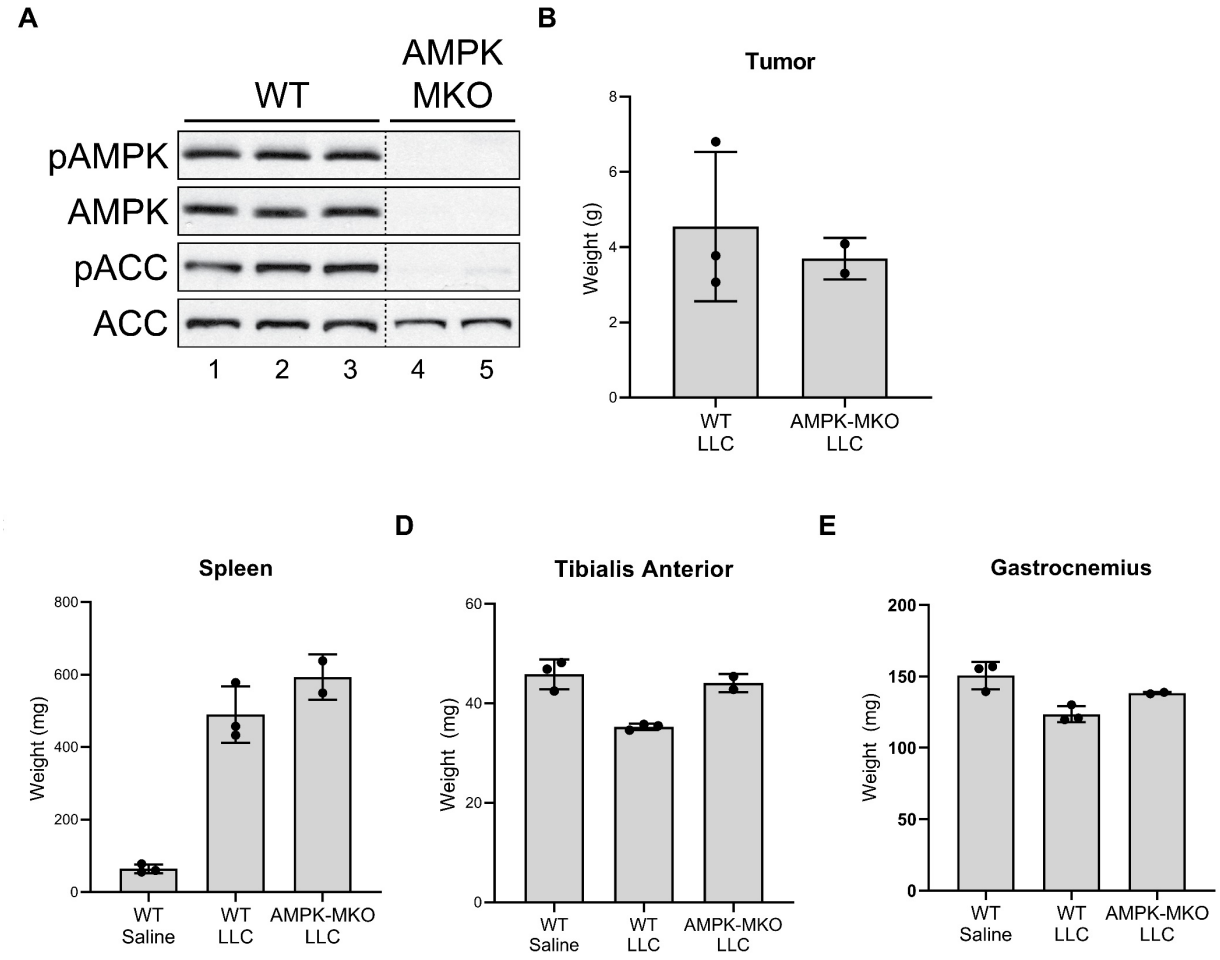

Figure 4.1: AMPK-MKO mice may be resistant to cancer-cachexia.

Wild-type C57BL/6 (WT) and C57BL/6 mice with muscle-specific genetic depletion of both subunits of the AMPK β-isoform (AMPK-MKO) were subcutaneously injected with 1.25 x 10^6 LLC cells or an equivalent volume of saline. After 25 days, mice were euthanized, and muscle and tissue samples were analyzed.

(A) Western blot analysis of pThr172-AMPK (pAMPK), total AMPK (AMPK), pSer79-ACC (pACC), and total ACC (ACC) from quadriceps protein content.

(B-E) Tissue weights of the tumor (B), spleen (C), tibialis anterior (D), and gastrocnemius (E).

Data information: Data points represent individual mice. Three WT, saline-treated (n = 3), three WT, LLC-treated (n = 3), and two AMPK-MKO, LLC-treated (n = 2) mice were analyzed. Error bars represent the standard deviation of the mean.

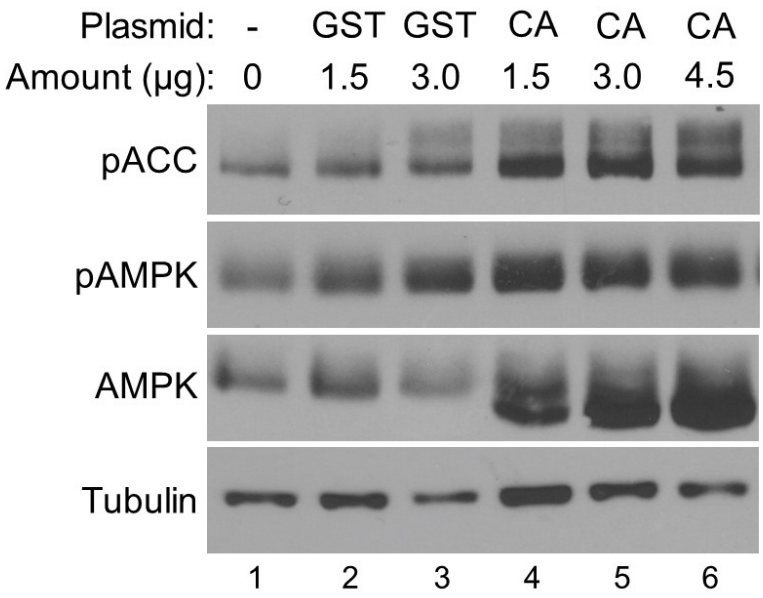

Figure 4.2: AMPK constitutively active mutant expression in C2C12 myotubes.

C2C12 myotubes were transiently transfected on day 0 of differentiation with a plasmid containing a GST-tagged, constitutively active (CA) AMPKα1 isoform with a truncated C-terminus (aa 1-312) or an empty vector control (GST). AMPK activity and expression were then assessed 5 days later by western blot analysis for pSer79-ACC (pACC), pThr172-AMPK (pAMPK), total AMPK (AMPK), and tubulin.

If the dual role of AMPK as a protector or mediator is confirmed, it raises the question of which methodology, activation or inhibition, is the better strategy for the treatment of cachexia. One important consideration will be the timing of treatment. Our study suggests that AMPK activation is more beneficial the earlier the treatment begins. Indeed, we saw that in the C26 model, the efficacy of AICAR was limited by delayed treatment and was not able to promote recovery, though it did spare further wasting (Fig. 2.14). In contrast, AMPK activation during the normal progression of cachexia appears to occur later in disease progression (White et al., 2011b). Therefore, it is possible that AMPK activation will be beneficial during early stages of cachexia, while AMPK inhibition may be beneficial during later stages. This presents several challenges. Diagnosis of cachexia early is difficult, and clinical classification of pre-cachectic stages is still an area of development (Blauwhoff-Buskermolen et al., 2014). Thus, it may be difficult to identify patients at a time when they are responsive to AMPK agonist treatment. In later stages, cachectic patients have difficulty tolerating drug therapy, potentially limiting the doses of anti-cachectic agents that can be administered (Andreyev et al., 1998; Dewys et al., 1980; Prado et al., 2007). Indeed, given the critical role of AMPK in metabolic homeostasis (Herzig and Shaw, 2018), AMPK inhibitors may exacerbate metabolic crisis arising from metabolic dysfunction in later stages of cachexia (Brown et al., 2017; White et al., 2011a). AMPK activators may also have toxicity issues in late-stage cachexia due to promotion of catabolic signaling and inhibition of anabolic signaling (Hardie, 2011). Thus, treatment timing and toxicity of AMPK activators and inhibitors will need to be carefully considered.

Another important consideration is how AMPK activation or inhibition affects other aspects of cachexia progression. Loss of AMPK expression in adipose tissue has been shown to promote adipose tissue wasting in cachexia, which can be reversed with an AMPK stabilizing peptide (Rohm et al., 2016). This suggests that AMPK inhibitors may exacerbate adipose tissue wasting, which can in turn affect lean body mass (Das et al., 2011; Kir et al., 2016; Rohm et al., 2016). However, AMPK activators can also promote fat tissue browning, which may contribute to a negative energy balance in cachexia (Desjardins and Steinberg, 2018). AMPK signaling also influences gut-barrier function, liver metabolic homeostasis, cardiac function, and hypothalamic activity (Ronnett et al., 2009; Shirwany and Zou, 2010; Sun and Zhu, 2017; Viollet et al., 2006).

Given our evolving understanding of how inter-organ crosstalk contributes to cachexia, understanding the potential impact of AMPK inhibition or activation in other organs during cachexia will be critical to developing an effective therapeutic strategy.

AMPK treatment strategies should also be tailored to the overlying condition driving cachexia. In cancer cachexia, as mentioned above, AMPK activation can be both pro- and anti-tumorigenic (Faubert et al., 2015; Zadra et al., 2015). Several mechanisms of AMPK oncogenic or tumor suppressor activity have been proposed, and it seems likely that the role of AMPK in tumorigenesis is highly context dependent. For example, AMPK activation or inhibition have both been associated with promotion or inhibition of the epithelial-mesenchymal transition (EMT) that facilitates invasion and metastasis (Chou et al., 2014; Saxena et al., 2018). In addition, AMPK activation can impair cancer growth by inhibiting protein and lipid synthesis (Zadra et al., 2015), but it can also confer a growth advantage to cancer cells experiencing nutrient deprivation (Vincent et al., 2015). Therefore, in cancer cachexia patients, treatments targeting AMPK should involve a precision medicine approach, accounting for the effects of AMPK activation on their specific cancer subtype and level of progression. AMPK may also modulate the overlying conditions in other forms of cachexia. In sepsis, AMPK activation has been shown to limit inflammatory metabolism and protect against sepsis-induced organ damage (Escobar et al., 2015; Fan et al., 2018; Huang et al., 2018). In CHF, AMPK activity is thought to reduce systolic dysfunction and ventricular hypertrophy (Beauloye et al., 2011). AMPK has also been suggested to be a therapeutic target for preventing lung damage in COPD (Zhang et al., 2018b). Thus, in cancer and other chronic diseases, accounting for the effects of AMPK activation or inhibition on the overlying condition will be critical to the success of treatment strategies.

Finally, the methodology of AMPK modulation needs to be considered. The primary focus of AMPK drug development has been on activation (Kim et al., 2016; Steinberg and Carling, 2019). As a result, there are numerous natural and synthetic compounds available to activate AMPK. In addition, AMPK can be activated by exercise (Richter and Ruderman, 2009). Exercise has consistently been shown to be beneficial for cachexia, and it is possible that AMPK activation contributes to these positive effects (Baracos et al., 2018; Hardee et al., 2019). Therefore, exercise may represent a viable alternative to AMPK drug therapy. However, in cachexia patients

for whom compliance with an exercise program is difficult for physical or psychological reasons, drug-therapy may be more effective (Wasley et al., 2018). Currently, the only AMPK inhibitor that is widely available is Compound C, which is nonspecific (Dasgupta and Seibel, 2018). This lack of inhibitors could be due to a lack of interest from pharmaceutical companies or may indicate technical challenges in the development of AMPK specific inhibitors. Regardless, this lack of viable chemical inhibitors poses a significant limitation to the idea of inhibiting AMPK in later stages of cachexia. Thus, while there is evidence that both AMPK activation and inhibition could be beneficial, AMPK activation is likely the more practical strategy.

4.3 The interactions between AMPK and iNOS: deciphering the signaling loop.

Our studies demonstrate that AMPK activation prevents muscle wasting during models of inflammatory-driven atrophy. We link this protective effect to the ability of direct AMPK activation to restore mitochondrial function and inhibit iNOS expression. However, the underlying mechanisms behind these outcomes were not fully explored. In addition, it remains to be determined why AMPK activation during the normal progression of cachexia does not inhibit iNOS expression or protect metabolic function. In Chapter 3, we find that iNOS activity inhibits OXPHOS and is upstream of the activation of AMPK during cytokine treatment. Given that AMPK activation can impair iNOS expression, this would suggest the presence of a negative feedback loop (Fig. 4.3A). However, it is clear that during cytokine treatment this potential negative feedback loop is not engaged, as both iNOS expression and significant AMPK activation occur simultaneously (Fig. 4.3B). In contrast, direct AMPK activation is able to reengage the feedback loop during cytokine treatment, limiting iNOS expression (Fig. 4.3C). One possible explanation for these differential outcomes is that metabolic dysfunction, through iNOS activity or metformin treatment, activates a different AMPK isoform than direct AMPK activators (Fig. 4.3D). AMPK is composed of three subunits, with several different isoforms for each (Tobias et al., 2018). AMPK complexes containing different isoforms have been shown to have different sensitivities to activation and preferences for downstream substrates (Klaus et al., 2012; Rajamohan et al., 2016; Ross et al., 2016; Schaffer et al., 2015). Therefore, it is possible that there exists a “protective” AMPK isoform complex that restores metabolic function and inhibits iNOS expression and an “atrophic” AMPK isoform that activates in response to energetic stress and

promotes catabolism. The differential expression, regulation, and activity of AMPK isoforms in muscle is complex, making speculation on the potential roles of different isoforms in our system difficult (Thomson, 2018). However, A-769662 is known to preferentially activate β1-containing complexes (Sanders et al., 2007). In addition, AICAR has been shown to preferentially activate the α2-catalytic subunit in L-6 rat myotubes, whereas metformin preferentially activated the α1-catalytic subunit (Bogachus and Turcotte, 2010). Thus, it is possible that preferential isoform activation underlies our observations, but this will need to be investigated experimentally.

An alternative explanation is that the ability of AMPK activation to protect muscle during cachexia is dependent on recovery or protection of mitochondrial function (Fig. 4.3E). AMPK activation is known to regulate mitochondrial homeostasis by promoting mitophagy and mitochondrial biogenesis, which helps to clear and replace damaged mitochondria (Herzig and Shaw, 2018). Thus, direct AMPK activators, which can activate AMPK independent of metabolic stress, may prime the cell to handle the mitochondrial dysfunction induced by cytokines. In contrast, AMPK activation by cytokine treatment, which only occurs after the onset of metabolic stress in our model, may be too late or insufficient to effectively recover mitochondrial activity. In this model, metformin treatment would be ineffective, as it would also inhibit mitochondria, effectively eliminating any potential benefit from AMPK activation. However, this model does not explain the differential effects on iNOS expression. Interestingly, the inhibition of mitochondria function has been associated with an increase in iNOS expression, suggesting that the iNOS-mitochondrial axis represents a feed-forward mechanism that re-enforces iNOS expression following cytokine simulation (Jeon et al., 2012). If true, direct AMPK activators may be indirectly impairing iNOS expression by restoring mitochondrial function. One way to assess this would be to delay treatment with AICAR and A-769662. If the effectiveness of AICAR and A-769662 is dependent on pre-emptively preparing the cell to handle metabolic stress, then iNOS expression should become refractory to AICAR and A-769662 treatment after metabolic dysfunction has become firmly established. Ultimately, deciphering why direct activation of AMPK is beneficial while indirect activation through energetic stress is not could facilitate the development of more targeted therapeutics.

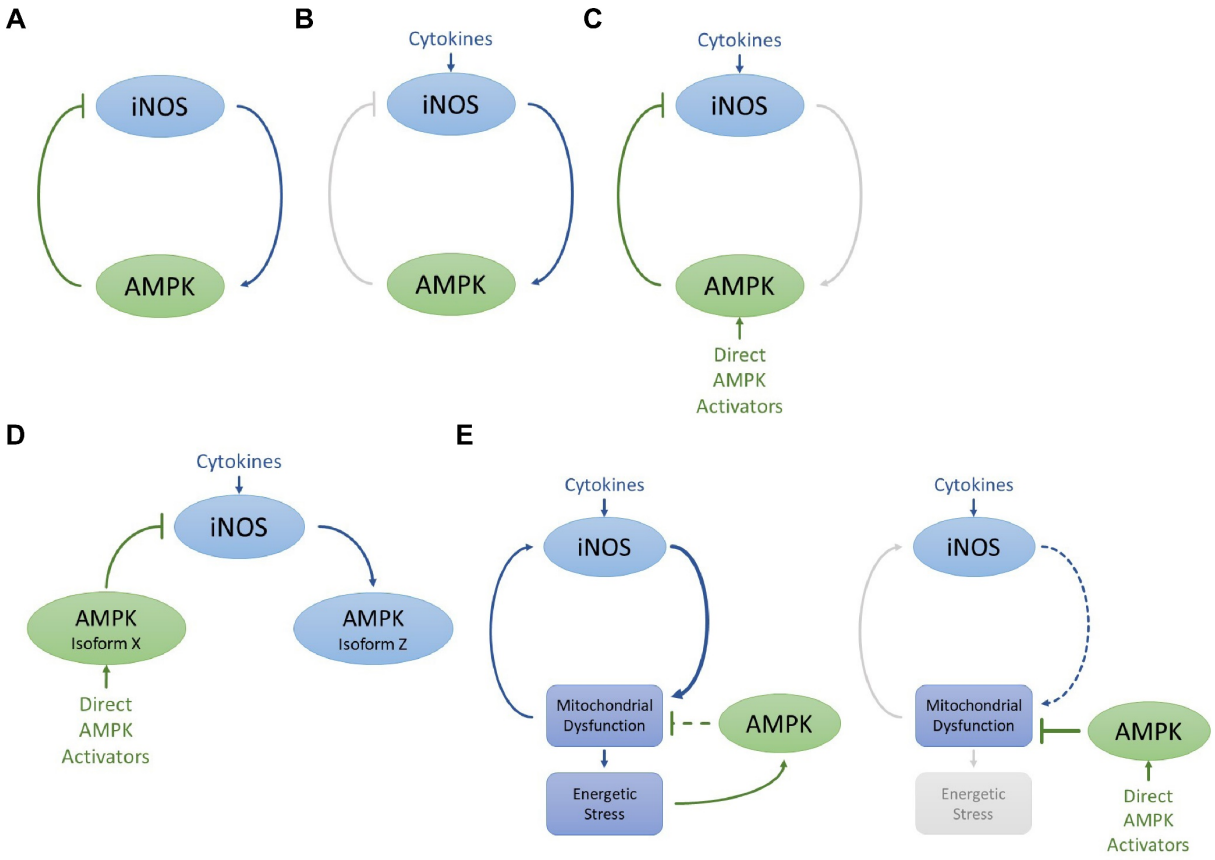

Figure 4.3: Potential models of differential AMPK and iNOS interactions.

Results from our studies indicate that iNOS can activate AMPK and that AMPK activation can inhibit iNOS, suggesting the presence of a negative feedback loop (A). However, in cytokine treated myotubes, the activation of AMPK does not lead to the inhibition of iNOS (B). Nevertheless, direct AMPK activators can still inhibit iNOS expression during cytokine treatment (C). One possible explanation for this apparent discrepancy is that direct AMPK activators and cytokine-induced iNOS expression activate different isoforms of AMPK with different downstream effects (D). Alternatively, inhibition of iNOS expression may be dependent on recovery of mitochondrial function. In cytokine treatment and metformin treatment, when AMPK is activated downstream of induction of severe energetic stress, AMPK activation is not sufficient to prevent dysfunction. In contrast, direct activation of AMPK primes the cell, preventing mitochondrial dysfunction before it becomes refractory to AMPK activation (E).

4.4 Understanding the mechanisms of the anti-cachectic effects of AMPK activation

Determining the mechanisms of the differential effects of direct versus indirect AMPK activation would be greatly facilitated by a better understanding of how AMPK activation inhibits iNOS expression and protects metabolic function. As discussed above, since iNOS appears to be involved in the inhibition of oxidative respiration, it is possible that AMPK restores metabolic function by inhibiting iNOS expression. However, AMPK activation is known to regulate many aspects of mitochondria activity and homeostasis, so it is likely that AMPK activation also affects mitochondria independent of iNOS. Of particular interest, as described above, is the role of AMPK in promoting mitophagy and mitochondrial biogenesis (Herzig and Shaw, 2018). Morphological analysis of mitochondria in cachectic muscle has shown an accumulation of damaged mitochondria (Fontes-Oliveira et al., 2013; Shum et al., 2012). In healthy tissue, damaged mitochondria can be cleared through mitophagy (Um and Yun, 2017). However, evidence suggests that mitophagy is impaired in cachectic muscle, despite a general increase in autophagy (Aversa et al., 2016; Brown et al., 2017; Talbert et al., 2014; White et al., 2012). Cachexia has also been associated with a deficit in PGC-1α expression, a master regulator of mitochondrial biogenesis (Sandri et al., 2006; White et al., 2011a; White et al., 2012). Both mitophagy and PGC-1α activity can be stimulated by AMPK (Herzig and Shaw, 2018). Thus, these observations raise the possibility that AMPK could help restore mitochondrial health in cachexia by increasing both the turnover of damaged mitochondria and promoting mitochondrial biogenesis.

Several possible mechanisms of action exist for the inhibition of iNOS by AMPK activation in cachectic muscle. AMPK is known to inhibit NF-κB and STAT3 activation, which transcriptionally control the expression of iNOS (Ma et al., 2017; Mancini et al., 2017; Nerstedt et al., 2010; Salminen et al., 2011). NF-κB and STAT3 do not appear to be direct targets of AMPK kinase activity, but rather are inhibited indirectly by modulation of upstream pathways (Mancini et al., 2017; Salminen et al., 2011). Interestingly, inhibition of STAT3 phosphorylation is more sensitive to AICAR than metformin in liver cells, and the inhibition of STAT3 by metformin is likely independent of AMPK activity (Lin et al., 2013; Nerstedt et al., 2010). Furthermore, studies showing that metformin inhibits STAT3 and NF-κB activity used significantly higher doses than

we used in our studies (Hattori et al., 2006; Nerstedt et al., 2010). Thus, it is possible that differential regulation of NF-κB and STAT3 activity are responsible for the reduction of iNOS expression in our system. We have begun to investigate this possibility by assessing NF-κB localization and STAT3 activity. NF-κB has been shown to activate with a biphasic pattern in myotubes treated with inflammatory cytokines (Ladner et al., 2003). Thus, we assessed NF-κB nuclear localization at 30m (phase 1) and 24h (phase 2). We observed that AICAR but not metformin prevented NF-κB localization only in the second phase (Fig. 4.4A). In contrast, we did not see any changes in the phosphorylation of STAT3 over the first 24h of treatment with IFNγ/TNFα (Fig. 4.4B-E). In keeping with inhibition of the second phase of NF-κB activation, we found that AICAR treatment did not affect the initial induction of iNOS mRNA expression, which reached peak expression after 12h of treatment, but did reduce iNOS mRNA levels after 24h of treatment (Fig. 4.4F). This preliminary data suggests that AICAR may inhibit the maintenance of iNOS expression by inhibiting the second phase of NF-κB activation, but more work is needed to validate these findings.

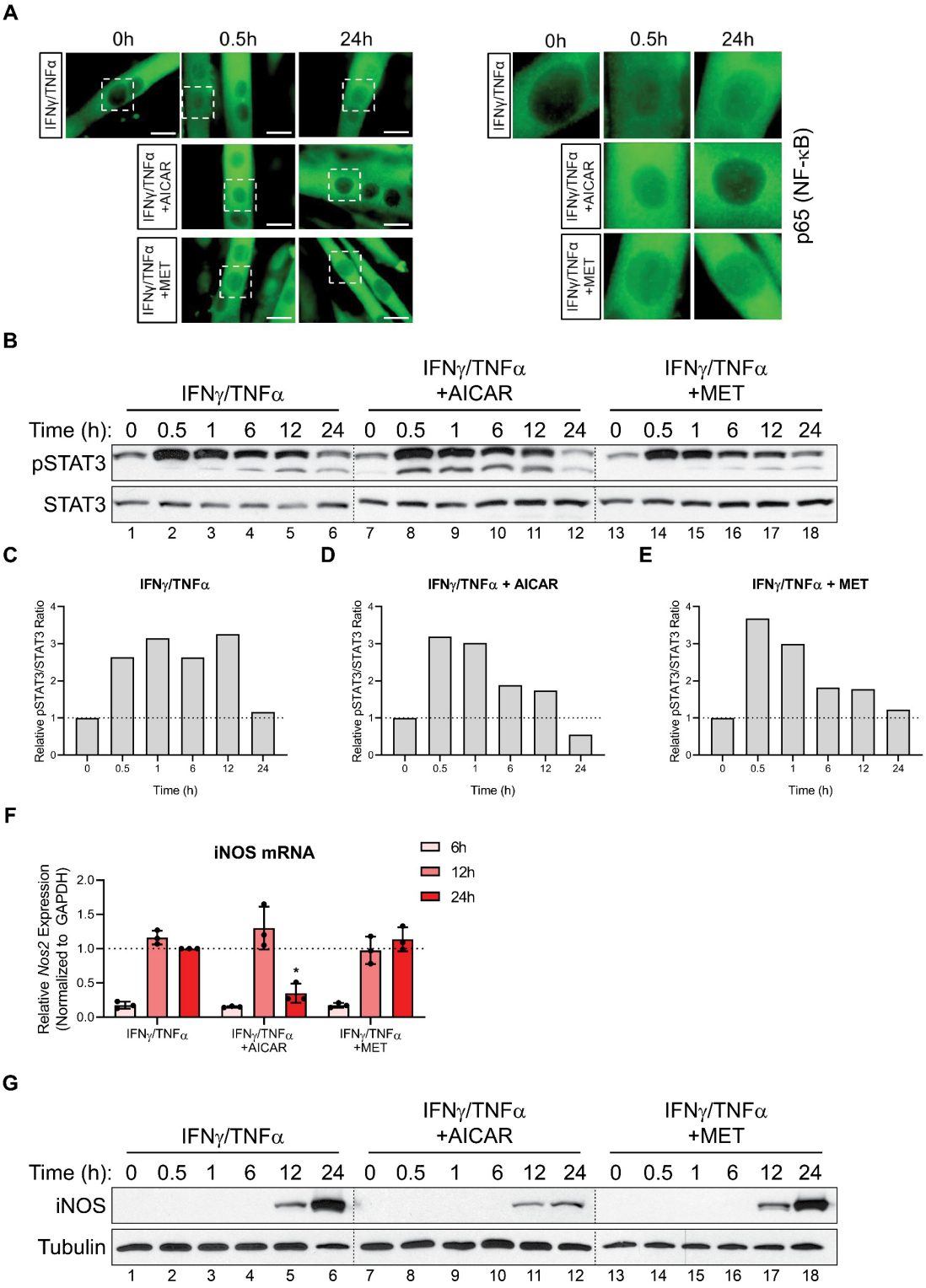

Figure 4.4: AICAR, but not metformin, prevents secondary phase NF-κB localization and iNOS expression without affecting STAT3 phosphorylation.

C2C12 myotubes were treated with IFNγ (100U/mL) and TNFα (20ng/mL) and with or without AICAR (0.5mM) or metformin (0.5mM).

(A) NF-κB subunit p65 localization was determined by immunofluorescence. Scale bar: 20μM.

(B) Western blot analysis for pTyr705-STAT3 (pSTAT3) and total STAT3 (STAT3).

(C-E) Quantification of the pSTAT3/STAT3 ratio relative to the 0h control time point.

(F) qPCR analysis of *Nos2* mRNA expression relative to the IFNγ/TNFα 24h timepoint. Expression was normalized to *Gapdh* mRNA.

(G) Western blot analysis of iNOS and tubulin protein expression.

Data Information: All panels except for F are results from one experiment (n = 1). Expression values from panel F were determined from three independent experiments (n = 3). 24h expression data in panel F was originally presented in Fig. 2.5B. Error bars represent the standard deviation of the mean. For statistical comparison in panel F, data was analyzed by a two-way ANOVA followed by a Tukey's post-hoc test for multiple comparisons. * indicates a statistically significant difference from the 24h IFNγ/TNFα sample ($\Delta = -0.65$, $p = 0.0001$).

It is also likely that post-transcriptional mechanisms play a role in the regulation of iNOS expression by AMPK. In our assessment of the kinetics of iNOS expression in cytokine-treated myotubes, we noted that AICAR treatment reduced iNOS protein expression levels at 12h, a timepoint when the mRNA levels are unaffected (Fig. 4.4F-G). This would suggest a posttranscriptional regulation of iNOS mRNA translation. We have previously shown that iNOS mRNA is regulated by HuR (Di Marco et al., 2005). In this study, we showed that HuR regulates the stability of the iNOS transcript. However, it is possible that HuR may also regulate its translation. Interestingly, we have previously seen that treatment of C2C12 myoblasts with 2mM of AICAR (a relatively high dose compared to what was utilized in our cachexia studies) sequesters HuR in the nucleus without affecting iNOS mRNA steady-state levels (Di Marco et al., 2005). In keeping with this, AMPK-mediated regulation of importin-1α has been shown to promote HuR nuclear import and decrease association with target messages (Wang et al., 2002; Wang et al., 2004). In addition to stability, HuR is known to promote nuclear export of messages and their recruitment to polysomes (Brennan et al., 2000; Durie et al., 2011). Therefore, it is possible that nuclear sequestration of HuR by AMPK activation limits either the export or recruitment of the iNOS transcript in an HuR-dependant manner. Assessment of these possibilities is warranted to better understand how AMPK activation might regulate the translation of iNOS mRNA.

Considering all the above discussion, I propose a two-staged regulation of iNOS expression that is inhibited by AMPK activation through regulation of mitochondrial function and HuR (Fig. 4.5). During the normal signal transduction of cytokine treatment, iNOS expression is initially induced by the first phase activation of NF-κB and STAT3. This initial production of iNOS leads to accumulation of nitric oxide and the impairment of mitochondrial respiration. Mitochondrial respiratory inhibition subsequently promotes and reinforces the expression of iNOS. One possible mechanism for this is the production of elevated ROS, which can activate NF-κB (Gloire et al., 2006). This ROS to NF-κB signaling axis may drive the second phase of NF-κB activation. Throughout this two-step induction, the stability and translation of the iNOS transcript is also regulated post-transcriptionally by HuR. Treatment with direct AMPK activators promotes mitochondrial turnover and primes the muscle cells to combat mitochondrial inhibition induced during the first phase of iNOS expression. In addition, nuclear sequestration of HuR by

phosphorylation of importin-1α leads to reduced translation of the iNOS transcript during this phase. Protection of mitochondria then prevents second phase activation of NF-κB, potentially by limiting ROS protection. This leads to the collapse of iNOS mRNA steady-state levels due to reduced transcription, further protecting the muscle mitochondria from nitrosative damage. Likely, this proposed mechanism does not encompass the complete nature of iNOS and mitochondrial regulation by AMPK. For example, AMPK may regulate NF-κB more directly through other signalling pathways (Salminen et al., 2011). However, experimental investigations into these potential mechanisms will help better our understanding of the crosstalk between inflammatory gene signaling and metabolic function in cachexia.

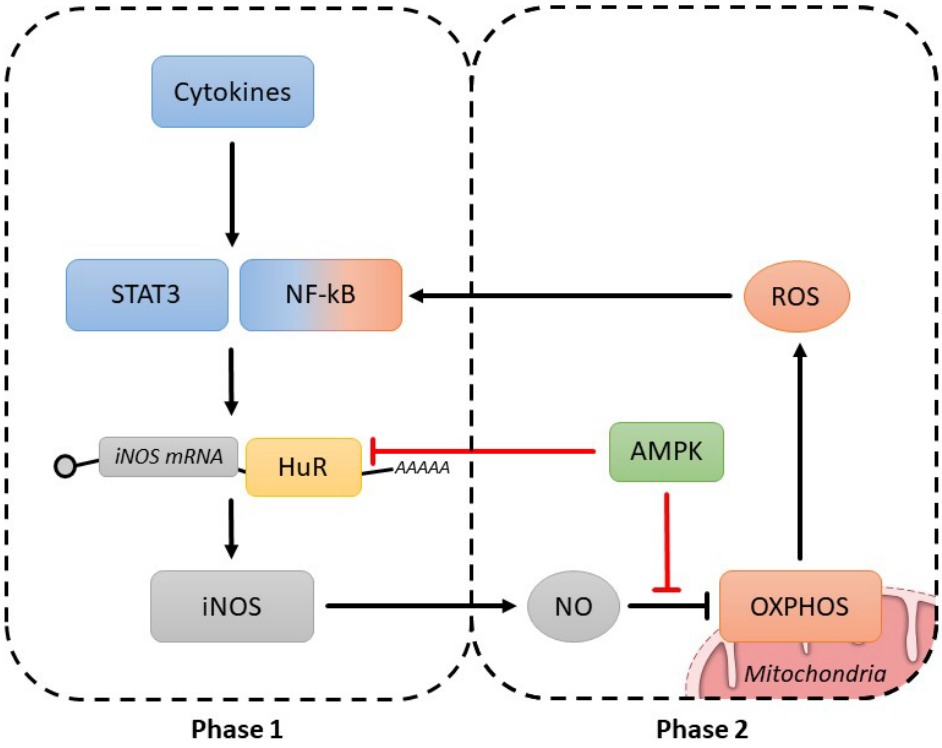

Figure 4.5: Proposed bi-phasic model of iNOS expression and potential mechanisms of AMPK mediated inhibition.

Cytokine treatment may induce iNOS expression in two phases in skeletal muscle cells. In the first phase, cytokine-mediated activation of STAT3 and NF-κB dramatically increases the transcription of the iNOS mRNA transcript, which is also stabilized by interaction with the RNA-binding protein HuR. In the second phase, elevated expression of iNOS leads to accumulation of nitric oxide, which subsequently inhibits oxidative phosphorylation (OXPHOS) in the mitochondria. Inhibition of OXPHOS leads to the release of ROS, which then activates NF-κB and reinforces the expression of iNOS. AMPK activation may inhibit iNOS expression by both sequestering HuR in the nucleus and by restoring mitochondrial OXPHOS. In doing so, it inhibits iNOS expression in both phases.

4.5 The potential of iNOS as a cachectic therapeutic target beyond metabolic dysfunction

The focus our studies was on the role of iNOS in inducing metabolic dysfunction during cachexia. However, targeting iNOS may have therapeutic benefits in cachexia beyond just metabolic homeostasis in mature muscle fibers. Indeed, nitric oxide signaling is known to regulate satellite cell function and muscle regeneration. Nitric oxide produced by nNOS is believed to stimulate satellite stem cell proliferation and expansion, a critical first step of the repair process (Anderson, 2000; Buono et al., 2012). General inhibition of NOS activity has been shown to limit this expansion and reduce Pax7 expression, demonstrating that regenerative signaling is sensitive to nitric oxide (Anderson, 2000; Buono et al., 2012; Filippin et al., 2011). In cachexia, chronic inflammatory signaling through NF-κB is believed to cause a regenerative deficit due to precocious activation of satellite cell expansion and chronic expression of Pax7, which limits commitment to subsequent differentiation steps (He et al., 2013). Since NO signaling is known to promote satellite cell expansion, one can speculate that elevation of iNOS, mediated by NF-κB activation, in satellite cells might be a cause of the persistent expression of Pax7 during cachexia. However, this will need to be investigated, as during injury-induced regeneration, iNOS expression appears to be limited to infiltrating macrophages (Rigamonti et al., 2013). Thus, it remains to be seen if satellite cells express iNOS in the context of chronic inflammation during cachexia. Importantly, iNOS knockout during injury-induced regeneration limits recovery by impairing the initial inflammatory response that plays a critical role in initiating myogenesis (Rigamonti et al., 2013). Therefore, the ultimate effect of iNOS inhibition on regeneration during cachexia will depend on the combination of its impact on the chronic inflammatory signaling that drives dysfunction and the physiological pathways that mediate normal regeneration. Regardless, it is likely that modulation of the muscle regenerative process will influence the therapeutic potential of iNOS inhibitors.

Beyond muscle, iNOS inhibition will also impact other physiological systems in cachectic patients. Most notably, iNOS plays a critical role in the inflammatory response, acting as a cytotoxic agent and regulator of immune cell differentiation (reviewed in (Xue et al., 2018)). As a result, iNOS inhibitors are likely to limit immune function in cachectic patients, which may be

beneficial or detrimental depending on the overlying condition. In vulnerable populations, it may also increase susceptibility to secondary infection. Nitric oxide signaling also plays an important role in the brain, regulating many aspects of CNS function under normal and inflammatory conditions (Calabrese et al., 2007). Indeed, iNOS expression is elevated in regions of the hypothalamus in both cancer-bearing and LPS-treated mice (Wang et al., 2005; Wong et al., 1996). Furthermore, treatment with an iNOS specific inhibitor reduced anorexia behavior in LPS-treated mice, indicating that iNOS inhibition can protect against cachexia-associated anorexia (Riediger et al., 2010). iNOS is also known to induce oxidative damage in liver hepatocytes under a variety of conditions, but its involvement in liver dysfunction during cachexia has yet to be determined (Iwakiri and Kim, 2015). In the heart of murine models of heart failure or hypertension, the inhibition of iNOS reduces contractile dysfunction, oxidative stress, and ventricular remodeling (Dias et al., 2010; Heusch et al., 2010; Liu et al., 2005). In addition, myocardium-specific overexpression of iNOS induces heart dysfunction, failure, and sudden cardiac death, indicating that chronic iNOS expression in cardiomyocytes is sufficient to induce cardiac pathology (Mungrue et al., 2002). However, as with the liver, the contribution of iNOS expression to cardiac dysfunction in cachexia is unknown. Finally, there is evidence that iNOS expression in the gut may contribute to intestinal permeability during cachexia. iNOS knockout mice exhibit resistance to bacterial translocation following ischemia-reperfusion injury and endotoxin injection (Mishima et al., 1997; Suzuki et al., 2000). In cachexia, a proposed mechanism for the role of iNOS in gut permeability is that elevated nitrate levels promote the growth of pathological *Enterobacteriaceae*, specifically *Klebsiella oxytoca,* which subsequently impair gut-barrier function (Potgens et al., 2018). Overall, the current evidence suggests that iNOS inhibition could protect against other critical aspects of the cachexia syndrome, such as anorexia and microbial dysbiosis. However, clinical development of iNOS inhibitors for cachexia should carefully monitor for signs of immunodeficiency, especially in more vulnerable populations, such as the elderly.

As for targeting AMPK, accounting for the impact of iNOS inhibition on the overlying conditions that induce cachexia will be a key component of therapeutic development. As described above, iNOS inhibition may limit immune function in response to septic infection. However, iNOS

inhibition has also been shown to limit the damage induced by septic shock (Takatani et al., 2018; Thiemermann, 1997). Thus, in patients with severe infection, co-administration of iNOS inhibitors with antibiotics may allow for both clearance of the infection and reduction of septic shock-associated cachexia. In CHF, iNOS inhibition or genetic depletion has been shown to prevent symptoms of myocardial infraction, hypertension, and ventricular pacing induced cardiac dysfunction (Dias et al., 2010; Heusch et al., 2010; Liu et al., 2005; Zhang et al., 2007). However, others have shown that iNOS knockout mice are not resistant to severe myocardial infraction, suggesting the efficacy of iNOS inhibition may depend on the severity of the CHF (Jones et al., 2005). iNOS inhibition has also been shown to have some beneficial effects on kidney function in high-fat diet induced CKD (Martin et al., 2018). In a model of smoking-induced COPD, iNOS depletion or inhibition was shown to prevent pulmonary hypertension and emphysema (Seimetz et al., 2011). Finally, iNOS may play a role in tumorigenesis, though its role in cancer development is complex. Indeed, it seems that, like AMPK, iNOS may serve both pro- or anti-tumorigenic functions depending on the cancer-type and cellular context (Vannini et al., 2015). Thus, accounting for the impact of iNOS inhibitors on cancer development will be important when using them for the treatment of cancer cachexia.

Collectively, the evidence suggests that iNOS inhibition has the potential to affect many aspects of cachexia beyond muscle metabolic dysfunction. As one of the greatest challenges for the treatment of cachexia is its multifactorial nature, it is tempting to speculate that iNOS inhibitors may therefore prove to be particularly effective. In addition, the fact that iNOS is upregulated in cachectic muscle of human patients across a spectrum of overlying conditions suggests that iNOS inhibition may be effective in a wide variety of cachexia subtypes (Adams et al., 2003; Agusti et al., 2004; Ramamoorthy et al., 2009). Since clinical inhibitors of iNOS have already been developed for other conditions, drug-repurposing may facilitate faster development of iNOS-targeting therapies for cachexia (Vitecek et al., 2012). Thus, iNOS inhibitors are a promising avenue of therapeutic development that warrants further investigation.

4.6 Final thoughts and future directions

This work identifies two novel therapeutic targets, AMPK and iNOS, for the treatment of cachexia, a devastating syndrome of body wasting that occurs in a variety of chronic diseases. In addition, it provides insights into the connections between inflammatory signaling and metabolic dysfunction that contribute to muscle weakness and atrophy in cachexia. While promising, several mechanistic questions remain that, if investigated, may provide key information for the development of the most effective therapies. For example, identification of a "protective" AMPK isoform would inform development or selection of AMPK agonists for the treatment of cachexia. However, a looming pitfall is if these strategies will translate from preclinical murine models to clinical, human cachexia. Indeed, translation of scientific findings in mice to human trials is notoriously difficult (Justice and Dhillon, 2016). This is likely to be particularly true in cachexia, where our lack of understanding of the human condition limits both the development of reflective mouse models and the proper design of clinical trials.

Although results from these studies provide mechanistic insight and efficacy proof-of-principle, the model systems used potentially limit the translatability of the findings. In culture, C2C12 myotubes do not perfectly replicate the biochemical function of muscle fibers (Cheng et al., 2014; Rodgers et al., 2014). In addition, a single application of cytokines does not reflect *in vivo* conditions with active extracellular milieu circulation. This system could be improved by utilizing primary myoblasts from mice or, ideally, humans, which may reflect the internal workings of muscle cells in the body more accurately, though not perfectly. Also, use of a perfusion-based culture system that allows for a constant stream of lower doses of inflammatory cytokines may more accurately reproduce the cachectic environment *in vitro*. Alternatively, co-culturing of primary myotubes with cancer cells is an efficient method of continuous cytokine delivery that could also be considered (Jackman et al., 2017). In our mouse models, we primarily employed subcutaneous injection of mature cancer cells into mice. While this model system is relatively inexpensive, widely used, and shown to replicate some of the clinical findings of cachexia, it does not accurately reflect normal disease progression (Bonetto et al., 2016). In essence, a non-cachectic mouse is given a mature, pro-cachectic cancer, almost immediately transitioning it into a cachectic or even refractory cachectic state. The lack of progressive development makes it

difficult to assess the efficacy of treatments, especially ones that might be more effective in earlier stages of disease development. Alternatively, development of genetically engineered mouse models (GEMM), which spontaneously develop cancer or other pro-cachectic conditions and progress through all stages of cachectic development, may more accurately reflect human cachexia and allow for the testing of therapeutic strategies at all stages of cachexia (Lee et al., 2016). Thus, while the tools used in this study have been widely used by us and others successfully, future work should also attempt to develop more effective models of cachexia.

The final pitfall of cachexia model and therapeutic development is a lack of understanding of the human cachexia condition. Indeed, cachexia diagnosis is complex and varies from region to region, making collective assessment of cachexia patients difficult (discussed in Chapter 1). Misclassification of pre-cachectic and refractory cachexia, in particular, could cause significant variance in cachexia clinical studies, limiting effective investigations into underlying mechanisms, biomarkers, or treatments. In addition to disease staging, another often over-looked consideration is the potential for cachexia sub-types in human populations. Indeed, molecular sub-typing of different cancers over the past several decades has revealed that physiologically similar diseases often present with unique underlying molecular mechanisms that dramatically influence patient outcome and response to therapy (Collisson et al., 2019; Dai et al., 2015). In cancer cachexia trials, patients from different cancers are often pooled in order to achieve a statistically relevant sampling size (Advani et al., 2018). However, it is likely that different overlying conditions induce cachexia through unique mechanisms. Indeed, one could imagine that induction of different profiles of cachectic cytokines through unique host-disease interactions could lead to a wide-breadth of cachexia sub-types with distinct molecular etiology. Determination of these potential cachexia-subtypes may help to identify patient populations that are at particular risk or that may be more responsive to certain therapies. In addition, accurate modeling of these different subtypes will help improve translatability of pre-clinical investigations. Doing so will be challenging and costly, but it may be necessary for the advancement of cachexia research and development of an effective treatment for this deadly syndrome.

Our understanding of cachexia has progressed rapidly over the past several decades, especially considering the relative lack of progress since its historical identification several hundred years ago. Experimental insights have provided new hope for patients suffering from the debilitating impact of this syndrome, with a few new therapies beginning to show promise in clinical trials (reviewed in (Advani et al., 2018)). However, there is still much to learn about how cachexia develops and how the complex interactions between the primary disease, the host immune system, and organs throughout the body drive a state of wasting. As the burden of chronic disease continues to grow, development of a treatment for cachexia will become imperative. The research presented here forms part of an emerging body of works looking into therapeutic targets in the molecular mechanisms of the cachectic condition. Hopefully, in the coming years, effective treatments for cachexia will become available and improve the lives of those suffering with chronic disease.

Appendix

i. Extended List of Publications

Journal Publications

- **Hall DT**, Griss, T, Ma JF, Sanchez BJ, Sadek J, Tremblay AK, Mubaid S, Omer A, Ford RJ, Bedard N, Pause A, Wing SS, Di Marco S, Steinberg GR, Jones RG, Gallouzi IE. "The AMPK agonist 5-Aminoimidazole-4-carboxamide ribonucleotide (AICAR), but not metformin, prevents inflammation-associated cachectic muscle wasting." (2018) EMBO Mol. Med. 10(7), pii: e8307
- Ma JF, Sanchez BJ, **Hall DT**, Tremblay AK, Di Marco S, Gallouzi IE. "STAT3 promotes IFNγ/TNFα-induced muscle wasting in an NF-κB-dependent and IL-6-independent manner." (2017) EMBO Mol. Med. 9(5), 622-637.
- Ma JF, **Hall DT**, and Gallouzi, IE. "The impact of mRNA turnover and translation on age-related muscle loss." (2012) Ageing Res. Rev. 11, 432-441.
- Di Marco S, Cammas A, Lian XJ, Kovacs EN, Ma JF, **Hall DT**, Mazroui R, Richardson J, Pelletier J, and Gallouzi IE. "The translation inhibitor pateamine A prevents cachexia-induced muscle wasting in mice." (2012) Nat. Communications. 3, 896.
- **Hall DT**, Ma JF, Marco SD, and Gallouzi IE. "Inducible nitric oxide synthase (iNOS) in muscle wasting syndrome, sarcopenia, and cachexia." (2011) Aging 3, 702-715.

Papers in Preparation or Under Revision

- **Hall DT**, Sadek J, Colalillo B, Tremblay AK, Di Marco S, and Gallouzi IE. "Inducible Nitric Oxide Synthase Impairs Mitochondria Oxidative Phosphorylation in Cachexia." *Manuscript in preparation.*
- **Hall DT**, Colalillo B, Sadek J, Di Marco S, and Gallouzi IE. "Therapeutic Targets in Metabolic Homeostasis for the Treatment of Cachexia." *Manuscript in preparation for an invited review in Cancers – Special Issue "Cancer Cachexia".*
- Mubaid S*, **Hall DT***, Lian XJ, Gagné J, Carlile G, Di Marco S, Poirier G, Thomas DY, and Gallouzi IE. "The Role of PARylation in the HuR-mediated Modulation of Muscle Fiber Formation." *Manuscript in preparation.*

  *co-first authors
- Sanchez BJ, Tremblay AK, Leduc-Gaudet J, **Hall DT**, Kovacs E, Ma JF, Mubaid S, Hallauer PL, Phillips BL, Vest KE, Corbett AH, Kontoyiannis DL, Hussain SNA, Hastings KEM, Di Marco S, and Gallouzi IE. "Depletion of HuR in murine skeletal muscle enhances exercise endurance and prevents cancer-induced muscle atrophy." *In press at Nature Communications.*

ii. List of Figures and Tables

iii. List of Abbreviations

4EBP	4E Binding Proteins
ACC	Acetyl-CoA Carboxylase
ActRIIB	Activin Receptor Type II B
AIDS	Acquired Immunodeficiency Syndrome
ALK	Activin Receptor-like Kinases
AMPK	AMP-Activated Protein Kinase
ATG9	Autophagy-related Protein 9
ATGL	Adipose Triglyceride Lipase
ATP5A	ATP Synthase F1 Subunit Alpha
BAT	Brown Adipose Tissue
BCAA	Branch-Chain Amino Acids
BMI	Body Mass Index
Bnip3	BCL2 Interacting Protein 3
C/EBP	CCAAT-Enhancer-Binding Proteins
CaMKKβ	Ca^{2+}/calmodulin-dependent Protein Kinase Kinase β
CASCO	Cachexia Score
CBS	Cystathionine β Synthase
CHF	Chronic Heart Failure
CHO	Chinese Hamster Ovary
CKD	Chronic Kidney Disease
CNS	Central Nervous System
COPD	Chronic Obstructive Pulmonary Disorder
CPT1	Carnitine Palmitoyltransferase I
CSS	Cachexia Staging Score
DMD	Duchenne Muscular Dystrophy
ECAR	Extracellular Acidification Rate
ECOG	Eastern Cooperative Oncology Group
eIF2B	Eukaryotic Initiation Factor 2B
eNOS	Endothelial Nitric Oxide Synthase
ETC	Electron Transport Chain
FFA	Free-Fatty Acids
FOXO	Forkhead Box Protein
GEMM	Genetic Engineered Mouse Model
GSK3β	Glycogen Synthase Kinase 3β
HIV	Human Immunodeficiency Virus
HPA	Hypothalamic-Pituitary-Adrenal
HSL	Hormone-Sensitive Lipase
HuR	Human Antigen R
IFNγ	Interferon γ

IGF-1	Insulin-like Growth Factor 1
IGFBP	Insulin-like Growth Factor Binding Protein
IKK	Inhibitor of κB Kinase
IL	Interleukin
iNOS	Inducible Nitric Oxide Synthase
JAK	Janus Kinases
J-ATP	ATP Production Rate
KSRP	KH-type Splicing Regulatory Protein
LDH	Lactate Dehydrogenase
LIF	Leukemia Inhibitor Factor
LKB1	Liver Kinase B1
LLC	Lewis Lung Carcinoma
LPS	Lipopolysaccharide
MCASCO	Mini-Cachexia Score
MTCO1	Mitochondrially Encoded Cytochrome C Oxidase I
mTOR	Mammalian Target of Rapamycin
MuRF1	Muscle RING-Finger Protein 1
MUSA1	Muscle Ubiquitin Ligase of the SCF Complex in Atrophy-1
Myf5	Myogenic Factor 5
NDUFB8	NADH:ubiquinone Oxidoreductase Subunit B8
NF-κB	Nuclear Factor κ-light-chain-enhancer of Activated B Cells
nNOS	Neuronal Nitric Oxide Synthase
NO	Nitric Oxide
NSCLC	Non-small-cell Lung Cancer
OCR	Oxygen Consumption Rate
OSM	Oncostatin M
OXPHOS	Oxidative Phosphorylation
Pax7	Paired Box 7
PDH	Pyruvate Dehydrogenase
PDK4	Pyruvate Dehydrogenase Kinase 4
PGC-1α	Peroxisome Proliferator-Activated Receptor-γ Coactivator 1α
PI3K	Phosphoinositide 3-Kinases
PINK	PTEN-induced Kinase
PTH	Parathyroid Hormone
PTHR	Parathyroid Hormone Receptor
PTHrP	Parathyroid Hormone Related Protein
REE	Resting Energy Expenditure
RNS	Reactive Nitrogen Species
ROS	Reactive Oxygen Species
S6	Ribosomal Protein S6

S6K	Ribosomal Protein S6 Kinase
SDHB	Succinate Dehydrogenase Complex Iron Sulfur Subunit B
SH2	Src Homology 2
SIRT1	Sirtuin 1
STAT3	Signal Transducers and Activators of Transcription-3
TAK1	Transforming Growth Factor-β-Activated Kinase 1
TCA	Tricarboxylic Acid
TGFβ	Transforming Growth Factor β
TNFα	Tumor Necrosis Factor α
TPP	Tristetraprolin
TRAF6	TNF Receptor Associated Factor 6
TSC2	Tuberous Sclerosis Complex 2
TWEAK	Tumor Necrosis Factor-like Weak Inducer of Apoptosis
UCP	Uncoupling Protein
ULK1	Unc-51-like Autophagy Activating Kinase
UPP	Ubiquitin-Proteasome Pathway
UQCRC2	Ubiquinol-cytochrome C Reductase Core Protein 2
UTR	Untranslated Region
VDAC	Voltage-dependent Anion Channel
WAT	White Adipose Tissue

iv. References

Abrigo, J., Elorza, A.A., Riedel, C.A., Vilos, C., Simon, F., Cabrera, D., Estrada, L., and Cabello-Verrugio, C. (2018). Role of Oxidative Stress as Key Regulator of Muscle Wasting during Cachexia. Oxid Med Cell Longev *2018*, 2063179.

Acharyya, S., Ladner, K.J., Nelsen, L.L., Damrauer, J., Reiser, P.J., Swoap, S., and Guttridge, D.C. (2004). Cancer cachexia is regulated by selective targeting of skeletal muscle gene products. J Clin Invest *114*, 370-378.

Adami, F., Guarini, A., Pini, M., Siviero, F., Sancetta, R., Massaia, M., Trentin, L., Foa, R., and Semenzato, G. (1994). Serum levels of tumour necrosis factor-alpha in patients with B-cell chronic lymphocytic leukaemia. European journal of cancer *30A*, 1259-1263.

Adams, V., Spate, U., Krankel, N., Schulze, P.C., Linke, A., Schuler, G., and Hambrecht, R. (2003). Nuclear factor-kappa B activation in skeletal muscle of patients with chronic heart failure: correlation with the expression of inducible nitric oxide synthase. Eur J Cardiovasc Prev Rehabil *10*, 273-277.

Advani, S.M., Advani, P.G., VonVille, H.M., and Jafri, S.H. (2018). Pharmacological management of cachexia in adult cancer patients: a systematic review of clinical trials. BMC cancer *18*, 1174.

Agusti, A., Morla, M., Sauleda, J., Saus, C., and Busquets, X. (2004). NF-kappaB activation and iNOS upregulation in skeletal muscle of patients with COPD and low body weight. Thorax *59*, 483-487.

Agustsson, T., Ryden, M., Hoffstedt, J., van Harmelen, V., Dicker, A., Laurencikiene, J., Isaksson, B., Permert, J., and Arner, P. (2007). Mechanism of increased lipolysis in cancer cachexia. Cancer research *67*, 5531-5537.

Agustsson, T., Wikrantz, P., Ryden, M., Brismar, T., and Isaksson, B. (2012). Adipose tissue volume is decreased in recently diagnosed cancer patients with cachexia. Nutrition *28*, 851-855.

Akdis, M., Aab, A., Altunbulakli, C., Azkur, K., Costa, R.A., Crameri, R., Duan, S., Eiwegger, T., Eljaszewicz, A., Ferstl, R*., et al.* (2016). Interleukins (from IL-1 to IL-38), interferons, transforming growth factor beta, and TNF-alpha: Receptors, functions, and roles in diseases. J Allergy Clin Immunol *138*, 984-1010.

Al-Shanti, N., and Stewart, C.E. (2012). Inhibitory effects of IL-6 on IGF-1 activity in skeletal myoblasts could be mediated by the activation of SOCS-3. J Cell Biochem *113*, 923-933.

Alvarez-Guardia, D., Palomer, X., Coll, T., Davidson, M.M., Chan, T.O., Feldman, A.M., Laguna, J.C., and Vazquez-Carrera, M. (2010). The p65 subunit of NF-kappaB binds to PGC-1alpha, linking inflammation and metabolic disturbances in cardiac cells. Cardiovasc Res *87*, 449-458.

Anderson, J.E. (2000). A role for nitric oxide in muscle repair: nitric oxide-mediated activation of muscle satellite cells. Molecular biology of the cell *11*, 1859-1874.

Andreyev, H.J., Norman, A.R., Oates, J., and Cunningham, D. (1998). Why do patients with weight loss have a worse outcome when undergoing chemotherapy for gastrointestinal malignancies? European journal of cancer *34*, 503-509.

Andrzejewski, S., Gravel, S.P., Pollak, M., and St-Pierre, J. (2014). Metformin directly acts on mitochondria to alter cellular bioenergetics. Cancer Metab *2*, 12.

Antoun, S., and Raynard, B. (2018). Muscle protein anabolism in advanced cancer patients: response to protein and amino acids support, and to physical activity. Ann Oncol *29*, ii10-ii17.

Antunes, D., Padrao, A.I., Maciel, E., Santinha, D., Oliveira, P., Vitorino, R., Moreira-Goncalves, D., Colaco, B., Pires, M.J., Nunes, C.*, et al.* (2014). Molecular insights into mitochondrial dysfunction in cancer-related muscle wasting. Biochim Biophys Acta *1841*, 896-905.

Anwar, A., Zahid, A.A., Scheidegger, K.J., Brink, M., and Delafontaine, P. (2002). Tumor necrosis factor-alpha regulates insulin-like growth factor-1 and insulin-like growth factor binding protein-3 expression in vascular smooth muscle. Circulation *105*, 1220-1225.

Aoyagi, T., Terracina, K.P., Raza, A., Matsubara, H., and Takabe, K. (2015). Cancer cachexia, mechanism and treatment. World J Gastrointest Oncol *7*, 17-29.

Arends, J., Baracos, V., Bertz, H., Bozzetti, F., Calder, P.C., Deutz, N.E.P., Erickson, N., Laviano, A., Lisanti, M.P., Lobo, D.N.*, et al.* (2017). ESPEN expert group recommendations for action against cancer-related malnutrition. Clinical nutrition *36*, 1187-1196.

Argiles, J.M., Alvarez, B., and Lopez-Soriano, F.J. (1997). The metabolic basis of cancer cachexia. Med Res Rev *17*, 477-498.

Argiles, J.M., Betancourt, A., Guardia-Olmos, J., Pero-Cebollero, M., Lopez-Soriano, F.J., Madeddu, C., Serpe, R., and Busquets, S. (2017). Validation of the CAchexia SCOre (CASCO). Staging Cancer Patients: The Use of miniCASCO as a Simplified Tool. Front Physiol *8*, 92.

Argiles, J.M., Busquets, S., Stemmler, B., and Lopez-Soriano, F.J. (2014). Cancer cachexia: understanding the molecular basis. Nature reviews Cancer *14*, 754-762.

Argiles, J.M., Busquets, S., Toledo, M., and Lopez-Soriano, F.J. (2009). The role of cytokines in cancer cachexia. Current opinion in supportive and palliative care *3*, 263-268.

Argiles, J.M., Lopez-Soriano, F.J., and Busquets, S. (2015a). Muscle wasting in cancer: the role of mitochondria. Curr Opin Clin Nutr Metab Care *18*, 221-225.

Argiles, J.M., Lopez-Soriano, F.J., Toledo, M., Betancourt, A., Serpe, R., and Busquets, S. (2011). The cachexia score (CASCO): a new tool for staging cachectic cancer patients. J Cachexia Sarcopenia Muscle *2*, 87-93.

Argiles, J.M., Stemmler, B., Lopez-Soriano, F.J., and Busquets, S. (2015b). Nonmuscle Tissues Contribution to Cancer Cachexia. Mediators Inflamm *2015*, 182872.

Argiles, J.M., Stemmler, B., Lopez-Soriano, F.J., and Busquets, S. (2018). Inter-tissue communication in cancer cachexia. Nat Rev Endocrinol *15*, 9-20.

Arora, G.K., Gupta, A., Narayanan, S., Guo, T., Iyengar, P., and Infante, R.E. (2018). Cachexia-associated adipose loss induced by tumor-secreted leukemia inhibitory factor is counterbalanced by decreased leptin. JCI Insight *3*.

Arthur, S.T., Noone, J.M., Van Doren, B.A., Roy, D., and Blanchette, C.M. (2014). One-year prevalence, comorbidities and cost of cachexia-related inpatient admissions in the USA. Drugs in context *3*, 212265.

Arthur, S.T., Van Doren, B.A., Roy, D., Noone, J.M., Zacherle, E., and Blanchette, C.M. (2016). Cachexia among US cancer patients. J Med Econ *19*, 874-880.

Asp, M.L., Tian, M., Kliewer, K.L., and Belury, M.A. (2011). Rosiglitazone delayed weight loss and anorexia while attenuating adipose depletion in mice with cancer cachexia. Cancer Biol Ther *12*, 957-965.

Assi, M., Derbre, F., Lefeuvre-Orfila, L., and Rebillard, A. (2016). Antioxidant supplementation accelerates cachexia development by promoting tumor growth in C26 tumor-bearing mice. Free Radic Biol Med *91*, 204-214.

Assi, M., and Rebillard, A. (2016). The Janus-Faced Role of Antioxidants in Cancer Cachexia: New Insights on the Established Concepts. Oxid Med Cell Longev *2016*, 9579868.

Atherton, P.J., and Smith, K. (2012). Muscle protein synthesis in response to nutrition and exercise. J Physiol *590*, 1049-1057.

Atta, M.G., De Seigneux, S., and Lucas, G.M. (2019). Clinical Pharmacology in HIV Therapy. Clin J Am Soc Nephrol *14*, 435-444.

Attard-Montalto, S.P., Camacho-Hubner, C., Cotterill, A.M., D'Souza-Li, L., Daley, S., Bartlett, K., Halliday, D., and Eden, O.B. (1998). Changes in protein turnover, IGF-I and IGF binding proteins in children with cancer. Acta Paediatr *87*, 54-60.

Aulino, P., Berardi, E., Cardillo, V.M., Rizzuto, E., Perniconi, B., Ramina, C., Padula, F., Spugnini, E.P., Baldi, A., Faiola, F.*, et al.* (2010). Molecular, cellular and physiological characterization of the cancer cachexia-inducing C26 colon carcinoma in mouse. BMC cancer *10*, 363.

Aust, S., Knogler, T., Pils, D., Obermayr, E., Reinthaller, A., Zahn, L., Radlgruber, I., Mayerhoefer, M.E., Grimm, C., and Polterauer, S. (2015). Skeletal Muscle Depletion and Markers for Cancer Cachexia Are Strong Prognostic Factors in Epithelial Ovarian Cancer. PLoS One *10*, e0140403.

Aversa, Z., Pin, F., Lucia, S., Penna, F., Verzaro, R., Fazi, M., Colasante, G., Tirone, A., Rossi Fanelli, F., Ramaccini, C*., et al.* (2016). Autophagy is induced in the skeletal muscle of cachectic cancer patients. Scientific reports *6*, 30340.

Baker, J.S., McCormick, M.C., and Robergs, R.A. (2010). Interaction among Skeletal Muscle Metabolic Energy Systems during Intense Exercise. J Nutr Metab *2010*, 905612.

Baltgalvis, K.A., Berger, F.G., Pena, M.M., Davis, J.M., Muga, S.J., and Carson, J.A. (2008). Interleukin-6 and cachexia in ApcMin/+ mice. Am J Physiol Regul Integr Comp Physiol *294*, R393-401.

Baracos, V.E., Martin, L., Korc, M., Guttridge, D.C., and Fearon, K.C.H. (2018). Cancer-associated cachexia. Nat Rev Dis Primers *4*, 17105.

Baracos, V.E., Mazurak, V.C., and Bhullar, A.S. (2019). Cancer cachexia is defined by an ongoing loss of skeletal muscle mass. Ann Palliat Med *8*, 3-12.

Barkhudaryan, A., Scherbakov, N., Springer, J., and Doehner, W. (2017). Cardiac muscle wasting in individuals with cancer cachexia. ESC Heart Fail *4*, 458-467.

Barreiro, E., de la Puente, B., Busquets, S., Lopez-Soriano, F.J., Gea, J., and Argiles, J.M. (2005). Both oxidative and nitrosative stress are associated with muscle wasting in tumour-bearing rats. FEBS Lett *579*, 1646-1652.

Barton, B.E., and Murphy, T.F. (2001). Cancer cachexia is mediated in part by the induction of IL-6-like cytokines from the spleen. Cytokine *16*, 251-257.

Beauloye, C., Bertrand, L., Horman, S., and Hue, L. (2011). AMPK activation, a preventive therapeutic target in the transition from cardiac injury to heart failure. Cardiovasc Res *90*, 224-233.

Beckendorf, L., and Linke, W.A. (2015). Emerging importance of oxidative stress in regulating striated muscle elasticity. J Muscle Res Cell Motil *36*, 25-36.

Bellinger, A.M., Reiken, S., Carlson, C., Mongillo, M., Liu, X., Rothman, L., Matecki, S., Lacampagne, A., and Marks, A.R. (2009). Hypernitrosylated ryanodine receptor calcium release channels are leaky in dystrophic muscle. Nature medicine *15*, 325-330.

Belloum, Y., Rannou-Bekono, F., and Favier, F.B. (2017). Cancer-induced cardiac cachexia: Pathogenesis and impact of physical activity (Review). Oncol Rep *37*, 2543-2552.

Beloribi-Djefaflia, S., Vasseur, S., and Guillaumond, F. (2016). Lipid metabolic reprogramming in cancer cells. Oncogenesis *5*, e189.

Bennani-Baiti, N., and Walsh, D. (2009). What is cancer anorexia-cachexia syndrome? A historical perspective. J R Coll Physicians Edinb *39*, 257-262.

Benny Klimek, M.E., Aydogdu, T., Link, M.J., Pons, M., Koniaris, L.G., and Zimmers, T.A. (2010). Acute inhibition of myostatin-family proteins preserves skeletal muscle in mouse models of cancer cachexia. Biochem Biophys Res Commun *391*, 1548-1554.

Berriel Diaz, M., Krones-Herzig, A., Metzger, D., Ziegler, A., Vegiopoulos, A., Klingenspor, M., Muller-Decker, K., and Herzig, S. (2008). Nuclear receptor cofactor receptor interacting protein 140 controls hepatic triglyceride metabolism during wasting in mice. Hepatology *48*, 782-791.

Bess, E., Fisslthaler, B., Fromel, T., and Fleming, I. (2011). Nitric oxide-induced activation of the AMP-activated protein kinase alpha2 subunit attenuates IkappaB kinase activity and inflammatory responses in endothelial cells. PLoS One *6*, e20848.

Beutler, B., Greenwald, D., Hulmes, J.D., Chang, M., Pan, Y.C., Mathison, J., Ulevitch, R., and Cerami, A. (1985a). Identity of tumour necrosis factor and the macrophage-secreted factor cachectin. Nature *316*, 552-554.

Beutler, B., Mahoney, J., Le Trang, N., Pekala, P., and Cerami, A. (1985b). Purification of cachectin, a lipoprotein lipase-suppressing hormone secreted by endotoxin-induced RAW 264.7 cells. J Exp Med *161*, 984-995.

Bindels, L.B., Beck, R., Schakman, O., Martin, J.C., De Backer, F., Sohet, F.M., Dewulf, E.M., Pachikian, B.D., Neyrinck, A.M., Thissen, J.P*., et al.* (2012). Restoring specific lactobacilli levels decreases inflammation and muscle atrophy markers in an acute leukemia mouse model. PLoS One *7*, e37971.

Bindels, L.B., Neyrinck, A.M., Claus, S.P., Le Roy, C.I., Grangette, C., Pot, B., Martinez, I., Walter, J., Cani, P.D., and Delzenne, N.M. (2016). Synbiotic approach restores intestinal homeostasis and prolongs survival in leukaemic mice with cachexia. ISME J *10*, 1456-1470.

Bindels, L.B., Neyrinck, A.M., Loumaye, A., Catry, E., Walgrave, H., Cherbuy, C., Leclercq, S., Van Hul, M., Plovier, H., Pachikian, B*., et al.* (2018). Increased gut permeability in cancer cachexia: mechanisms and clinical relevance. Oncotarget *9*, 18224-18238.

Bindels, L.B., Neyrinck, A.M., Salazar, N., Taminiau, B., Druart, C., Muccioli, G.G., Francois, E., Blecker, C., Richel, A., Daube, G*., et al.* (2015). Non Digestible Oligosaccharides Modulate the Gut Microbiota to Control the Development of Leukemia and Associated Cachexia in Mice. PLoS One *10*, e0131009.

Birben, E., Sahiner, U.M., Sackesen, C., Erzurum, S., and Kalayci, O. (2012). Oxidative stress and antioxidant defense. World Allergy Organ J *5*, 9-19.

Blaauw, B., and Reggiani, C. (2014). The role of satellite cells in muscle hypertrophy. J Muscle Res Cell Motil *35*, 3-10.

Blauwhoff-Buskermolen, S., de van der Schueren, M.A., Verheul, H.M., and Langius, J.A. (2014). 'Pre-cachexia': a non-existing phenomenon in cancer? Ann Oncol *25*, 1668-1669.

Blum, D., Stene, G.B., Solheim, T.S., Fayers, P., Hjermstad, M.J., Baracos, V.E., Fearon, K., Strasser, F., Kaasa, S., and Euro, I. (2014). Validation of the Consensus-Definition for Cancer Cachexia and evaluation of a classification model--a study based on data from an international multicentre project (EPCRC-CSA). Ann Oncol *25*, 1635-1642.

Bogachus, L.D., and Turcotte, L.P. (2010). Genetic downregulation of AMPK-alpha isoforms uncovers the mechanism by which metformin decreases FA uptake and oxidation in skeletal muscle cells. American journal of physiology Cell physiology *299*, C1549-1561.

Bohm, A., Hoffmann, C., Irmler, M., Schneeweiss, P., Schnauder, G., Sailer, C., Schmid, V., Hudemann, J., Machann, J., Schick, F.*, et al.* (2016). TGF-beta Contributes to Impaired Exercise Response by Suppression of Mitochondrial Key Regulators in Skeletal Muscle. Diabetes *65*, 2849-2861.

Bonaldo, P., and Sandri, M. (2013). Cellular and molecular mechanisms of muscle atrophy. Disease models & mechanisms *6*, 25-39.

Bonetto, A., Aydogdu, T., Jin, X., Zhang, Z., Zhan, R., Puzis, L., Koniaris, L.G., and Zimmers, T.A. (2012). JAK/STAT3 pathway inhibition blocks skeletal muscle wasting downstream of IL-6 and in experimental cancer cachexia. Am J Physiol Endocrinol Metab *303*, E410-421.

Bonetto, A., Aydogdu, T., Kunzevitzky, N., Guttridge, D.C., Khuri, S., Koniaris, L.G., and Zimmers, T.A. (2011). STAT3 activation in skeletal muscle links muscle wasting and the acute phase response in cancer cachexia. PLoS One *6*, e22538.

Bonetto, A., Rupert, J.E., Barreto, R., and Zimmers, T.A. (2016). The Colon-26 Carcinoma Tumor-bearing Mouse as a Model for the Study of Cancer Cachexia. J Vis Exp.

Bonnard, C., Durand, A., Peyrol, S., Chanseaume, E., Chauvin, M.A., Morio, B., Vidal, H., and Rieusset, J. (2008). Mitochondrial dysfunction results from oxidative stress in the skeletal muscle of diet-induced insulin-resistant mice. J Clin Invest *118*, 789-800.

Bost, F., Decoux-Poullot, A.G., Tanti, J.F., and Clavel, S. (2016). Energy disruptors: rising stars in anticancer therapy? Oncogenesis *5*, e188.

Bowtell, J.L., Marwood, S., Bruce, M., Constantin-Teodosiu, D., and Greenhaff, P.L. (2007). Tricarboxylic acid cycle intermediate pool size: functional importance for oxidative metabolism in exercising human skeletal muscle. Sports Med *37*, 1071-1088.

Boyden, S.E., Mahoney, L.J., Kawahara, G., Myers, J.A., Mitsuhashi, S., Estrella, E.A., Duncan, A.R., Dey, F., DeChene, E.T., Blasko-Goehringer, J.M.*, et al.* (2012). Mutations in the satellite cell gene MEGF10 cause a recessive congenital myopathy with minicores. Neurogenetics *13*, 115-124.

Brand, M.D., and Nicholls, D.G. (2011). Assessing mitochondrial dysfunction in cells. Biochem J *435*, 297-312.

Braun, T.P., Grossberg, A.J., Krasnow, S.M., Levasseur, P.R., Szumowski, M., Zhu, X.X., Maxson, J.E., Knoll, J.G., Barnes, A.P., and Marks, D.L. (2013). Cancer- and endotoxin-induced cachexia require intact glucocorticoid signaling in skeletal muscle. FASEB J *27*, 3572-3582.

Braun, T.P., and Marks, D.L. (2015). The regulation of muscle mass by endogenous glucocorticoids. Front Physiol *6*, 12.

Brennan, C.M., Gallouzi, I.E., and Steitz, J.A. (2000). Protein ligands to HuR modulate its interaction with target mRNAs in vivo. J Cell Biol *151*, 1-14.

Bridges, H.R., Jones, A.J., Pollak, M.N., and Hirst, J. (2014). Effects of metformin and other biguanides on oxidative phosphorylation in mitochondria. Biochem J *462*, 475-487.

Brink, M., Price, S.R., Chrast, J., Bailey, J.L., Anwar, A., Mitch, W.E., and Delafontaine, P. (2001). Angiotensin II induces skeletal muscle wasting through enhanced protein degradation and down-regulates autocrine insulin-like growth factor I. Endocrinology *142*, 1489-1496.

Brink, M., Wellen, J., and Delafontaine, P. (1996). Angiotensin II causes weight loss and decreases circulating insulin-like growth factor I in rats through a pressor-independent mechanism. J Clin Invest *97*, 2509-2516.

Brookes, P.S., Yoon, Y., Robotham, J.L., Anders, M.W., and Sheu, S.S. (2004). Calcium, ATP, and ROS: a mitochondrial love-hate triangle. American journal of physiology Cell physiology *287*, C817-833.

Brown, G.C. (2001). Regulation of mitochondrial respiration by nitric oxide inhibition of cytochrome c oxidase. Biochim Biophys Acta *1504*, 46-57.

Brown, G.C., and Borutaite, V. (2004). Inhibition of mitochondrial respiratory complex I by nitric oxide, peroxynitrite and S-nitrosothiols. Biochim Biophys Acta *1658*, 44-49.

Brown, J.L., Lee, D.E., Rosa-Caldwell, M.E., Brown, L.A., Perry, R.A., Haynie, W.S., Huseman, K., Sataranatarajan, K., Van Remmen, H., Washington, T.A.*, et al.* (2018). Protein imbalance in the development of skeletal muscle wasting in tumour-bearing mice. J Cachexia Sarcopenia Muscle *9*, 987-1002.

Brown, J.L., Rosa-Caldwell, M.E., Lee, D.E., Blackwell, T.A., Brown, L.A., Perry, R.A., Haynie, W.S., Hardee, J.P., Carson, J.A., Wiggs, M.P.*, et al.* (2017). Mitochondrial degeneration precedes the

development of muscle atrophy in progression of cancer cachexia in tumour-bearing mice. J Cachexia Sarcopenia Muscle *8*, 926-938.

Brunet, L.R., Finkelman, F.D., Cheever, A.W., Kopf, M.A., and Pearce, E.J. (1997). IL-4 protects against TNF-alpha-mediated cachexia and death during acute schistosomiasis. Journal of immunology *159*, 777-785.

Buck, M., and Chojkier, M. (1996). Muscle wasting and dedifferentiation induced by oxidative stress in a murine model of cachexia is prevented by inhibitors of nitric oxide synthesis and antioxidants. The EMBO journal *15*, 1753-1765.

Buettner, G.R. (2011). Superoxide dismutase in redox biology: the roles of superoxide and hydrogen peroxide. Anticancer Agents Med Chem *11*, 341-346.

Bujak, A.L., Crane, J.D., Lally, J.S., Ford, R.J., Kang, S.J., Rebalka, I.A., Green, A.E., Kemp, B.E., Hawke, T.J., Schertzer, J.D.*, et al.* (2015). AMPK activation of muscle autophagy prevents fasting-induced hypoglycemia and myopathy during aging. Cell metabolism *21*, 883-890.

Bung, N., Surepalli, S., Seshadri, S., Patel, S., Peddasomayajula, S., Kummari, L.K., Kumar, S.T., Babu, P.P., Parsa, K.V.L., Poondra, R.R.*, et al.* (2018). 2-[2-(4-(trifluoromethyl)phenylamino)thiazol-4-yl]acetic acid (Activator-3) is a potent activator of AMPK. Scientific reports *8*, 9599.

Buono, R., Vantaggiato, C., Pisa, V., Azzoni, E., Bassi, M.T., Brunelli, S., Sciorati, C., and Clementi, E. (2012). Nitric oxide sustains long-term skeletal muscle regeneration by regulating fate of satellite cells via signaling pathways requiring Vangl2 and cyclic GMP. Stem Cells *30*, 197-209.

Busquets, S., Almendro, V., Barreiro, E., Figueras, M., Argiles, J.M., and Lopez-Soriano, F.J. (2005). Activation of UCPs gene expression in skeletal muscle can be independent on both circulating fatty acids and food intake. Involvement of ROS in a model of mouse cancer cachexia. FEBS Lett *579*, 717-722.

Busquets, S., Carbo, N., Almendro, V., Figueras, M., Lopez-Soriano, F.J., and Argiles, J.M. (2001). Hyperlipemia: a role in regulating UCP3 gene expression in skeletal muscle during cancer cachexia? FEBS Lett *505*, 255-258.

Busquets, S., Toledo, M., Orpi, M., Massa, D., Porta, M., Capdevila, E., Padilla, N., Frailis, V., Lopez-Soriano, F.J., Han, H.Q.*, et al.* (2012). Myostatin blockage using actRIIB antagonism in mice bearing the Lewis lung carcinoma results in the improvement of muscle wasting and physical performance. J Cachexia Sarcopenia Muscle *3*, 37-43.

Cai, D., Frantz, J.D., Tawa, N.E., Jr., Melendez, P.A., Oh, B.C., Lidov, H.G., Hasselgren, P.O., Frontera, W.R., Lee, J., Glass, D.J.*, et al.* (2004). IKKbeta/NF-kappaB activation causes severe muscle wasting in mice. Cell *119*, 285-298.

Cala, M.P., Agullo-Ortuno, M.T., Prieto-Garcia, E., Gonzalez-Riano, C., Parrilla-Rubio, L., Barbas, C., Diaz-Garcia, C.V., Garcia, A., Pernaut, C., Adeva, J.*, et al.* (2018). Multiplatform plasma fingerprinting in cancer cachexia: a pilot observational and translational study. J Cachexia Sarcopenia Muscle *9*, 348-357.

Calabrese, M.F., Rajamohan, F., Harris, M.S., Caspers, N.L., Magyar, R., Withka, J.M., Wang, H., Borzilleri, K.A., Sahasrabudhe, P.V., Hoth, L.R.*, et al.* (2014). Structural basis for AMPK activation: natural and synthetic ligands regulate kinase activity from opposite poles by different molecular mechanisms. Structure *22*, 1161-1172.

Calabrese, V., Mancuso, C., Calvani, M., Rizzarelli, E., Butterfield, D.A., and Stella, A.M. (2007). Nitric oxide in the central nervous system: neuroprotection versus neurotoxicity. Nat Rev Neurosci *8*, 766-775.

Callahan, L.A., and Supinski, G.S. (2009). Sepsis-induced myopathy. Crit Care Med *37*, S354-367.

Carbone, J.W., McClung, J.P., and Pasiakos, S.M. (2012). Skeletal muscle responses to negative energy balance: effects of dietary protein. Adv Nutr *3*, 119-126.

Carling, D., Sanders, M.J., and Woods, A. (2008). The regulation of AMP-activated protein kinase by upstream kinases. Int J Obes (Lond) *32 Suppl 4*, S55-59.

Carnio, S., LoVerso, F., Baraibar, M.A., Longa, E., Khan, M.M., Maffei, M., Reischl, M., Canepari, M., Loefler, S., Kern, H.*, et al.* (2014). Autophagy impairment in muscle induces neuromuscular junction degeneration and precocious aging. Cell Rep *8*, 1509-1521.

Carson, J.A., and Baltgalvis, K.A. (2010). Interleukin 6 as a key regulator of muscle mass during cachexia. Exerc Sport Sci Rev *38*, 168-176.

Cassina, A., and Radi, R. (1996). Differential inhibitory action of nitric oxide and peroxynitrite on mitochondrial electron transport. Arch Biochem Biophys *328*, 309-316.

Chacon-Cabrera, A., Fermoselle, C., Urtreger, A.J., Mateu-Jimenez, M., Diament, M.J., de Kier Joffe, E.D., Sandri, M., and Barreiro, E. (2014). Pharmacological strategies in lung cancer-induced cachexia: effects on muscle proteolysis, autophagy, structure, and weakness. J Cell Physiol *229*, 1660-1672.

Chang, N.C., Chevalier, F.P., and Rudnicki, M.A. (2016). Satellite Cells in Muscular Dystrophy - Lost in Polarity. Trends Mol Med *22*, 479-496.

Chen, C.L., Chen, J., Rawale, S., Varadharaj, S., Kaumaya, P.P., Zweier, J.L., and Chen, Y.R. (2008). Protein tyrosine nitration of the flavin subunit is associated with oxidative modification of mitochondrial complex II in the post-ischemic myocardium. J Biol Chem *283*, 27991-28003.

Chen, J.L., Walton, K.L., Hagg, A., Colgan, T.D., Johnson, K., Qian, H., Gregorevic, P., and Harrison, C.A. (2017). Specific targeting of TGF-beta family ligands demonstrates distinct roles in the regulation of muscle mass in health and disease. Proc Natl Acad Sci U S A *114*, E5266-E5275.

Chen, J.L., Walton, K.L., Qian, H., Colgan, T.D., Hagg, A., Watt, M.J., Harrison, C.A., and Gregorevic, P. (2016). Differential Effects of IL6 and Activin A in the Development of Cancer-Associated Cachexia. Cancer research *76*, 5372-5382.

Chen, L.F., Mu, Y., and Greene, W.C. (2002). Acetylation of RelA at discrete sites regulates distinct nuclear functions of NF-kappaB. The EMBO journal *21*, 6539-6548.

Cheng, C.S., El-Abd, Y., Bui, K., Hyun, Y.E., Hughes, R.H., Kraus, W.E., and Truskey, G.A. (2014). Conditions that promote primary human skeletal myoblast culture and muscle differentiation in vitro. American journal of physiology Cell physiology *306*, C385-395.

Cheung, W., Yu, P.X., Little, B.M., Cone, R.D., Marks, D.L., and Mak, R.H. (2005). Role of leptin and melanocortin signaling in uremia-associated cachexia. J Clin Invest *115*, 1659-1665.

Chitti, S.V., Fonseka, P., and Mathivanan, S. (2018). Emerging role of extracellular vesicles in mediating cancer cachexia. Biochemical Society transactions *46*, 1129-1136.

Choi, Y., Oh, D.Y., Kim, T.Y., Lee, K.H., Han, S.W., Im, S.A., Kim, T.Y., and Bang, Y.J. (2015). Skeletal Muscle Depletion Predicts the Prognosis of Patients with Advanced Pancreatic Cancer Undergoing Palliative Chemotherapy, Independent of Body Mass Index. PLoS One *10*, e0139749.

Chou, C.C., Lee, K.H., Lai, I.L., Wang, D., Mo, X., Kulp, S.K., Shapiro, C.L., and Chen, C.S. (2014). AMPK reverses the mesenchymal phenotype of cancer cells by targeting the Akt-MDM2-Foxo3a signaling axis. Cancer research *74*, 4783-4795.

Christensen, H.M., Kistorp, C., Schou, M., Keller, N., Zerahn, B., Frystyk, J., Schwarz, P., and Faber, J. (2013). Prevalence of cachexia in chronic heart failure and characteristics of body composition and metabolic status. Endocrine *43*, 626-634.

Collins, P., Bing, C., McCulloch, P., and Williams, G. (2002). Muscle UCP-3 mRNA levels are elevated in weight loss associated with gastrointestinal adenocarcinoma in humans. British journal of cancer *86*, 372-375.

Collisson, E.A., Bailey, P., Chang, D.K., and Biankin, A.V. (2019). Molecular subtypes of pancreatic cancer. Nat Rev Gastroenterol Hepatol *16*, 207-220.

Colombini, M., Blachly-Dyson, E., and Forte, M. (1996). VDAC, a channel in the outer mitochondrial membrane. Ion Channels *4*, 169-202.

Conley, K.E. (2016). Mitochondria to motion: optimizing oxidative phosphorylation to improve exercise performance. The Journal of experimental biology *219*, 243-249.

Constantinou, C., Fontes de Oliveira, C.C., Mintzopoulos, D., Busquets, S., He, J., Kesarwani, M., Mindrinos, M., Rahme, L.G., Argiles, J.M., and Tzika, A.A. (2011). Nuclear magnetic resonance in conjunction with functional genomics suggests mitochondrial dysfunction in a murine model of cancer cachexia. Int J Mol Med *27*, 15-24.

Cool, B., Zinker, B., Chiou, W., Kifle, L., Cao, N., Perham, M., Dickinson, R., Adler, A., Gagne, G., Iyengar, R.*, et al.* (2006). Identification and characterization of a small molecule AMPK activator that treats key components of type 2 diabetes and the metabolic syndrome. Cell metabolism *3*, 403-416.

Copeland, S., Warren, H.S., Lowry, S.F., Calvano, S.E., Remick, D., Inflammation, and the Host Response to Injury, I. (2005). Acute inflammatory response to endotoxin in mice and humans. Clin Diagn Lab Immunol *12*, 60-67.

Costelli, P., Muscaritoli, M., Bossola, M., Moore-Carrasco, R., Crepaldi, S., Grieco, G., Autelli, R., Bonelli, G., Pacelli, F., Lopez-Soriano, F.J.*, et al.* (2005). Skeletal muscle wasting in tumor-bearing rats is associated with MyoD down-regulation. Int J Oncol *26*, 1663-1668.

Costelli, P., Muscaritoli, M., Bossola, M., Penna, F., Reffo, P., Bonetto, A., Busquets, S., Bonelli, G., Lopez-Soriano, F.J., Doglietto, G.B.*, et al.* (2006). IGF-1 is downregulated in experimental cancer cachexia. Am J Physiol Regul Integr Comp Physiol *291*, R674-683.

Crute, B.E., Seefeld, K., Gamble, J., Kemp, B.E., and Witters, L.A. (1998). Functional domains of the alpha1 catalytic subunit of the AMP-activated protein kinase. J Biol Chem *273*, 35347-35354.

Cui, P., Huang, C., Guo, J., Wang, Q., Liu, Z., Zhuo, H., and Lin, D. (2019a). Metabolic Profiling of Tumors, Sera, and Skeletal Muscles from an Orthotopic Murine Model of Gastric Cancer Associated-Cachexia. J Proteome Res *18*, 1880-1892.

Cui, P., Shao, W., Huang, C., Wu, C.J., Jiang, B., and Lin, D. (2019b). Metabolic derangements of skeletal muscle from a murine model of glioma cachexia. Skeletal muscle *9*, 3.

Cuzzocrea, S., Chatterjee, P.K., Mazzon, E., McDonald, M.C., Dugo, L., Di Paola, R., Serraino, I., Britti, D., Caputi, A.P., and Thiemermann, C. (2002). Beneficial effects of GW274150, a novel, potent and selective inhibitor of iNOS activity, in a rodent model of collagen-induced arthritis. Eur J Pharmacol *453*, 119-129.

Dahele, M., Skipworth, R.J., Wall, L., Voss, A., Preston, T., and Fearon, K.C. (2007). Objective physical activity and self-reported quality of life in patients receiving palliative chemotherapy. Journal of pain and symptom management *33*, 676-685.

Dahlman, I., Mejhert, N., Linder, K., Agustsson, T., Mutch, D.M., Kulyte, A., Isaksson, B., Permert, J., Petrovic, N., Nedergaard, J.*, et al.* (2010). Adipose tissue pathways involved in weight loss of cancer cachexia. British journal of cancer *102*, 1541-1548.

Dai, X., Li, T., Bai, Z., Yang, Y., Liu, X., Zhan, J., and Shi, B. (2015). Breast cancer intrinsic subtype classification, clinical use and future trends. Am J Cancer Res *5*, 2929-2943.

Dalal, S. (2019). Lipid metabolism in cancer cachexia. Ann Palliat Med *8*, 13-23.

Das, S.K., Eder, S., Schauer, S., Diwoky, C., Temmel, H., Guertl, B., Gorkiewicz, G., Tamilarasan, K.P., Kumari, P., Trauner, M.*, et al.* (2011). Adipose triglyceride lipase contributes to cancer-associated cachexia. Science *333*, 233-238.

Dasgupta, B., and Seibel, W. (2018). Compound C/Dorsomorphin: Its Use and Misuse as an AMPK Inhibitor. Methods Mol Biol *1732*, 195-202.

de Matos-Neto, E.M., Lima, J.D., de Pereira, W.O., Figueredo, R.G., Riccardi, D.M., Radloff, K., das Neves, R.X., Camargo, R.G., Maximiano, L.F., Tokeshi, F.*, et al.* (2015). Systemic Inflammation in Cachexia - Is Tumor Cytokine Expression Profile the Culprit? Front Immunol *6*, 629.

de Miguel Diez, J., Chancafe Morgan, J., and Jimenez Garcia, R. (2013). The association between COPD and heart failure risk: a review. Int J Chron Obstruct Pulmon Dis *8*, 305-312.

Deans, D.A., Tan, B.H., Ross, J.A., Rose-Zerilli, M., Wigmore, S.J., Howell, W.M., Grimble, R.F., and Fearon, K.C. (2009). Cancer cachexia is associated with the IL10 -1082 gene promoter polymorphism in patients with gastroesophageal malignancy. The American journal of clinical nutrition *89*, 1164-1172.

Del Fabbro, E., Hui, D., Dalal, S., Dev, R., Nooruddin, Z.I., and Bruera, E. (2011). Clinical outcomes and contributors to weight loss in a cancer cachexia clinic. J Palliat Med *14*, 1004-1008.

Delgoffe, G.M., and Vignali, D.A. (2013). STAT heterodimers in immunity: A mixed message or a unique signal? JAKSTAT *2*, e23060.

Der-Torossian, H., Wysong, A., Shadfar, S., Willis, M.S., McDunn, J., and Couch, M.E. (2013). Metabolic derangements in the gastrocnemius and the effect of Compound A therapy in a murine model of cancer cachexia. J Cachexia Sarcopenia Muscle *4*, 145-155.

Deribe, Y.L., Pawson, T., and Dikic, I. (2010). Post-translational modifications in signal integration. Nat Struct Mol Biol *17*, 666-672.

Desjardins, E.M., and Steinberg, G.R. (2018). Emerging Role of AMPK in Brown and Beige Adipose Tissue (BAT): Implications for Obesity, Insulin Resistance, and Type 2 Diabetes. Curr Diab Rep *18*, 80.

Dewys, W.D., Begg, C., Lavin, P.T., Band, P.R., Bennett, J.M., Bertino, J.R., Cohen, M.H., Douglass, H.O., Jr., Engstrom, P.F., Ezdinli, E.Z.*, et al.* (1980). Prognostic effect of weight loss prior to chemotherapy in cancer patients. Eastern Cooperative Oncology Group. Am J Med *69*, 491-497.

Di Marco, S., Cammas, A., Lian, X.J., Kovacs, E.N., Ma, J.F., Hall, D.T., Mazroui, R., Richardson, J., Pelletier, J., and Gallouzi, I.E. (2012). The translation inhibitor pateamine A prevents cachexia-induced muscle wasting in mice. Nat Commun *3*, 896.

Di Marco, S., Mazroui, R., Dallaire, P., Chittur, S., Tenenbaum, S.A., Radzioch, D., Marette, A., and Gallouzi, I.E. (2005). NF-(kappa)B-mediated MyoD decay during muscle wasting requires nitric oxide synthase mRNA stabilization, HuR protein, and nitric oxide release. Molecular and cellular biology *25*, 6533-6545.

Dial, A.G., Ng, S.Y., Manta, A., and Ljubicic, V. (2018). The Role of AMPK in Neuromuscular Biology and Disease. Trends in endocrinology and metabolism: TEM *29*, 300-312.

Dias, F.A., Urboniene, D., Yuzhakova, M.A., Biesiadecki, B.J., Pena, J.R., Goldspink, P.H., Geenen, D.L., and Wolska, B.M. (2010). Ablation of iNOS delays cardiac contractile dysfunction in chronic hypertension. Front Biosci (Elite Ed) *2*, 312-324.

Dikalov, S.I., and Harrison, D.G. (2014). Methods for detection of mitochondrial and cellular reactive oxygen species. Antioxid Redox Signal *20*, 372-382.

Dite, T.A., Ling, N.X.Y., Scott, J.W., Hoque, A., Galic, S., Parker, B.L., Ngoei, K.R.W., Langendorf, C.G., O'Brien, M.T., Kundu, M.*, et al.* (2017). The autophagy initiator ULK1 sensitizes AMPK to allosteric drugs. Nat Commun *8*, 571.

Doyle, A., Zhang, G., Abdel Fattah, E.A., Eissa, N.T., and Li, Y.P. (2011). Toll-like receptor 4 mediates lipopolysaccharide-induced muscle catabolism via coordinate activation of ubiquitin-proteasome and autophagy-lysosome pathways. FASEB J *25*, 99-110.

Drake, J.C., and Yan, Z. (2017). Mitophagy in maintaining skeletal muscle mitochondrial proteostasis and metabolic health with ageing. J Physiol *595*, 6391-6399.

Drott, C., Svaninger, G., and Lundholm, K. (1988). Increased urinary excretion of cortisol and catecholami-NES in malnourished cancer patients. Ann Surg *208*, 645-650.

Ducommun, S., Ford, R.J., Bultot, L., Deak, M., Bertrand, L., Kemp, B.E., Steinberg, G.R., and Sakamoto, K. (2014). Enhanced activation of cellular AMPK by dual-small molecule treatment: AICAR and A769662. Am J Physiol Endocrinol Metab *306*, E688-696.

Dumas, J.F., Goupille, C., Julienne, C.M., Pinault, M., Chevalier, S., Bougnoux, P., Servais, S., and Couet, C. (2011). Efficiency of oxidative phosphorylation in liver mitochondria is decreased in a rat model of peritoneal carcinosis. J Hepatol *54*, 320-327.

Durie, D., Lewis, S.M., Liwak, U., Kisilewicz, M., Gorospe, M., and Holcik, M. (2011). RNA-binding protein HuR mediates cytoprotection through stimulation of XIAP translation. Oncogene *30*, 1460-1469.

Eisele, P.S., Salatino, S., Sobek, J., Hottiger, M.O., and Handschin, C. (2013). The peroxisome proliferator-activated receptor gamma coactivator 1alpha/beta (PGC-1) coactivators repress the transcriptional activity of NF-kappaB in skeletal muscle cells. J Biol Chem *288*, 2246-2260.

Eley, H.L., and Tisdale, M.J. (2007). Skeletal muscle atrophy, a link between depression of protein synthesis and increase in degradation. J Biol Chem *282*, 7087-7097.

Emery, P.W., Edwards, R.H., Rennie, M.J., Souhami, R.L., and Halliday, D. (1984a). Protein synthesis in muscle measured in vivo in cachectic patients with cancer. Br Med J (Clin Res Ed) *289*, 584-586.

Emery, P.W., Lovell, L., and Rennie, M.J. (1984b). Protein synthesis measured in vivo in muscle and liver of cachectic tumor-bearing mice. Cancer research *44*, 2779-2784.

Engineer, D.R., and Garcia, J.M. (2012). Leptin in anorexia and cachexia syndrome. Int J Pept *2012*, 287457.

Engvall, I.L., Elkan, A.C., Tengstrand, B., Cederholm, T., Brismar, K., and Hafstrom, I. (2008). Cachexia in rheumatoid arthritis is associated with inflammatory activity, physical disability, and low bioavailable insulin-like growth factor. Scand J Rheumatol *37*, 321-328.

Escobar, D.A., Botero-Quintero, A.M., Kautza, B.C., Luciano, J., Loughran, P., Darwiche, S., Rosengart, M.R., Zuckerbraun, B.S., and Gomez, H. (2015). Adenosine monophosphate-activated protein kinase activation protects against sepsis-induced organ injury and inflammation. J Surg Res *194*, 262-272.

Espinosa, A., Henriquez-Olguin, C., and Jaimovich, E. (2016). Reactive oxygen species and calcium signals in skeletal muscle: A crosstalk involved in both normal signaling and disease. Cell Calcium *60*, 172-179.

Evans, W.J., Morley, J.E., Argiles, J., Bales, C., Baracos, V., Guttridge, D., Jatoi, A., Kalantar-Zadeh, K., Lochs, H., Mantovani, G.*, et al.* (2008). Cachexia: a new definition. Clinical nutrition *27*, 793-799.

Fan, J., Molina, P.E., Gelato, M.C., and Lang, C.H. (1994). Differential tissue regulation of insulin-like growth factor-I content and binding proteins after endotoxin. Endocrinology *134*, 1685-1692.

Fan, K., Lin, L., Ai, Q., Wan, J., Dai, J., Liu, G., Tang, L., Yang, Y., Ge, P., Jiang, R.*, et al.* (2018). Lipopolysaccharide-Induced Dephosphorylation of AMPK-Activated Protein Kinase Potentiates Inflammatory Injury via Repression of ULK1-Dependent Autophagy. Front Immunol *9*, 1464.

Farkas, J., von Haehling, S., Kalantar-Zadeh, K., Morley, J.E., Anker, S.D., and Lainscak, M. (2013). Cachexia as a major public health problem: frequent, costly, and deadly. J Cachexia Sarcopenia Muscle *4*, 173-178.

Faubert, B., Boily, G., Izreig, S., Griss, T., Samborska, B., Dong, Z., Dupuy, F., Chambers, C., Fuerth, B.J., Viollet, B*., et al.* (2013). AMPK is a negative regulator of the Warburg effect and suppresses tumor growth in vivo. Cell metabolism *17*, 113-124.

Faubert, B., Vincent, E.E., Poffenberger, M.C., and Jones, R.G. (2015). The AMP-activated protein kinase (AMPK) and cancer: many faces of a metabolic regulator. Cancer Lett *356*, 165-170.

Fearon, K., Strasser, F., Anker, S.D., Bosaeus, I., Bruera, E., Fainsinger, R.L., Jatoi, A., Loprinzi, C., MacDonald, N., Mantovani, G*., et al.* (2011). Definition and classification of cancer cachexia: an international consensus. The Lancet Oncology *12*, 489-495.

Fearon, K.C., Glass, D.J., and Guttridge, D.C. (2012). Cancer cachexia: mediators, signaling, and metabolic pathways. Cell metabolism *16*, 153-166.

Fearon, K.C., Von Meyenfeldt, M.F., Moses, A.G., Van Geenen, R., Roy, A., Gouma, D.J., Giacosa, A., Van Gossum, A., Bauer, J., Barber, M.D*., et al.* (2003). Effect of a protein and energy dense N-3 fatty acid enriched oral supplement on loss of weight and lean tissue in cancer cachexia: a randomised double blind trial. Gut *52*, 1479-1486.

Ferber, E.C., Peck, B., Delpuech, O., Bell, G.P., East, P., and Schulze, A. (2012). FOXO3a regulates reactive oxygen metabolism by inhibiting mitochondrial gene expression. Cell Death Differ *19*, 968-979.

Fermoselle, C., Garcia-Arumi, E., Puig-Vilanova, E., Andreu, A.L., Urtreger, A.J., de Kier Joffe, E.D., Tejedor, A., Puente-Maestu, L., and Barreiro, E. (2013). Mitochondrial dysfunction and therapeutic approaches in respiratory and limb muscles of cancer cachectic mice. Exp Physiol *98*, 1349-1365.

Filippin, L.I., Cuevas, M.J., Lima, E., Marroni, N.P., Gonzalez-Gallego, J., and Xavier, R.M. (2011). Nitric oxide regulates the repair of injured skeletal muscle. Nitric Oxide *24*, 43-49.

Flint, T.R., Janowitz, T., Connell, C.M., Roberts, E.W., Denton, A.E., Coll, A.P., Jodrell, D.I., and Fearon, D.T. (2016). Tumor-Induced IL-6 Reprograms Host Metabolism to Suppress Anti-tumor Immunity. Cell metabolism *24*, 672-684.

Flores, E.A., Bistrian, B.R., Pomposelli, J.J., Dinarello, C.A., Blackburn, G.L., and Istfan, N.W. (1989). Infusion of tumor necrosis factor/cachectin promotes muscle catabolism in the rat. A synergistic effect with interleukin 1. J Clin Invest *83*, 1614-1622.

Fontes-Oliveira, C.C., Busquets, S., Toledo, M., Penna, F., Paz Aylwin, M., Sirisi, S., Silva, A.P., Orpi, M., Garcia, A., Sette, A*., et al.* (2013). Mitochondrial and sarcoplasmic reticulum abnormalities in cancer cachexia: altered energetic efficiency? Biochim Biophys Acta *1830*, 2770-2778.

Fouladiun, M., Korner, U., Gunnebo, L., Sixt-Ammilon, P., Bosaeus, I., and Lundholm, K. (2007). Daily physical-rest activities in relation to nutritional state, metabolism, and quality of life in

cancer patients with progressive cachexia. Clinical cancer research : an official journal of the American Association for Cancer Research *13*, 6379-6385.

Friesen, D.E., Baracos, V.E., and Tuszynski, J.A. (2015). Modeling the energetic cost of cancer as a result of altered energy metabolism: implications for cachexia. Theor Biol Med Model *12*, 17.

Frost, R.A., Nystrom, G.J., and Lang, C.H. (2009). Endotoxin and interferon-gamma inhibit translation in skeletal muscle cells by stimulating nitric oxide synthase activity. Shock *32*, 416-426.

Fu, X., Zhu, M.J., Dodson, M.V., and Du, M. (2015). AMP-activated protein kinase stimulates Warburg-like glycolysis and activation of satellite cells during muscle regeneration. J Biol Chem *290*, 26445-26456.

Fujiki, F., Mukaida, N., Hirose, K., Ishida, H., Harada, A., Ohno, S., Bluethmann, H., Kawakami, M., Akiyama, M., Sone, S.*, et al.* (1997). Prevention of adenocarcinoma colon 26-induced cachexia by interleukin 10 gene transfer. Cancer research *57*, 94-99.

Fujimoto-Ouchi, K., Tamura, S., Mori, K., Tanaka, Y., and Ishitsuka, H. (1995). Establishment and characterization of cachexia-inducing and -non-inducing clones of murine colon 26 carcinoma. International journal of cancer *61*, 522-528.

Fukawa, T., Yan-Jiang, B.C., Min-Wen, J.C., Jun-Hao, E.T., Huang, D., Qian, C.N., Ong, P., Li, Z., Chen, S., Mak, S.Y.*, et al.* (2016). Excessive fatty acid oxidation induces muscle atrophy in cancer cachexia. Nature medicine *22*, 666-671.

Galic, S., Fullerton, M.D., Schertzer, J.D., Sikkema, S., Marcinko, K., Walkley, C.R., Izon, D., Honeyman, J., Chen, Z.P., van Denderen, B.J.*, et al.* (2011). Hematopoietic AMPK beta1 reduces mouse adipose tissue macrophage inflammation and insulin resistance in obesity. J Clin Invest *121*, 4903-4915.

Gannavarapu, B.S., Lau, S.K.M., Carter, K., Cannon, N.A., Gao, A., Ahn, C., Meyer, J.J., Sher, D.J., Jatoi, A., Infante, R.*, et al.* (2018). Prevalence and Survival Impact of Pretreatment Cancer-Associated Weight Loss: A Tool for Guiding Early Palliative Care. J Oncol Pract *14*, e238-e250.

Gao, S., and Carson, J.A. (2016). Lewis lung carcinoma regulation of mechanical stretch-induced protein synthesis in cultured myotubes. American journal of physiology Cell physiology *310*, C66-79.

Garrido, P., Shalaby, A., Walsh, E.M., Keane, N., Webber, M., Keane, M.M., Sullivan, F.J., Kerin, M.J., Callagy, G., Ryan, A.E.*, et al.* (2017). Impact of inducible nitric oxide synthase (iNOS) expression on triple negative breast cancer outcome and activation of EGFR and ERK signaling pathways. Oncotarget *8*, 80568-80588.

Gaude, E., Schmidt, C., Gammage, P.A., Dugourd, A., Blacker, T., Chew, S.P., Saez-Rodriguez, J., O'Neill, J.S., Szabadkai, G., Minczuk, M.*, et al.* (2018). NADH Shuttling Couples Cytosolic Reductive

Carboxylation of Glutamine with Glycolysis in Cells with Mitochondrial Dysfunction. Molecular cell *69*, 581-593 e587.

Gloire, G., Legrand-Poels, S., and Piette, J. (2006). NF-kappaB activation by reactive oxygen species: fifteen years later. Biochemical pharmacology *72*, 1493-1505.

Goodman, C.A., McNally, R.M., Hoffmann, F.M., and Hornberger, T.A. (2013). Smad3 induces atrogin-1, inhibits mTOR and protein synthesis, and promotes muscle atrophy in vivo. Mol Endocrinol *27*, 1946-1957.

Goransson, O., McBride, A., Hawley, S.A., Ross, F.A., Shpiro, N., Foretz, M., Viollet, B., Hardie, D.G., and Sakamoto, K. (2007). Mechanism of action of A-769662, a valuable tool for activation of AMP-activated protein kinase. J Biol Chem *282*, 32549-32560.

Grahame Hardie, D. (2016). Regulation of AMP-activated protein kinase by natural and synthetic activators. Acta Pharm Sin B *6*, 1-19.

Granados-Principal, S., Liu, Y., Guevara, M.L., Blanco, E., Choi, D.S., Qian, W., Patel, T., Rodriguez, A.A., Cusimano, J., Weiss, H.L*., et al.* (2015). Inhibition of iNOS as a novel effective targeted therapy against triple-negative breast cancer. Breast Cancer Res *17*, 25.

Gray, L.R., Tompkins, S.C., and Taylor, E.B. (2014). Regulation of pyruvate metabolism and human disease. Cell Mol Life Sci *71*, 2577-2604.

Groarke, J.D., Cheng, S., Jones, L.W., and Moslehi, J. (2013). Cancer cachexia: getting to the heart of the matter. European heart journal.

Gross, D.N., van den Heuvel, A.P., and Birnbaum, M.J. (2008). The role of FoxO in the regulation of metabolism. Oncogene *27*, 2320-2336.

Grossberg, A.J., Scarlett, J.M., and Marks, D.L. (2010). Hypothalamic mechanisms in cachexia. Physiol Behav *100*, 478-489.

Grumati, P., Coletto, L., Schiavinato, A., Castagnaro, S., Bertaggia, E., Sandri, M., and Bonaldo, P. (2011). Physical exercise stimulates autophagy in normal skeletal muscles but is detrimental for collagen VI-deficient muscles. Autophagy *7*, 1415-1423.

Gullett, N.P., Mazurak, V.C., Hebbar, G., and Ziegler, T.R. (2011). Nutritional interventions for cancer-induced cachexia. Curr Probl Cancer *35*, 58-90.

Guttridge, D.C., Mayo, M.W., Madrid, L.V., Wang, C.Y., and Baldwin, A.S., Jr. (2000). NF-kappaB-induced loss of MyoD messenger RNA: possible role in muscle decay and cachexia. Science *289*, 2363-2366.

Hall, D.T., Griss, T., Ma, J.F., Sanchez, B.J., Sadek, J., Tremblay, A.M.K., Mubaid, S., Omer, A., Ford, R.J., Bedard, N*., et al.* (2018). The AMPK agonist 5-aminoimidazole-4-carboxamide ribonucleotide

(AICAR), but not metformin, prevents inflammation-associated cachectic muscle wasting. EMBO Mol Med *10*.

Hall, D.T., Ma, J.F., Marco, S.D., and Gallouzi, I.E. (2011). Inducible nitric oxide synthase (iNOS) in muscle wasting syndrome, sarcopenia, and cachexia. Aging (Albany NY) *3*, 702-715.

Halle, J.L., Pena, G.S., Paez, H.G., Castro, A.J., Rossiter, H.B., Visavadiya, N.P., Whitehurst, M.A., and Khamoui, A.V. (2019). Tissue-specific dysregulation of mitochondrial respiratory capacity and coupling control in colon-26 tumor-induced cachexia. Am J Physiol Regul Integr Comp Physiol.

Hambrecht, R., Schulze, P.C., Gielen, S., Linke, A., Mobius-Winkler, S., Yu, J., Kratzsch, J.J., Baldauf, G., Busse, M.W., Schubert, A*., et al.* (2002). Reduction of insulin-like growth factor-I expression in the skeletal muscle of noncachectic patients with chronic heart failure. J Am Coll Cardiol *39*, 1175-1181.

Han, J., Meng, Q., Shen, L., and Wu, G. (2018). Interleukin-6 induces fat loss in cancer cachexia by promoting white adipose tissue lipolysis and browning. Lipids Health Dis *17*, 14.

Hardee, J.P., Counts, B.R., and Carson, J.A. (2019). Understanding the Role of Exercise in Cancer Cachexia Therapy. Am J Lifestyle Med *13*, 46-60.

Hardee, J.P., Counts, B.R., Gao, S., VanderVeen, B.N., Fix, D.K., Koh, H.J., and Carson, J.A. (2018). Inflammatory signalling regulates eccentric contraction-induced protein synthesis in cachectic skeletal muscle. J Cachexia Sarcopenia Muscle *9*, 369-383.

Hardie, D.G. (2011). AMP-activated protein kinase: an energy sensor that regulates all aspects of cell function. Genes Dev *25*, 1895-1908.

Hardie, D.G., Ross, F.A., and Hawley, S.A. (2012). AMPK: a nutrient and energy sensor that maintains energy homeostasis. Nature reviews Molecular cell biology *13*, 251-262.

Hasselgren, P.O., Alamdari, N., Aversa, Z., Gonnella, P., Smith, I.J., and Tizio, S. (2010). Corticosteroids and muscle wasting: role of transcription factors, nuclear cofactors, and hyperacetylation. Curr Opin Clin Nutr Metab Care *13*, 423-428.

Hattori, Y., Suzuki, K., Hattori, S., and Kasai, K. (2006). Metformin inhibits cytokine-induced nuclear factor kappaB activation via AMP-activated protein kinase activation in vascular endothelial cells. Hypertension *47*, 1183-1188.

He, W.A., Berardi, E., Cardillo, V.M., Acharyya, S., Aulino, P., Thomas-Ahner, J., Wang, J., Bloomston, M., Muscarella, P., Nau, P*., et al.* (2013). NF-kappaB-mediated Pax7 dysregulation in the muscle microenvironment promotes cancer cachexia. J Clin Invest *123*, 4821-4835.

Heberle, A.M., Prentzell, M.T., van Eunen, K., Bakker, B.M., Grellscheid, S.N., and Thedieck, K. (2015). Molecular mechanisms of mTOR regulation by stress. Mol Cell Oncol *2*, e970489.

Heineke, J., Auger-Messier, M., Xu, J., Sargent, M., York, A., Welle, S., and Molkentin, J.D. (2010). Genetic deletion of myostatin from the heart prevents skeletal muscle atrophy in heart failure. Circulation *121*, 419-425.

Hershey, J.W., Sonenberg, N., and Mathews, M.B. (2012). Principles of translational control: an overview. Cold Spring Harbor perspectives in biology *4*.

Herzig, S., and Shaw, R.J. (2018). AMPK: guardian of metabolism and mitochondrial homeostasis. Nature reviews Molecular cell biology *19*, 121-135.

Heusch, P., Aker, S., Boengler, K., Deindl, E., van de Sand, A., Klein, K., Rassaf, T., Konietzka, I., Sewell, A., Menazza, S*., et al.* (2010). Increased inducible nitric oxide synthase and arginase II expression in heart failure: no net nitrite/nitrate production and protein S-nitrosylation. American journal of physiology Heart and circulatory physiology *299*, H446-453.

Hong, N., Yoon, H.J., Lee, Y.H., Kim, H.R., Lee, B.W., Rhee, Y., Kang, E.S., Cha, B.S., and Lee, H.C. (2016). Serum PTHrP Predicts Weight Loss in Cancer Patients Independent of Hypercalcemia, Inflammation, and Tumor Burden. J Clin Endocrinol Metab *101*, 1207-1214.

Hopkinson, J.B. (2014). Psychosocial impact of cancer cachexia. J Cachexia Sarcopenia Muscle *5*, 89-94.

Hornberger, T.A., Sukhija, K.B., Wang, X.R., and Chien, S. (2007). mTOR is the rapamycin-sensitive kinase that confers mechanically-induced phosphorylation of the hydrophobic motif site Thr(389) in p70(S6k). FEBS Lett *581*, 4562-4566.

Hou, Y.C., Wang, C.J., Chao, Y.J., Chen, H.Y., Wang, H.C., Tung, H.L., Lin, J.T., and Shan, Y.S. (2018). Elevated Serum Interleukin-8 Level Correlates with Cancer-Related Cachexia and Sarcopenia: An Indicator for Pancreatic Cancer Outcomes. J Clin Med *7*.

Houten, S.M., Violante, S., Ventura, F.V., and Wanders, R.J. (2016). The Biochemistry and Physiology of Mitochondrial Fatty Acid beta-Oxidation and Its Genetic Disorders. Annual review of physiology *78*, 23-44.

Hu, W., Ru, Z., Xiao, W., Xiong, Z., Wang, C., Yuan, C., Zhang, X., and Yang, H. (2018). Adipose tissue browning in cancer-associated cachexia can be attenuated by inhibition of exosome generation. Biochem Biophys Res Commun *506*, 122-129.

Huang, J., Liu, K., Zhu, S., Xie, M., Kang, R., Cao, L., and Tang, D. (2018). AMPK regulates immunometabolism in sepsis. Brain Behav Immun *72*, 89-100.

Huynh, J., Chand, A., Gough, D., and Ernst, M. (2019). Therapeutically exploiting STAT3 activity in cancer - using tissue repair as a road map. Nature reviews Cancer *19*, 82-96.

Inoki, K., Kim, J., and Guan, K.L. (2012). AMPK and mTOR in cellular energy homeostasis and drug targets. Annual review of pharmacology and toxicology *52*, 381-400.

Iseki, H., Kajimura, N., Ohue, C., Tanaka, R., Akiyama, Y., and Yamaguchi, K. (1995). Cytokine production in five tumor cell lines with activity to induce cancer cachexia syndrome in nude mice. Japanese journal of cancer research : Gann *86*, 562-567.

Iwakiri, Y., and Kim, M.Y. (2015). Nitric oxide in liver diseases. Trends Pharmacol Sci *36*, 524-536.

Iwase, S., Murakami, T., Saito, Y., and Nakagawa, K. (2004). Steep elevation of blood interleukin-6 (IL-6) associated only with late stages of cachexia in cancer patients. Eur Cytokine Netw *15*, 312-316.

Jackman, R.W., Floro, J., Yoshimine, R., Zitin, B., Eiampikul, M., El-Jack, K., Seto, D.N., and Kandarian, S.C. (2017). Continuous Release of Tumor-Derived Factors Improves the Modeling of Cachexia in Muscle Cell Culture. Front Physiol *8*, 738.

Jager, S., Handschin, C., St-Pierre, J., and Spiegelman, B.M. (2007). AMP-activated protein kinase (AMPK) action in skeletal muscle via direct phosphorylation of PGC-1alpha. Proc Natl Acad Sci U S A *104*, 12017-12022.

Jain, S., Gautam, V., and Naseem, S. (2011). Acute-phase proteins: As diagnostic tool. J Pharm Bioallied Sci *3*, 118-127.

Jatoi, A., Dakhil, S.R., Nguyen, P.L., Sloan, J.A., Kugler, J.W., Rowland, K.M., Jr., Soori, G.S., Wender, D.B., Fitch, T.R., Novotny, P.J*., et al.* (2007). A placebo-controlled double blind trial of etanercept for the cancer anorexia/weight loss syndrome: results from N00C1 from the North Central Cancer Treatment Group. Cancer *110*, 1396-1403.

Jatoi, A., Ritter, H.L., Dueck, A., Nguyen, P.L., Nikcevich, D.A., Luyun, R.F., Mattar, B.I., and Loprinzi, C.L. (2010). A placebo-controlled, double-blind trial of infliximab for cancer-associated weight loss in elderly and/or poor performance non-small cell lung cancer patients (N01C9). Lung Cancer *68*, 234-239.

Jeon, M.J., Leem, J., Ko, M.S., Jang, J.E., Park, H.S., Kim, H.S., Kim, M., Kim, E.H., Yoo, H.J., Lee, C.H*., et al.* (2012). Mitochondrial dysfunction and activation of iNOS are responsible for the palmitate-induced decrease in adiponectin synthesis in 3T3L1 adipocytes. Exp Mol Med *44*, 562-570.

Jeon, S.M., and Hay, N. (2015). The double-edged sword of AMPK signaling in cancer and its therapeutic implications. Arch Pharm Res *38*, 346-357.

Jeong, J.Y., Jeoung, N.H., Park, K.G., and Lee, I.K. (2012). Transcriptional regulation of pyruvate dehydrogenase kinase. Diabetes Metab J *36*, 328-335.

Jin, B., and Li, Y.P. (2007). Curcumin prevents lipopolysaccharide-induced atrogin-1/MAFbx upregulation and muscle mass loss. J Cell Biochem *100*, 960-969.

Joanisse, S., Nederveen, J.P., Snijders, T., McKay, B.R., and Parise, G. (2017). Skeletal Muscle Regeneration, Repair and Remodelling in Aging: The Importance of Muscle Stem Cells and Vascularization. Gerontology *63*, 91-100.

Johns, N., Hatakeyama, S., Stephens, N.A., Degen, M., Degen, S., Frieauff, W., Lambert, C., Ross, J.A., Roubenoff, R., Glass, D.J.*, et al.* (2014). Clinical classification of cancer cachexia: phenotypic correlates in human skeletal muscle. PLoS One *9*, e83618.

Johnston, A.J., Murphy, K.T., Jenkinson, L., Laine, D., Emmrich, K., Faou, P., Weston, R., Jayatilleke, K.M., Schloegel, J., Talbo, G.*, et al.* (2015). Targeting of Fn14 Prevents Cancer-Induced Cachexia and Prolongs Survival. Cell *162*, 1365-1378.

Jones, A., Friedrich, K., Rohm, M., Schafer, M., Algire, C., Kulozik, P., Seibert, O., Muller-Decker, K., Sijmonsma, T., Strzoda, D.*, et al.* (2013). TSC22D4 is a molecular output of hepatic wasting metabolism. EMBO Mol Med *5*, 294-308.

Jones, S.P., Greer, J.J., Ware, P.D., Yang, J., Walsh, K., and Lefer, D.J. (2005). Deficiency of iNOS does not attenuate severe congestive heart failure in mice. American journal of physiology Heart and circulatory physiology *288*, H365-370.

Jose, C., Hebert-Chatelain, E., Bellance, N., Larendra, A., Su, M., Nouette-Gaulain, K., and Rossignol, R. (2011). AICAR inhibits cancer cell growth and triggers cell-type distinct effects on OXPHOS biogenesis, oxidative stress and Akt activation. Biochim Biophys Acta *1807*, 707-718.

Julienne, C.M., Dumas, J.F., Goupille, C., Pinault, M., Berri, C., Collin, A., Tesseraud, S., Couet, C., and Servais, S. (2012). Cancer cachexia is associated with a decrease in skeletal muscle mitochondrial oxidative capacities without alteration of ATP production efficiency. J Cachexia Sarcopenia Muscle *3*, 265-275.

Julienne, C.M., Tardieu, M., Chevalier, S., Pinault, M., Bougnoux, P., Labarthe, F., Couet, C., Servais, S., and Dumas, J.F. (2014). Cardiolipin content is involved in liver mitochondrial energy wasting associated with cancer-induced cachexia without the involvement of adenine nucleotide translocase. Biochim Biophys Acta *1842*, 726-733.

Justice, M.J., and Dhillon, P. (2016). Using the mouse to model human disease: increasing validity and reproducibility. Disease models & mechanisms *9*, 101-103.

Kalantar-Zadeh, K., Rhee, C., Sim, J.J., Stenvinkel, P., Anker, S.D., and Kovesdy, C.P. (2013). Why cachexia kills: examining the causality of poor outcomes in wasting conditions. J Cachexia Sarcopenia Muscle *4*, 89-94.

Kapur, S., Bedard, S., Marcotte, B., Cote, C.H., and Marette, A. (1997). Expression of nitric oxide synthase in skeletal muscle: a novel role for nitric oxide as a modulator of insulin action. Diabetes *46*, 1691-1700.

Kayacan, O., Karnak, D., Beder, S., Gullu, E., Tutkak, H., Senler, F.C., and Koksal, D. (2006). Impact of TNF-alpha and IL-6 levels on development of cachexia in newly diagnosed NSCLC patients. Am J Clin Oncol *29*, 328-335.

Kemp, B.E. (2004). Bateman domains and adenosine derivatives form a binding contract. J Clin Invest *113*, 182-184.

Khansari, N., Shakiba, Y., and Mahmoudi, M. (2009). Chronic inflammation and oxidative stress as a major cause of age-related diseases and cancer. Recent Pat Inflamm Allergy Drug Discov *3*, 73-80.

Kim, J., Yang, G., Kim, Y., Kim, J., and Ha, J. (2016). AMPK activators: mechanisms of action and physiological activities. Exp Mol Med *48*, e224.

Kim, S.J., and Yoon, S. (2016). Activated Rac1 regulates the degradation of IkappaBalpha and the nuclear translocation of STAT3-NFkappaB complexes in starved cancer cells. Exp Mol Med *48*, e231.

Kim, Y.D., Kim, Y.H., Cho, Y.M., Kim, D.K., Ahn, S.W., Lee, J.M., Chanda, D., Shong, M., Lee, C.H., and Choi, H.S. (2012). Metformin ameliorates IL-6-induced hepatic insulin resistance via induction of orphan nuclear receptor small heterodimer partner (SHP) in mouse models. Diabetologia *55*, 1482-1494.

Kim, Y.M., Kim, M.Y., Kim, H.J., Roh, G.S., Ko, G.H., Seo, H.G., Lee, J.H., and Chang, K.C. (2011). Compound C independent of AMPK inhibits ICAM-1 and VCAM-1 expression in inflammatory stimulants-activated endothelial cells in vitro and in vivo. Atherosclerosis *219*, 57-64.

Kimball, S.R. (1999). Eukaryotic initiation factor eIF2. Int J Biochem Cell Biol *31*, 25-29.

Kir, S., Komaba, H., Garcia, A.P., Economopoulos, K.P., Liu, W., Lanske, B., Hodin, R.A., and Spiegelman, B.M. (2016). PTH/PTHrP Receptor Mediates Cachexia in Models of Kidney Failure and Cancer. Cell metabolism *23*, 315-323.

Kir, S., White, J.P., Kleiner, S., Kazak, L., Cohen, P., Baracos, V.E., and Spiegelman, B.M. (2014). Tumour-derived PTH-related protein triggers adipose tissue browning and cancer cachexia. Nature *513*, 100-104.

Klaus, A., Polge, C., Zorman, S., Auchli, Y., Brunisholz, R., and Schlattner, U. (2012). A two-dimensional screen for AMPK substrates identifies tumor suppressor fumarate hydratase as a preferential AMPKalpha2 substrate. J Proteomics *75*, 3304-3313.

Kliewer, K.L., Ke, J.Y., Tian, M., Cole, R.M., Andridge, R.R., and Belury, M.A. (2015). Adipose tissue lipolysis and energy metabolism in early cancer cachexia in mice. Cancer Biol Ther *16*, 886-897.

Klok, M.D., Jakobsdottir, S., and Drent, M.L. (2007). The role of leptin and ghrelin in the regulation of food intake and body weight in humans: a review. Obes Rev *8*, 21-34.

Kostourou, V., Cartwright, J.E., Johnstone, A.P., Boult, J.K., Cullis, E.R., Whitley, G., and Robinson, S.P. (2011). The role of tumour-derived iNOS in tumour progression and angiogenesis. British journal of cancer *104*, 83-90.

Kourelis, T.V., and Siegel, R.D. (2012). Metformin and cancer: new applications for an old drug. Medical oncology *29*, 1314-1327.

Krawiec, B.J., Nystrom, G.J., Frost, R.A., Jefferson, L.S., and Lang, C.H. (2007). AMP-activated protein kinase agonists increase mRNA content of the muscle-specific ubiquitin ligases MAFbx and MuRF1 in C2C12 cells. Am J Physiol Endocrinol Metab *292*, E1555-1567.

Kudryashova, E., Kramerova, I., and Spencer, M.J. (2012). Satellite cell senescence underlies myopathy in a mouse model of limb-girdle muscular dystrophy 2H. J Clin Invest *122*, 1764-1776.

Kumar, A., Bhatnagar, S., and Paul, P.K. (2012). TWEAK and TRAF6 regulate skeletal muscle atrophy. Curr Opin Clin Nutr Metab Care *15*, 233-239.

Kumar, A., Yamauchi, J., Girgenrath, T., and Girgenrath, M. (2011). Muscle-specific expression of insulin-like growth factor 1 improves outcome in Lama2Dy-w mice, a model for congenital muscular dystrophy type 1A. Hum Mol Genet *20*, 2333-2343.

Ladner, K.J., Caligiuri, M.A., and Guttridge, D.C. (2003). Tumor necrosis factor-regulated biphasic activation of NF-kappa B is required for cytokine-induced loss of skeletal muscle gene products. J Biol Chem *278*, 2294-2303.

Laflamme, N., and Rivest, S. (1999). Effects of systemic immunogenic insults and circulating proinflammatory cytokines on the transcription of the inhibitory factor kappaB alpha within specific cellular populations of the rat brain. J Neurochem *73*, 309-321.

Lagalice, L., Pichon, J., Gougeon, E., Soussi, S., Deniaud, J., Ledevin, M., Maurier, V., Leroux, I., Durand, S., Ciron, C*., et al.* (2018). Satellite cells fail to contribute to muscle repair but are functional in Pompe disease (glycogenosis type II). Acta Neuropathol Commun *6*, 116.

Langendorf, C.G., and Kemp, B.E. (2015). Choreography of AMPK activation. Cell Res *25*, 5-6.

Langendorf, C.G., Ngoei, K.R.W., Scott, J.W., Ling, N.X.Y., Issa, S.M.A., Gorman, M.A., Parker, M.W., Sakamoto, K., Oakhill, J.S., and Kemp, B.E. (2016). Structural basis of allosteric and synergistic activation of AMPK by furan-2-phosphonic derivative C2 binding. Nat Commun *7*, 10912.

Langstein, H.N., Doherty, G.M., Fraker, D.L., Buresh, C.M., and Norton, J.A. (1991). The roles of gamma-interferon and tumor necrosis factor alpha in an experimental rat model of cancer cachexia. Cancer research *51*, 2302-2306.

Lautaoja, J.H., Lalowski, M., Nissinen, T.A., Hentila, J., Shi, Y., Ritvos, O., Cheng, S., and Hulmi, J.J. (2019). Muscle and serum metabolomes are dysregulated in colon-26 tumor-bearing mice

despite amelioration of cachexia with activin receptor type 2B ligand blockade. Am J Physiol Endocrinol Metab *316*, E852-E865.

Lazarus, D.D., Moldawer, L.L., and Lowry, S.F. (1993). Insulin-like growth factor-1 activity is inhibited by interleukin-1 alpha, tumor necrosis factor-alpha, and interleukin-6. Lymphokine Cytokine Res *12*, 219-223.

Le Grand, F., and Rudnicki, M.A. (2007). Skeletal muscle satellite cells and adult myogenesis. Curr Opin Cell Biol *19*, 628-633.

Lecker, S.H., Goldberg, A.L., and Mitch, W.E. (2006). Protein degradation by the ubiquitin-proteasome pathway in normal and disease states. J Am Soc Nephrol *17*, 1807-1819.

Lee, J.W., Komar, C.A., Bengsch, F., Graham, K., and Beatty, G.L. (2016). Genetically Engineered Mouse Models of Pancreatic Cancer: The KPC Model (LSL-Kras(G12D/+) ;LSL-Trp53(R172H/+) ;Pdx-1-Cre), Its Variants, and Their Application in Immuno-oncology Drug Discovery. Curr Protoc Pharmacol *73*, 14 39 11-14 39 20.

Li, H., Malhotra, S., and Kumar, A. (2008). Nuclear factor-kappa B signaling in skeletal muscle atrophy. Journal of molecular medicine *86*, 1113-1126.

Li, Q., and Verma, I.M. (2002). NF-kappaB regulation in the immune system. Nat Rev Immunol *2*, 725-734.

Liguori, I., Russo, G., Curcio, F., Bulli, G., Aran, L., Della-Morte, D., Gargiulo, G., Testa, G., Cacciatore, F., Bonaduce, D.*, et al.* (2018). Oxidative stress, aging, and diseases. Clin Interv Aging *13*, 757-772.

Lin, C.C., Yeh, H.H., Huang, W.L., Yan, J.J., Lai, W.W., Su, W.P., Chen, H.H., and Su, W.C. (2013). Metformin enhances cisplatin cytotoxicity by suppressing signal transducer and activator of transcription-3 activity independently of the liver kinase B1-AMP-activated protein kinase pathway. Am J Respir Cell Mol Biol *49*, 241-250.

Linker, K., Pautz, A., Fechir, M., Hubrich, T., Greeve, J., and Kleinert, H. (2005). Involvement of KSRP in the post-transcriptional regulation of human iNOS expression-complex interplay of KSRP with TTP and HuR. Nucleic Acids Res *33*, 4813-4827.

Lionetti, V., Stanley, W.C., and Recchia, F.A. (2011). Modulating fatty acid oxidation in heart failure. Cardiovasc Res *90*, 202-209.

Liu, T., Zhang, L., Joo, D., and Sun, S.C. (2017). NF-kappaB signaling in inflammation. Signal Transduct Target Ther *2*.

Liu, Y.H., Carretero, O.A., Cingolani, O.H., Liao, T.D., Sun, Y., Xu, J., Li, L.Y., Pagano, P.J., Yang, J.J., and Yang, X.P. (2005). Role of inducible nitric oxide synthase in cardiac function and remodeling

in mice with heart failure due to myocardial infarction. American journal of physiology Heart and circulatory physiology *289*, H2616-2623.

Llovera, M., Garcia-Martinez, C., Lopez-Soriano, J., Agell, N., Lopez-Soriano, F.J., Garcia, I., and Argiles, J.M. (1998). Protein turnover in skeletal muscle of tumour-bearing transgenic mice overexpressing the soluble TNF receptor-1. Cancer Lett *130*, 19-27.

Loumaye, A., de Barsy, M., Nachit, M., Lause, P., Frateur, L., van Maanen, A., Trefois, P., Gruson, D., and Thissen, J.P. (2015). Role of Activin A and myostatin in human cancer cachexia. J Clin Endocrinol Metab *100*, 2030-2038.

Loumaye, A., de Barsy, M., Nachit, M., Lause, P., van Maanen, A., Trefois, P., Gruson, D., and Thissen, J.P. (2017). Circulating Activin A predicts survival in cancer patients. J Cachexia Sarcopenia Muscle *8*, 768-777.

Lukey, M.J., Katt, W.P., and Cerione, R.A. (2017). Targeting amino acid metabolism for cancer therapy. Drug Discov Today *22*, 796-804.

Luo, Y., Yoneda, J., Ohmori, H., Sasaki, T., Shimbo, K., Eto, S., Kato, Y., Miyano, H., Kobayashi, T., Sasahira, T.*, et al.* (2014). Cancer usurps skeletal muscle as an energy repository. Cancer research *74*, 330-340.

Ma, J., Matkar, S., He, X., and Hua, X. (2018). FOXO family in regulating cancer and metabolism. Semin Cancer Biol *50*, 32-41.

Ma, J.F., **Hall, D.T.**, and Gallouzi, I.E. (2012). The impact of mRNA turnover and translation on age-related muscle loss. Ageing research reviews *11*, 432-441.

Ma, J.F., Sanchez, B.J., Hall, D.T., Tremblay, A.K., Di Marco, S., and Gallouzi, I.E. (2017). STAT3 promotes IFNgamma/TNFalpha-induced muscle wasting in an NF-kappaB-dependent and IL-6-independent manner. EMBO Mol Med *9*, 622-637.

MacDonald, A.J., Johns, N., Stephens, N., Greig, C., Ross, J.A., Small, A.C., Husi, H., Fearon, K.C., and Preston, T. (2015). Habitual Myofibrillar Protein Synthesis Is Normal in Patients with Upper GI Cancer Cachexia. Clinical cancer research : an official journal of the American Association for Cancer Research *21*, 1734-1740.

MacLellan, J.D., Gerrits, M.F., Gowing, A., Smith, P.J., Wheeler, M.B., and Harper, M.E. (2005). Physiological increases in uncoupling protein 3 augment fatty acid oxidation and decrease reactive oxygen species production without uncoupling respiration in muscle cells. Diabetes *54*, 2343-2350.

Mali, S.B. (2015). Review of STAT3 (Signal Transducers and Activators of Transcription) in head and neck cancer. Oral Oncol *51*, 565-569.

Mancini, S.J., White, A.D., Bijland, S., Rutherford, C., Graham, D., Richter, E.A., Viollet, B., Touyz, R.M., Palmer, T.M., and Salt, I.P. (2017). Activation of AMP-activated protein kinase rapidly suppresses multiple pro-inflammatory pathways in adipocytes including IL-1 receptor-associated kinase-4 phosphorylation. Molecular and cellular endocrinology *440*, 44-56.

Mangili, A., Murman, D.H., Zampini, A.M., and Wanke, C.A. (2006). Nutrition and HIV infection: review of weight loss and wasting in the era of highly active antiretroviral therapy from the nutrition for healthy living cohort. Clin Infect Dis *42*, 836-842.

Manning, B.D., and Cantley, L.C. (2007). AKT/PKB signaling: navigating downstream. Cell *129*, 1261-1274.

Marchildon, F., Lala, N., Li, G., St-Louis, C., Lamothe, D., Keller, C., and Wiper-Bergeron, N. (2012). CCAAT/enhancer binding protein beta is expressed in satellite cells and controls myogenesis. Stem Cells *30*, 2619-2630.

Marchildon, F., Lamarche, E., Lala-Tabbert, N., St-Louis, C., and Wiper-Bergeron, N. (2015). Expression of CCAAT/Enhancer Binding Protein Beta in Muscle Satellite Cells Inhibits Myogenesis in Cancer Cachexia. PLoS One *10*, e0145583.

Marin, T.L., Gongol, B., Zhang, F., Martin, M., Johnson, D.A., Xiao, H., Wang, Y., Subramaniam, S., Chien, S., and Shyy, J.Y. (2017). AMPK promotes mitochondrial biogenesis and function by phosphorylating the epigenetic factors DNMT1, RBBP7, and HAT1. Sci Signal *10*.

Marinho, R., Alcantara, P.S.M., Ottoch, J.P., and Seelaender, M. (2017). Role of Exosomal MicroRNAs and myomiRs in the Development of Cancer Cachexia-Associated Muscle Wasting. Front Nutr *4*, 69.

Marks, D.L., Ling, N., and Cone, R.D. (2001). Role of the central melanocortin system in cachexia. Cancer research *61*, 1432-1438.

Martin, B., Caron, N., Jadot, I., Colombaro, V., Federici, G., Depommier, C., and Decleves, A.E. (2018). Evaluation of inducible nitric oxide synthase inhibition on kidney function and structure in high-fat diet-induced kidney disease. Exp Physiol *103*, 125-140.

Martin, L., Senesse, P., Gioulbasanis, I., Antoun, S., Bozzetti, F., Deans, C., Strasser, F., Thoresen, L., Jagoe, R.T., Chasen, M.*, et al.* (2015). Diagnostic criteria for the classification of cancer-associated weight loss. Journal of clinical oncology : official journal of the American Society of Clinical Oncology *33*, 90-99.

Massague, J. (2012). TGFbeta signalling in context. Nature reviews Molecular cell biology *13*, 616-630.

Matthys, P., Dijkmans, R., Proost, P., Van Damme, J., Heremans, H., Sobis, H., and Billiau, A. (1991a). Severe cachexia in mice inoculated with interferon-gamma-producing tumor cells. International journal of cancer *49*, 77-82.

Matthys, P., Heremans, H., Opdenakker, G., and Billiau, A. (1991b). Anti-interferon-gamma antibody treatment, growth of Lewis lung tumours in mice and tumour-associated cachexia. European journal of cancer *27*, 182-187.

McBride, A., Ghilagaber, S., Nikolaev, A., and Hardie, D.G. (2009). The glycogen-binding domain on the AMPK beta subunit allows the kinase to act as a glycogen sensor. Cell metabolism *9*, 23-34.

McDonald, J.J., McMillan, D.C., and Laird, B.J.A. (2018). Targeting IL-1alpha in cancer cachexia: a narrative review. Current opinion in supportive and palliative care *12*, 453-459.

McLean, J.B., Moylan, J.S., and Andrade, F.H. (2014). Mitochondria dysfunction in lung cancer-induced muscle wasting in C2C12 myotubes. Front Physiol *5*, 503.

Melzer, K. (2011). Carbohydrate and fat utilization during rest and physical activity. e-SPEN, the European e-Journal of Clinical Nutrition and Metabolism *6*, e45-e52.

Mercier, S., Breuille, D., Mosoni, L., Obled, C., and Patureau Mirand, P. (2002). Chronic inflammation alters protein metabolism in several organs of adult rats. J Nutr *132*, 1921-1928.

Miron, M.J., Gallouzi, I.E., Lavoie, J.N., and Branton, P.E. (2004). Nuclear localization of the adenovirus E4orf4 protein is mediated through an arginine-rich motif and correlates with cell death. Oncogene *23*, 7458-7468.

Mishima, S., Xu, D., Lu, Q., and Deitch, E.A. (1997). Bacterial translocation is inhibited in inducible nitric oxide synthase knockout mice after endotoxin challenge but not in a model of bacterial overgrowth. Arch Surg *132*, 1190-1195.

Mookerjee, S.A., Gerencser, A.A., Nicholls, D.G., and Brand, M.D. (2017). Quantifying intracellular rates of glycolytic and oxidative ATP production and consumption using extracellular flux measurements. J Biol Chem *292*, 7189-7207.

Mookerjee, S.A., Gerencser, A.A., Nicholls, D.G., and Brand, M.D. (2018). Quantifying intracellular rates of glycolytic and oxidative ATP production and consumption using extracellular flux measurements. J Biol Chem *293*, 12649-12652.

Morley, J.E., Thomas, D.R., and Wilson, M.M. (2006). Cachexia: pathophysiology and clinical relevance. The American journal of clinical nutrition *83*, 735-743.

Mounier, R., Theret, M., Arnold, L., Cuvellier, S., Bultot, L., Goransson, O., Sanz, N., Ferry, A., Sakamoto, K., Foretz, M*., et al.* (2013). AMPKalpha1 regulates macrophage skewing at the time of resolution of inflammation during skeletal muscle regeneration. Cell metabolism *18*, 251-264.

Moustakas, A., Souchelnytskyi, S., and Heldin, C.H. (2001). Smad regulation in TGF-beta signal transduction. Journal of cell science *114*, 4359-4369.

Muhlfeld, C., Das, S.K., Heinzel, F.R., Schmidt, A., Post, H., Schauer, S., Papadakis, T., Kummer, W., and Hoefler, G. (2011). Cancer induces cardiomyocyte remodeling and hypoinnervation in the left ventricle of the mouse heart. PLoS One *6*, e20424.

Mulligan, H.D., Beck, S.A., and Tisdale, M.J. (1992). Lipid metabolism in cancer cachexia. British journal of cancer *66*, 57-61.

Munday, M.R. (2002). Regulation of mammalian acetyl-CoA carboxylase. Biochemical Society transactions *30*, 1059-1064.

Mungrue, I.N., Gros, R., You, X., Pirani, A., Azad, A., Csont, T., Schulz, R., Butany, J., Stewart, D.J., and Husain, M. (2002). Cardiomyocyte overexpression of iNOS in mice results in peroxynitrite generation, heart block, and sudden death. J Clin Invest *109*, 735-743.

Murphy, K.T. (2016). The pathogenesis and treatment of cardiac atrophy in cancer cachexia. American journal of physiology Heart and circulatory physiology *310*, H466-477.

Murphy, K.T., Chee, A., Gleeson, B.G., Naim, T., Swiderski, K., Koopman, R., and Lynch, G.S. (2011). Antibody-directed myostatin inhibition enhances muscle mass and function in tumor-bearing mice. Am J Physiol Regul Integr Comp Physiol *301*, R716-726.

Murphy, K.T., Chee, A., Trieu, J., Naim, T., and Lynch, G.S. (2012). Importance of functional and metabolic impairments in the characterization of the C-26 murine model of cancer cachexia. Disease models & mechanisms *5*, 533-545.

Murphy, M.P. (2009). How mitochondria produce reactive oxygen species. Biochem J *417*, 1-13.

Muscaritoli, M., Anker, S.D., Argiles, J., Aversa, Z., Bauer, J.M., Biolo, G., Boirie, Y., Bosaeus, I., Cederholm, T., Costelli, P*., et al.* (2010). Consensus definition of sarcopenia, cachexia and pre-cachexia: joint document elaborated by Special Interest Groups (SIG) "cachexia-anorexia in chronic wasting diseases" and "nutrition in geriatrics". Clinical nutrition *29*, 154-159.

Nair, A.B., and Jacob, S. (2016). A simple practice guide for dose conversion between animals and human. J Basic Clin Pharm *7*, 27-31.

Naito, T., Okayama, T., Aoyama, T., Ohashi, T., Masuda, Y., Kimura, M., Shiozaki, H., Murakami, H., Kenmotsu, H., Taira, T*., et al.* (2017). Unfavorable impact of cancer cachexia on activity of daily living and need for inpatient care in elderly patients with advanced non-small-cell lung cancer in Japan: a prospective longitudinal observational study. BMC cancer *17*, 800.

Nakashima, K., and Yakabe, Y. (2007). AMPK activation stimulates myofibrillar protein degradation and expression of atrophy-related ubiquitin ligases by increasing FOXO transcription factors in C2C12 myotubes. Bioscience, biotechnology, and biochemistry *71*, 1650-1656.

Narsale, A.A., and Carson, J.A. (2014). Role of interleukin-6 in cachexia: therapeutic implications. Current opinion in supportive and palliative care *8*, 321-327.

Narsale, A.A., Enos, R.T., Puppa, M.J., Chatterjee, S., Murphy, E.A., Fayad, R., Pena, M.O., Durstine, J.L., and Carson, J.A. (2015). Liver inflammation and metabolic signaling in ApcMin/+ mice: the role of cachexia progression. PLoS One *10*, e0119888.

Nerstedt, A., Johansson, A., Andersson, C.X., Cansby, E., Smith, U., and Mahlapuu, M. (2010). AMP-activated protein kinase inhibits IL-6-stimulated inflammatory response in human liver cells by suppressing phosphorylation of signal transducer and activator of transcription 3 (STAT3). Diabetologia *53*, 2406-2416.

Neumann, D. (2018). Is TAK1 a Direct Upstream Kinase of AMPK? Int J Mol Sci *19*.

O'Neill, H.M., Maarbjerg, S.J., Crane, J.D., Jeppesen, J., Jorgensen, S.B., Schertzer, J.D., Shyroka, O., Kiens, B., van Denderen, B.J., Tarnopolsky, M.A.*, et al.* (2011). AMP-activated protein kinase (AMPK) beta1beta2 muscle null mice reveal an essential role for AMPK in maintaining mitochondrial content and glucose uptake during exercise. Proc Natl Acad Sci U S A *108*, 16092-16097.

O'Neill, L.A., and Hardie, D.G. (2013). Metabolism of inflammation limited by AMPK and pseudo-starvation. Nature *493*, 346-355.

Olguin, H.C., and Pisconti, A. (2012). Marking the tempo for myogenesis: Pax7 and the regulation of muscle stem cell fate decisions. J Cell Mol Med *16*, 1013-1025.

Op den Kamp, C.M., Langen, R.C., Minnaard, R., Kelders, M.C., Snepvangers, F.J., Hesselink, M.K., Dingemans, A.C., and Schols, A.M. (2012). Pre-cachexia in patients with stages I-III non-small cell lung cancer: systemic inflammation and functional impairment without activation of skeletal muscle ubiquitin proteasome system. Lung Cancer *76*, 112-117.

Op den Kamp, C.M., Langen, R.C., Snepvangers, F.J., de Theije, C.C., Schellekens, J.M., Laugs, F., Dingemans, A.M., and Schols, A.M. (2013). Nuclear transcription factor kappa B activation and protein turnover adaptations in skeletal muscle of patients with progressive stages of lung cancer cachexia. The American journal of clinical nutrition *98*, 738-748.

Owen, O.E., Kalhan, S.C., and Hanson, R.W. (2002). The key role of anaplerosis and cataplerosis for citric acid cycle function. J Biol Chem *277*, 30409-30412.

Ozorio, G.A., Barao, K., and Forones, N.M. (2017). Cachexia Stage, Patient-Generated Subjective Global Assessment, Phase Angle, and Handgrip Strength in Patients with Gastrointestinal Cancer. Nutr Cancer *69*, 772-779.

Pacher, P., Beckman, J.S., and Liaudet, L. (2007). Nitric oxide and peroxynitrite in health and disease. Physiological reviews *87*, 315-424.

Padrao, A.I., Figueira, A.C., Faustino-Rocha, A.I., Gama, A., Loureiro, M.M., Neuparth, M.J., Moreira-Goncalves, D., Vitorino, R., Amado, F., Santos, L.L.*, et al.* (2017). Long-term exercise

training prevents mammary tumorigenesis-induced muscle wasting in rats through the regulation of TWEAK signalling. Acta Physiol (Oxf) *219*, 803-813.

Padrao, A.I., Moreira-Goncalves, D., Oliveira, P.A., Teixeira, C., Faustino-Rocha, A.I., Helguero, L., Vitorino, R., Santos, L.L., Amado, F., Duarte, J.A*., et al.* (2015). Endurance training prevents TWEAK but not myostatin-mediated cardiac remodelling in cancer cachexia. Arch Biochem Biophys *567*, 13-21.

Padrao, A.I., Oliveira, P., Vitorino, R., Colaco, B., Pires, M.J., Marquez, M., Castellanos, E., Neuparth, M.J., Teixeira, C., Costa, C*., et al.* (2013). Bladder cancer-induced skeletal muscle wasting: disclosing the role of mitochondria plasticity. Int J Biochem Cell Biol *45*, 1399-1409.

Palikaras, K., Lionaki, E., and Tavernarakis, N. (2015). Balancing mitochondrial biogenesis and mitophagy to maintain energy metabolism homeostasis. Cell Death Differ *22*, 1399-1401.

Palmela, C., Chevarin, C., Xu, Z., Torres, J., Sevrin, G., Hirten, R., Barnich, N., Ng, S.C., and Colombel, J.F. (2018). Adherent-invasive Escherichia coli in inflammatory bowel disease. Gut *67*, 574-587.

Parzych, K.R., and Klionsky, D.J. (2014). An overview of autophagy: morphology, mechanism, and regulation. Antioxid Redox Signal *20*, 460-473.

Patel, H.J., and Patel, B.M. (2017). TNF-alpha and cancer cachexia: Molecular insights and clinical implications. Life Sci *170*, 56-63.

Pauly, M., Daussin, F., Burelle, Y., Li, T., Godin, R., Fauconnier, J., Koechlin-Ramonatxo, C., Hugon, G., Lacampagne, A., Coisy-Quivy, M*., et al.* (2012). AMPK activation stimulates autophagy and ameliorates muscular dystrophy in the mdx mouse diaphragm. The American journal of pathology *181*, 583-592.

Pautz, A., Art, J., Hahn, S., Nowag, S., Voss, C., and Kleinert, H. (2010). Regulation of the expression of inducible nitric oxide synthase. Nitric Oxide *23*, 75-93.

Penna, F., Bonetto, A., Muscaritoli, M., Costamagna, D., Minero, V.G., Bonelli, G., Rossi Fanelli, F., Baccino, F.M., and Costelli, P. (2010). Muscle atrophy in experimental cancer cachexia: is the IGF-1 signaling pathway involved? International journal of cancer *127*, 1706-1717.

Penna, F., Costamagna, D., Pin, F., Camperi, A., Fanzani, A., Chiarpotto, E.M., Cavallini, G., Bonelli, G., Baccino, F.M., and Costelli, P. (2013). Autophagic degradation contributes to muscle wasting in cancer cachexia. The American journal of pathology *182*, 1367-1378.

Petruzzelli, M., Schweiger, M., Schreiber, R., Campos-Olivas, R., Tsoli, M., Allen, J., Swarbrick, M., Rose-John, S., Rincon, M., Robertson, G*., et al.* (2014). A switch from white to brown fat increases energy expenditure in cancer-associated cachexia. Cell metabolism *20*, 433-447.

Peyta, L., Jarnouen, K., Pinault, M., Coulouarn, C., Guimaraes, C., Goupille, C., de Barros, J.P., Chevalier, S., Dumas, J.F., Maillot, F.*, et al.* (2015). Regulation of hepatic cardiolipin metabolism by TNFalpha: Implication in cancer cachexia. Biochim Biophys Acta *1851*, 1490-1500.

Pfeffer, G., and Chinnery, P.F. (2013). Diagnosis and treatment of mitochondrial myopathies. Ann Med *45*, 4-16.

Phaniendra, A., Jestadi, D.B., and Periyasamy, L. (2015). Free radicals: properties, sources, targets, and their implication in various diseases. Indian J Clin Biochem *30*, 11-26.

Pigna, E., Berardi, E., Aulino, P., Rizzuto, E., Zampieri, S., Carraro, U., Kern, H., Merigliano, S., Gruppo, M., Mericskay, M.*, et al.* (2016). Aerobic Exercise and Pharmacological Treatments Counteract Cachexia by Modulating Autophagy in Colon Cancer. Scientific reports *6*, 26991.

Pin, F., Barreto, R., Couch, M.E., Bonetto, A., and O'Connell, T.M. (2019a). Cachexia induced by cancer and chemotherapy yield distinct perturbations to energy metabolism. J Cachexia Sarcopenia Muscle *10*, 140-154.

Pin, F., Novinger, L.J., Huot, J.R., Harris, R.A., Couch, M.E., O'Connell, T.M., and Bonetto, A. (2019b). PDK4 drives metabolic alterations and muscle atrophy in cancer cachexia. FASEB J *33*, 7778-7790.

Ponikowski, P., Piepoli, M., Chua, T.P., Banasiak, W., Francis, D., Anker, S.D., and Coats, A.J. (1999). The impact of cachexia on cardiorespiratory reflex control in chronic heart failure. European heart journal *20*, 1667-1675.

Porporato, P.E. (2016). Understanding cachexia as a cancer metabolism syndrome. Oncogenesis *5*, e200.

Potgens, S.A., Brossel, H., Sboarina, M., Catry, E., Cani, P.D., Neyrinck, A.M., Delzenne, N.M., and Bindels, L.B. (2018). Klebsiella oxytoca expands in cancer cachexia and acts as a gut pathobiont contributing to intestinal dysfunction. Scientific reports *8*, 12321.

Powers, S.K., Morton, A.B., Ahn, B., and Smuder, A.J. (2016). Redox control of skeletal muscle atrophy. Free Radic Biol Med *98*, 208-217.

Prado, C.M., Baracos, V.E., McCargar, L.J., Mourtzakis, M., Mulder, K.E., Reiman, T., Butts, C.A., Scarfe, A.G., and Sawyer, M.B. (2007). Body composition as an independent determinant of 5-fluorouracil-based chemotherapy toxicity. Clinical cancer research : an official journal of the American Association for Cancer Research *13*, 3264-3268.

Prokopchuk, O., Steinacker, J.M., Nitsche, U., Otto, S., Bachmann, J., Schubert, E.C., Friess, H., and Martignoni, M.E. (2017). IL-4 mRNA Is Downregulated in the Liver of Pancreatic Cancer Patients Suffering from Cachexia. Nutr Cancer *69*, 84-91.

Puig-Vilanova, E., Rodriguez, D.A., Lloreta, J., Ausin, P., Pascual-Guardia, S., Broquetas, J., Roca, J., Gea, J., and Barreiro, E. (2015). Oxidative stress, redox signaling pathways, and autophagy in cachectic muscles of male patients with advanced COPD and lung cancer. Free Radic Biol Med *79*, 91-108.

Puppa, M.J., Gao, S., Narsale, A.A., and Carson, J.A. (2014a). Skeletal muscle glycoprotein 130's role in Lewis lung carcinoma-induced cachexia. FASEB J *28*, 998-1009.

Puppa, M.J., Murphy, E.A., Fayad, R., Hand, G.A., and Carson, J.A. (2014b). Cachectic skeletal muscle response to a novel bout of low-frequency stimulation. Journal of applied physiology *116*, 1078-1087.

Puppa, M.J., White, J.P., Sato, S., Cairns, M., Baynes, J.W., and Carson, J.A. (2011). Gut barrier dysfunction in the Apc(Min/+) mouse model of colon cancer cachexia. Biochim Biophys Acta *1812*, 1601-1606.

Puppa, M.J., White, J.P., Velazquez, K.T., Baltgalvis, K.A., Sato, S., Baynes, J.W., and Carson, J.A. (2012). The effect of exercise on IL-6-induced cachexia in the Apc (Min/+) mouse. J Cachexia Sarcopenia Muscle *3*, 117-137.

Quan-Jun, Y., Yan, H., Yong-Long, H., Li-Li, W., Jie, L., Jin-Lu, H., Jin, L., Peng-Guo, C., Run, G., and Cheng, G. (2017). Selumetinib Attenuates Skeletal Muscle Wasting in Murine Cachexia Model through ERK Inhibition and AKT Activation. Molecular cancer therapeutics *16*, 334-343.

Quan, H., Kim, J.M., Lee, H.J., Lee, S.H., Choi, J.I., and Bae, H.B. (2015). AICAR Enhances the Phagocytic Ability of Macrophages towards Apoptotic Cells through P38 Mitogen Activated Protein Kinase Activation Independent of AMP-Activated Protein Kinase. PLoS One *10*, e0127885.

Radi, R. (2013a). Peroxynitrite, a stealthy biological oxidant. J Biol Chem *288*, 26464-26472.

Radi, R. (2013b). Protein tyrosine nitration: biochemical mechanisms and structural basis of functional effects. Acc Chem Res *46*, 550-559.

Radi, R., Rodriguez, M., Castro, L., and Telleri, R. (1994). Inhibition of mitochondrial electron transport by peroxynitrite. Arch Biochem Biophys *308*, 89-95.

Rajamohan, F., Reyes, A.R., Frisbie, R.K., Hoth, L.R., Sahasrabudhe, P., Magyar, R., Landro, J.A., Withka, J.M., Caspers, N.L., Calabrese, M.F*., et al.* (2016). Probing the enzyme kinetics, allosteric modulation and activation of alpha1- and alpha2-subunit-containing AMP-activated protein kinase (AMPK) heterotrimeric complexes by pharmacological and physiological activators. Biochem J *473*, 581-592.

Ramamoorthy, S., Donohue, M., and Buck, M. (2009). Decreased Jun-D and myogenin expression in muscle wasting of human cachexia. Am J Physiol Endocrinol Metab *297*, E392-401.

Rao, E., Zhang, Y., Li, Q., Hao, J., Egilmez, N.K., Suttles, J., and Li, B. (2016). AMPK-dependent and independent effects of AICAR and compound C on T-cell responses. Oncotarget *7*, 33783-33795.

Reich, N.C. (2013). STATs get their move on. JAKSTAT *2*, e27080.

Reim, D., and Friess, H. (2016). Feeding Challenges in Patients with Esophageal and Gastroesophageal Cancers. Gastrointest Tumors *2*, 166-177.

Rennie, M.J., Edwards, R.H., Emery, P.W., Halliday, D., Lundholm, K., and Millward, D.J. (1983). Depressed protein synthesis is the dominant characteristic of muscle wasting and cachexia. Clinical physiology *3*, 387-398.

Richter, E.A., and Ruderman, N.B. (2009). AMPK and the biochemistry of exercise: implications for human health and disease. Biochem J *418*, 261-275.

Riediger, T., Cordani, C., Potes, C.S., and Lutz, T.A. (2010). Involvement of nitric oxide in lipopolysaccharide induced anorexia. Pharmacol Biochem Behav *97*, 112-120.

Rigamonti, E., Touvier, T., Clementi, E., Manfredi, A.A., Brunelli, S., and Rovere-Querini, P. (2013). Requirement of inducible nitric oxide synthase for skeletal muscle regeneration after acute damage. Journal of immunology *190*, 1767-1777.

Rodgers, B.D., Wiedeback, B.D., Hoversten, K.E., Jackson, M.F., Walker, R.G., and Thompson, T.B. (2014). Myostatin stimulates, not inihibits, C2C12 myoblast proliferation. Endocrinology *155*, 670-675.

Rodriguez-Pascual, F., Hausding, M., Ihrig-Biedert, I., Furneaux, H., Levy, A.P., Forstermann, U., and Kleinert, H. (2000). Complex contribution of the 3'-untranslated region to the expressional regulation of the human inducible nitric-oxide synthase gene. Involvement of the RNA-binding protein HuR. J Biol Chem *275*, 26040-26049.

Rodriguez, J., Vernus, B., Chelh, I., Cassar-Malek, I., Gabillard, J.C., Hadj Sassi, A., Seiliez, I., Picard, B., and Bonnieu, A. (2014). Myostatin and the skeletal muscle atrophy and hypertrophy signaling pathways. Cell Mol Life Sci *71*, 4361-4371.

Rohm, M., Schafer, M., Laurent, V., Ustunel, B.E., Niopek, K., Algire, C., Hautzinger, O., Sijmonsma, T.P., Zota, A., Medrikova, D*., et al.* (2016). An AMP-activated protein kinase-stabilizing peptide ameliorates adipose tissue wasting in cancer cachexia in mice. Nature medicine *22*, 1120-1130.

Ronnett, G.V., Ramamurthy, S., Kleman, A.M., Landree, L.E., and Aja, S. (2009). AMPK in the brain: its roles in energy balance and neuroprotection. J Neurochem *109 Suppl 1*, 17-23.

Ross, F.A., Hawley, S.A., Auciello, F.R., Gowans, G.J., Atrih, A., Lamont, D.J., and Hardie, D.G. (2017). Mechanisms of Paradoxical Activation of AMPK by the Kinase Inhibitors SU6656 and Sorafenib. Cell Chem Biol *24*, 813-824 e814.

Ross, F.A., Jensen, T.E., and Hardie, D.G. (2016). Differential regulation by AMP and ADP of AMPK complexes containing different gamma subunit isoforms. Biochem J *473*, 189-199.

Rousset, S., Alves-Guerra, M.C., Mozo, J., Miroux, B., Cassard-Doulcier, A.M., Bouillaud, F., and Ricquier, D. (2004). The biology of mitochondrial uncoupling proteins. Diabetes *53 Suppl 1*, S130-135.

Roux, P.P., Shahbazian, D., Vu, H., Holz, M.K., Cohen, M.S., Taunton, J., Sonenberg, N., and Blenis, J. (2007). RAS/ERK signaling promotes site-specific ribosomal protein S6 phosphorylation via RSK and stimulates cap-dependent translation. J Biol Chem *282*, 14056-14064.

Salazar-Degracia, A., Busquets, S., Argiles, J.M., Lopez-Soriano, F.J., and Barreiro, E. (2017). Formoterol attenuates increased oxidative stress and myosin protein loss in respiratory and limb muscles of cancer cachectic rats. PeerJ *5*, e4109.

Salminen, A., Hyttinen, J.M., and Kaarniranta, K. (2011). AMP-activated protein kinase inhibits NF-kappaB signaling and inflammation: impact on healthspan and lifespan. Journal of molecular medicine *89*, 667-676.

Salminen, A., Kaarniranta, K., and Kauppinen, A. (2016). Age-related changes in AMPK activation: Role for AMPK phosphatases and inhibitory phosphorylation by upstream signaling pathways. Ageing research reviews *28*, 15-26.

Salt, I.P., and Palmer, T.M. (2012). Exploiting the anti-inflammatory effects of AMP-activated protein kinase activation. Expert opinion on investigational drugs *21*, 1155-1167.

Sanchis, D., Busquets, S., Alvarez, B., Ricquier, D., Lopez-Soriano, F.J., and Argiles, J.M. (1998). Skeletal muscle UCP2 and UCP3 gene expression in a rat cancer cachexia model. FEBS Lett *436*, 415-418.

Sanders, K.J., Kneppers, A.E., van de Bool, C., Langen, R.C., and Schols, A.M. (2016). Cachexia in chronic obstructive pulmonary disease: new insights and therapeutic perspective. J Cachexia Sarcopenia Muscle *7*, 5-22.

Sanders, M.J., Ali, Z.S., Hegarty, B.D., Heath, R., Snowden, M.A., and Carling, D. (2007). Defining the mechanism of activation of AMP-activated protein kinase by the small molecule A-769662, a member of the thienopyridone family. J Biol Chem *282*, 32539-32548.

Sandri, M. (2016). Protein breakdown in cancer cachexia. Semin Cell Dev Biol *54*, 11-19.

Sandri, M., Lin, J., Handschin, C., Yang, W., Arany, Z.P., Lecker, S.H., Goldberg, A.L., and Spiegelman, B.M. (2006). PGC-1alpha protects skeletal muscle from atrophy by suppressing FoxO3 action and atrophy-specific gene transcription. Proc Natl Acad Sci U S A *103*, 16260-16265.

Sartori, R., Milan, G., Patron, M., Mammucari, C., Blaauw, B., Abraham, R., and Sandri, M. (2009). Smad2 and 3 transcription factors control muscle mass in adulthood. American journal of physiology Cell physiology *296*, C1248-1257.

Saunier, E., Benelli, C., and Bortoli, S. (2016). The pyruvate dehydrogenase complex in cancer: An old metabolic gatekeeper regulated by new pathways and pharmacological agents. International journal of cancer *138*, 809-817.

Saxena, M., Balaji, S.A., Deshpande, N., Ranganathan, S., Pillai, D.M., Hindupur, S.K., and Rangarajan, A. (2018). AMP-activated protein kinase promotes epithelial-mesenchymal transition in cancer cells through Twist1 upregulation. Journal of cell science *131*.

Schaaf, G.J., van Gestel, T.J.M., In 't Groen, S.L.M., de Jong, B., Boomaars, B., Tarallo, A., Cardone, M., Parenti, G., van der Ploeg, A.T., and Pijnappel, W. (2018). Satellite cells maintain regenerative capacity but fail to repair disease-associated muscle damage in mice with Pompe disease. Acta Neuropathol Commun *6*, 119.

Schaffer, B.E., Levin, R.S., Hertz, N.T., Maures, T.J., Schoof, M.L., Hollstein, P.E., Benayoun, B.A., Banko, M.R., Shaw, R.J., Shokat, K.M.*, et al.* (2015). Identification of AMPK Phosphorylation Sites Reveals a Network of Proteins Involved in Cell Invasion and Facilitates Large-Scale Substrate Prediction. Cell metabolism *22*, 907-921.

Schakman, O., Gilson, H., de Coninck, V., Lause, P., Verniers, J., Havaux, X., Ketelslegers, J.M., and Thissen, J.P. (2005). Insulin-like growth factor-I gene transfer by electroporation prevents skeletal muscle atrophy in glucocorticoid-treated rats. Endocrinology *146*, 1789-1797.

Schakman, O., Kalista, S., Barbe, C., Loumaye, A., and Thissen, J.P. (2013). Glucocorticoid-induced skeletal muscle atrophy. Int J Biochem Cell Biol *45*, 2163-2172.

Schiaffino, S., and Mammucari, C. (2011). Regulation of skeletal muscle growth by the IGF1-Akt/PKB pathway: insights from genetic models. Skeletal muscle *1*, 4.

Schmidt, K., von Haehling, S., Doehner, W., Palus, S., Anker, S.D., and Springer, J. (2011). IGF-1 treatment reduces weight loss and improves outcome in a rat model of cancer cachexia. J Cachexia Sarcopenia Muscle *2*, 105-109.

Schmitt, T.L., Martignoni, M.E., Bachmann, J., Fechtner, K., Friess, H., Kinscherf, R., and Hildebrandt, W. (2007). Activity of the Akt-dependent anabolic and catabolic pathways in muscle and liver samples in cancer-related cachexia. Journal of molecular medicine *85*, 647-654.

Schneider, C.A., Rasband, W.S., and Eliceiri, K.W. (2012). NIH Image to ImageJ: 25 years of image analysis. Nature methods *9*, 671-675.

Scott, J.W., Ling, N., Issa, S.M., Dite, T.A., O'Brien, M.T., Chen, Z.P., Galic, S., Langendorf, C.G., Steinberg, G.R., Kemp, B.E.*, et al.* (2014). Small molecule drug A-769662 and AMP synergistically activate naive AMPK independent of upstream kinase signaling. Chemistry & biology *21*, 619-627.

Scott, J.W., van Denderen, B.J., Jorgensen, S.B., Honeyman, J.E., Steinberg, G.R., Oakhill, J.S., Iseli, T.J., Koay, A., Gooley, P.R., Stapleton, D.*, et al.* (2008). Thienopyridone drugs are selective activators of AMP-activated protein kinase beta1-containing complexes. Chemistry & biology *15*, 1220-1230.

Seimetz, M., Parajuli, N., Pichl, A., Veit, F., Kwapiszewska, G., Weisel, F.C., Milger, K., Egemnazarov, B., Turowska, A., Fuchs, B.*, et al.* (2011). Inducible NOS inhibition reverses tobacco-smoke-induced emphysema and pulmonary hypertension in mice. Cell *147*, 293-305.

Seto, D.N., Kandarian, S.C., and Jackman, R.W. (2015). A Key Role for Leukemia Inhibitory Factor in C26 Cancer Cachexia. J Biol Chem *290*, 19976-19986.

Shaarawy, M., and Abdel-Aziz, O. (1992). Serum tumour necrosis factor alpha levels in benign and malignant lesions of the endometrium in postmenopausal women. A preliminary study. Acta Oncol *31*, 417-420.

Shao, Y., and Williamson, C. (2012). The HIV-1 epidemic: low- to middle-income countries. Cold Spring Harb Perspect Med *2*, a007187.

Sharpe, M.A., and Cooper, C.E. (1998). Interaction of peroxynitrite with mitochondrial cytochrome oxidase. Catalytic production of nitric oxide and irreversible inhibition of enzyme activity. J Biol Chem *273*, 30961-30972.

Shavlakadze, T., White, J., Hoh, J.F., Rosenthal, N., and Grounds, M.D. (2004). Targeted expression of insulin-like growth factor-I reduces early myofiber necrosis in dystrophic mdx mice. Mol Ther *10*, 829-843.

Shaw, R.J. (2009). LKB1 and AMP-activated protein kinase control of mTOR signalling and growth. Acta Physiol (Oxf) *196*, 65-80.

Shibutani, M., Maeda, K., Nagahara, H., Iseki, Y., Hirakawa, K., and Ohira, M. (2016). The significance of the C-reactive protein to albumin ratio as a marker for predicting survival and monitoring chemotherapeutic effectiveness in patients with unresectable metastatic colorectal cancer. Springerplus *5*, 1798.

Shimomura, Y., Murakami, T., Nakai, N., Nagasaki, M., and Harris, R.A. (2004). Exercise promotes BCAA catabolism: effects of BCAA supplementation on skeletal muscle during exercise. J Nutr *134*, 1583S-1587S.

Shirwany, N.A., and Zou, M.H. (2010). AMPK in cardiovascular health and disease. Acta pharmacologica Sinica *31*, 1075-1084.

Shum, A.M., Mahendradatta, T., Taylor, R.J., Painter, A.B., Moore, M.M., Tsoli, M., Tan, T.C., Clarke, S.J., Robertson, G.R., and Polly, P. (2012). Disruption of MEF2C signaling and loss of sarcomeric and mitochondrial integrity in cancer-induced skeletal muscle wasting. Aging (Albany NY) *4*, 133-143.

Silva, K.A., Dong, J., Dong, Y., Dong, Y., Schor, N., Tweardy, D.J., Zhang, L., and Mitch, W.E. (2015). Inhibition of Stat3 activation suppresses caspase-3 and the ubiquitin-proteasome system, leading to preservation of muscle mass in cancer cachexia. J Biol Chem *290*, 11177-11187.

Smeitink, J., van den Heuvel, L., and DiMauro, S. (2001). The genetics and pathology of oxidative phosphorylation. Nat Rev Genet *2*, 342-352.

Smiles, W.J., Hawley, J.A., and Camera, D.M. (2016). Effects of skeletal muscle energy availability on protein turnover responses to exercise. The Journal of experimental biology *219*, 214-225.

Smith, A.M., Depp, C., Ryan, B.J., Johnston, G.I., Alegre-Abarrategui, J., Evetts, S., Rolinski, M., Baig, F., Ruffmann, C., Simon, A.K.*, et al.* (2018). Mitochondrial dysfunction and increased glycolysis in prodromal and early Parkinson's blood cells. Mov Disord *33*, 1580-1590.

Smith, K.L., and Tisdale, M.J. (1993). Increased protein degradation and decreased protein synthesis in skeletal muscle during cancer cachexia. British journal of cancer *67*, 680-685.

Socher, S.H., Martinez, D., Craig, J.B., Kuhn, J.G., and Oliff, A. (1988). Tumor necrosis factor not detectable in patients with clinical cancer cachexia. J Natl Cancer Inst *80*, 595-598.

Song, Y.H., Li, Y., Du, J., Mitch, W.E., Rosenthal, N., and Delafontaine, P. (2005). Muscle-specific expression of IGF-1 blocks angiotensin II-induced skeletal muscle wasting. J Clin Invest *115*, 451-458.

Songur, N., Kuru, B., Kalkan, F., Ozdilekcan, C., Cakmak, H., and Hizel, N. (2004). Serum interleukin-6 levels correlate with malnutrition and survival in patients with advanced non-small cell lung cancer. Tumori *90*, 196-200.

Stamler, J.S., and Meissner, G. (2001). Physiology of nitric oxide in skeletal muscle. Physiological reviews *81*, 209-237.

Stein, S.C., Woods, A., Jones, N.A., Davison, M.D., and Carling, D. (2000). The regulation of AMP-activated protein kinase by phosphorylation. Biochem J *345 Pt 3*, 437-443.

Steinberg, G.R., and Carling, D. (2019). AMP-activated protein kinase: the current landscape for drug development. Nat Rev Drug Discov *18*, 527-551.

Steinberg, G.R., and Kemp, B.E. (2009). AMPK in Health and Disease. Physiological reviews *89*, 1025-1078.

Stephens, N.A., Gallagher, I.J., Rooyackers, O., Skipworth, R.J., Tan, B.H., Marstrand, T., Ross, J.A., Guttridge, D.C., Lundell, L., Fearon, K.C.*, et al.* (2010). Using transcriptomics to identify and validate novel biomarkers of human skeletal muscle cancer cachexia. Genome Med *2*, 1.

Stephens, N.A., Skipworth, R.J., Gallagher, I.J., Greig, C.A., Guttridge, D.C., Ross, J.A., and Fearon, K.C. (2015). Evaluating potential biomarkers of cachexia and survival in skeletal muscle of upper gastrointestinal cancer patients. J Cachexia Sarcopenia Muscle *6*, 53-61.

Strassmann, G., Fong, M., Kenney, J.S., and Jacob, C.O. (1992a). Evidence for the involvement of interleukin 6 in experimental cancer cachexia. J Clin Invest *89*, 1681-1684.

Strassmann, G., Jacob, C.O., Evans, R., Beall, D., and Fong, M. (1992b). Mechanisms of experimental cancer cachexia. Interaction between mononuclear phagocytes and colon-26 carcinoma and its relevance to IL-6-mediated cancer cachexia. Journal of immunology *148*, 3674-3678.

Strassmann, G., Masui, Y., Chizzonite, R., and Fong, M. (1993). Mechanisms of experimental cancer cachexia. Local involvement of IL-1 in colon-26 tumor. Journal of immunology *150*, 2341-2345.

Strijdom, H., Chamane, N., and Lochner, A. (2009). Nitric oxide in the cardiovascular system: a simple molecule with complex actions. Cardiovasc J Afr *20*, 303-310.

Sullivan-Gunn, M.J., Campbell-O'Sullivan, S.P., Tisdale, M.J., and Lewandowski, P.A. (2011). Decreased NADPH oxidase expression and antioxidant activity in cachectic skeletal muscle. J Cachexia Sarcopenia Muscle *2*, 181-188.

Sun, F., Sun, Y., Zhang, D., Zhang, J., Song, B., and Zheng, H. (2010). Association of interleukin-10 gene polymorphism with cachexia in Chinese patients with gastric cancer. Ann Clin Lab Sci *40*, 149-155.

Sun, X., and Zhu, M.J. (2017). AMP-activated protein kinase: a therapeutic target in intestinal diseases. Open Biol *7*.

Suzuki, K., Ichikawa, T., Furuse, H., Tsuda, T., Tokui, K., Masaki, Y., Okazawa, S., Kambara, K., Inomata, M., Yamada, T*., et al.* (2015). Relationship of the urine cortisol level with the performance status of patients with lung cancer: a retrospective study. Support Care Cancer *23*, 2129-2133.

Suzuki, Y., Deitch, E.A., Mishima, S., Lu, Q., and Xu, D. (2000). Inducible nitric oxide synthase gene knockout mice have increased resistance to gut injury and bacterial translocation after an intestinal ischemia-reperfusion injury. Crit Care Med *28*, 3692-3696.

Suzuki, Y.J., Carini, M., and Butterfield, D.A. (2010). Protein carbonylation. Antioxid Redox Signal *12*, 323-325.

Szabo, C., Ischiropoulos, H., and Radi, R. (2007). Peroxynitrite: biochemistry, pathophysiology and development of therapeutics. Nat Rev Drug Discov *6*, 662-680.

Tabony, A.M., Yoshida, T., Galvez, S., Higashi, Y., Sukhanov, S., Chandrasekar, B., Mitch, W.E., and Delafontaine, P. (2011). Angiotensin II upregulates protein phosphatase 2Calpha and inhibits AMP-activated protein kinase signaling and energy balance leading to skeletal muscle wasting. Hypertension *58*, 643-649.

Takahashi, M., Terashima, M., Takagane, A., Oyama, K., Fujiwara, H., and Wakabayashi, G. (2009). Ghrelin and leptin levels in cachectic patients with cancer of the digestive organs. Int J Clin Oncol *14*, 315-320.

Takatani, Y., Ono, K., Suzuki, H., Inaba, M., Sawada, M., and Matsuda, N. (2018). Inducible nitric oxide synthase during the late phase of sepsis is associated with hypothermia and immune cell migration. Lab Invest *98*, 629-639.

Takayama, K., Atagi, S., Imamura, F., Tanaka, H., Minato, K., Harada, T., Katakami, N., Yokoyama, T., Yoshimori, K., Takiguchi, Y.*, et al.* (2016). Quality of life and survival survey of cancer cachexia in advanced non-small cell lung cancer patients-Japan nutrition and QOL survey in patients with advanced non-small cell lung cancer study. Support Care Cancer *24*, 3473-3480.

Talarmin, H., Derbre, F., Lefeuvre-Orfila, L., Leon, K., Droguet, M., Pennec, J.P., and Giroux-Metges, M.A. (2017). The diaphragm is better protected from oxidative stress than hindlimb skeletal muscle during CLP-induced sepsis. Redox Rep *22*, 218-226.

Talbert, E.E., Metzger, G.A., He, W.A., and Guttridge, D.C. (2014). Modeling human cancer cachexia in colon 26 tumor-bearing adult mice. J Cachexia Sarcopenia Muscle *5*, 321-328.

Tan, B.H., and Fearon, K.C. (2008). Cachexia: prevalence and impact in medicine. Curr Opin Clin Nutr Metab Care *11*, 400-407.

Tanaka, Y., Eda, H., Tanaka, T., Udagawa, T., Ishikawa, T., Horii, I., Ishitsuka, H., Kataoka, T., and Taguchi, T. (1990). Experimental cancer cachexia induced by transplantable colon 26 adenocarcinoma in mice. Cancer research *50*, 2290-2295.

Tang, A.M., Jacobson, D.L., Spiegelman, D., Knox, T.A., and Wanke, C. (2005). Increasing risk of 5% or greater unintentional weight loss in a cohort of HIV-infected patients, 1995 to 2003. J Acquir Immune Defic Syndr *40*, 70-76.

Tang, H., Pang, S., Wang, M., Xiao, X., Rong, Y., Wang, H., and Zang, Y.Q. (2010). TLR4 activation is required for IL-17-induced multiple tissue inflammation and wasting in mice. Journal of immunology *185*, 2563-2569.

Tardif, N., Klaude, M., Lundell, L., Thorell, A., and Rooyackers, O. (2013). Autophagic-lysosomal pathway is the main proteolytic system modified in the skeletal muscle of esophageal cancer patients. The American journal of clinical nutrition *98*, 1485-1492.

Tarricone, R., Ricca, G., Nyanzi-Wakholi, B., and Medina-Lara, A. (2016). Impact of cancer anorexia-cachexia syndrome on health-related quality of life and resource utilisation: A systematic review. Crit Rev Oncol Hematol *99*, 49-62.

Taylor, C.T., and Moncada, S. (2010). Nitric oxide, cytochrome C oxidase, and the cellular response to hypoxia. Arterioscler Thromb Vasc Biol *30*, 643-647.

Terawaki, K., Sawada, Y., Kashiwase, Y., Hashimoto, H., Yoshimura, M., Suzuki, M., Miyano, K., Sudo, Y., Shiraishi, S., Higami, Y*., et al.* (2014). New cancer cachexia rat model generated by implantation of a peritoneal dissemination-derived human stomach cancer cell line. Am J Physiol Endocrinol Metab *306*, E373-387.

Teunissen, S.C., Wesker, W., Kruitwagen, C., de Haes, H.C., Voest, E.E., and de Graeff, A. (2007). Symptom prevalence in patients with incurable cancer: a systematic review. Journal of pain and symptom management *34*, 94-104.

Thiemermann, C. (1997). Nitric oxide and septic shock. Gen Pharmacol *29*, 159-166.

Thomson, D.M. (2018). The Role of AMPK in the Regulation of Skeletal Muscle Size, Hypertrophy, and Regeneration. Int J Mol Sci *19*.

Thoresen, L., Frykholm, G., Lydersen, S., Ulveland, H., Baracos, V., Prado, C.M., Birdsell, L., and Falkmer, U. (2013). Nutritional status, cachexia and survival in patients with advanced colorectal carcinoma. Different assessment criteria for nutritional status provide unequal results. Clinical nutrition *32*, 65-72.

Thornalley, P.J. (2003). Use of aminoguanidine (Pimagedine) to prevent the formation of advanced glycation endproducts. Arch Biochem Biophys *419*, 31-40.

Tian, M., Nishijima, Y., Asp, M.L., Stout, M.B., Reiser, P.J., and Belury, M.A. (2010). Cardiac alterations in cancer-induced cachexia in mice. Int J Oncol *37*, 347-353.

Tiano, J.P., Springer, D.A., and Rane, S.G. (2015). SMAD3 negatively regulates serum irisin and skeletal muscle FNDC5 and peroxisome proliferator-activated receptor gamma coactivator 1-alpha (PGC-1alpha) during exercise. J Biol Chem *290*, 7671-7684.

Tisdale, M.J. (1997). Biology of Cachexia. Journal of the National Cancer Institute *89*, 1763-1773.

Tisdale, M.J. (1999). Wasting in cancer. J Nutr *129*, 243S-246S.

Tisdale, M.J. (2009). Mechanisms of cancer cachexia. Physiological reviews *89*, 381-410.

Tobias, I.S., Lazauskas, K.K., Arevalo, J.A., Bagley, J.R., Brown, L.E., and Galpin, A.J. (2018). Fiber type-specific analysis of AMPK isoforms in human skeletal muscle: advancement in methods via capillary nanoimmunoassay. Journal of applied physiology *124*, 840-849.

Towler, M.C., and Hardie, D.G. (2007). AMP-activated protein kinase in metabolic control and insulin signaling. Circulation research *100*, 328-341.

Toyama, E.Q., Herzig, S., Courchet, J., Lewis, T.L., Jr., Loson, O.C., Hellberg, K., Young, N.P., Chen, H., Polleux, F., Chan, D.C.*, et al.* (2016). Metabolism. AMP-activated protein kinase mediates mitochondrial fission in response to energy stress. Science *351*, 275-281.

Tracey, K.J., Lowry, S.F., and Cerami, A. (1988). Cachectin: a hormone that triggers acute shock and chronic cachexia. J Infect Dis *157*, 413-420.

Trendelenburg, A.U., Meyer, A., Rohner, D., Boyle, J., Hatakeyama, S., and Glass, D.J. (2009). Myostatin reduces Akt/TORC1/p70S6K signaling, inhibiting myoblast differentiation and myotube size. American journal of physiology Cell physiology *296*, C1258-1270.

Tseng, Y.C., Kulp, S.K., Lai, I.L., Hsu, E.C., He, W.A., Frankhouser, D.E., Yan, P.S., Mo, X., Bloomston, M., Lesinski, G.B.*, et al.* (2015). Preclinical Investigation of the Novel Histone Deacetylase Inhibitor AR-42 in the Treatment of Cancer-Induced Cachexia. J Natl Cancer Inst *107*, djv274.

Tsoli, M., Schweiger, M., Vanniasinghe, A.S., Painter, A., Zechner, R., Clarke, S., and Robertson, G. (2014). Depletion of white adipose tissue in cancer cachexia syndrome is associated with inflammatory signaling and disrupted circadian regulation. PLoS One *9*, e92966.

Twig, G., Elorza, A., Molina, A.J., Mohamed, H., Wikstrom, J.D., Walzer, G., Stiles, L., Haigh, S.E., Katz, S., Las, G.*, et al.* (2008). Fission and selective fusion govern mitochondrial segregation and elimination by autophagy. The EMBO journal *27*, 433-446.

Tzika, A.A., Fontes-Oliveira, C.C., Shestov, A.A., Constantinou, C., Psychogios, N., Righi, V., Mintzopoulos, D., Busquets, S., Lopez-Soriano, F.J., Milot, S.*, et al.* (2013). Skeletal muscle mitochondrial uncoupling in a murine cancer cachexia model. Int J Oncol *43*, 886-894.

Um, J.H., and Yun, J. (2017). Emerging role of mitophagy in human diseases and physiology. BMB Rep *50*, 299-307.

Utech, A.E., Tadros, E.M., Hayes, T.G., and Garcia, J.M. (2012). Predicting survival in cancer patients: the role of cachexia and hormonal, nutritional and inflammatory markers. J Cachexia Sarcopenia Muscle *3*, 245-251.

Valvona, C.J., Fillmore, H.L., Nunn, P.B., and Pilkington, G.J. (2016). The Regulation and Function of Lactate Dehydrogenase A: Therapeutic Potential in Brain Tumor. Brain Pathol *26*, 3-17.

van de Worp, W., Theys, J., van Helvoort, A., and Langen, R.C.J. (2018). Regulation of muscle atrophy by microRNAs: 'AtromiRs' as potential target in cachexia. Curr Opin Clin Nutr Metab Care *21*, 423-429.

van der Meij, B.S., Schoonbeek, C.P., Smit, E.F., Muscaritoli, M., van Leeuwen, P.A., and Langius, J.A. (2013). Pre-cachexia and cachexia at diagnosis of stage III non-small-cell lung carcinoma: an exploratory study comparing two consensus-based frameworks. Br J Nutr *109*, 2231-2239.

van Norren, K., Dwarkasing, J.T., and Witkamp, R.F. (2017). The role of hypothalamic inflammation, the hypothalamic-pituitary-adrenal axis and serotonin in the cancer anorexia-cachexia syndrome. Curr Opin Clin Nutr Metab Care *20*, 396-401.

VanderVeen, B.N., Fix, D.K., and Carson, J.A. (2017). Disrupted Skeletal Muscle Mitochondrial Dynamics, Mitophagy, and Biogenesis during Cancer Cachexia: A Role for Inflammation. Oxid Med Cell Longev *2017*, 3292087.

VanderVeen, B.N., Fix, D.K., Montalvo, R.N., Counts, B.R., Smuder, A.J., Murphy, E.A., Koh, H.J., and Carson, J.A. (2019). The regulation of skeletal muscle fatigability and mitochondrial function by chronically elevated interleukin-6. Exp Physiol *104*, 385-397.

VanderVeen, B.N., Hardee, J.P., Fix, D.K., and Carson, J.A. (2018). Skeletal muscle function during the progression of cancer cachexia in the male Apc(Min/+) mouse. Journal of applied physiology *124*, 684-695.

Vannini, F., Kashfi, K., and Nath, N. (2015). The dual role of iNOS in cancer. Redox Biol *6*, 334-343.

Vaughan, V.C., Martin, P., and Lewandowski, P.A. (2013). Cancer cachexia: impact, mechanisms and emerging treatments. J Cachexia Sarcopenia Muscle *4*, 95-109.

Vazeille, C., Jouinot, A., Durand, J.P., Neveux, N., Boudou-Rouquette, P., Huillard, O., Alexandre, J., Cynober, L., and Goldwasser, F. (2017). Relation between hypermetabolism, cachexia, and survival in cancer patients: a prospective study in 390 cancer patients before initiation of anticancer therapy. The American journal of clinical nutrition *105*, 1139-1147.

Velloso, C.P. (2008). Regulation of muscle mass by growth hormone and IGF-I. Br J Pharmacol *154*, 557-568.

Vichai, V., and Kirtikara, K. (2006). Sulforhodamine B colorimetric assay for cytotoxicity screening. Nat Protoc *1*, 1112-1116.

Vigano, A., Del Fabbro, E., Bruera, E., and Borod, M. (2012). The cachexia clinic: from staging to managing nutritional and functional problems in advanced cancer patients. Crit Rev Oncog *17*, 293-303.

Vigano, A.A.L., Morais, J.A., Ciutto, L., Rosenthall, L., di Tomasso, J., Khan, S., Olders, H., Borod, M., and Kilgour, R.D. (2017). Use of routinely available clinical, nutritional, and functional criteria to classify cachexia in advanced cancer patients. Clinical nutrition *36*, 1378-1390.

Vincent, E.E., Coelho, P.P., Blagih, J., Griss, T., Viollet, B., and Jones, R.G. (2015). Differential effects of AMPK agonists on cell growth and metabolism. Oncogene *34*, 3627-3639.

Viollet, B., Foretz, M., Guigas, B., Horman, S., Dentin, R., Bertrand, L., Hue, L., and Andreelli, F. (2006). Activation of AMP-activated protein kinase in the liver: a new strategy for the management of metabolic hepatic disorders. J Physiol *574*, 41-53.

Viollet, B., Guigas, B., Sanz Garcia, N., Leclerc, J., Foretz, M., and Andreelli, F. (2012). Cellular and molecular mechanisms of metformin: an overview. Clinical science *122*, 253-270.

Vitecek, J., Lojek, A., Valacchi, G., and Kubala, L. (2012). Arginine-based inhibitors of nitric oxide synthase: therapeutic potential and challenges. Mediators Inflamm *2012*, 318087.

von Haehling, S., Anker, M.S., and Anker, S.D. (2016). Prevalence and clinical impact of cachexia in chronic illness in Europe, USA, and Japan: facts and numbers update 2016. J Cachexia Sarcopenia Muscle *7*, 507-509.

von Haehling, S., and Anker, S.D. (2010). Cachexia as a major underestimated and unmet medical need: facts and numbers. J Cachexia Sarcopenia Muscle *1*, 1-5.

von Haehling, S., and Anker, S.D. (2014). Prevalence, incidence and clinical impact of cachexia: facts and numbers-update 2014. J Cachexia Sarcopenia Muscle *5*, 261-263.

von Haehling, S., Doehner, W., and Anker, S.D. (2007). Nutrition, metabolism, and the complex pathophysiology of cachexia in chronic heart failure. Cardiovasc Res *73*, 298-309.

von Roretz, C., Beauchamp, P., Di Marco, S., and Gallouzi, I.E. (2011). HuR and myogenesis: being in the right place at the right time. Biochim Biophys Acta *1813*, 1663-1667.

Wallengren, O., Lundholm, K., and Bosaeus, I. (2013). Diagnostic criteria of cancer cachexia: relation to quality of life, exercise capacity and survival in unselected palliative care patients. Support Care Cancer *21*, 1569-1577.

Wan, J.J., Qin, Z., Wang, P.Y., Sun, Y., and Liu, X. (2017). Muscle fatigue: general understanding and treatment. Exp Mol Med *49*, e384.

Wang, F., Liu, H., Hu, L., Liu, Y., Duan, Y., Cui, R., and Tian, W. (2018a). The Warburg effect in human pancreatic cancer cells triggers cachexia in athymic mice carrying the cancer cells. BMC cancer *18*, 360.

Wang, G., Biswas, A.K., Ma, W., Kandpal, M., Coker, C., Grandgenett, P.M., Hollingsworth, M.A., Jain, R., Tanji, K., Lomicronpez-Pintado, S*., et al.* (2018b). Metastatic cancers promote cachexia through ZIP14 upregulation in skeletal muscle. Nature medicine *24*, 770-781.

Wang, W., Fan, J., Yang, X., Furer-Galban, S., Lopez de Silanes, I., von Kobbe, C., Guo, J., Georas, S.N., Foufelle, F., Hardie, D.G*., et al.* (2002). AMP-activated kinase regulates cytoplasmic HuR. Mol Cell Biol *22*, 3425-3436.

Wang, W., Svanberg, E., Delbro, D., and Lundholm, K. (2005). NOS isoenzyme content in brain nuclei as related to food intake in experimental cancer cachexia. Brain Res Mol Brain Res *134*, 205-214.

Wang, W., Yang, X., Kawai, T., Lopez de Silanes, I., Mazan-Mamczarz, K., Chen, P., Chook, Y.M., Quensel, C., Kohler, M., and Gorospe, M. (2004). AMP-activated protein kinase-regulated phosphorylation and acetylation of importin alpha1: involvement in the nuclear import of RNA-binding protein HuR. J Biol Chem *279*, 48376-48388.

Waning, D.L., Mohammad, K.S., Reiken, S., Xie, W., Andersson, D.C., John, S., Chiechi, A., Wright, L.E., Umanskaya, A., Niewolna, M*., et al.* (2015). Excess TGF-beta mediates muscle weakness associated with bone metastases in mice. Nature medicine *21*, 1262-1271.

Wanke, C.A., Silva, M., Knox, T.A., Forrester, J., Speigelman, D., and Gorbach, S.L. (2000). Weight loss and wasting remain common complications in individuals infected with human immunodeficiency virus in the era of highly active antiretroviral therapy. Clin Infect Dis *31*, 803-805.

Warren, S. (1932). The immediate causes of death in cancer. Am J Med Sci *184*, 610-615.

Wasley, D., Gale, N., Roberts, S., Backx, K., Nelson, A., van Deursen, R., and Byrne, A. (2018). Patients with established cancer cachexia lack the motivation and self-efficacy to undertake regular structured exercise. Psychooncology *27*, 458-464.

Wesseltoft-Rao, N., Hjermstad, M.J., Ikdahl, T., Dajani, O., Ulven, S.M., Iversen, P.O., and Bye, A. (2015). Comparing two classifications of cancer cachexia and their association with survival in patients with unresected pancreatic cancer. Nutr Cancer *67*, 472-480.

Wheelwright, S., Darlington, A.S., Hopkinson, J.B., Fitzsimmons, D., White, A., and Johnson, C.D. (2013). A systematic review of health-related quality of life instruments in patients with cancer cachexia. Support Care Cancer *21*, 2625-2636.

White, J.P., Baltgalvis, K.A., Puppa, M.J., Sato, S., Baynes, J.W., and Carson, J.A. (2011a). Muscle oxidative capacity during IL-6-dependent cancer cachexia. Am J Physiol Regul Integr Comp Physiol *300*, R201-211.

White, J.P., Baynes, J.W., Welle, S.L., Kostek, M.C., Matesic, L.E., Sato, S., and Carson, J.A. (2011b). The regulation of skeletal muscle protein turnover during the progression of cancer cachexia in the Apc(Min/+) mouse. PLoS One *6*, e24650.

White, J.P., Puppa, M.J., Gao, S., Sato, S., Welle, S.L., and Carson, J.A. (2013). Muscle mTORC1 suppression by IL-6 during cancer cachexia: a role for AMPK. Am J Physiol Endocrinol Metab *304*, E1042-1052.

White, J.P., Puppa, M.J., Sato, S., Gao, S., Price, R.L., Baynes, J.W., Kostek, M.C., Matesic, L.E., and Carson, J.A. (2012). IL-6 regulation on skeletal muscle mitochondrial remodeling during cancer cachexia in the ApcMin/+ mouse. Skeletal muscle *2*, 14.

Wiedenmann, B., Malfertheiner, P., Friess, H., Ritch, P., Arseneau, J., Mantovani, G., Caprioni, F., Van Cutsem, E., Richel, D., DeWitte, M.*, et al.* (2008). A multicenter, phase II study of infliximab plus gemcitabine in pancreatic cancer cachexia. J Support Oncol *6*, 18-25.

Williamson, D.L., Bolster, D.R., Kimball, S.R., and Jefferson, L.S. (2006). Time course changes in signaling pathways and protein synthesis in C2C12 myotubes following AMPK activation by AICAR. Am J Physiol Endocrinol Metab *291*, E80-89.

Winbanks, C.E., Murphy, K.T., Bernardo, B.C., Qian, H., Liu, Y., Sepulveda, P.V., Beyer, C., Hagg, A., Thomson, R.E., Chen, J.L.*, et al.* (2016). Smad7 gene delivery prevents muscle wasting associated with cancer cachexia in mice. Sci Transl Med *8*, 348ra398.

Windsor, J.A., and Hill, G.L. (1988). Risk factors for postoperative pneumonia. The importance of protein depletion. Ann Surg *208*, 209-214.

Wiseman, D.A., and Thurmond, D.C. (2012). The good and bad effects of cysteine S-nitrosylation and tyrosine nitration upon insulin exocytosis: a balancing act. Curr Diabetes Rev *8*, 303-315.

Wisse, B.E., Frayo, R.S., Schwartz, M.W., and Cummings, D.E. (2001). Reversal of cancer anorexia by blockade of central melanocortin receptors in rats. Endocrinology *142*, 3292-3301.

Wolf, I., Sadetzki, S., Kanety, H., Kundel, Y., Pariente, C., Epstein, N., Oberman, B., Catane, R., Kaufman, B., and Shimon, I. (2006). Adiponectin, ghrelin, and leptin in cancer cachexia in breast and colon cancer patients. Cancer *106*, 966-973.

Wong, M.L., Rettori, V., al-Shekhlee, A., Bongiorno, P.B., Canteros, G., McCann, S.M., Gold, P.W., and Licinio, J. (1996). Inducible nitric oxide synthase gene expression in the brain during systemic inflammation. Nature medicine *2*, 581-584.

Wu, Q., Sun, S., Li, Z., Yang, Q., Li, B., Zhu, S., Wang, L., Wu, J., Yuan, J., Yang, C.*, et al.* (2018). Tumour-originated exosomal miR-155 triggers cancer-associated cachexia to promote tumour progression. Mol Cancer *17*, 155.

Xiao, B., Sanders, M.J., Underwood, E., Heath, R., Mayer, F.V., Carmena, D., Jing, C., Walker, P.A., Eccleston, J.F., Haire, L.F.*, et al.* (2011). Structure of mammalian AMPK and its regulation by ADP. Nature *472*, 230-233.

Xu, J., Ji, J., and Yan, X.H. (2012). Cross-talk between AMPK and mTOR in regulating energy balance. Crit Rev Food Sci Nutr *52*, 373-381.

Xue, Q., Yan, Y., Zhang, R., and Xiong, H. (2018). Regulation of iNOS on Immune Cells and Its Role in Diseases. Int J Mol Sci *19*.

Yabar, C.S., and Winter, J.M. (2016). Pancreatic Cancer: A Review. Gastroenterol Clin North Am *45*, 429-445.

Yavuzsen, T., Walsh, D., Davis, M.P., Kirkova, J., Jin, T., LeGrand, S., Lagman, R., Bicanovsky, L., Estfan, B., Cheema, B*., et al.* (2009). Components of the anorexia-cachexia syndrome: gastrointestinal symptom correlates of cancer anorexia. Support Care Cancer *17*, 1531-1541.

Ye, F., Mathur, S., Liu, M., Borst, S.E., Walter, G.A., Sweeney, H.L., and Vandenborne, K. (2013). Overexpression of insulin-like growth factor-1 attenuates skeletal muscle damage and accelerates muscle regeneration and functional recovery after disuse. Exp Physiol *98*, 1038-1052.

Yoshida, T., Semprun-Prieto, L., Sukhanov, S., and Delafontaine, P. (2010). IGF-1 prevents ANG II-induced skeletal muscle atrophy via Akt- and Foxo-dependent inhibition of the ubiquitin ligase atrogin-1 expression. American journal of physiology Heart and circulatory physiology *298*, H1565-1570.

Youle, R.J., and van der Bliek, A.M. (2012). Mitochondrial fission, fusion, and stress. Science *337*, 1062-1065.

Zadra, G., Batista, J.L., and Loda, M. (2015). Dissecting the Dual Role of AMPK in Cancer: From Experimental to Human Studies. Mol Cancer Res *13*, 1059-1072.

Zhang, G., Liu, Z., Ding, H., Zhou, Y., Doan, H.A., Sin, K.W.T., Zhu, Z.J., Flores, R., Wen, Y., Gong, X*., et al.* (2017). Tumor induces muscle wasting in mice through releasing extracellular Hsp70 and Hsp90. Nat Commun *8*, 589.

Zhang, L., Pan, J., Dong, Y., Tweardy, D.J., Dong, Y., Garibotto, G., and Mitch, W.E. (2013). Stat3 activation links a C/EBPdelta to myostatin pathway to stimulate loss of muscle mass. Cell metabolism *18*, 368-379.

Zhang, P., Xu, X., Hu, X., van Deel, E.D., Zhu, G., and Chen, Y. (2007). Inducible nitric oxide synthase deficiency protects the heart from systolic overload-induced ventricular hypertrophy and congestive heart failure. Circulation research *100*, 1089-1098.

Zhang, X., Yang, S., Chen, J., and Su, Z. (2018a). Unraveling the Regulation of Hepatic Gluconeogenesis. Front Endocrinol (Lausanne) *9*, 802.

Zhang, Y., Qiu, J., Wang, X., Zhang, Y., and Xia, M. (2011). AMP-activated protein kinase suppresses endothelial cell inflammation through phosphorylation of transcriptional coactivator p300. Arterioscler Thromb Vasc Biol *31*, 2897-2908.

Zhang, Z., Cheng, X., Yue, L., Cui, W., Zhou, W., Gao, J., and Yao, H. (2018b). Molecular pathogenesis in chronic obstructive pulmonary disease and therapeutic potential by targeting AMP-activated protein kinase. J Cell Physiol *233*, 1999-2006.

Zhou, G., Myers, R., Li, Y., Chen, Y., Shen, X., Fenyk-Melody, J., Wu, M., Ventre, J., Doebber, T., Fujii, N.*, et al.* (2001). Role of AMP-activated protein kinase in mechanism of metformin action. J Clin Invest *108*, 1167-1174.

Zhou, J., and Cidlowski, J.A. (2005). The human glucocorticoid receptor: one gene, multiple proteins and diverse responses. Steroids *70*, 407-417.

Zhou, T., Wang, B., Liu, H., Yang, K., Thapa, S., Zhang, H., Li, L., and Yu, S. (2018). Development and validation of a clinically applicable score to classify cachexia stages in advanced cancer patients. J Cachexia Sarcopenia Muscle *9*, 306-314.

Zhou, T., Yang, K., Thapa, S., Liu, H., Wang, B., and Yu, S. (2017). Differences in Symptom Burden Among Cancer Patients With Different Stages of Cachexia. Journal of pain and symptom management *53*, 919-926.

Zhou, X., Wang, J.L., Lu, J., Song, Y., Kwak, K.S., Jiao, Q., Rosenfeld, R., Chen, Q., Boone, T., Simonet, W.S.*, et al.* (2010). Reversal of cancer cachexia and muscle wasting by ActRIIB antagonism leads to prolonged survival. Cell *142*, 531-543.

Zimmers, T.A., Davies, M.V., Koniaris, L.G., Haynes, P., Esquela, A.F., Tomkinson, K.N., McPherron, A.C., Wolfman, N.M., and Lee, S.J. (2002). Induction of cachexia in mice by systemically administered myostatin. Science *296*, 1486-1488.

Zimmers, T.A., Jiang, Y., Wang, M., Liang, T.W., Rupert, J.E., Au, E.D., Marino, F.E., Couch, M.E., and Koniaris, L.G. (2017). Exogenous GDF11 induces cardiac and skeletal muscle dysfunction and wasting. Basic Res Cardiol *112*, 48.

Zong, H., Ren, J.M., Young, L.H., Pypaert, M., Mu, J., Birnbaum, M.J., and Shulman, G.I. (2002). AMP kinase is required for mitochondrial biogenesis in skeletal muscle in response to chronic energy deprivation. Proc Natl Acad Sci U S A *99*, 15983-15987.

Zugmaier, G., Paik, S., Wilding, G., Knabbe, C., Bano, M., Lupu, R., Deschauer, B., Simpson, S., Dickson, R.B., and Lippman, M. (1991). Transforming growth factor beta 1 induces cachexia and systemic fibrosis without an antitumor effect in nude mice. Cancer research *51*, 3590-3594.